NASA TECHNICAL NOTE

NASA TN D-7944

NASA TN D-7944

DESIGN AND PERFORMANCE AT A LOCAL MACH NUMBER OF 6 OF AN INLET FOR AN INTEGRATED SCRAMJET CONCEPT

Carl A. Trexler and Sue W. Souders

Langley Research Center
Hampton, Va. 23665

NATIONAL AERONAUTICS AND SPACE ADMINISTRATION • WASHINGTON, D. C. • AUGUST 1975

1. Report No. NASA TN D-7944	2. Government Accession No.	3. Recipient's Catalog No.
4. Title and Subtitle DESIGN AND PERFORMANCE AT A LOCAL MACH NUMBER OF 6 OF AN INLET FOR AN INTEGRATED SCRAMJET CONCEPT		5. Report Date August 1975 6. Performing Organization Code
7. Author(s) Carl A. Trexler and Sue W. Souders		8. Performing Organization Report No. L-10000
9. Performing Organization Name and Address NASA Langley Research Center Hampton, Va. 23665		10. Work Unit No. 505-05-41-01 11. Contract or Grant No.
12. Sponsoring Agency Name and Address National Aeronautics and Space Administration Washington, D.C. 20546		13. Type of Report and Period Covered Technical Note 14. Sponsoring Agency Code
15. Supplementary Notes		

16. Abstract

A research program on hypersonic propulsion at the NASA Langley Research Center is focused on the development of a concept for a modular supersonic combustion ramjet (Langley Scramjet Module), which is designed to integrate with the airframe of a hypersonic vehicle. The present paper reports the design philosophy and results of experiments at Mach 6 to evaluate the performance of the scramjet inlet. The inlet was designed with modest contraction ratio, fixed geometry, and three fuel injection struts which contribute to the inlet flow compression and provide a short combustor design that results in low internal cooling requirements. The baseline inlet configuration is rectangular in cross-sectional shape, has planar compression surfaces swept at 48°, and has an opening upstream of the cowl leading edge through which spillage occurs for starting. The inlet model has a projected geometric capture area measuring 19.05 cm high by 15.24 cm wide. The average throat Mach number was 3.1. The kinetic energy efficiency was 97.7 percent, and the average inlet aerodynamic contraction ratio was 7.0, which does not include the compression expected from the vehicle bow shock. The inlet captured 94 percent of the flow at its face; and, overall, the inlet performance was well within the acceptable range for high engine performance.

17. Key Words (Suggested by Author(s))	18. Distribution Statement
Hypersonic inlet Integrated scramjet Hypersonic propulsion	Unclassified – Unlimited New Subject Category 07

19. Security Classif. (of this report)	20. Security Classif. (of this page)	21. No. of Pages	22. Price*
Unclassified	Unclassified	140	$5.75

*For sale by the National Technical Information Service, Springfield, Virginia 22151

CONTENTS

	Page
SUMMARY	1
INTRODUCTION	2
SYMBOLS	3
INLET DESIGN CRITERIA AND CONCEPT	5
Airframe-Engine Integration	5
The Scramjet Engine	6
The Inlet Concept	6
Inlet Starting	7
INLET MODEL DESIGN	8
Sweep Angle	8
Mach 6 Shock-Wave System	8
Inlet Design Performance	9
End Effects	9
Off-Design Performance	10
APPARATUS AND TEST PROCEDURE	11
The Inlet Model	11
Boundary-Layer Trips	12
Model Instrumentation	12
Pressure Survey Rakes	12
Mach 6 Test Facility	13
Facility Instrumentation	13
DATA-REDUCTION PROCEDURE	14
RESULTS AND DISCUSSION	14
Initial Inlet Tests	14
Modified Inlet Configuration	15
Inlet Entrance Conditions	16
Wall Static-Pressure Distribution	16
Oil-Flow Study	17
Wall Surface Temperature and Boundary-Layer Analysis	17
Throat Surveys	18
Throat Contour Maps	19
Capture Measurement Results	19
Performance Results	20

Page

CONCLUDING REMARKS 20

APPENDIX A – ANALYTICAL CALCULATIONS OF SWEPT SHOCK WAVES . . . 22

APPENDIX B – INLET PERFORMANCE FOR LOW REYNOLDS NUMBER AND UNSTARTED OPERATION 48

APPENDIX C – CAPTURE MEASUREMENT DATA 49

REFERENCES 50

TABLES 51

FIGURES 55

DESIGN AND PERFORMANCE AT A LOCAL MACH NUMBER OF 6 OF AN INLET FOR AN INTEGRATED SCRAMJET CONCEPT

Carl A. Trexler and Sue W. Souders
Langley Research Center

SUMMARY

A research program on hypersonic propulsion at the NASA Langley Research Center is focused on the development of a concept for a modular supersonic combustion ramjet (Langley Scramjet Module). The modular engine concept is designed to integrate with the airframe; precompression of the engine airflow will be produced by the vehicle bow shock and additional expansion of the nozzle exhaust will be produced by the vehicle afterbody. As part of this research program, component investigations are in progress on the baseline inlet configuration and the present paper reports the design philosophy and results of experiments at Mach 6 to evaluate the performance of the inlet.

With the integration advantages, the inlet was designed with modest contraction ratios and fixed geometry. Three fuel injection struts contribute to the inlet flow compression and provide a short combustor design that results in low internal cooling requirements. The baseline inlet configuration is rectangular in cross-sectional shape, has sweptback sidewall planar compression surfaces, has an opening upstream of the cowl leading edge through which spillage occurs for starting and normal operation, and has the external cowl surface alined with the local flow to provide a minimal external drag. The inlet model had a projected geometric capture area measuring 19.05 cm high by 15.24 cm wide. The sidewalls and struts had 48^{o} swept leading edges and nominal compression surface angles of 6^{o}.

Tests were conducted in the Langley 20-inch Mach 6 tunnel and the inlet model was instrumented to obtain both wall and survey pressure measurements which were used in computing performance and capture flow. The data-reduction system provided integrated performance data as well as contour maps of parameters such as total-pressure recovery and Mach number in the inlet throat. The difficulty and importance of properly positioning the shock waves in the throats of hypersonic inlets were demonstrated, but no adverse effects were noted as a result of the inlet ingesting a boundary layer on the top surface which simulated the boundary layer that would be ingested from the vehicle forebody.

The average throat Mach number was 3.1 compared with the predicted value of 3.4. The kinetic energy efficiency was 97.7 percent (0.59 recovery) compared with prediction

of 98.3 percent (0.67 recovery), which did not account for all sources of total-pressure loss. The average inlet aerodynamic contraction ratio was 7.0, which does not include the compression expected from the vehicle bow shock. The inlet captured 94 percent of the flow at its face; and, overall, the inlet performance was well within the acceptable range for high engine performance.

INTRODUCTION

The attractive potential of hypersonic flight with air-breathing propulsion has been recognized for the past 15 years; however, major advances in technology are required. Exploratory research on concepts for hypersonic air-breathing engines has been pursued in substantial research and development programs and a broad technology base has been established. See, for example, references 1 to 4. The investigation of several small-scale, hydrogen fueled, supersonic combustion ramjet (scramjet) engine designs has shown that the scramjet is a feasible engine concept and practical levels of thrust have been demonstrated (ref. 5). Hypersonic research and technology programs have been conducted (refs. 6 and 7) which illustrate the next logical step in scramjet evolution, which is the development of engine concepts which will integrate with the airframe. Integration includes the use of the vehicle forebody to precompress the engine airflow before it enters the inlet and the use of the vehicle afterbody for additional expansion and thrust vectoring of the nozzle exhaust gas. Other principal design criteria for hypersonic systems are minimum engine cooling requirements to make part of the heat sink of the hydrogen fuel available for active cooling of the airframe, fixed geometry to reduce weight and system complexity, and minimum external drag.

Detailed analytical and experimental studies at the Langley Research Center have resulted in the definition of the Langley Scramjet Module, with design features in both the inlet and combustor which will satisfy the engine design criteria, when the benefits of vehicle and propulsion system integration are included. This report deals primarily with the design and performance evaluation for the hypersonic inlet concept for the Langley Scramjet Module. The design criteria were met with the use of swept compression surfaces, which produced oblique shock waves, and a matching swept throat and combustor. Because of the complexity of the flow, it was necessary to optimize the selected inlet configuration from the experimental results of several earlier configuration studies. Once the concept was derived, computer programs aided in locating shock waves within the inlet, determined boundary-layer corrections to the interior walls, provided theoretical performance results, and reduced experimental test data.

A model of the inlet portion of the Langley Scramjet Module, 19.05 cm high by 15.24 cm wide, was tested in the Langley 20-inch Mach 6 wind tunnel. This test

condition represents local inlet face conditions for a flight Mach number of approximately 7.6 after compression from the vehicle forebody. The tunnel free-stream total temperature and pressure were 467 K and 11.9 atm (1 atm = 101.3 KN/m^2), respectively, and provided a Reynolds number per meter of approximately 9.8×10^6. One run was made at a reduced Reynolds number per meter of 3.3×10^6.

SYMBOLS

When two symbols are given for the same concept, the second one is that used for the computer data.

A	cross-sectional area of a stream tube
A*	cross-sectional area of a stream tube with sonic velocity
A/A_1	aerodynamic contraction ratio, $\frac{A_1}{A_1^*}\frac{p_t}{p_{t,1}}\frac{A^*}{A}$
c,C	distance from cowl tip (fig. 13(d))
c',C'	distance from cowl leading edge (fig. 13(d))
H	inlet height, 19.05 cm (7.5 in.)
M	Mach number
p,P	static pressure
p_1,P1	static pressure in front of inlet
p_t	total pressure
p_{pitot},PITOT	pitot pressure
R	Reynolds number
s	distance from foreplate leading edge (fig. 13(a))

s'	distance from sidewall leading edge (fig. 13(c))
s''	distance from strut leading edge (figs. 13(e) to 13(g))
T	temperature
T_{aw}	adiabatic wall temperature
T_t	total temperature
V	velocity vector
v	velocity
W	throat gap or width of capture measurement station, cm (figs. 11 and 25)
X	distance downstream of intersection of sidewall with foreplate (fig. 13(b))
x	axis parallel to free-stream flow (fig. 57)
Y	distance from foreplate (fig. 13(c))
y	axis perpendicular to free-stream flow (fig. 57)
Z	distance away from model center line (figs. 13(a) and 13(d))
Z'	distance across throat or across duct (fig. 11)
z	axis perpendicular to free-stream flow and y-axis (figs. 4 and 57)
δ	boundary-layer thickness
δ_n	flow turning angle normal to leading edge of swept wedge (fig. 57)
δ_{xy}	cross-flow angle (fig. 57)
δ_{xz}	wedge angle or flow turning angle in xz-plane (fig. 57)

ϵ_{xz} shock-wave angle in xz-plane (fig. 57)

η_k kinetic energy efficiency

Λ sweep angle measured in xy-plane, deg

λ distance around capture measurement station (fig. 62)

ρ density

ϕ dihedral angle measured perpendicular to ridge line, deg

ψ dihedral parameter

Subscripts:

1 conditions at inlet face or ahead of a shock wave

2,3,4 conditions behind 1st, 2d, and 3d shock waves, respectively

n normal to leading edge (fig. 57)

t tangential to leading edge (fig. 57)

∞ free stream (in front of vehicle)

INLET DESIGN CRITERIA AND CONCEPT

Airframe-Engine Integration

The advantages of integrating the airframe and engine of a hypersonic vehicle are well known. The parametric analysis of reference 8 indicates that the contributions of the vehicle forebody and afterbody are responsible for up to 70 percent of the thrust. At hypersonic speeds very large engine airflows are required for adequate thrust in spite of the high-energy potential of the hydrogen fuel. These engine airflow requirements are best met by utilizing the precompression obtained from the vehicle forebody and locating the engine on the underside of the vehicle toward the aft end. (See fig. 1.) A method of designing the forebody is discussed in reference 6. The propulsion system inlet area is therefore restricted to the space between the vehicle undersurface and the bow shock and is several times wider than it is high, as shown in the cross section of figure 1. This

geometry concept suggests the arrangement of a number of adjacent rectangular engine modules, and the use of modules also permits development in ground test facilities of reasonable size. The relatively thick turbulent boundary layer generated on the vehicle forebody is an unfavorable characteristic which must be considered in the inlet design. The design of the vehicle afterbody, discussed in reference 7, is also important because of the large gross-thrust and moment forces involved, which can generate large trim drag penalties if not correctly considered.

The Scramjet Engine

The primary objectives of the scramjet engine design are: to provide a high level of thrust and specific impulse with efficient capture over the flight Mach number range from 3.5 to 10, to have low cooling requirements in order to make a portion of the fuel heat sink available for active cooling of the vehicle structure at high Mach numbers, to have satisfactory operating characteristics over the Mach number range including the establishment of supersonic flow (starting) within the inlet at the low end of the Mach number range, to have fixed geometry in order to reduce system complexity as well as joint and seal problems, to ingest successfully the vehicle-forebody boundary layer, and to produce low external drag. Many of these objectives are interrelated and trade-offs discussed in reference 7 indicate that a fixed geometry inlet with moderate contraction for starting at a low Mach number is desirable. A moderate contraction and low internal pressure will not only mean a reduction in engine weight and cooling requirements but also an increased ability for the engine to ingest the vehicle-forebody boundary layer.

Because the use of only fuel injection from the sidewalls would produce very long mixing lengths for this type of modular design, the scramjet engine concept of figure 2 has three struts to provide six planes of instream fuel injection. This feature not only reduces cooling and shortens the combustor but also the inlet, since the struts provide a significant part of the inlet flow compression. The sidewalls are the main inlet compression surfaces, whereas the top surface partially eliminates expansions produced by the downflow created by the swept shock-wave system, which is a unique characteristic of the swept inlet design. The cowl is kept nearly parallel to the vehicle underbody to minimize external drag.

The Inlet Concept

The inlet must efficiently compress the airflow captured for the combustor. Reference 7 indicates that a contraction ratio between 6 and 10 would be satisfactory for a fixed geometry inlet at a flight Mach number of about $7\frac{1}{2}$, and several inlet configurations were investigated which would fit into the area provided beneath the vehicle. Inlet interior walls consisting of swept planar surfaces were assumed; this assumption simplifies the analysis and avoids the need for three-dimensional characteristic computer programs.

Compression angles between 6° and 8° were employed; these angles are a compromise between high angles which contribute to high total-pressure losses from shock waves and increase the possibility of shock-induced boundary-layer separation and low compression angles which make the inlet long.

Prior to the development of the inlet shown in figure 2, a design utilizing swept compression surfaces in which the top surface was the primary compression surface was considered and is discussed in reference 9. Disadvantages to this design were: a corner flow problem originating at the top surface and covering much of the inlet throat; difficulty in obtaining good capture characteristics over the Mach number range; and no effective way of dealing with the vehicle-forebody boundary layer. Therefore sidewalls with swept leading edges were made the primary compression surface for the inlet in figure 2. Because planes of constant flow properties tend to be parallel to the sweep lines, the fuel injection struts and all downstream stations are also swept at the same angle. This design generates a system of swept shock waves which turns the flow away from the top surface and thus reduces the corner flow and boundary-layer problems on that surface. A cowl design which would provide 100-percent capture at high Mach numbers was tested on a preliminary design, and those results indicated that better starting and operating performance could be obtained with the pointed cowl leading edge located near the struts as shown in figure 2. Good capture characteristics can be obtained over the Mach number range with the fixed geometry design; and spillage, produced by the flow being turned toward the opening in front of the cowl by a transient shock system, permits starting at a low Mach number. The downflow produced by the sweep during normal operation tends to reduce the static-pressure rise near the top surface and should make possible the ingestion of the vehicle-forebody boundary layer without separation.

Inlet Starting

Inlet starting at the low end of the Mach number range is primarily a function of contraction ratio, which is influenced by the amount of sweep, the strut design, and the cowl leading-edge location. From simple one-dimensional considerations at an entrance Mach number of 3.0, an area contraction of less than 30 percent is necessary downstream of the plane of closure corresponding to the cowl leading edge. However, in figure 3 the normal plane B-B having the minimum cross-sectional flow area is shown to be located at the cowl leading edge; therefore, on the average there is no contraction downstream of the cowl leading edge. This is a strong indication that the inlet will have no starting problem, and early investigations of similar designs substantiate this conclusion.

The frontal height-width ratio also contributes to the starting characteristics of the inlet. If the width is greater than the height, the inlet is longer and end effects from the top surface and cowl begin to dominate the throat. If the width is much less than the height, the struts become slender and structural problems can appear. Based on

preliminary investigations, a width-height ratio of 0.8 was selected for the inlet design to reduce end effects and to permit a reasonable flight weight structure.

INLET MODEL DESIGN

Sweep Angle

In order to develop the swept shock-wave system for these inlet configurations, it was necessary to understand the process that the supersonic flow undergoes as it strikes a swept wedge. A detailed discussion of the calculation procedure for obtaining the shock-wave angle ϵ_{xz}, downflow δ_{xy}, and the flow properties behind the shock wave is given in reference 9, and a method for predicting the complete shock-wave train for the inlet is developed in appendix A.

A shock wave may be attached or detached depending on the sweep angle and Mach number; consequently, the sweep angle determines the lowest Mach number at which the shock waves can be attached at the strut leading edges. If the sweep is too high, low Mach number operation will result in shock waves being detached well upstream in the inlet ahead of the struts. These detached shock waves may create a situation where disturbances originating in the combustor may extend upstream of the struts locally and produce an undesirable inlet combustor interaction. Too little sweep means the internal contraction is high and no mechanism is provided for sufficient flow spillage for inlet starting at low Mach numbers. Because of the difficulty in analyzing inlet performance at low Mach numbers when the shock waves become detached, two models with struts were built and tested over the Mach number range of 2.3 to 6.0. These models had sweep angles of 60° and 56°. Several smaller models without struts but with sweeps of 50° and 0° were also tested at Mach 4. The results of these tests indicated that a sweep angle lower than 50° could be obtained with adequate starting capability and a sweep angle of 48° was selected.

Mach 6 Shock-Wave System

The theoretical shock diagram for a Mach number of 6 is shown in figure 4 with tables for the various flow passages and struts within the inlet. Section A-A is a horizontal plane parallel to the vehicle underbody and cowl. The sidewall compression angle was kept low to prevent the possibility of boundary-layer separation due to boundary-layer—shock interactions. (See ref. 10.) A detail of the predicted shock-wave structure in the vicinity of the struts is given in figure 5, and the properties of each numbered bay are listed in table I. The struts provide approximately 75 percent of the inlet static-pressure rise (46-percent decrease in throat area measured in the xz-plane). The side struts were positioned within the inlet so that two-thirds of the flow area available was in front of the center passages. This flow division permits the fuel to be injected equally from the surfaces of both the center strut and side struts (only six injection planes).

Boundary-layer transition on the sidewalls is expected to occur ahead of the struts, and the correction of 0.4^{o} (based on flat-plate predictions) in conjunction with the sidewall angle provides a nominal turning of 6^{o}. Because the chords of the struts are small, the thin boundary layer of the struts is expected to be largely laminar in front of the throats, and separation of this thin boundary layer is expected to be of little consequence. Although it is impossible to prevent the sidewall shocks from merging with the strut shocks at some flight Mach number, the situation is relieved for the Mach 6 shock-wave system by changing the wall slope of the struts at appropriate locations and either canceling or reducing the shock strength.

Inlet Design Performance

As previously mentioned, cooling requirements are a major consideration in combustor design and tend to limit the inlet contraction ratio. The inviscid design aerodynamic contraction ratio (which is computed from Mach number at the face of the inlet, throat Mach number, and total-pressure recovery) for the inlet at Mach 6 was 6.85 for the side passage (bay 6) and 7.57 for the center passage (bay 10) and yielded a mass flow weighted average theoretical contraction of 7.3. The geometric throat gaps between the struts are greater than those for a two-dimensional inlet of the same contraction, because a portion of the contraction is produced when the flow is turned toward the cowl (δ_{xy} in table I). In this inlet design the ratio of throat gap to inlet height is 0.042 for each center passage and 0.041 for each boundary-layer-corrected side passage. The width ratio measured in the xz-plane sidewall leading edges to the throats is 5.74 for the inviscid side passages and 6.17 for the center passages when the predicted flow split of 67 percent for the center passage and 33 percent for the side passage is assumed.

In the inviscid flow the average throat Mach number is 3.4 and the total-pressure recovery is 0.88; as a result, there is an adiabatic kinetic energy efficiency of 99.5 percent. The inclusion of the estimated boundary-layer losses on the struts, sidewalls, and top surface reduces the total-pressure recovery to approximately 0.67 (η_k = 98.3 percent); but this value still does not include corner effects. Inlet capture at Mach 6 was predicted to be 93 percent for the cowl location discussed in the next section. This predicted capture is based on the spillage generated when the flow is turned toward the opening in front of the cowl which is computed from matching pressure and flow direction between the external and internal streams.

End Effects

Although no attempt was made to analyze viscous corner boundary-layer interaction regions in the inlet throat, inviscid calculations of the flow near the top surface and cowl were made. Because the flow is turned away from the top surface as it proceeds through the inlet, a fillet was added as shown in figure 6(a). To match precisely the downflow, the

top-surface contour must vary with local Mach number, but to avoid this complication, a single contour angle and position was selected. The angle was kept small (4^o) to avoid shock interactions which could lead to separation of the thick, top-surface boundary layer. The leading edge of the top-surface fillet coincides with the location of the sidewall shocks with a Mach number of 5 in front of the inlet. With Mach 6 in front of the inlet, the top-surface fillet is upstream of the sidewall shock wave, and a 4^o shock wave is produced as illustrated in section B-B of figure 6(a). At the throat the fillet displaces approximately the same amount or cross-sectional area as it would have if it had been on design for each bay, the Mach number in front of the inlet being equal to 6. The corrected values of flow parameters near the top surface for this constant-angle fillet are given in table II(a), where the angle of flow δ_{xy} in each bay has been corrected to match the 4^o slope.

When the internal flow strikes the cowl, the flow must be turned back parallel to the cowl internal surface; as a result, a cowl shock wave and a high-pressure region are produced. The results of this flow turning are given in table II(b) where $\delta_{xy} = 0^o$. To compensate partially for this high pressure, the throat area next to the cowl was opened by relieving the struts and sidewalls. (See fig. 6(b).) This relief area begins where the shock wave from the cowl leading edge strikes the struts and sidewalls, and because the center strut is located downstream of the cowl leading edge, the strut does not extend to the cowl surface. For the inlet model, this cantilevered center strut was secured to the cowl with a pin located behind the strut maximum thickness.

Selection of the proper cowl leading-edge shape was based upon previous model testing. Cowls which enclosed the area behind the sidewall shock waves providing 100-percent capture made the model difficult to start, produced a cowl shock covering most of the inlet throat, and generated a very large corner interaction region between the sidewalls and cowl. A partial cowl whose leading edges were swept back at 50^o (fig. 6(c)) was selected, which provided an open area near the inlet throats. This open area permits spillage for low Mach number inlet starting and provides for some sidewall boundary-layer bleed. The exact location of the cowl relative to the struts was determined from additional model testing as described in a later section.

Off-Design Performance

Although the inlet is not a point design at a local Mach 6 in the conventional sense, it is designed to give the highest relative performance at this Mach number. As the Mach number is decreased as shown in figure 7, the shock-wave system shifts forward, and experimental observations on previous models indicate an increased spillage and lower aerodynamic contraction. For this design at a Mach number of about 3.5, the shock waves become detached from the strut leading edges. With this swept inlet concept, the aerodynamic contraction will increase with increasing Mach number until the shock waves are fully attached in the throat region. At still higher Mach numbers the number of shock

waves in the inlet decreases as they pass through the throat and the contraction begins to decrease slightly.

The combination of detached shock waves, with resulting spillage and variable contraction with Mach number, permits the inlet to have fixed geometry, to start at a low Mach number, and to provide enough contraction for successful operation at a high Mach number.

APPARATUS AND TEST PROCEDURE

The Inlet Model

A photograph of the inlet model designed with regard to the aforementioned concepts appears in figure 8. One sidewall has been removed in figure 8(a) and several pressure rakes can be seen. The model is shown upside down, and the 45.72-cm (18-in.) plate extending ahead of the sidewalls generates a simulated vehicle-forebody boundary layer. The boundary layer from this plate encounters early transition by trips located near the leading edge and the resulting boundary-layer profile entering the inlet is measured by a three-prong adjustable rake.

The model is 90.2 cm (35.5 in.) long not including the foreplate, and inlet frontal dimensions are 19.05 cm (7.5 in.) high by 15.24 cm (6.0 in.) wide. The aluminum top surface was machined in one piece, the foreplate being detachable. Assembly consisted of pinning and bolting the aluminum sidewalls to the top surface and then the stainless-steel cowl to the sidewalls in any one of three possible positions. Three stainless-steel struts were bolted in slots machined in the top surface which were then sealed. The struts were attached to the cowl by pins instead of bolts to reduce thermal stresses created by changes in the lengths of the struts and heights of the sidewalls. The normal to the leading-edge radii of the sidewalls, cowl, and struts was about 0.01 cm (0.004 in.), whereas the foreplate leading-edge radius was 0.06 cm (0.023 in.). Partially visible in the upper left of figure 8(b) is the actuator mechanism which moved pressure survey rakes inside the model.

Schematic drawings of the model are given in figure 9. Stainless-steel cheeks attached to the exterior of the sidewalls simulated adjacent inlet modules up to the inlet closeoff station next to the cowl. A survey station for measuring inlet capture was provided by a swept flat section of sidewall located downstream of the struts. A sidewall relief area next to the cowl is also illustrated, along with the footprint of the side struts on the cowl in section D-D. Detailed strut dimensions (fig. 10) and the relative positions of the struts and cowl (fig. 11) are measured in any xz-plane parallel to the foreplate and away from the relieved area near the cowl. The "station" positions are relative to the sidewall leading edges in the same xz-plane. A second center strut, which provides an

increase in contraction, is also described in figure 10. The difference in contour for this second center strut is similarly shown by the dashed lines on some subsequent figures in the report.

Boundary-Layer Trips

To insure a turbulent boundary layer entering the throat passages, boundary-layer trips were attached to the sidewalls as well as to the foreplate. (See fig. 12.) The diameter of the steel balls (0.159 cm) was approximately equal to the estimated, flat-plate, boundary-layer thickness measured 7.6 cm downstream from the foreplate leading edge. The balls were spotwelded to steel strips which were in turn fastened with epoxy to the aluminum surfaces. The trips on the foreplate were utilized to increase the thickness of the boundary layer which would be entering the inlet, to determine whether there were any adverse effects associated with ingesting the boundary layer of a vehicle forebody.

Model Instrumentation

Figure 13 locates the 116 static-pressure orifices distributed throughout the inlet model. The orifices were strategically located to determine inlet starting, pinpoint shock-wave position, and aid in evaluating inlet contraction. Because of the variety of locations, the position reference varies for each group of orifices. Iron-constantan thermocouples were installed in the right sidewall as shown in figure 14. Each thermocouple lead was spotwelded to the aluminum surface instead of the leads being welded together, in order to determine more precisely the surface temperature.

Pressure Survey Rakes

The three-pronged foreplate boundary-layer probe is described in figure 15. This probe, alined with the sidewall leading edge at $Y/H = 0$ and $Z/H = 0.133$, was adjusted in height between tests to obtain detailed inlet entrance conditions near the top surface. The remaining survey probes were positioned laterally, by an electric motor and actuator attached to the model (fig. 16), in one of five access locations. Locations 1 to 4 provided for probe surveys across the inlet's throats, whereas location 5 provided access to the capture measurement station downstream of the struts. Tubing for the throat survey probes (fig. 17) was routed through the hollow actuator shaft, whereas capture measurement probe (fig. 18) tubes were carried out the rear of the model as illustrated in figure 8(a). The throat pitot probes were designed to survey one side and one center passage simultaneously, and the static survey probe surveyed only one center passage. It was necessary to rely on wall static data for the side passage. The capture measurement station 6.35 cm (2.5 in.) downstream from the struts was surveyed by the seven-prong

pitot and static probes of figure 18(a). A single, stationary tube (0.102 cm I.D.) extended through the top surface and was bent toward the flow to obtain pitot pressure data in the front of a center passage near the top surface. This tube was bent to different locations across the passage between test runs.

Because of the static-pressure gradients in the small throat area to be surveyed, a conventional static-pressure probe, with the orifices located 10 to 20 diameters downstream from the tip, was found to be unsatisfactory. Therefore, a new static probe design (ref. 11), with the orifices approximately 3 tube diameters downstream from the probe tip and on a 3^{o} conical shoulder, was used for both the throat and capture measurement surveys. These static-pressure probes were calibrated at a Mach number of 4.0, and the recorded pressures were found to be in error by less than 5 percent.

Mach 6 Test Facility

Figure 19 is a sketch of the Langley 20-inch Mach 6 tunnel. Tunnel test-section characteristics and flow calibrations can be found in the appendix of reference 12. The tunnel total temperature and pressure were normally 467 K and 11.9 atm, respectively, and provided a Reynolds number per meter of 9.8×10^{6}. One run was made at a reduced Reynolds number per meter of 3.3×10^{6} at a pressure of 4.4 atm, and all runs in the blowdown tunnel were restricted to less than 2 min. The model was mounted upside down in the center of the 50.8-cm-square test section with two 15.24-cm steel channels bolted to the tunnel floor as shown in figure 20.

Facility Instrumentation

Tunnel pressure was recorded with strain-gage pressure transducers, and model static pressures were divided between six 48-port scanivalves. Pitot pressures and all survey data were measured by either strain-gage pressure transducers or multirange capacitance-type pressure transducers. Pitot position was determined with an electronic bridge circuit, and all data were processed by an electronic data processing system.

Because of the short time in which data could be taken $\left(\text{less than } 1\frac{1}{2} \text{ min}\right)$, the scanivalve stepping mechanism was used to trigger the recording system, once each second, while the survey probe was moved continuously across the flow. Before the test the speed of the throat probes was selected by varying the voltage to the dc motor until the probe would span the flow in one test run. At the capture measurement station two test runs were required to span the flow area with the probe. An analysis of the survey data also indicated that pressure lag was not significant even though the connecting tubing was up to $\approx$3 m in length.

DATA-REDUCTION PROCEDURE

A curve-fitting interpolation procedure was utilized to expand the pitot and static survey data into a grid network. Mach number, total pressure, and unit mass flow were calculated for each grid point; and contour maps of each parameter were plotted by the computer's graphic system. Inserted into the program for each grid point was an upper limit on total-pressure recovery which was obtained from the inviscid shock diagram. (See fig. 5.) If the total pressure was greater than this limit, the measured pitot pressure and the limiting total pressure were used to compute the flow parameters including the static pressure. The measured static pressure was discarded when the recovery limit was exceeded for any particular grid point because of the relative inaccuracy of the static-pressure measurements. After completing the grid, numerical integrations were performed to compute a mass-weighted Mach number and total-pressure recovery for the inlet throats and a value for a capture parameter $\rho v/\rho_1 v_1$ at the capture measurement station.

RESULTS AND DISCUSSION

Initial Inlet Tests

The results of the first inlet tests at Mach 6 indicated the model was not operating as expected. Initial testing of the model at Mach 6 indicated too much compression and possible choking was occurring within the center passage as indicated in figure 21. Upon investigation, it was discovered that the 6° sidewall shock wave was striking the side strut too near the leading edge. This shock wave then combined with the 4° side-strut shock wave and produced a 10° wave which reflected between the side and center struts (fig. 22) unlike the expected pattern of figure 5. The location of this sidewall shock wave was also determined by removing the struts and observing the sidewall static-pressure distribution (fig. 23). The error in shock-wave position as measured in the xz-plane was only about 0.64 cm ($\Delta/H = 0.033$) measured approximately 36 cm from the sidewall leading edge. The effect of the increased compression of the center passage extended across the inlet in the vicinity of the cowl to the sidewall, as indicated by the disturbance in the oil-streak photograph of figure 24(a). More detail concerning the oil study is provided in a later section, but proof that the sidewall disturbance was created by the center passage is illustrated in figure 24(b) with the center strut removed. This photograph shows no disturbance next to the cowl. The measured capture was only 81 percent with the choked cowl compared with 92 percent with the center strut removed.

Modified Inlet Configuration

To deal with the miscalculated sidewall shock-wave location, the strut arrangement was altered to move the shock waves toward the center-passage throat. The three struts and cowl were moved forward $\Delta X/H = 0.213$ ($\Delta X \approx 4.06$ cm); and the side struts were moved toward the sidewalls $\Delta Z/H = 0.022$ ($\Delta Z \approx 0.43$ cm) to maintain the same contraction and percent of flow in the side passage. The resulting configuration is shown in figure 25. It was also observed that the experimentally determined location of the sidewall shock waves could be duplicated theoretically by the addition of 0.83° to the sidewall compression angle. This correction is necessary because of end effects from the top surface, or model misalinement, or the use of flat-plate boundary-layer calculations on the swept sidewalls and struts. There was some concern for the inlet operation at lower Mach numbers when the shock wave moved forward along the side strut. However, the shock waves become detached from the swept compression surfaces and should prevent boundary-layer separation and choking by spreading the static-pressure rise along the strut surfaces. In fact, unpublished data from low Mach number tests support this conclusion.

The shock waves were recomputed with the new strut locations and the corrected inviscid sidewall compression angle, and the results are given in figures 26, 27, and in tables III and IV. Compression in the side passage increased because of the stronger sidewall shock wave. Mach number, recovery, and aerodynamic contraction changed from 3.51, 87.9 percent, and 6.85 to 3.45, 86.2 percent, and 7.07, respectively. The center-passage throat is now divided between bays 10, 14, and 16. The predicted, inviscid, mass-weighted average Mach number, recovery, and aerodynamic contraction for the inlet changed from 3.44, 88 percent, and 7.3 to 3.37, 85 percent, and 7.6, respectively, for the modified design.

From the initial inlet tests, moving the cowl to the forward position (fig. 11) aggravated the choking situation next to the cowl; and the cowl at the most rearward position failed to help the design. Therefore, the center position of the cowl relative to the struts (fig. 25) was maintained for the new configuration. This movement of the cowl forward ($\Delta X/H = 0.213$) relative to the sidewalls increased the theoretical capture by 2 percent to 95 percent.

The center-passage-throat gap was increased when the struts were moved forward, although the inlet aerodynamic contraction increased slightly. The purpose of center strut 2 was to decrease again the center-passage-throat gap and to determine operating sensitivity of the inlets on this parameter.

Inlet Entrance Conditions

The foreplate static-pressure distribution and the Mach number profile for the flow entering the inlet are given in figure 28. The static pressure on the foreplate was above the free-stream value because no boundary-layer correction was applied; in addition, the boundary layer was thicker than predicted by the flat-plate calculations probably as a result of trip losses.

Wall Static-Pressure Distribution

Figures 29 to 41 present the results of the static-pressure data throughout the model, which are compared with the predicted results of figures 26 and 27, and of tables III and IV. The solid symbols are data from orifices used to check flow symmetry with the two passages on the right side of the model. The round symbols are data obtained with the initial configuration and the x-position of this data has been shifted to correspond to the new strut locations. These data indicate in figures 29 to 33 that there was reasonable agreement between predicted and measured operation of the side passage away from the cowl. Some additional compression was observed on the cowl of the modified configuration (fig. 32) that was probably due to corner interaction phenomenon and blunt leading-edge effects. The static-pressure distribution along the side-passage throat is summarized in figure 33. The symbols of figure 33(b) were obtained from orifices located on the side strut; and, because no static surveys were made in the side passage, a linear pressure distribution was assumed across the throat between the strut and sidewall for data analysis. The data from the sidewall throat (squares in fig. 33(a)) of the new configuration were neglected because these orifices were no longer at the throat but downstream of the struts.

Data in the center passage are given in figures 34 to 41. The center passage of the initial design also operated as anticipated near the top surface (fig. 34), unlike the evidence of too much compression on the side strut at $Y/H = 0.43$ (fig. 21 or 35). The cowl pressures were greatly reduced with the modified configuration (figs. 38 and 39), but no theoretical value is shown because of the complicated flow generated by the strut relief (fig. 6(b)). The hump in the center-passage-throat pressure distribution (fig. 40) is attributed to a corner effect from the top surface creating a relocation of the strut shock waves. In general the center-passage compression was slightly greater than that predicted because no boundary-layer correction was made on the struts. The diamond symbols of figures 33 to 41 correspond to the larger center strut. From figure 27 it is clear that the larger center strut reduces the gap between the struts and moves the throat downstream. None of the experimental measurements would be expected to be affected by the larger strut except wall statics on the side strut in the downstream portion of bay 16 (fig. 27). Figure 35 does, in fact, show a higher pressure on the most downstream

static orifice. In all other instances the larger strut had a negligible effect on the pressure measurements and it is concluded that the strut could be used successfully at Mach 6 to provide added contraction ratio. The static pressure on the small center strut (fig. 41) is lower because the orifices were located downstream of the strut shoulder. Appendix B presents pressure levels found within the model for a low-pressure test ($R = 3.3 \times 10^6$ per meter) and also an unstarted condition.

Oil-Flow Study

Although static pressures could be, and were, monitored to detect inlet starting, the most rapid and reliable method was to observe, by closed circuit television, the oil-flow pattern formed as the blackened oil droplets moved across the model's surface under the approaching flow. If the model did not start, all the oil on the sidewall moved in a curved path toward the bottom of the model. The only evidence of any shock wave was observed well upstream of the sidewall leading edges on the top surface. With the started inlet (fig. 42), the oil on the sidewall moves toward the throat along a line parallel to the line of intersection between the top surface and the sidewall. The exception was the oil near the bottom edge of the sidewall which followed the path of the flow spilled from the inlet. When the oil reached the high-pressure region formed by the side strut shock wave on the sidewall, it turned toward the cowl along a line approximately parallel to the swept leading edges. This oil accumulation line extended out the bottom of the inlet in front of the cowl with no interruptions, unlike the original strut configuration (fig. 24(a)).

Wall Surface Temperature and Boundary-Layer Analysis

The inlet did not reach an equilibrium temperature (fig. 43) because of a test time limit; however, the temperature was fairly uniform because of the high thermal conductivity of the aluminum. The dashed lines of figure 43 represent the wall temperature distribution selected for the boundary-layer analysis conducted with a modified version of the boundary-layer program of reference 13. This integral method computer program provided a viscous correction to the top-surface sidewalls and struts and reduced the total-pressure recovery from 86.2 percent to 54 percent for the side passage. The center-passage recovery changed from 84 percent to 73 percent, and the inlet average recovery was decreased from 85 percent to 67 percent. Because the surface of the cowl was small, it was neglected in the analysis, but the computed boundary-layer thickness for the rest of the inlet was nondimensionalized by the inlet height and plotted in figure 44. Transition was forced on the top surface 7.62 cm from the foreplate leading edge because of the trips. Natural transition was assumed at $s'/H \approx 0.8$ for the sidewall where the Reynolds number based on momentum thickness was equal to 1000. The sidewall boundary-layer trips had been removed prior to the modified configuration test when it was observed

that they had little effect on the side-passage experimental data. The boundary-layer flow over the struts was assumed to be turbulent from the swept leading edges.

Throat Surveys

Pitot pressure distributions for both the side and center passage are presented in figure 45, where W is the throat gap and Z' is equal to zero at the sidewall for the side-passage throat and equal to zero at the side strut for the center-passage throat. At the top of the model ($Y/H = 0.14$), the center throat data were obtained from the fixed tube, which was bent to a new Z' position for each test. The side-passage pitot profile ($Y/H = 0.17$) was obtained from the theoretical boundary-layer profile at $Z/W = 0.5$ and then assumed similarity with the profile at the adjacent side throat station of $Y/H = 0.26$. The solid symbols were not data points but depended on theoretical boundary layer calculations to extend each survey (dashed lines) to the wall static value for data reduction.

Data station $Y/H = 0.43$ was considered the station least influenced by top-surface and cowl flow effects, and surveys for the low Reynolds number test and the large center strut test are presented for this station in figures 45(g) and 45(h). The dashed lines in these two figures were taken from the standard tests (fig. 45(c)) and indicate that neither the large center strut nor the low Reynolds number tests had any significant effect on inlet operation.

The static survey data (fig. 46), obtained for the center passage, were faired to the wall values as indicated by the solid symbols. As mentioned earlier, when the measured static pressure was low and the total-pressure recovery exceeded the set upper limit (88 percent), a new static pressure based on the upper recovery limit was computed as illustrated by the dashed lines. To check the effect of this restriction, it was determined that a 10-percent increase in the limit increased the mass-weighted total-pressure recovery by approximately 3 percent. The straight lines are the static-pressure distributions assumed for the side passage and are based on neighboring wall static values. Other static-pressure data estimated from neighborhood statics for both the center- and side-passage throats near the top surface and cowl are given in figure 47. These additional estimated distributions made possible an analysis of a greater part of the throat flow area as defined by the pitot surveys.

The throat stations at $Y/H = 0.43$ were selected to be compared with the theoretical inviscid and boundary-layer calculations, and the resulting Mach number profiles are found in figure 48. The agreement is good for both passages; the dip next to the center-passage side strut may be caused by a probe-tip shock-wave interaction. The small hash marks indicate the pitot measurement closest to the sidewall or strut, and the remainder of the curve is the result of fairing the pitot pressure to the wall static-pressure level.

Throat Contour Maps

Contour maps of the results of compiling the throat pitot and static data are given in figures 49 to 52. Figures 49 and 50 are maps of the data input used to compute the Mach number and recovery maps of figures 51 and 52. Each map is shown with the width scale seven times the height, which makes the relief area next to the cowl (illustrated in fig. 51) appear to be out of proportion. The side-passage Mach number contours (fig. 51) are relatively symmetrical, and the prediction of boundary-layer thickness δ agrees well for the top and side surface. The top-surface boundary-layer thickness for the side passage had to agree because of the imposed boundary conditions. A nearly horizontal shock of about 8^{o} turning was generated by the cowl leading edge and is still near the cowl surface at the throat. This discrete shock is smeared by the computer programs interpolation process; and consequently a vertical Mach number gradient extending well beyond the predicted δ for the cowl is indicated. There is some rounding of the contours at the corners, but no flow separation is detected. The Mach number contours for the center passage are not as symmetrical because of the greater shock-wave concentration (fig. 51(b)); however, the Mach 3 (mass-weighted average equals 3.11) contour encloses the major portion of the total area. The mass-weighted total-pressure recovery recorded in figure 52 for both the throat passages was obtained by a computer program which averaged the values of approximately 1000 grid points, evenly spaced over the throat area. One case was also integrated by hand with negligible difference, and the results verified the computed results. The mass-weighted average recovery for the two passages is 59 percent when the losses on the foreplate are included and 61 percent when they are neglected. The central area of nearly constant total-pressure recovery in figure 52(b) is in part a result of the assumption of a total-pressure recovery limit in regions where the measured static-pressure level was too low (fig. 46); however, this assumption is considered to be justified on a phenomenological basis as well as by the similarity in shape between the measured and derived static-pressure profiles (fig. 46) and the reasonable agreement between theory and data (for example, fig. 48).

Capture Measurement Results

The procedure for analyzing the flow at the capture measurement station was identical to that of the inlet throats. At this station static survey data were taken at each pitot survey location. Each rake had seven probe tips. The data from which the Mach number and capture parameter $\rho v/\rho_1 v_1$ were derived for figures 53 and 54 are discussed in appendix C. The wakes of the three struts, which are about 7.5 cm upstream, are detectable in the Mach number map (fig. 53); in general, lines of constant Mach number are parallel to the sidewalls. Besides measuring inlet capture flow, the capture parameter (fig. 54) is a good indicator of flow gradient direction because it is less sensitive to static-pressure error than either Mach number or recovery. The average

value of $\rho v/\rho_1 v_1$ was 3.18 for the inlet at the capture measurement station; before capture flow could be calculated, however, some estimate of flow direction to determine cross-sectional area had to be made. The assumptions in figure 55 are: flow parallel to the top surface in the top-surface boundary layer; flow parallel to the cowl below the estimated location of the cowl shock wave; and flow down at 8° for the remainder of the area. This 8° downflow was the flow turning which was computed from the rise in static pressure due to the cowl shock. The flow was also assumed to be parallel to the sidewalls at this station. With these restrictions a capture of about 94 percent was computed for the inlet at Mach 6.

Performance Results

Because the struts were positioned within the inlet to provide two-thirds of the flow to the center passage, the captured flow (94 percent) was assumed to be split between the center and side passages in the ratio of 63/31. With this criteria the Mach 6 integrated performance parameters based on the tunnel free-stream conditions are tabulated for each passage, and the total inlet, in figure 56. The side-passage total-pressure recovery was lower than the center-passage recovery because of the relatively thicker boundary layer on the sidewalls. The average viscous total-pressure recovery was 0.59 compared with the predicted value of 0.67 for the initial inlet configuration, which did not include corner effects. The aerodynamic contraction ratio, which is based on the average throat Mach number and total pressure, is 7.0 instead of the design value of 7.3. This is because moving the struts upstream increased the throat width somewhat and because the measured total-pressure recovery was slightly lower. The larger center strut increased the contraction, but no data were taken at the new center-passage throat location. Included in figure 56 are curves from reference 7 predicting the inlet kinetic energy efficiency and capture over the flight Mach number range of 4 to 10. The Mach 6.0 inlet data have been entered in the figure for a flight Mach number of 7.6, which indicates a representative amount of vehicle forebody compression. The measured kinetic energy efficiency as determined by adiabatic process was 97.7 percent compared with the predicted tunnel value of 98.3 percent. The predicted curve is slightly high primarily because the cowl shock and viscous corner interactions were not included. The measured captured mass flow from in front of the inlet was 94 percent and matched the predicted value. The theory is expected to be less accurate at low Mach numbers because of the formation of detached shock waves. (See fig. 7.)

CONCLUDING REMARKS

As part of a Langley research and technology program focused on the development of a concept for an airframe-integrated scramjet engine (Langley Scramjet Module), a

detailed performance evaluation of the baseline inlet configuration at Mach 6 (simulated flight Mach number of approximately 7.6) has been conducted.

Mach number profiles in the inlet throat agreed reasonably well with the predicted results both for the inviscid flow and the boundary-layer calculations on the struts and sidewall. The mass-weighted average throat Mach number was 3.0 for the side passage and 3.1 for the center passage. This value compares with the inviscid values of 3.4 for each of the two passages. This additional compression was produced by the boundary layer, viscous corner interactions, and other end effects (for example, the internal cowl shock).

An adiabatic kinetic energy efficiency of 97.7 percent (0.59 recovery) was measured and compared with a predicted value of 98.3 percent (0.67), which does not include corner or end effects.

The average inlet aerodynamic contraction ratio was 7.0 instead of the predicted value of 7.3 because of the slightly lower total-pressure recovery. However, the results indicated that the contraction ratio can be increased by the use of a larger center strut, which operated successfully but no survey data were taken.

The measured inlet capture flow was 94 percent which agrees with the predicted value of 95 percent.

The difficulty and importance of properly positioning the shock waves in the throats of hypersonic inlets were demonstrated, but no adverse effects were noted as a result of the inlet ingesting a boundary layer on the top surface which simulated the boundary layer that would be ingested from the vehicle forebody. Overall, the inlet performance is well within the acceptable range for high engine performance.

Langley Research Center,
National Aeronautics and Space Administration,
Hampton, Va., April 22, 1975.

APPENDIX A

ANALYTICAL CALCULATIONS OF SWEPT SHOCK WAVES

Shock-wave systems for swept inlet configurations require a three-dimensional coordinate system to locate the shock waves correctly and to compute the flow properties. A selected two-dimensional coordinate system (the xz-plane of fig. 4) is also helpful in maintaining visual contact with the problem. Figure 57 illustrates the flow striking a swept wedge (surface AGFED) and helps to describe the development of the swept shock wave. Points A, H, I, and D lie in the xy-plane and points A, H, G, and B lie in the xz-plane. The flow strikes the leading edge at point A; and if the wedge were not swept, the flow would only be turned away from the xy-plane by angle δ_{xz} and would follow the path AC However, sweeping the wedge requires the flow to traverse the surface along AF, the flo also being turned away from the xz-plane as shown by angle δ_{xy} which is measured in the xy-plane. A swept shock wave (plane ABCD) attached to the leading edge is produce and is located with angle ϵ_{xz} which is measured in the xz-plane. As long as the wedge is assumed to be of infinite length, no end effects are encountered; if the wedge is assum to extend from the xz-plane, a reduced pressure, nonuniform flow region will exist in th proximity of the xz-plane. To eliminate this region, a fillet (AGFB) is added which extends out to the shock wave and fills the void left by the flow being turned away from the xz-plane.

A detailed discussion of the calculation procedure for obtaining the shock wave angle ϵ_{xz}, downflow δ_{xy}, and the flow properties behind the shock wave is given in reference 9, which describes the flow velocity being broken into vector components normal and tangential to the leading edge as shown in the sketch of figure 57. Although the velocity component tangential to the leading edge V_t remains unchanged $\left(V_{t,1} = V_{t,2}\right)$, the component perpendicular to the leading edge $V_{n,1}$ is reduced because it is turned by when it encounters the wedge. The vectors on the wedge surface, $V_{n,2}$, and $V_{t,2}$, are then combined to obtain the velocity and direction of flow on the wedge surface. One limitation to the procedure occurs when either the sweep angle or the wedge angle is too gre and the velocity component $V_{n,2}$ becomes subsonic. The shock wave may become detached from the wedge leading edge, as illustrated in the sketch, and the downstream flow is not uniform.

The Swept Shock-Wave System

To determine the shock-wave orientation and flow properties for a train of shock waves as illustrated in figure 58, additional steps are required to compute the shock an in the xz-plane. The computation must include the change in sweep angle and normal

turning angle as the flow crosses each successive shock wave and is turned further from the xz-plane.

A computer program has been written to compute an inviscid shock wave system for an inlet, when the inlet geometry and the initial Mach number are specified. Inlet geometry consists of plane wedges defined by sweep angle measured in the xy-plane and flow turning angles which are measured in the xz-plane. The shock-wave computational procedure is described for the three shock waves of figure 58. The second shock wave reflects from a plane of symmetry along line AB, strikes the sidewall (line BB), and is again reflected. The flow vectors behind the three shock waves are labeled V_2, V_3, and V_4, respectively. Because the flow angle with respect to the top surface (xz-plane) increases as the flow crosses each successive shock wave, a new fillet is required to eliminate three-dimensional end effects. The downstream fillets have complex orientations which are functions of Mach number; but, because they are small and considered to have minimal influence on the flow, these effects were neglected in the inlet design.

The sidewall is the generator of the first shock wave and may be considered to be a wedge or wing with sweep Λ_1 measured in the xy-plane, angle of attack δ_{xz} and dihedral as measured by the angle ϕ_1. The second shock wave is reflected from the plane of symmetry along line AA and is illustrated in detail in figure 59. For this reflected wave the computer program solves the problem of flow across a wedge or wing with sweep Λ_2, angle of attack $\delta_{(xz)'}$, and zero dihedral $(\phi_2 = 0)$. The reference axes are x', y', and z'. Because the flow has been turned toward the y-axis by the first shock wave, the sweep angle Λ_2 increased from the value of Λ_1. Once V_3 and the shock-wave angle $\epsilon_{(xz)'}$ have been computed, the shock wave is defined in the original xz-plane with angle ϵ_{xz}.

The third shock wave is illustrated in detail in figure 60, where the flow in front of the wave V_3 approaches a swept wedge (sidewall) which is in the x'', y'', and z'' coordinate system. The sweep angle is Λ_3. The angle of attack is $\delta_{(xz)''}$, and the dihedral is ϕ_3. The computer program treats this wave in the same manner as the first wave to compute $\epsilon_{(xz)''}$, and then defines the shock wave in the xz-plane with ϵ_{xz}.

The first and third shock waves are coded "type A" waves by the program whereas waves reflected from the plane of symmetry are coded "type B." The flow turning across each wave, measured in the xz-plane, can be put into the program, which means the strength of the reflected wave (type B) may be made different from the strength of the incident (type A) wave. To compute a shock train, the program always begins with a wave of type A, but the wave types do not have to alternate as the wave type of each shock wave is input to the program. When two type B waves are together, the nomenclature must be reversed and the second type B wave considered to be type A; then this new orientation is continued.

The program transfers all shock angles back to the xz-plane, where the angle is measured with respect to the flow direction in front of the wave for a type A wave; and the shock angle is measured with respect to the flow direction behind the wave for a type B wave. For a selected path of shock waves the sweep angle and dihedral for the first wave are input to the program. Subsequent sweep angles are internally computed, as is the dihedral, which is a function of the wave type. The number of shock waves in the train is input, and the program will continue to calculate across successive shock waves until shock-wave detachment occurs.

Because the flow properties in oblique shock-wave systems are path dependent, it may become necessary to iterate on pressure and flow direction, when waves of different turning strengths are encountered. Usually, however, the differences in shock-wave turning angles are small enough to insure that such effects can be neglected. If a correction is deemed to be necessary, an iteration can be done either by hand as the program computes across one wave at a time, or by following several flow paths with the program and averaging the results in the selected downstream flow bay.

The Computer Program

The program is written in FORTRAN IV and is adapted to the CDC 6600 computer located at the Langley Research Center, Hampton, Virginia. Although the primary purpose of the program is to compute flow properties for swept, weak, oblique shock-wave systems, additional versatility is available as shown in the input listing attached to this appendix. Either perfect-gas or thermally perfect-gas (gas with caloric imperfections as defined in ref. 14) problems may be computed by the listed program. Also operational, but not included in the program listing, is a subroutine for real-air calculations. This real-air subroutine uses either thermodynamic tables or equations of air in thermochemical equilibrum to compute flow properties behind shock waves.

For the thermally perfect gas, the local total properties are computed; and the specific heat ratio γ is computed as a function of static temperature from equation (180) of reference 14. The gas characteristics that are assumed for air and are used currently in the program are:

Molecular vibrational-energy constant, θ_v	3076 K
Perfect gas specific heat ratio, γ_p	1.4
Gas constant, $\overline{R}$	1545.31
Molecular weight	28.9644

Both weak and strong shock waves and perfect-gas Prandtl-Meyer expansion calculations are possible. For the expansion fan, the angles of the leading, trailing, and average waves are printed.

The dihedral ϕ is measured in a plane perpendicular to the wedge ridge line (line AG of fig. 57) and is defined in a parameter ψ where

$$\psi \equiv 1 - \frac{\cot \Lambda \tan \phi}{\sin \delta_{XZ}}$$

This parameter is defined in reference 9 as the ratio of the lengths of two line segments (DE/AD) and is used to define the location of the wedge leading edge with respect to the xy-plane. For the first wave of a shock train, the wedge dihedral ϕ does not have to be calculated because the leading edge is assumed to lie in the xy-plane and ψ has a value of zero. For a single-wave calculation the leading edge may be lifted out of the xy-plane; and when the dihedral is zero, ψ has a value of 1.

Program Input

Card 1 – FORMAT(4F10.4,2F5.2,2F10.4,5I1)

OC — Number of successive waves (Maximum = 20) (cols. 1 to 10)

XM — Initial Mach number, M (cols. 11 to 20)

ALP — Sweep angle, Λ, deg (cols. 21 to 30)

E1 — Wedge ridge angle, δ_{XZ}, deg (cols. 31 to 40)

DEADR — Dihedral parameter, $\psi \equiv 1 - \frac{\cot \Lambda \tan \phi}{\sin \delta_{XZ}}$ (cols. 41 to 45)

GAM — Specific heat ratio, γ, for perfect gas (cols. 46 to 50)

P1 — Static pressure, p_1, psia (cols. 51 to 60)
Set equal to 1.0 if left blank

T1 — Static temperature, T_1, ^{o}R (cols. 61 to 70)
Set equal to 500^{o} R if left blank

K1 — Type of gas calculation (col. 71)
- 0 perfect gas
- 2 thermally perfect gas

K2 — Flag indicates value of turning angle for each shock wave to follow on card 2 (col. 72)
- 0 all waves will have δ_{XZ} = E1
- 2 OC values of δ_{XZ} will follow on card 2

K3 — Flag indicates wave type for each shock wave to follow on card 3 (col. 73)
- 0 no card 3 necessary, waves will alternate Type A and Type B
- 2 OC wave types to follow on card 3

K4 Flag indicates strength of shock wave (col. 74)

- 0 weak shock waves
- 2 strong shock wave (limited to OC = 1)

K5 Special input case for dihedral (col. 75)

- 0 DEADR = Dihedral parameter, ψ
- 2 DEADR = Dihedral angle, deg

Card 2 – FORMAT (16F5.3). Do not use if K2 = 0

E11A Value of δ_{XZ} for each wave, deg
Expansion waves are entered as negative

Card 3 – FORMAT (16F5.3). Do not use if K3 = 0

TYPE Wave types

- 1. Type A
- -1. Type B

The first wave of a shock train must be type A.

A listing of the computer program follows:

```
      PROGRAM INLET    (INPUT,OUTPUT,TAPE5=INPUT,TAPE6=OUTPUT,TAPE8)                  100000
C                                                                                     200000
C           SWEPT SHOCK WAVE PROGRAM   A1991       BY C.A. TREXLER    10/22/74      300000
C                                                                                     400000
C     INPUT FOR CARD 1   FORMAT(4F10.4,2F5.2,2F10.4,5I1)                            500000
CNO.WAVES MACH NO.  SWEEP     DELTA     DIH   GAM   P1          T1        KKKKK     600000
C                   DEG.      DEG.      DE/AD       PSIA        DEG.R     12345     700000
C                                                                                     800000
C        SWEEP= SWEEP ANGLE MEASURED IN XY PLANE                                      900000
C        DELTA= FLOW TURNING ANGLE IN XZ PLANE                                        1000000
C        DIH=   DIHEDRAL PARAMETER (DE/AD)                                            1100000
C        GAM=   SPECIFIC HEAT RATIO      **  SET EQUAL TO 1.4 IF LEFT BLANK           1200000
C        P1=    STATIC PRESSURE, PSIA    **  SET EQUAL TO 1.0 IF LEFT BLANK           1300000
C        T1=    STAT TEMP., DEG R        **  SET EQUAL TO 500. IF LEFT BLANK          1400000
C        ADDITIONAL ENGLISH UNITS                                                     1500000
C                 DENSITY -- LBM/FT**3                                                1600000
C                 VELOCITY - FT/SEC                                                   1700000
C                 ENTHALPY - BTU/LBM                                                  1800000
C                                                                                     1900000
C    K1= BLANK, PERFECT GAS                ///   K1= 2, THERMALLY PERFECT GAS        2000000
C                 K1= 4, REAL AIR - EQUATIONS  (IF T1=0  P1= ALTITUDE, FT.)           2100000
C                 K1= 6, REAL AIR - TABLES     (IF T1=0  P1= ALTITUDE, FT.)           2200000
C    K2= BLANK, WAVE STRENGTHS NOT INPUT   ///   K2= 2, WAVE STRENGTHS INPUT          2300000
C    K3= BLANK, WAVE TYPES NOT INPUT       ///   K3= 2, WAVE TYPES INPUT             2400000
C    K4= BLANK, WEAK SHOCK WAVE            ///   K4= 2, STRONG SHOCK WAVE            2500000
C    K5= BLANK, DIH = DE/AD                ///   K5= 2, SPECIAL CASE                 2600000
C       *SPECIAL CASE* DIHEDRAL (DIH) DEFINED BY AN ANGLE MEASURED                    2700000
C                      IN A PLANE PERPENDICULAR TO RIDGE LINE.                        2800000
C                      SWEEP MEASURED WITH LEADING EDGE IN XY PLANE,                  2900000
C                      AND WEDGE AT ZERO ANGLE OF ATTACK.                             3000000
C                                                                                     3100000
C    INPUT FOR CARD 2   FORMAT(16F5.2)   NOT INPUT IF K2= BLANK                       3200000
CD(1) D(2) D(3) D(4).....D(NW)                                                        3300000
C        D=     FLOW TURNING ANGLE IN XZ PLANE (DEG)                                  3400000
C        NW=    NO. WAVES                                                             3500000
C                                                                                     3600000
C    INPUT FOR CARD 3   FORMAT(16F5.2)   NOT INPUT IF K3= BLANK                       3700000
CT(1) T(2) T(3) T(4).....T(NW)                                                        3800000
C        T=     WAVE TYPE ****** T= 1. FOR TYPE A    ///   T= -1. FOR TYPE B        3900000
C        NW=    NO. WAVES                                                             4000000
C                                                                                     4100000
000003      COMMON C,THV,GAMP,RBAR,XMWT,P1,T1,XM,XMNORM,TO                            4200000
```

```
00003          COMMON P2,T2,DELTN,GAM,XM2N,EPD,RHOR                                4300000
00003          COMMON EMAX,DELTNM,N,KGAS,MC                                        4400000
00003          COMMON EPDF,TPRA,AR,XM1T,XM2T                                       4500000
00003          COMMON NDEBUG                                                       4600000
00003          DIMENSION E11A(20), TYPE(20)                                        4700000
00003          C=3.14159265/180.0                                                  4800000
00005          GAM=1.400                                                           4900000
00006          THV=5537.0                                                          5000000
00007          GAMP=1.4                                                            5100000
00010          RBAR=1545.31                                                        5200000
00012          XMWT=28.9644                                                        5300000
00013          NDEBUG=0                                                            5400000
00014          JJ=0                                                                5500000
00016        5 READ(5,101)OC,XM,ALP,E1,DEADR,GAM,P1,T1,KGAS,NDELT,NORDER,N,KSP     5600000
00054      101 FORMAT(4F10.4,2F5.2,2F10.4,5I1)                                     5700000
00054          IF(EOF,5)6,70                                                       5800000
00057        6 STOP                                                                5900000
00061       70 CONTINUE                                                          6000000
00061          T0=0.                                                             6100000
00062          DIH=DEADR                                                         6200000
00063          NSTR=N                                                            6300000
00065          IF(GAM.LT..001)GAM=1.4                                            6400000
00071          IF(KGAS.GT.3)GO TO 400                                            6500000
00075          IF(P1.EQ.0.)P1=1.                                                 6600000
00077          IF(T1.EQ.0.)T1=500.                                               6700000
00101      400 CONTINUE                                                          6800000
00101          IF(KGAS.EQ.0)KGAS=0                                               6900000
00103          IF(NDELT.EQ.0)NDELT=0                                             7000000
00105          IF(NORDER.EQ.0)NORDER=0                                           7100000
00107          IF(NSTR.EQ.0)NSTR=0                                               7200000
00111          IF(KSP.EQ.0)KSP=0                                                 7300000
00113          IF(ALP.EQ.0.)GO TO 700                                            7400000
00114          IF(E1.EQ.0.)GO TO 700                                             7500000
00115          IF(KSP.EQ.2)DEADR=1.-TAN(DEADR*C)/(SIN(E1*C)*TAN(ALP*C))          7600000
00136      700 CONTINUE                                                          7700000
00136          XMINF=XM                                                          7800000
00137          PINFR=1.0                                                         7900000
00141          TINFR=1.0                                                         8000000
00141          RINFR=1.0                                                         8100000
00142          KKGAS=KGAS                                                        8200000
00144          IF(KGAS.EQ.0)KGAS=1                                               8300000
00146          MC=OC                                                             8400000
00150          DO 3 I=1,MC                                                       8500000
00152          E11A(I)=E1                                                        8600000
00154          TYPE(I)=0.                                                        8700000
00155        3 CONTINUE                                                          8800000
00157          IF(NDELT.EQ.0)GO TO 4                                             8900000
00160          READ(5,102)(E11A(NO),NO=1,MC)                                     9000000
00172          E1=E11A(1)                                                        9100000
00174      102 FORMAT(16F5.3)                                                    9200000
00174        4 CONTINUE                                                          9300000
00174          IF(NORDER.EQ.2)READ(5,102)(TYPE(NO),NO=1,MC)                      9400000
00211          OC=1.0                                                            9500000
00212          I=1                                                               9600000
00213          COI3PT=0.0                                                        9700000
00214          ARCA=1.0                                                          9800000
00215          TPRA=1.0                                                          9900000
00216          K=1                                                              10000000
00217          NN=0                                                             10100000
00220          JJ=JJ+1                                                          10200000
00222          ALI=ALP                                                          10300000
00224        7 CONTINUE                                                         10400000
00224          PRINT 106                                                        10500000
00230      106 FORMAT(1H1)                                                      10600000
00230          PRINT 126, JJ,K                                                  10700000
00240      126 FORMAT(1X,7HCASE NO,I3,10X,7HWAVE NO,I3,39X2HK1,2X2HK2,2X2HK3,2X 10800000
               1 2HK4,2X2HK5)                                                   10900000
00240          IF(NSTR.EQ.2.AND.E1.GE..01)PRINT 121,KKGAS,NDELT,NORDER,NSTR,KSP 11000000
00267          IF(NSTR.NE.2.AND.E1.GE.0.)PRINT 122,KKGAS,NDELT,NORDER,NSTR,KSP  11100000
00315          IF(NSTR.NE.2.AND.E1.LT.0.)PRINT 123,KKGAS,NDELT,NORDER,NSTR,KSP  11200000
00343          IF(NSTR.EQ.2.AND.E1.LT..01)PRINT 124,KKGAS,NDELT,NORDER,NSTR,KSP 11300000
00372          IF(KSP.EQ.2)PRINT 125, DIH                                       11400000
00402      121 FORMAT(45X14H(STRONG SHOCK),9X6I4)                               11500000
00402      122 FORMAT(45X14H(WEAK SHOCK)  ,9X6I4)                               11600000
00402      123 FORMAT(45X14H(EXPANSION)   ,9X6I4)                               11700000
00402      124 FORMAT(45X14H(NORMAL SHOCK),9X6I4)                               11800000
00402      125 FORMAT(70X26H(DIHEDRAL = SPECIAL CASE =,F7.3,5H DEG))            11900000
00402          J=1                                                              12000000
```

```
000403      600 CONTINUE                                                    12100000
000403          ALPH=ALP*C                                                  12200000
000405          E=E1*C                                                      12300000
000406          IF(ALPH.GT..001)GO TO 9                                     12400000
000412          XM1N=XM                                                     12500000
000412          XM1T=0.                                                     12600000
000413          XMNORM=XM                                                   12700000
000414          DELTN=E                                                     12800000
000416          DELTNP=DELTN                                                12900000
000420          GO TO 14                                                    13000000
000420        9 CONTINUE                                                    13100000
000420          ACOD=90.*C-ALPH                                             13200000
000423          CD=OC*TAN(ACOD)                                             13300000
000426          OD=OC/COS(ACOD)                                             13400000
000431          BC=OC*TAN(E)                                                13500000
000434          AD=BC                                                       13600000
000436          DE=AD*DEADR                                                 13700000
000437          PSI=ATAN2(DE,OD)                                            13800000
000442          OE=(OD**2+DE**2)**.5                                        13900000
000450          OB=(BC**2+OC**2)**.5                                        14000000
000456          AE=ABS(AD-DE)                                               14100000
000461          BE=(CD**2+AE**2)**.5                                        14200000
000467          THETA=ACOS(OC/OE)                                           14300000
000473          ABOE=ACOS((OB**2+OE**2-BE**2)/(2.0*OB*OE))                  14400000
000504          XM1T=XM*OC/OE                                               14500000
000507          XM1N=XM*SIN(THETA)                                          14600000
000512          IF(XM1N-1.0)203,203,8                                       14700000
000515        8 CONTINUE                                                    14800000
000515          OG=OC*OC/OE                                                 14900000
000517          CG=OC*SIN(THETA)                                            15000000
000522          HG=OG*TAN(ABOE)                                             15100000
000525          OH=(HG**2+OG**2)**.5                                        15200000
000532          HC=(OH**2+OC**2-2.0*OH*OC*COS(E))**.5                       15300000
000544          DELTN=ACOS((HG**2+CG**2-HC**2)/(2.0*HG*CG))                 15400000
000554          IF(E11A(K).LT.0.)DELTN=-DELTN                               15500000
000560          DELTNP=DELTN                                                15600000
000561          XMNORM=XM1N                                                 15700000
000563       14 CONTINUE                                                    15800000
000563          GR=(GAM+1.)/(GAM-1.)                                        15900000
000567          EMAX=SQRT((GAM+1.)*(1.+(GAM-1.)/2.*XM1N**2+(GAM+1.)/16.*XM1N**4))  16000000
000605          EMAX=(1./(GAM*XM1N**2))*((GAM+1.)/4.*XM1N**2-1.+EMAX)       16100000
000620          EMAX=ASIN(SQRT(EMAX))                                       16200000
000624          DELTNM =(GAM+1.)*XM1N**2/(2.*(XM1N**2* (SIN(EMAX)**2)-1.))  16300000
000635          DELTNM=(DELTNM-1.)*TAN(EMAX)                                16400000
000642          DELTNM=ATAN(1./DELTNM)                                      16500000
000645          DLIMIT=DELTNM+10.*C                                         16600000
000650          IF(XM1N.LT.2.)DLIMIT=DELTNM+2.*C                            16700000
000656          IF(DLIMIT.GT.DELTN)GO TO 15                                 16800000
000662          KGAS=1                                                      16900000
000663       15 CONTINUE                                                    17000000
000663          IF(KGAS-1)10,10,11                                          17100000
000666       11 CONTINUE                                                    17200000
000666          IF(KGAS.GT.3)CALL RAIR(ZFT,NSTR)                            17300000
000673          IF(KGAS.GT.3)GO TO 16                                       17400000
000677          CALL REALG (NSTR)                                           17500000
000700          IF(N.LT.100)GO TO 16                                        17600000
000703          KGAS=1                                                      17700000
000703          IF(DELTNM.LT.DELTN)GO TO 10                                 17800000
000706          IF(N.EQ.100)GO TO 5                                         17900000
000707       16 CONTINUE                                                    18000000
000707          TR=T2/T1                                                    18100000
000711          PR1=P2/P1                                                   18200000
000713          RR=RHOR                                                     18300000
000714          EP=EPD*C                                                    18400000
000716          EPF=EPDF*C                                                  18500000
000717          IF(ALPH.LT..001)GO TO 21                                    18600000
000722       10 CONTINUE                                                    18700000
000722          IF(KGAS-1)12,12,25                                          18800000
000725       12 CALL PGAS                                                   18900000
000726          IF(N.EQ.100)GO TO 5                                         19000000
000730          TR=T2/T1                                                    19100000
000732          PR1=P2/P1                                                   19200000
000734          RR=RHOR                                                     19300000
000735          EP=EPD*C                                                    19400000
000737          EPF=EPDF*C                                                  19500000
000740          IF(ALPH.GT..001)GO TO 13                                    19600000
000744       21 CONTINUE                                                    19700000
000744          ARCA=ARCA*AR                                                19800000
```

```
000746          DELTN1=DELTNP/C                                                 19900000
000747          DELTM=DELTNM/C                                                  20000000
000751          EMAX1=EMAX/C                                                    20100000
000752          EEF=1.-(2./(GAM-1.)*((1./TPRA)**((GAM-1.)/GAM)-1.)/XMINF**2)    20200000
000766          PINFR=PINFR*PR1                                                 20300000
000770          TINFR=TINFR*TR                                                  20400000
000771          RINFR=RINFR*RR                                                  20500000
000773          PRINT 115                                                       20600000
000777      115 FORMAT(// *          SUMMARY OF FLOW PROPERTIES ACROSS UNSWEPT WEDGE  20700000
                1  *)                                                          20800000
000777          PRINT 17, XM,ALP,DELTN1,EPD,P1,T1                               20900000
001017       17 FORMAT(/1X,3HM1=,F8.3,7X6HSWEEP=,F7.3,7X6HDELTA=,F7.3,12X4HEPS=,  21000000
               1 F7.3,7X3HP1=,F8.4,6X3HT1=,F8.2)                                21100000
001017          PRINT 19, XM2N,PINFR,RINFR,TINFR,GAM                            21200000
001035       19 FORMAT(/1X,3HM2=,F8.3,6X,7HP/PINF=,F8.4,5X7HR/RINF=,F8.4,9X7HT/TIN  21300000
               1F=,F8.4,5X4HGAM=,F7.4)                                          21400000
001035          PRINT 120,TPRA,EEF                                              21500000
001045      120 FORMAT(/1X,22HRECOVERY (PT/PTINF) =,F8.4,7X20HKINETIC ENERGY EFF.  21600000
               1=,F9.5)                                                         21700000
001045          PRINT 18,ARCA,DELTM,EMAX1                                       21800000
001057       18 FORMAT(/1X,22HCONTRACTION (AINF/A) =, F8.4,27X10HDELTA MAX=,F8.4,  21900000
               14X8HEPS MAX=,F8.4)                                              22000000
001057          IF(DELTN1.GT.DELTM)PRINT 119                                    22100000
001065      119 FORMAT(60X28H***SHOCK WAVE IS DETACHED***)                      22200000
001065          IF(DELTN.GT.DELTNM)GO TO 5                                      22300000
001071          I=I+1                                                           22400000
001072          IF(MC-I)5,20,20                                                 22500000
001074       20 CONTINUE                                                        22600000
001074          K=K+1                                                           22700000
001076          P1=P2                                                           22800000
001077          T1=T2                                                           22900000
001100          XM=XM2N                                                         23000000
001102          E1=E11A(K)                                                      23100000
001104          GO TO 7                                                         23200000
001104       13 CONTINUE                                                        23300000
001104          XM2T= XM1T*(1./TR)**.5                                          23400000
001112       25 CONTINUE                                                        23500000
001112          XM2=(XM2T**2+XM2N**2)**.5                                       23600000
001120          ARC=AR*XMNORM*XM2/(XM2N*XM)                                     23700000
001124          ARCA=ARCA*ARC                                                   23800000
001126          ACHG=ACOS((HC**2+HG**2-CG**2)/(2.*HC*HG))                       23900000
001136          AJHG=180.*C-ACHG                                                24000000
001141          IF(E11A(K).LT.0.)AJHG=ACHG                                      24100000
001145          AJGH = EP - DELTN                                               24200000
001147          AHJG=180.*C-(AJHG+AJGH)                                         24300000
001153          GJ=HG*(SIN(AJHG)/SIN(AHJG))                                     24400000
001161          HJ=HG*(SIN(AJGH)/SIN(AHJG))                                     24500000
001167          CJ=HC+HJ                                                        24600000
001171          IF(E11A(K).LT.0.)CJ=HJ-HC                                       24700000
001175          OJ=(GJ**2+OG**2)**.5                                            24800000
001203          EPXZP=ACOS((OJ**2+OC**2-CJ**2)/(2.*OJ*OC))                      24900000
001214          EXZPF=EPXZP                                                     25000000
001216          EXZAVG=0.0                                                      25100000
001216          IF(E11A(K))505,500,500                                          25200000
001221      505 AJGHF=EPF                                                       25300000
001222          AHJGF=180.*C-(AJHG+AJGHF)                                       25400000
001226          GJF=HG*(SIN(ACHG)/SIN(AHJGF))                                   25500000
001234          HJF=HG*(SIN(AJGHF)/SIN(AHJGF))                                  25600000
001242          CJF=HJF-HC                                                      25700000
001244          IF((EPF+DELTN).LT.0.)CJF=HC-HJF                                 25800000
001251          OJF=(GJF**2+OG**2)**.5                                          25900000
001257          EXZPF =ACOS((OJF**2+OC**2-CJF**2)/(2.*OJF*OC))                  26000000
001270          IF((EPF+DELTN).LE.0.)EXZPF=-EXZPF                               26100000
001274          EXZAVG= EPXZP-.5*(EPXZP- EXZPF)                                 26200000
001300      500 CONTINUE                                                        26300000
001300      300 FORMAT(10F10.5)                                                 26400000
001300          AEOI1P=ATAN2(XM2N,XM2T)                                         26500000
001302          ABOI1P=ABOE-AEOI1P                                              26600000
001304          ABEO=ASIN(OB*SIN(ABOE)/BE)                                      26700000
001312          AOBE=180.*C-(ABEO+ABOE)                                         26800000
001316          ABI1PO=180.*C-(AOBE+ABOI1P)                                     26900000
001321          IF(ABOI1P)304,303,303                                           27000000
001322      304 ABI1PO=AOBE- ABS(ABOI1P)                                        27100000
001325      303 CONTINUE                                                        27200000
001325          BI1P=OB*(SIN(ABOI1P)/SIN(ABI1PO))                               27300000
001333          AABE=ATAN(AE/CD)                                                27400000
001337          T1PI2P= BI1P*COS(AABE)                                          27500000
001342          ACOI3P = ATAN(T1PI2P/OC)                                        27600000
001346          AFOC= ATAN2(DE,OC)                                              27700000
```

```
001351          ABOF= ABS(E-AFOC)                                                27800000
001354          BI2P=(BI1P**2-T1PI2P**2)**.5                                     27900000
001362          IF(DEADR-1.)200,200,201                                          28000000
001365      200 CI2P = BC -BI2P                                                  28100000
001367          ACOI2P=ATAN(CI2P/OC)                                             28200000
001374          GO TO 203                                                        28300000
001374      201 CI2P = BC +BI2P                                                  28400000
001376          ACOI2P=ATAN(CI2P/OC)                                             28500000
001403      203 CONTINUE                                                         28600000
001403          EQ=EP/C                                                          28700000
001405          THET1=THETA/C                                                    28800000
001406          DELTN1=DELTN/C                                                   28900000
001410          EPX1=EPXZP/C                                                     29000000
001411          EPX1F=EXZPF/C                                                    29100000
001413          EXZ1AV=EXZAVG/C                                                  29200000
001415          COI3P= ACOI3P/C                                                  29300000
001416          OUT2=COI3P                                                       29400000
001420          COI2P=ACOI2P/C                                                   29500000
001421          EOI1P= AEOI1P/C                                                  29600000
001423          AABE1=AABE/C                                                     29700000
001425          DELTM=DELTNM/C                                                   29800000
001426          EMAX1=EMAX/C                                                     29900000
001430          ABOE1=ABOE/C                                                     30000000
001431          ABEO1=ABEO/C                                                     30100000
001433          DELTN1=DELTNP/C                                                  30200000
001435          EEF=1.-(2./(GAM-1.)*((1./TPRA)**((GAM-1.)/GAM)-1.)/XMINF**2)     30300000
001451          PINFR=PINFR*PR1                                                  30400000
001453          TINFR=TINFR*TR                                                   30500000
001454          RINFR=RINFR*RR                                                   30600000
001456          PRINT 114                                                        30700000
001462      114 FORMAT(// *        FLOW PROPERTIES REFERENCED TO SWEPT WEDGE*)   30800000
001462          PRINT 110                                                        30900000
001466      110 FORMAT(/4X,3HM1N,7X3HM1T,7X3HM2N,7X3HM2T,8X2HM2,6X6HP/PINF,5X6HR/R  31000000
               1INF,5X6HT/TINF,6X3HGAM)                                         31100000
001466          PRINT 111, XM1N,XM1T,XM2N,XM2T,XM2,PINFR,RINFR,TINFR,GAM         31200000
001514      111 FORMAT(1X,9F10.5)                                                31300000
001514          PRINT 112                                                        31400000
001520      112 FORMAT(/3X6HDELTAN,5X4HEPSN,6X4HAJOC,5X6HACOI2P,4X6HACOI3P,      31500000
               14X6HAEOI1P,5X5HTHETA,4X10HDELTAN MAX,3X8HEPSN MAX,3X1HN)        31600000
001520          PRINT 113, DELTN1,EQ,EPX1,COI2P,COI3P,EOI1P,THET1,DELTM,EMAX1,N  31700000
001550      113 FORMAT(1X,9F10.5,I7)                                             31800000
001550          IF(DELTN1.GT.DELTM)PRINT 119                                     31900001
001556          PRINT 109, XM,ALP,E1,DEADR,P1,T1                                 32000000
001576      109 FORMAT(                    /1X,3HM1=,F8.3, 7X6HSWEEP=,F8.3, 7X12HR  32100000
               1IDGE ANGLE=,F8.3,7X6HDE/AD=,F6.3,7X3HP1=,F8.4,7X3HT1=,F8.2)     32200000
001576          PRINT 19, XM2, PINFR,RINFR,TINFR,GAM                             32300000
001614          PRINT 120,TPRA,EEF                                               32400000
001624          PRINT 108, ARCA,EPX1,COI3P                                       32500000
001636      108 FORMAT(/1X,22HCONTRACTION (AINF/A) =,  F8.4,7X4HEPS=,F8.3,7X11HCRO  32600000
               1SS FLOW=,F8.3)                                                  32700000
001636          IF(DELTN1.LT.0.)PRINT 508,EPX1,EPX1F,EXZ1AV                      32800000
001651      508 FORMAT(/2X,14HEXPANSION FAN*,9X,10HLEAD WAVE=,F8.4,5X11HFINAL WAVE  32900000
               1=,F8.4,5X9HAVG WAVE=,F8.4)                                      33000000
001651          PRINT 118                                                        33100000
001655      118 FORMAT(// *        FLOW PROPERTIES REFERENCED TO INITIAL XYZ COORDI  33200000
               1NATE SYSTEM*)                                                   33300000
001655          WR=ARCA*SIN((90.-ALI-COI3P)*C)/COS(ALI*C)                        33400000
001671          IF(K.EQ.1)PRINT 117,XM2,E11A(K),EPX1                             33500000
001705      117 FORMAT(/1X3HM2=,F8.3,8X9HDELTA XZ=,F8.3,10X7HEPS XZ=,F8.3)       33600000
001705          IF(K.EQ.1.AND.DELTN1.LT.0.)PRINT 508,EPX1,EPX1F,EXZ1AV           33700000
001727          IF(K.EQ.1)PRINT 116,COI3P,WR                                     33800000
001741      116 FORMAT(/1X29HTOTAL CROSS FLOW (DELTA XY)=,F8.3,10X               33900000
               118HGAP RATIO (W1/W2)=,F8.3)                                     34000000
001741          IF(MC.EQ.1)GO TO 5                                               34100000
001743      274 IF(NN)276,606,275                                                34200000
001745      606 IF(TYPE(K+1))601,601,602                                         34300000
001750      276 CONTINUE                                                         34400000
001750          XJOC2=EPXZP                                                      34500000
001751          ACOI2P=COI2P*C                                                   34600000
001753          COI3P1=COI3PT*C                                                  34700000
001755          ALP1=(90.-ALI)*C                                                 34800000
001757          EXZP = TAN(XJOC2-ACOI2P)*TAN(ALP1)/(COS(COI3P1)*(TAN(ALP1)-TAN(COI  34900000
               13P1)))                                                          35000000
002000          EXZP=ATAN(EXZP)/C                                                35100000
002003          XJMUP = EXZPF-ACOI2P                                             35200000
002005          IF(EXZPF.LT.0.)XJMUP=EXZPF                                       35300000
002010          EXZPF=TAN(   XJMUP      )*TAN(ALP1)/(COS(COI3P1)*(TAN(ALP1)-TAN(COI3  35400000
               1P1)))                                                           35500000
```

```
002027          EXZPF=ATAN(EXZPF)/C                                          35600000
002032          EXZAVG=EXZP-.5*(EXZP-EXZPF)                                  35700000
002036          OUT2= (ABOE-AEOI1P)/C                                        35800000
002041          OUTT=COI3PT+OUT2                                             35900000
002043          WR = ARCA*SIN((90.-AL1-OUTT)*C)/COS(AL1*C)                   36000000
002057          PRINT 117, XM2,E11A(K),EXZP                                  36100000
002070          IF(DELTN1.LT.0.)PRINT 508,EXZP,EXZPF,EXZAVG                  36200000
002103          PRINT 116, OUTT,WR                                           36300000
002113          IF(DELTN.GT.DELTNM)GO TO 5                                   36400000
002117          I=I+1                                                        36500000
002120          IF(MC-I)5,5,604                                              36600000
002122      604 IF(TYPE(K+1))601,602,602                                     36700000
002125      275 CONTINUE                                                     36800000
002125          OFT=COI3PT*C                                                 36900000
002127          XJOC3=EPXZP                                                  37000000
002130          CAP1=(90.-AL1)*C                                             37100000
002133          EXZP=TAN(CAP1)*TAN(OFT)*TAN(XJOC3)/(SIN(OFT)*(TAN(CAP1)-TAN(OFT)))  37200000
002155          EXZP=ATAN(EXZP)/C                                            37300000
002160          EXZPF=TAN(CAP1)*TAN(OFT)*TAN( EXZPF)/(SIN(OFT)*(TAN(CAP1)-TAN(OFT)  37400000
               1))                                                          37500000
002202          EXZPF = ATAN(EXZPF)/C                                        37600000
002205          EXZAVG= EXZP - .5*(EXZP-EXZPF)                               37700000
002211          OUTF=COI3PT+COI3P                                            37800000
002213          WR = ARCA*SIN((90.-AL1-OUTF)*C)/COS(AL1*C)                   37900000
002230          PRINT 117, XM2,E11A(K),EXZP                                  38000000
002241          IF(DELTN1.LT.0.)PRINT 508,EXZP,EXZPF,EXZAVG                  38100000
002254          PRINT 116, OUTF,WR                                           38200000
002264          IF(DELTN.GT.DELTNM)GO TO 5                                   38300000
002270          I=I+1                                                        38400000
002271          IF(MC-I)5,5,605                                              38500000
002273      605 IF(TYPE(K+1))601,601,602                                     38600000
002275      601 CONTINUE                                                     38700000
002275          NN=-1                                                        38800000
002276          COI3PT=COI3PT+COI3P                                          38900000
002300          AIOI3P=ATAN(TAN(COI2P*C)*COS(COI3PT*C))/C                    39000000
002313          ALP=ATAN((TAN((90.-AL1-COI3PT)*C))/COS(AIOI3P*C))            39100000
002330          ALP=90.-ALP/C                                                39200000
002333          K=K+1                                                        39300000
002335          E11=E11A(K-1)                                                39400000
002336          TE1=(TAN(E11*C)-TAN(E11*C-E11A(K)*C))*TAN(AIOI3P*C)/TAN(E11*C)  39500000
002363          E1=ATAN(TE1)/C                                               39600000
002366          XM=XM2                                                       39700000
002370          T1=T2                                                        39800000
002371          P1=P2                                                        39900000
002373          DEADR=ABS(TAN(AIOI3P*C)/TAN(E1*C))                           40000000
002405          GO TO 7                                                      40100000
002405      602 CONTINUE                                                     40200000
002405          NN=1                                                         40300000
002406          COI3PT=COI3PT+OUT2                                           40400000
002410          ALP=AL1+COI3PT                                               40500000
002411          SIGMA=(90.-AL1)*C                                            40600000
002414          SIGMA1=COI3PT*C                                              40700000
002415          K=K+1                                                        40800000
002417          E12 = E11A(K)                                                40900000
002420          E1=ATAN(TAN(E12*C)*(TAN(SIGMA)-TAN(SIGMA1))*SIN(SIGMA1)/(TAN(SIGMA  41000000
               1)*TAN(SIGMA1)))                                             41100000
002446          E1=E1/C                                                      41200000
002450          XM=XM2                                                       41300000
002452          T1=T2                                                        41400000
002453          P1=P2                                                        41500000
002455          DEADR=0.0                                                    41600000
002456          GO TO 7                                                      41700000
002456          END                                                          41800000
                SUBROUTINE REALG (NSTR)                                      41900000
          C   THIS SUBROUTINE COMPUTES WAVE PROPERTIES FOR A THERMALLY PERFECT GAS  42000000
000003          COMMON C,THV,GAMP,RBAR,XMWT,P1,T1,XM,XMNORM,TO               42100000
000003          COMMON P2,T2,DELTN,GAM,XM2N,EPD,RHOR                         42200000
000003          COMMON EMAX,DELTNM,N,KGAS,MC                                 42300000
000003          COMMON EPDF,TPRA,AR,XM1T,XM2T                                42400000
000003          COMMON NDEBUG                                                42500000
000003          DIMENSION P(4),T(4),PJ(4)                                    42600000
000003          FGA(T )=1.+(GAMP-1.)/(1.+(GAMP-1.)*(THETA/T)**2*EXP(THETA/T)/(  42700000
               2EXP(THETA/T)-1.)**2)                                        42800000
000035          FW(T2)=A**2-Q*(A**2-4.*R*T2)**.5-2.*R*T2-DD+GG*R*(T2-T1)+4.*R*  42900000
               1THETA*(1./(EXP(THETA/T2)-1.)-E1)                            43000000
000075          EPDF=0.                                                      43100000
000076          EPDAVG=0.                                                    43200000
000076          GC=32.1741                                                   43300000
000100          GG=4.0*GAMP/(GAMP-1.)                                        43400000
```

```
000103          R=GC*PBAR/XMWT                                                  43500000
000106          R1=P1*144./(RBAR/XMWT*T1)                                       43600000
000112          THETA=THV                                                       43700000
000114          XM1=XMNORM                                                      43800000
000115          ARA=1.0                                                         43900000
000117          J=1                                                             44000000
000120          I=N                                                             44100000
000122   117    CONTINUE                                                        44200000
000122          DELT=DELTN                                                      44300000
000123          IF(DELTN.LT.0.)PRINT 118                                        44400000
000132      118 FORMAT(1X27H***THERMALLY PERFECT GAS***,14X16HAPPROX. SOLUTION) 44500000
000132          IF(DELTN.GE.0.)PRINT 6                                          44600000
000141        6 FORMAT(1X27H***THERMALLY PERFECT GAS***)                        44700000
000141          PRINT 9                                                         44800000
000145        9 FORMAT(38X16HIN FRONT OF WAVE)                                  44900000
000145          CALL TOTAL (P1,T1,XM,TO,PT1)                                    45000000
000151          GAM1=FGA(T1)                                                    45100000
000154          XM1N=XM1                                                        45200000
000156          GAM=GAM1                                                        45300000
000157          SOUND =(R*T1*GAM1)**.5                                          45400000
000165          IF(DELTN.LT.0.) GO TO 446                                       45500000
000167          EMAX=SQRT((GAM+1.)*(1.+(GAM-1.)/2.*XM1N**2+(GAM+1.)/16.*XM1N**4)) 45600000
000204          EMAX=(1./(GAM*XM1N**2))*((GAM+1.)/4.*XM1N**2-1.+EMAX)           45700000
000217          EMAX=ASIN(SQRT(EMAX))                                           45800000
000223          DELTNM =(GAM+1.)*XM1N**2/(2.*(XM1N**2* (SIN(EMAX)**2)-1.))      45900000
000234          DELTNM=(DELTNM-1.)*TAN(EMAX)                                    46000000
000241          DELTNM=ATAN(1./DELTNM)                                          46100000
000244          V1=XM1*SOUND                                                    46200000
000246          PIE=3.141592654                                                 46300000
000250          N2=4                                                            46400000
000251          IF(I.EQ.2)N2=0                                                  46500000
000255          IF(MC.GT.1)N2=4                                                 46600000
000261          DEL2=DELTN                                                      46700000
000262          IF(DELTNM.LT.DELTN)DEL2=DELTNM                                  46800000
000266          GAN=GAM1                                                        46900000
000267          XM12=XM1**2                                                     47000000
000271          XM14=XM1**4                                                     47100000
000272          BB=-(XM12+2.)/XM12-GAN*SIN(DEL2)**2                             47200000
000301          CC=(2.*XM12+1)/XM14+((GAN+1.)**2/4.+(GAN-1.)/XM12)*SIN(DEL2)**2 47300000
000320          D2=-COS(DEL2)**2/XM14                                           47400000
000324          EX=      (9.*BB*CC/2.-BB**3-27.*D2/2.)/(BB**2-3.*CC)**1.5       47500000
000344          IF(EX.GT.1)EX=1.                                                47600000
000352          IF(EX.LT.-1)EX=-1                                               47700000
000357          EE=ACOS(EX)                                                     47800000
000361          FF=COS((EE+N2*PIE)/3.)                                          47900000
000370          G2=(-BB/3.+(2*(BB**2-3.*CC)**.5/3.)*FF)**.5                     48000000
000406          EPS=ASIN(G2)                                                    48100000
000410          IF(NSTR.EQ.2.AND.DEL2.LT..01)GO TO 1000                         48200000
000423          GO TO 1001                                                      48300000
000423     1000 EPS=90.*C                                                       48400000
000425          GO TO 1004                                                      48500000
000426     1001 CONTINUE                                                        48600000
000426          RR=TAN(EPS)/TAN(EPS-DEL2)                                       48700000
000435          PR1=1.+GAN* XM1**2*SIN(EPS)**2*(1.-1./RR)                       48800000
000447     1004 CONTINUE                                                        48900000
000447          EP1=EPS/C                                                       49000000
000451          M=1                                                             49100000
000452          N=1                                                             49200000
000453          NN=1                                                            49300000
000454          E1=1./(EXP(THETA/T1)-1.)                                        49400000
000462          NT=1                                                            49500000
000464   111    CONTINUE                                                        49600000
000464          KK=-1                                                           49700000
000465          U1=V1*SIN(EPS)                                                  49800000
000470          A=U1+R*T1/U1                                                    49900000
000474          Q=A                                                             50000000
000475          DD=2.0*U1**2                                                    50100000
000477          HH=XM1**2*(SIN(EPS))**2                                         50200000
000503          HK=(2.*GAM1*HH-(GAM1-1.))*((GAM1-1.)*HH+2.)/((GAM1+1.)**2*HH)   50300000
000516          STR=((-.2/9000.)*TO+1.0)*HK                                     50400000
000523          TMAX=A**2/(4.*R)-.000001                                        50500000
000530          IF(N.EQ.1.AND.NDEBUG.GT.0)PRINT 223                             50600000
000544      223 FORMAT(/)                                                       50700000
000544          IF(NDEBUG.EQ.0)GO TO 120                                        50800000
000545          PRINT 222, TMAX,A,R,U1,T1,V1,EP1,PR1,PR2                        50900000
000573      222 FORMAT(1X9HSUB REALG,9F12.4)                                    51000000
000573      120 CONTINUE                                                        51100000
000573          WMAX=FW(TMAX)                                                   51200000
```

```
000576          IF(WMAX)140,10,143                                      51300000
000600      140 Q=-Q                                                    51400000
000601          NT=2                                                    51500000
000602          T21=TMAX                                                51600000
000603          T22=T21                                                 51700000
000605          W1=FW(TMAX)                                             51800000
000610      703 T22=T22-.1*(T21-T1)                                     51900000
000614          W2=FW(T22)                                              52000000
000616          NT=NT+1                                                 52100000
000620          IF(NT-12)803,803,802                                    52200000
000622      803 IF(W2)703,19,707                                        52300000
000624      707 T21=T22+.1*(T21-T1)                                     52400000
000630          W1=FW(T21)                                              52500000
000632          T21=-W1/(W2-W1)*(T22-T21)+T21                           52600000
000640          IF(T21-TMAX)706,706,708                                 52700000
000642      708 T21=TMAX-.00001                                         52800000
000644      706 CONTINUE                                                52900000
000644          W1=FW(T21)                                              53000000
000646          T22=T21-.01*(T21-T1)                                    53100000
000652          W2=FW(T22)                                              53200000
000655          T21=-W1/(W2-W1)*(T22-T21)+T21                           53300000
000663          IF(T21-TMAX)712,711,711                                 53400000
000665      711 T21=TMAX                                                53500000
000667      712 CONTINUE                                                53600000
000667          W1=FW(T21)                                              53700000
000672          GO TO 802                                               53800000
000672       19 CONTINUE                                                53900000
000672          W1=W2                                                   54000000
000673          T21=T22                                                 54100000
000675          GO TO 802                                               54200000
000676      143 CONTINUE                                                54300000
000676          T21=STR*T1+40.                                          54400000
000701          IF(T21-TMAX)300,300,301                                 54500000
000704      301 T21=TMAX                                                54600000
000706      300 T22=T21-10.*XM1                                         54700000
000711          W1=FW(T21)                                              54800000
000713          W2=FW(T22)                                              54900000
000716          T21=-W1/(W2-W1)*(T22-T21)+T21                           55000000
000724          IF(T21-TMAX)11,11,14                                    55100000
000726       14 T21=TMAX                                                55200000
000730       11 T22=T21-2.*XM1                                          55300000
000733          W1=FW(T21)                                              55400000
000735          W2=FW(T22)                                              55500000
000740          T21=-W1/(W2-W1)*(T22-T21)+T21                           55600000
000746          IF(T21-TMAX)141,141,305                                 55700000
000750      305 T21=TMAX                                                55800000
000752      141 T22=T21-.8*XM1                                          55900000
000755          W1=FW(T21)                                              56000000
000757          W2=FW(T22)                                              56100000
000762          T21=-W1/(W2-W1)*(T22-T21)+T21                           56200000
000770          IF(T21-TMAX)12,12,142                                   56300000
000772      142 T21=TMAX                                                56400000
000774       12 T22=T21-.1*XM1                                          56500000
000777          W1=FW(T21)                                              56600000
001001          W2=FW(T22)                                              56700000
001004          T21=-W1/(W2-W1)*(T22-T21)+T21                           56800000
001012          IF(T21-TMAX)15,15,10                                    56900000
001014       10 T21=TMAX                                                57000000
001016   15     CONTINUE                                                57100000
001016          W1=FW(T21)                                              57200000
001021      802 CONTINUE                                                57300000
001021          XNT=NT                                                  57400000
001022          XNN=NN                                                  57500000
001024          TRR=T21/T1                                              57600000
001026          T2=T21                                                  57700000
001027       13 CONTINUE                                                57800000
001027          GAM2=FGA(T2)                                            57900000
001031          XM2=2.0*T1/(GAM2*T2)*((GAM1*XM1**2/2.0)+(GAMP/(GAMP-1.0))*(1.0-  58000000
                2T2/T1)+THETA/T1*(1./(EXP(THETA/T1)-1.0)-1./(EXP(THETA/T2)-1.0)))  58100000
001067          IF(XM2)28,28,307                                        58200000
001072      307 CONTINUE                                                58300000
001072          XM2=XM2**.5                                             58400000
001076          PR2=1./2.*((1.+GAM2*XM2**2)-T1/T2*(1.+GAM1*XM1**2)+(((((1.+GAM2*  58500000
                2XM2**2)-T1/T2*(1.+GAM1*XM1**2))**2)+4.*T1/T2)**.5))            58600000
001123          PR2=1./PR2                                              58700000
001125          ROR=(((GAM2/GAM1)*(T2/T1)*(XM2/XM1)**2-1.)/SIN(EPS)**2)+1.  58800000
001137          IF(ROR)100,101,102                                      58900000
```

```
001143      101 CONTINUE                                                    59000000
001143          ROR=.000001                                                 59100000
001145      102 CONTINUE                                                    59200000
001145          ROR=ROR**.5                                                 59300000
001151      100 CONTINUE                                                    59400000
001151          ROR=1./ROR                                                  59500000
001153          PR3=ROR*T2/T1                                               59600000
001155          EP1=EPS/C                                                   59700000
001157          IF(NSTR.EQ.2.AND.DEL2.LT..01)GO TO 1002                     59800000
001170          GO TO 1003                                                  59900000
001170      1002 PR1=PR2                                                    60000000
001172          GO TO 25                                                    60100000
001172      1003 CONTINUE                                                   60200000
001172          IF(ABS(PR2-PR1)-.001)25,25,27                               60300000
001177      27  N=N+1                                                       60400000
001201          NAP=N                                                       60500000
001201          IF(M-2)55,56,56                                             60600000
001204      55  PRY=PR2                                                    60700000
001205          PRX=PR1                                                     60800000
001207          IF(NN-2)304,303,303                                         60900000
001212      304 PR1=PR1+.5*(PR2-PR1)                                        61000000
001216          NN=2                                                        61100000
001217      303 CONTINUE                                                    61200000
001217          PR1=PR1+.01*(PR2-PR1)                                       61300000
001223          M=M+1                                                       61400000
001225          GO TO 191                                                   61500000
001225      56  S=(PRY-PR2)/(PRX-PR1)                                      61600000
001231          PR1=(1./(1.-S))*(-S*PRX+PRY)                                61700000
001237          M=M-1                                                       61800000
001241      306 CONTINUE                                                    61900000
001241      191 CONTINUE                                                    62000000
001241          COTD=1.0/TAN(DELT)                                          62100000
001244          EPS=ATAN(COTD/(GAM1*XM1**2/(PR1-1.)-1.))                    62200000
001254          EP1=EPS/C                                                   62300000
001256          IF(EP1.LT.1.)GO TO 28                                       62400000
001262          IF(N-20)111,28,28                                           62500000
001265      28  PRINT 112,EP1,T2,JJ,J,JAA,NN,N,XM2                         62600000
001311      112 FORMAT(//21H PR DID NOT CONVERGE ,3X4HEP1=,F10.4,3X3HT2=,F10.4,3X3  62700000
               2HJJ=,I4,3X2HJ=,I4,3X4HJAA=,3I6,F10.4)                       62800000
001311          N=100                                                       62900000
001312          RETURN                                                      63000000
001313      25  CONTINUE                                                   63100000
001313          P2=PR1*P1                                                   63200000
001315          R2=ROR*R1                                                   63300000
001317          GO TO 447                                                   63400000
001321      446 CONTINUE                                                    63500000
          C     C  EXPANSION WAVE CALCULATIONS FOR TPG                      63600000
001321          XNUDF=-DELTN/C                                              63700000
001323          XNUD=XNUDF                                                  63800000
001324          XMI=XM1                                                     63900000
001326          TD2=TD                                                      64000000
001327          AW=SQRT((GAM+1.)/(GAM-1.))                                  64100000
001336          AAW=SQRT((GAM-1.)/(GAM+1.)*(XMI**2-1.))                     64200000
001350          XMU=90.-ACOS(1./XMI)/C                                      64300000
001357          XNUS=AW*ATAN(AAW)/C-(90.-XMU)                               64400000
001366          XNUB=XNUS+XNUDF                                             64500000
001367          BW=1./AW                                                    64600000
001371          CW=(GAM-1.)/2.                                              64700000
001374          DW=(GAM+1.)/(2.*(GAM-1.))                                   64800000
001377          EW=-GAM/(GAM-1.)                                            64900000
001402          XMW=XMI                                                     65000000
001403          XNUX=XNUS*C                                                 65100000
001405          NW=0                                                        65200000
001406      444 DO 445 JW=1,30                                              65300000
001411          XNU=AW*ATAN(BW*SQRT(XMW*XMW-1.))-ATAN(SQRT(XMW*XMW-1.))     65400000
001432          DIFF=XNUX-XNU                                               65500000
001433          IF(ABS(DIFF)-.00001)22,22,33                                65600000
001440      33  DM=(XMW/SQRT(XMW*XMW-1.))*(1.+CW*XMW*XMW)*DIFF             65700000
001452          XMW=XMW+DM                                                  65800000
001453      445 CONTINUE                                                    65900000
001456          PRINT80                                                     66000000
001462      80  FORMAT(30H MAX NO OF ITERATIONS EXCEEDED)                  66100000
001462      22  XMU=ATAN(1./SQRT(XMW*XMW-1.))/C                            66200000
001472          PR=(1.+CW*XMW*XMW)**EW                                      66300000
001501          IF(NW)64,64,66                                              66400000
001504      64  CONTINUE                                                   66500000
001504          XMU1=XMU                                                    66600000
001505          PRT1=PR                                                     66700000
```

```
001507          XNUD=XNUDF                                                      66800000
001510          NW=NW+1                                                         66900000
001512          XNUX=(XNUS+FLOAT(NW)*XNUD)*C                                    67000000
001516          IF(XNUX-XNUB*C)444,444,66                                       67100000
001522       66 CONTINUE                                                        67200000
001522          XM2N=XMW                                                        67300000
001523          XM2=XM2N                                                        67400000
001525          TR=(1.+(GAM-1.)/2.*XM1N**2)/(1.+(GAM-1.)/2.*XM2N**2)            67500000
001537          T2=T1*TR                                                        67600000
001541          GAM2=FGA(T2)                                                    67700000
001543          PR1=PR/PRT1                                                     67800000
001545          P2=P1*PR1                                                       67900000
001547          R2=P2*144./(RBAR/XMWT*T2)                                       68000000
001553          RHOR=R2/R1                                                      68100000
001555          EPD=XMU1                                                        68200000
001556          EP1=EPD                                                         68300000
001557          EPDF=XMU                                                        68400000
001561          EPDAVG=EPD-.5*(EPD-EPDF)                                        68500000
001564          B=1.0                                                           68600000
001566          N=JW                                                            68700000
001567          AR=RHOR*(XM2N/XMNORM)*TR**.5                                    68800000
001576          RNFR=RHOR*XM2N/(XMNORM*TR**.26)                                 68900000
001604          GAMM1=GAM-1.                                                    69000000
001606          TPR=((GAM+1.)*B/(GAMM1*B+2.))**(GAM/GAMM1)*((GAM+1.)/(2.*GAM*   69100000
                1B-(GAMM1)))**(1./GAMM1)                                        69200000
001630          TPRA=TPRA*TPR                                                   69300000
001632          DELTN1=DELTN/C                                                  69400000
              C THIS PACKAGE OVER RIDES PERFECT GAS PRESSURE RATIO AND USES TPG EQ 69500000
001634          GAX = GAMP/(GAMP-1.)                                            69600000
001636          ETT=EXP(THETA/T2)                                               69700000
001642          ETTM1=ETT-1.                                                    69800000
001644          ETTT=EXP(THETA/TO2)                                             69900000
001650          ETTTM1=ETTT-1.                                                  70000000
001652          ETR=ETTTM1/ETTM1                                                70100000
001654          TTTR=T2/TO2                                                     70200000
001656          THTR=THETA/T2                                                   70300000
001660          THTTR=THETA/TO2                                                 70400000
001661          EX1=ETT/ETTM1                                                   70500000
001663          EX2=ETTT/ETTTM1                                                 70600000
001665          PTPR=ETR*TTTR**GAX*EXP(THTR*EX1-THTTR*EX2)                      70700000
001700          P2=PT1*PTPR                                                     70800000
001702          R2=P2*144./(RBAR/XMWT*T2)                                       70900000
001706          RHOR=R2/R1                                                      71000000
001710      447 CONTINUE                                                        71100000
001710          TR=T2/T1                                                        71200000
001712          XM2T=XM1T*((GAM1*T1)/(GAM2*T2))**.5                             71300000
001717          XM2F=(XM2T**2+XM2**2)**.5                                       71400000
001725          PRINT 7                                                         71500000
001731        7 FORMAT(/38X11HBEHIND WAVE)                                      71600000
001731          CALL TOTAL(P2,T2,XM2F,TO2,PT2)                                  71700000
001735          PTR=PT2/PT1                                                     71800000
001737          TPRA=TPRA*PTR                                                   71900000
001740          DELTD=DELT/C                                                    72000000
001742          SND2=(R*T2*GAM2)**.5                                            72100000
001747          AR=R2*XM2*SND2/(R1*XM1*SCUND)                                   72200000
001754          ARA=ARA*AR                                                      72300000
001755          PRINT 8                                                         72400000
001761        8 FORMAT(// *        FLOW PROPERTIES MEASURED NORMAL TO WEDGE LEADING 72500000
                1 EDGE    *)                                                    72600000
001761          PRINT113,XM1,DELTD,P1,R1,T1,PT1,GAM1                            72700000
002003      113 FORMAT(/2X4HM1N=,F6.3,4X7HDELTAN=,F7.3,5X3HP1=,F8.4,6X3HR1=,F8.4, 72800000
              26X3HT1=,F8.2,6X4HPT1=,F10.4,6X5HGAM1=,F6.4)                      72900000
002003          PRINT114,XM2,EP1,P2,R2,T2,PT2,GAM2                              73000000
002025      114 FORMAT(2X4HM2N=,F6.3,7X4HEPN=,F7.3,5X3HP2=,F8.4,6X3HR2=,F8.4,   73100000
              26X3HT2=,F8.2,6X4HPT2=,F10.4,6X5HGAM2=,F6.4)                      73200000
002025          RHOR=R2/R1                                                      73300000
002027          RNFR=RHOR*XM2/(XM1*(T2/T1)**0.26)                               73400000
002036          PRINT 115,RNFR,AR,PR1,RHOR,TR,PTR,NAP                           73500000
002060      115 FORMAT(1X,5HREYN=,F6.3,5X6HA1/A2=,F7.3,2X6HP2/P1=,F8.4,3X6HR2/R1=, 73600000
              1F8.4,3X6HT2/T1=,F8.4,6X4HTPR=,F10.4,9X2HN=,I6)                   73700000
002060          IF(DELTD .LT.0.)PRINT 116, EPD,EPDF,EPDAVG                      73800000
002075      116 FORMAT(/2X,14HEXPANSION FAN*,9X,10HLEAD WAVE=,F8.4,5X11HFINAL WAVE 73900000
              1=,F8.4,5X9HAVG WAVE=,F8.4)                                       74000000
002075          J=J+1                                                           74100000
002077          XM2N=XM2                                                        74200000
002100          EPD=EP1                                                         74300000
002102          RETURN                                                          74400000
002103      109 STOP                                                            74500000
002105          END                                                             74600000
```

```
                SUBROUTINE PGAS                                                 74700000
      C     THIS SUBROUTINE COMPUTES WAVE PROPERTIES FOR A PERFECT GAS          74800000
      C     INPUT= XM1,  DELT,  N          OUTPUT= EP                           74900000
      C     NN= 0 FOR  STRONG  SHOCK                                            75000000
      C     NN= 4 FOR  WEAK  SHOCK                                              75100000
000002        COMMON C,THV,GAMP,RBAR,XMWT,P1,T1,XM,XMNORM,TO                    75200000
000002        COMMON P2,T2,DELTN,GAM,XM2N,EPD,RHOR                              75300000
000002        COMMON EMAX,DELTNM,N,KGAS,MC                                      75400000
000002        COMMON EPDF,TPRA,AR,XM1T,XM2T                                     75500000
000002        COMMON NDEBUG                                                     75600000
000002        RBAR=1545.31                                                      75700000
000003        XMWT=28.9644                                                      75800000
000005        XM1N=XMNORM                                                       75900000
000006        EPDF=0.                                                           76000000
000007        EPDAVG=0.                                                         76100000
000010        GR=(GAM+1.)/(GAM-1.)                                              76200000
000015        NN=4                                                              76300000
000016        IF(MC.GT.1)N=0                                                    76400000
000022        IF(N.EQ.2)NN=0                                                    76500000
000025        IF(N.EQ.0)NN=4                                                    76600000
000027        IF(DELTNM.LT.DELTN)DELTN=DELTNM                                   76700000
000032        XM1=XM1N                                                          76800000
000033        DELT=DELTN                                                        76900000
000035        PRINT 6                                                           77000000
000040      6 FORMAT(1X17H***PERFECT GAS***)                                    77100000
000040        PRINT 9                                                           77200000
000044      9 FORMAT(38X16HIN FRONT OF WAVE)                                    77300000
000044        CALL TOPG(P1,T1,XM,TO,PT1)                                        77400000
000050        IF(DELTN.LT.0.)GO TO 500                                          77500000
000052        PIE=3.141592654                                                   77600000
000053        XM12=XM1**2                                                       77700000
000054        XM14=XM1**4                                                       77800000
000055        BB=-(XM12+2.)/XM12-GAM*SIN(DELT)**2                               77900000
000064        CC=(2.*XM12+1.)/XM14+((GAM+1.)**2/4.+(GAM-1.)/XM12)*SIN(DELT)**2  78000000
000102        DD=-COS(DELT)**2/XM14                                             78100000
000106        EX=     (9.*BB*CC/2.-BB**3-27.*DD/2.)/(BB**2-3.*CC)**1.5          78200000
000126        IF(EX.GT.1)EX=1.                                                  78300000
000133        IF(EX.LT.-1)EX=-1                                                 78400000
000140        EE=ACOS(EX)                                                       78500000
000142        FF=COS((EE+NN*PIE)/3.)                                            78600000
000151        GG=(-BB/3.+(2*(BB**2-3.*CC)**.5/3.)*FF)**.5                       78700000
000167        EP=ASIN(GG)                                                       78800000
000171        EPD=EP/C                                                          78900000
000173        IF(EPD.GE.89.999)GO TO 25                                         79000000
000176        RR=TAN(EP)/TAN(EP-DELTN)                                          79100000
000206     25 CONTINUE                                                          79200000
000206        IF(EPD.GT.89.999)RR= (GAM+1.)*XM1**2/(((GAM-1.)*XM1**2)+2.)       79300000
000220        PR1=1.+GAM*XM1N**2*SIN(EP)**2*(1.-1./RR)                          79400000
000231        N=NN                                                              79500000
000232        B=XM1N**2*SIN(EP)**2                                              79600000
000236        BB=((GAM-1.)*B+2.)/(2.*GAM*B-(GAM-1.))                            79700000
000244        XM2N = (BB/(SIN(EP-DELTN))**2)**.5                                79800000
000255        TR=((2.0*GAM*B-(GAM-1.))*((GAM-1.)*B+2.))/((GAM+1.)**2*B)         79900000
000270        T2=TR*T1                                                          80000000
000272        P2=PR1*P1                                                         80100000
000274        PR=P2/P1                                                          80200000
000275        RHOR=RR                                                           80300000
000276        EPD=EP/C                                                          80400000
000300        GO TO 502                                                         80500000
000301    500 CONTINUE                                                          80600000
      C       EXPANSION WAVE CALCULATION                                      80700000
000301        XMI=XM1N                                                          80800000
000302        XNUDF=-DELTN/C                                                    80900000
000304        XNUD=XNUDF                                                        81000000
000306        AW=SQRT((GAM+1.)/(GAM-1.))                                        81100000
000314        AAW=SQRT((GAM-1.)/(GAM+1.)*(XMI**2-1.))                           81200000
000326        XMU=90.-ACOS(1./XMI)/C                                            81300000
000335        XNUS=AW*ATAN(AAW)/C-(90.-XMU)                                     81400000
000344        XNUB=XNUS+XNUDF                                                   81500000
000345        BW=1./AW                                                          81600000
000347        CW=(GAM-1.)/2.                                                    81700000
000352        DW=(GAM+1.)/(2.*(GAM-1.))                                         81800000
000355        EW=-GAM/(GAM-1.)                                                  81900000
000360        XMW=XMI                                                           82000000
000361        XNUX=XNUS*C                                                       82100000
000363        NW=0                                                              82200000
000364    444 DO100JW=1,30                                                      82300000
```

```
000366          XNU=AW*ATAN(BW*SQRT(XMW*XMW-1.))-ATAN(SQRT(XMW*XMW-1.))                 82400000
000407          DIFF=XNUX-XNU                                                           82500000
000410          IF(ABS(DIFF)-.00001)22,22,33                                            82600000
000414       33 DM=(XMW/SQRT(XMW*XMW-1.))*(1.+CW*XMW*XMW)*DIFF                          82700000
000426          XMW=XMW+DM                                                              82800000
000427       10 CONTINUE                                                                82900000
000432          PRINT80                                                                 83000000
000435       80 FORMAT(30H MAX NO OF ITERATIONS EXCEEDED)                               83100000
000435       22 XMU=ATAN(1./SQRT(XMW*XMW-1.))/C                                        83200000
000445          PR=(1.+CW*XMW*XMW)**EW                                                  83300000
000454          IF(NW)55,55,66                                                          83400000
000456       55 CONTINUE                                                                83500000
000456          XMU1=XMU                                                                83600000
000457          PRT1=PR                                                                 83700000
000461          XNUD=XNUDF                                                              83800000
000462          NW=NW+1                                                                 83900000
000464          XNUX=(XNUS+FLOAT(NW)*XNUD)*C                                            84000000
000470          IF(XNUX-XNUB*C)444,444,66                                               84100000
000474       66 CONTINUE                                                                84200000
000474          XM2N=XMW                                                                84300000
000475          PR1=PR/PRT1                                                             84400000
000477          TR=(1.+(GAM-1.)/2.*XM1N**2)/(1.+(GAM-1.)/2.*XM2N**2)                    84500000
000512          T2=T1*TR                                                                84600000
000514          P2=P1*PR1                                                               84700000
000516          RHOR=PR1/TR                                                             84800000
000517          EPD=XMU1                                                                84900000
000521          EPDF=XMU                                                                85000000
000522          EPDAVG=EPD-.5*(EPD-EPDF)                                                85100000
000526          B=1.0                                                                   85200000
000530          N=JW                                                                    85300000
000532       502 CONTINUE                                                               85400000
000532          AR=RHOR*(XM2N/XMNORM)*TR**.5                                            85500000
000541          RNFR=RHOR*XM2N/(XMNORM*TR**.26)                                         85600000
000547          GAMM1=GAM-1.                                                            85700000
000551          TPR=((GAM+1.)*B/(GAMM1*B+2.))**(GAM/GAMM1)*((GAM+1.)/(2.*GAM*           85800000
               18-(GAMM1)))**(1./GAMM1)                                                 85900000
000573          XM2T=XM1T*(T1/T2)**.5                                                   86000000
000600          XM2F=(XM2T**2+XM2N**2)**.5                                              86100000
000606          PRINT 7                                                                 86200000
000612        7 FORMAT(/38X11HBEHIND WAVE)                                              86300000
000612          CALL TOPG(P2,T2,XM2F,TO2,PT2)                                           86400000
000616          TPRA=TPRA*TPR                                                           86500000
000620          DELTN1=DELTN/C                                                          86600000
000621          ACR=0.                                                                  86700000
000622          GAM1=GAM                                                                86800000
000624          GAM2=GAM                                                                86900000
000624          R1=P1*144./(RBAR*T1/XMWT)                                               87000000
000630          R2=P2*144./(RBAR*T2/XMWT)                                               87100000
000634          RHOR=R2/R1                                                              87200000
000636          PRINT 8                                                                 87300000
000642        8 FORMAT(// *        FLOW PROPERTIES MEASURED NORMAL TO WEDGE LEADING    87400000
               1 EDGE    *)                                                           87500000
000642          PRINT 3,XMNORM,DELTN1,P1,R1,T1,PT1,GAM1                                 87600000
000664       3 FORMAT(/2X4HM1N=,F6.3,4X7HDELTAN=,F7.3,5X3HP1=,F8.4,6X3HR1=,F8.4,        87700000
               26X3HT1=,F8.2,6X4HPT1=,F10.4,6X5HGAM1=,F6.4)                             87800000
000664          PRINT 4, XM2N,EPD,P2,R2,T2,PT2,GAM2                                     87900000
000706       4 FORMAT(2X4HM2N=,F6.3,7X4HEPN=,F7.3,5X3HP2=,F8.4,6X3HR2=,F8.4,            88000000
               26X3HT2=,F8.2,6X4HPT2=,F10.4,6X5HGAM2=,F6.4)                             88100000
000706          PRINT  2,RNFR,AR,PR1,RHOR,TR,TPR,N                                      88200000
000730       2 FORMAT(1X,5HREYR=,F6.3,5X6HA1/A2=,F7.3,2X6HP2/P1=,F8.4,3X6HR2/R1=,       88300000
               1F8.4,3X6HT2/T1=,F8.4,6X4HTPR=,F10.4,9X2HN=,I6)                          88400000
000730          IF(DELTN1.LT.0.)PRINT 5, EPD,EPDF,EPDAVG                                88500000
000743       5 FORMAT(/2X,14HEXPANSION FAN*,9X,10HLEAD WAVE=,F8.4,5X11HFINAL WAVE       88600000
               1=,F8.4,5X9HAVG WAVE=,F8.4)                                              88700000
000743          RETURN                                                                  88800000
000744          END                                                                     88900000

                SUBROUTINE TOTAL(P,T,YM,TTOT,PO)                                        89000000
          C  THIS SUBROUTINE COMPUTES TOTAL PROPERTIES FOR A THERMALLY PERFECT GAS       89100000
000010          COMMON C,THV,GAMP,RBAR,XMWT,P1,T1,XM,XMNORM,TO                          89200000
000010          COMMON P2,T2,DELTN,GAM,XM2N,EPD,RHOR                                    89300000
000010          COMMON EMAX,DELTNM,N,KGAS,MC                                            89400000
000010          COMMON EPDF,TPRA,AR,XM1T,XM2T                                           89500000
000010          COMMON NDEBUG                                                           89600000
000010          FGA(T )=1.+(GAMP-1.)/(1.+(GAMP-1.)*(THETA/T)**2*EXP(THETA/T)/(          89700000
               2EXP(THETA/T)-1.)**2)                                                    89800000
000044          FXM(TO) = SQRT((A*TO-7./GAM)+B*(1./(EXP(THV/TO)-1.)-E))                 89900000
```

```
000072          THETA=THV                                                    90000000
000074          PRINT2                                                       90100000
000077        2 FORMAT( 49X,*TOTAL PROPERTIES*)                              90200000
000077          PRINT3                                                       90300000
000103        3 FORMAT(8X1HM,9X6HMCHECK,7X2HTO,9X4HT/TO,8X2HPO,10X4HP/PO,9X1HR,  90400000
               11)X4HR/RO,8X3HGAM,6X1HN)                                   90500000
000103          N=1                                                        90600000
000104          GAM=FGA(T)                                                 90700000
000111          RHO=P*144./(RBAR*T/XMWT)                                   90800000
000115          A= 7./(GAM*T)                                              90900000
000120          B= 2.*THV/(GAM*T)                                          91000000
000122          ET= EXP(THV/T)                                             91100000
000130          E=1./(ET-1.)                                               91200000
000133          T01 = T*(1.+(GAM-1.)*YM**2/2.)                             91300000
000140          T02=T01-50.                                                91400000
000142        8 XM1=FXM(T01)                                               91500000
000144          XM2= FXM(T02)                                              91600000
000147          TO=(YM-XM1)/(XM2-XM1)*(T02-T01)+T01                        91700000
000156          XM3=FXM(TO)                                                91800000
000161          IF(ABS(YM-XM3)-.0001)10,10,5                               91900000
000166        5 T01=TO                                                     92000000
000167          T02=TO-10.                                                 92100000
000171          N=N+1                                                      92200000
000173          IF(N-25)9,9,10                                             92300000
000175        9 GO TO 8                                                    92400000
000176       10 CONTINUE                                                   92500000
000176          ETO=EXP(THV/TO)                                            92600000
000202          ET01=ETO-1.                                                92700000
000204          ET1=ET-1.                                                  92800000
000206          APR=EXP((THV*ET/(T*ET1))-(THV*ETO/(TO*ET01)))              92900000
000225          PR= ET01*(T/TO)**(GAMP/(GAMP-1.))*APR/ET1                  93000000
000236          RHOR =  ET01*(T/TO)**(1./(GAMP-1.))*APR/ET1                93100000
000247          TR=T/TO                                                    93200000
000251          PO=P/PR                                                    93300000
000253          TTOT=TO                                                    93400000
000253          PRINT1,YM,XM3,TO,TR,PO,PR,RHO,RHOR,GAM,N                   93500000
000303        1 FORMAT(1X,2F12.5,F12.3,F10.5,F13.3,F13.9,F12.6,F13.9,F9.5,I5)  93600000
000303          RETURN                                                     93700000
000304          END                                                        93800000
                SUBROUTINE TOPG(P,T,YM,TTOT,PO)                            93900000
      C  THIS SUBROUTINE COMPUTES TOTAL PROPERTIES FOR A PERFECT GAS       94000000
000010          COMMON C,THV,GAMP,RBAR,XMWT,P1,T1,XM,XMNORM,TO             94100000
000010          COMMON P2,T2,DELTN,GAM,XM2N,EPD,RHOR                       94200000
000010          COMMON EMAX,DELTNM,N,KGAS,MC                               94300000
000010          COMMON EPDF,TPRA,AR,XM1T,XM2T                              94400000
000010          COMMON NDEBUG                                              94500000
000010          PRINT2                                                     94600000
000013        2 FORMAT( 49X,*TOTAL PROPERTIES*)                            94700000
000013          PRINT3                                                     94800000
000017        3 FORMAT(8X1HM,9X6HMCHECK,7X2HTO,9X4HT/TO,8X2HPO,10X4HP/PO,9X1HR,  94900000
               110X4HR/RO,8X3HGAM,6X1HN)                                   95000000
000017          RBAR=1545.31                                               95100000
000020          XMWT=28.9644                                               95200000
000022          RHO=P*144./(RBAR*T/XMWT)                                   95300000
000030          A = (GAM-1.)/2.*YM**2                                      95400000
000034          TR = 1./(1.+A)                                             95500000
000036          PR = (1./(1.+A))**(GAM/(GAM-1.))                           95600000
000045          RHOR = (1./(1.+A))**(1./(GAM-1.))                          95700000
000055          TO=T/TR                                                    95800000
000057          PO=P/PR                                                    95900000
000060          TTOT=TO                                                    96000000
000061          XM3=YM                                                     96100000
000062          PRINT1,YM,XM3,TO,TR,PO,PR,RHO,RHOR,GAM                     96200000
000110        1 FORMAT(1X,2F12.5,F12.3,F10.5,F13.3,F13.9,F12.6,F13.9,F9.5,I5)  96300000
000110          RETURN                                                     96400000
000111          END                                                        96500000
```

**** SAMPLE CASES ****

CASE NO. 1 -- FOR AN INITIAL SWEEP ANGLE OF 48 DEGREES, THIS CASE COMPUTES FLOW PROPERTIES ACROSS 3 SUCCESSIVE SHOCK WAVES. THE WAVES ALTERNATE TYPE A, TYPE B, AND TYPE A, WITH THE FLOW TURNING ACROSS EACH SHOCK WAVE EQUAL TO 6 DEGREES WHEN MEASURED IN THE XZ PLANE.

INPUT FOR CASE NO. 1

```
3.      6.0     48.     6.0     0.      1.4                     02200
6.      6.      6.
1.      -1.     1.
```

CASE NO. 2 -- THIS IS ALSO A PERFECT GAS CASE, WITH AN INITIAL SWEEP ANGLE OF 48 DEGREES. THE FIRST WAVE IS A SHOCK FOLLOWED BY AN EXPANSION FAN. BOTH WAVES ARE TYPE A, AND THE FLOW TURNING ACROSS EACH WAVE IS EQUAL TO 6 DEGREES WHEN MEASURED IN THE XZ PLANE.

INPUT FOR CASE NO. 2

```
2.      6.0     48.     6.0     0.      1.4                     02200
6.      -6.
1.      1.
```

CASE NO. 3 -- THIS CASE IS A REPEAT OF CASE NO. 1, BUT FOR A THERMALLY PERFECT GAS AND AT A FLIGHT DYNAMIC PRESSURE OF 1000 PSF.

INPUT FOR CASE NO. 3

```
3.      6.0     48.     6.0     0.      .2775   402.    22200
6.      6.      6.
1.      -1.     1.
```

CASE NO 1 WAVE NO 1 (WEAK SHOCK)

K1	K2	K3	K4	K5
0	2	2	0	0

PERFECT GAS

IN FRONT OF WAVE

TOTAL PROPERTIES

M	MCHECK	TO	T/TO	PO	P/PO	R	R/RO	GAM	N
6.00000	6.00000	4100.000	.12195	1578.878	.000633361	.005398	.005193563	1.40000	

BEHIND WAVE

TOTAL PROPERTIES

M	MCHECK	TO	T/TO	PO	P/PO	R	R/RO	GAM	N
5.17681	5.17681	4100.000	.15724	1490.317	.001541448	.009618	.009803422	1.40000	

FLOW PROPERTIES MEASURED NORMAL TO WEDGE LEADING EDGE

M1N= 4.015	DELTAN= 8.927	P1= 1.0000	R1= .0054	T1= 500.00	PT1= 1578.8777	GAM1=1.4000
M2N= 3.373	EPN= 21.221	P2= 2.2972	R2= .0096	T2= 644.67	PT2= 1490.3174	GAM2=1.4000
REYR= 1.401	A1/A2= 1.700	P2/P1= 2.2972	R2/R1= 1.7817	T2/T1= 1.2893	TPR= .9439	N= 4

FLOW PROPERTIES REFERENCED TO SWEPT WEDGE

M1N	M1T	M2N	M2T	M2	P/PINF	R/RINF	T/TINF	GAM
4.01478	4.45887	3.37334	3.92683	5.17681	2.29725	1.78173	1.28933	1.40000

DELTAN	EPSN	AJOC	ACOI2P	ACOI3P	AEOI1P	THETA	DELTAN MAX	EPSN MAX	N
8.92684	21.22146	14.56494	5.80584	1.68065	40.66416	42.00000	38.82060	66.06870	4

M1= 6.000 SWEEP= 48.000 RIDGE ANGLE= 6.000 DE/AD= 0.000 P1= 1.0000 T1= 500.00

M2= 5.177 P/PINF= 2.2972 R/RINF= 1.7817 T/TINF= 1.2893 GAM= 1.4000

RECOVERY (PT/PTINF) = .9439 KINETIC ENERGY EFF.= .99769

CONTRACTION (AINF/A) = 1.7456 EPS= 14.565 CROSS FLOW= 1.681

FLOW PROPERTIES REFERENCED TO INITIAL XYZ COORDINATE SYSTEM

M2= 5.177 DELTA XZ= 6.000 EPS XZ= 14.565

TOTAL CROSS FLOW (DELTA XY)= 1.681 GAP RATIO (W1/W2)= 1.688

CASE NO 1 WAVE NO 2 (WEAK SHOCK)

K1	K2	K3	K4	K5
0	2	2	0	0

PERFECT GAS

IN FRONT OF WAVE

TOTAL PROPERTIES

M	MCHECK	TO	T/TO	PO	P/PO	R	R/RO	GAM	N
5.17681	5.17681	4100.000	.15724	1490.317	.001541448	.009618	.009803422	1.40000	

BEHIND WAVE

TOTAL PROPERTIES

M	MCHECK	TO	T/TO	PO	P/PO	R	R/RO	GAM	N
4.54388	4.54388	4100.000	.19496	1436.267	.003271737	.015867	.016781921	1.40000	

FLOW PROPERTIES MEASURED NORMAL TO WEDGE LEADING EDGE

M1N= 3.373	DELTAN= 8.927	P1= 2.2972	R1= .0096	T1= 644.67	PT1= 1490.3174	GAM1=1.4000
M2N= 2.865	EPN= 24.092	P2= 4.6991	R2= .0159	T2= 799.32	PT2= 1436.2673	GAM2=1.4000
REYR= 1.325	A1/A2= 1.560	P2/P1= 2.0455	R2/R1= 1.6498	T2/T1= 1.2399	TPR= .9637	N= 4

FLOW PROPERTIES REFERENCED TO SWEPT WEDGE

M1N	M1T	M2N	M2T	M2	P/PINF	R/RINF	T/TINF	GAM
3.37334	3.92683	2.85536	3.52655	4.54388	4.69909	2.93943	1.59864	1.40000

DELTAN	EPSN	AJOC	ACOI2P	ACOI3P	AEOI1P	THETA	DELTAN MAX	EPSN MAX	N
8.92684	24.09216	15.75064	5.80336	1.23139	39.09427	40.66416	36.26086	65.58180	4

M1= 5.177 SWEEP= 49.535 RIDGE ANGLE= 5.803 DE/AD= 1.000 P1= 2.2972 T1= 644.67

M2= 4.544 P/PINF= 4.6991 R/RINF= 2.9394 T/TINF= 1.5986 GAM= 1.4000

RECOVERY (PT/PTINF) = .9097 KINETIC ENERGY EFF.= .99619

CONTRACTION (AINF/A) = 2.8146 EPS= 15.751 CROSS FLOW= 1.231

FLOW PROPERTIES REFERENCED TO INITIAL XYZ COORDINATE SYSTEM

M2= 4.544 DELTA XZ= 6.000 EPS XZ= 10.280

TOTAL CROSS FLOW (DELTA XY)= 2.906 GAP RATIO (W1/W2)= 2.653

CASE NO 1 WAVE NO 3 (WEAK SHOCK)

K1	K2	K3	K4	K5
0	2	2	0	0

PERFECT GAS

IN FRONT OF WAVE

TOTAL PROPERTIES

M	MCHECK	TO	T/TO	PO	P/PO	R	R/RO	GAM	N
4.54388	4.54388	4100.000	.19496	1436.267	.003271737	.015867	.016781921	1.40000	

BEHIND WAVE

TOTAL PROPERTIES

M	MCHECK	TO	T/TO	PO	P/PO	R	R/RO	GAM	N
4.03831	4.03831	4100.000	.23465	1401.402	.006258880	.024607	.026672824	1.40000	

FLOW PROPERTIES MEASURED NORMAL TO WEDGE LEADING EDGE

M1N= 2.865	DELTAN= 8.927	P1= 4.6991	R1= .0159	T1= 799.32	PT1= 1436.2673	GAM1=1.4000
M2N= 2.444	EPN= 27.434	P2= 8.7712	R2= .0246	T2= 962.08	PT2= 1401.4016	GAM2=1.4000
REYR= 1.261	A1/A2= 1.451	P2/P1= 1.8666	R2/R1= 1.5508	T2/T1= 1.2036	TPR= .9757	N= 4

FLOW PROPERTIES REFERENCED TO SWEPT WEDGE

M1N	M1T	M2N	M2T	M2	P/PINF	R/RINF	T/TINF	GAM
2.86536	3.52655	2.44447	3.21443	4.03831	8.77120	4.55846	1.92416	1.40000

DELTAN	EPSN	AJOC	ACOI2P	ACOI3P	AEOI1P	THETA	DELTAN MAX	EPSN MAX	N
8.92684	27.43391	18.12559	5.39357	2.17835	37.25179	39.09427	33.10175	65.11211	4

M1= 4.544 SWEEP= 50.906 RIDGE ANGLE= 5.657 DE/AD= 0.000 P1= 4.6991 T1= 799.32

M2= 4.038 P/PINF= 8.7712 R/RINF= 4.5585 T/TINF= 1.9242 GAM= 1.4000

RECOVERY (PT/PTINF) = .8876 KINETIC ENERGY EFF.= .99519

CONTRACTION (AINF/A) = 4.2559 EPS= 18.126 CROSS FLOW= 2.178

FLOW PROPERTIES REFERENCED TO INITIAL XYZ COORDINATE SYSTEM

M2= 4.038 DELTA XZ= 6.000 EPS XZ= 19.155

TOTAL CROSS FLOW (DELTA XY)= 5.084 GAP RATIO (W1/W2)= 3.820

CASE NO 2 WAVE NO 1 (WEAK SHOCK) K1 K2 K3 K4 K5 = 0 2 2 0 0

PERFECT GAS

IN FRONT OF WAVE

TOTAL PROPERTIES

M	MCHECK	TO	T/TO	PO	P/PO	R	R/RO	GAM	N
6.00000	6.00000	4100.000	.12195	1578.878	.000633361	.005398	.005193563	1.40000	

BEHIND WAVE

TOTAL PROPERTIES

M	MCHECK	TO	T/TO	PO	P/PO	R	R/RO	GAM	N
5.17681	5.17681	4100.000	.15724	1490.317	.001541448	.009618	.009803422	1.40000	

FLOW PROPERTIES MEASURED NORMAL TO WEDGE LEADING EDGE

M1N=	4.015	DELTAN=	8.927	P1=	1.0000	R1=	.0054	T1=	500.00	PT1=	1578.8777	GAM1=1.4000
M2N=	3.373	EPN=	21.221	P2=	2.2972	R2=	.0096	T2=	644.67	PT2=	1490.3174	GAM2=1.4000
REYR=	1.401	A1/A2=	1.700	P2/P1=	2.2972	R2/R1=	1.7817	T2/T1=	1.2893	TPR=	.9439	N= 4

FLOW PROPERTIES REFERENCED TO SWEPT WEDGE

M1N	M1T	M2N	M2T	M2	P/PINF	R/RINF	T/TINF	GAM
4.01478	4.45887	3.37334	5.92683	5.17681	2.29725	1.78173	1.28933	1.40000

DELTAN	EPSN	AJOC	ACOI2P	ACOI3P	AEOI1P	THETA	DELTAN MAX	EPSN MAX	N
8.92684	21.22146	14.56494	5.80584	1.68065	40.66416	42.00000	38.82060	66.06870	4

M1= 6.000 SWEEP= 48.000 RIDGE ANGLE= 6.000 DE/AD= 0.000 P1= 1.0000 T1= 500.00

M2= 5.177 P/PINF= 2.2972 R/RINF= 1.7817 T/TINF= 1.2893 GAM= 1.4000

RECOVERY (PT/PTINF) = .9439 KINETIC ENERGY EFF.= .99769

CONTRACTION (AINF/A) = 1.7456 EPS= 14.565 CROSS FLOW= 1.681

FLOW PROPERTIES REFERENCED TO INITIAL XYZ COORDINATE SYSTEM

M2= 5.177 DELTA XZ= 6.000 EPS XZ= 14.565

TOTAL CROSS FLOW (DELTA XY)= 1.681 GAP RATIO (W1/W2)= 1.688

CASE NO 2 WAVE NO 2 (EXPANSION) K1 K2 K3 K4 K5
0 2 2 0 0

PERFECT GAS

IN FRONT OF WAVE
TOTAL PROPERTIES

M	MCHECK	TO	T/TO	PO	P/PO	R	R/RO	GAM	N
5.17681	5.17681	4100.000	.15724	1490.317	.001541448	.009618	.009803422	1.40000	

BEHIND WAVE
TOTAL PROPERTIES

M	MCHECK	TO	T/TO	PO	P/PO	R	R/RO	GAM	N
5.93700	5.93700	4100.000	.12423	1490.317	.000675761	.005337	.005439594	1.40000	

FLOW PROPERTIES MEASURED NORMAL TO WEDGE LEADING EDGE

M1N= 3.350 DELTAN= -8.927 P1= 2.2972 R1= .0096 T1= 644.67 PT1= 1490.3174 GAM1=1.4000
M2N= 3.941 EPN= 17.370 P2= 1.0071 R2= .0053 T2= 509.34 PT2= 1490.3174 GAM2=1.4000
REYR= .694 A1/A2= .580 P2/P1= .4384 R2/R1= .5549 T2/T1= .7901 TPR= 1.0000 N= 4

EXPANSION FAN* LEAD WAVE= 17.3699 FINAL WAVE= 14.7001 AVG WAVE= 16.0350

FLOW PROPERTIES REFERENCED TO SWEPT WEDGE

M1N	M1T	M2N	M2T	M2	P/PINF	R/RINF	T/TINF	GAM
3.34964	3.94706	3.94075	4.44054	5.93700	1.00710	.98862	1.01869	1.40000

DELTAN	EPSN	AJOC	ACOI2P	ACOI3P	AEOI1P	THETA	DELTAN MAX	EPSN MAX	N
-8.92684	17.36989	11.44203	-5.91259	-.92163	41.58737	40.31935	36.14072	65.56125	4

M1= 5.177 SWEEP= 49.681 RIDGE ANGLE= -5.803 DE/AD= 0.000 P1= 2.2972 T1= 644.67

M2= 5.937 P/PINF= 1.0071 R/RINF= .9886 T/TINF= 1.0187 GAM= 1.4000

RECOVERY (PT/PTINF) = .9439 KINETIC ENERGY EFF.= .99769

CONTRACTION (AINF/A) = .9873 EPS= 11.442 CROSS FLOW= -.922

EXPANSION FAN* LEAD WAVE= 11.4420 FINAL WAVE= 3.7429 AVG WAVE= 7.5925

FLOW PROPERTIES REFERENCED TO INITIAL XYZ COORDINATE SYSTEM

M2= 5.937 DELTA XZ= -6.000 EPS XZ= 11.822

EXPANSION FAN* LEAD WAVE= 11.8217 FINAL WAVE= 3.8703 AVG WAVE= 7.8460

TOTAL CROSS FLOW (DELTA XY)= .759 GAP RATIO (W1/W2)= .973

CASE NO 3 WAVE NO 1 (WEAK SHOCK)

K1	K2	K3	K4	K5
2	2	2	0	0

THERMALLY PERFECT GAS

IN FRONT OF WAVE

TOTAL PROPERTIES

M	MCHECK	TO	T/TO	PO	P/PO	R	R/RO	GAM	N
6.00000	5.99999	2999.707	.13401	528.661	.000524911	.001863	.003916865	1.39997	2

BEHIND WAVE

TOTAL PROPERTIES

M	MCHECK	TO	T/TO	PO	P/PO	R	R/RO	GAM	N
5.17765	5.17764	2999.706	.17273	498.961	.001277606	.003320	.007394459	1.39958	2

FLOW PROPERTIES MEASURED NORMAL TO WEDGE LEADING EDGE

M1N= 4.015	DELTAN= 8.927	P1= .2775	R1= .0019	T1= 402.00	PT1= 528.6610	GAM1=1.4000
M2N= 3.374	EPN= 21.221	P2= .6375	R2= .0033	T2= 518.29	PT2= 498.9614	GAM2=1.3996
REYR= 1.402	A1/A2= 1.700	P2/P1= 2.2972	R2/R1= 1.7819	T2/T1= 1.2893	TPR= .9438	N= R

FLOW PROPERTIES REFERENCED TO SWEPT WEDGE

M1N	M1T	M2N	M2T	M2	P/PINF	R/RINF	T/TINF	GAM
4.01478	4.45887	3.37387	3.92747	5.17765	2.29721	1.78194	1.28927	1.39958

DELTAN	EPSN	AJOC	ACOI2P	ACOI3P	AEOI1P	THETA	DELTAN MAX	EPSN MAX	N
8.92684	21.22136	14.56486	5.80582	1.68078	40.66402	42.00000	38.82164	66.06918	2

M1= 6.000 SWEEP= 48.000 RIDGE ANGLE= 6.000 DE/AD= 0.000 P1= .2775 T1= 402.00

M2= 5.178 P/PINF= 2.2972 R/RINF= 1.7819 T/TINF= 1.2893 GAM= 1.3996

RECOVERY (PT/PTINF) = .9438 KINETIC ENERGY EFF.= .99769

CONTRACTION (AINF/A) = 1.7458 EPS= 14.565 CROSS FLOW= 1.681

FLOW PROPERTIES REFERENCED TO INITIAL XYZ COORDINATE SYSTEM

M2= 5.178 DELTA XZ= 6.000 EPS XZ= 14.565

TOTAL CROSS FLOW (DELTA XY)= 1.681 GAP RATIO (W1/W2)= 1.688

CASE NO 3 WAVE NO 2 (WEAK SHOCK)

K1	K2	K3	K4	K5
2	2	2	0	0

THERMALLY PERFECT GAS

IN FRONT OF WAVE

TOTAL PROPERTIES

M	MCHECK	TO	T/TO	PO	P/PO	R	R/RO	GAM	N
5.17765	5.17764	2999.706	.17278	498.961	.001277606	.003320	.007394459	1.39958	2

BEHIND WAVE

TOTAL PROPERTIES

M	MCHECK	TO	T/TO	PO	P/PO	R	R/RO	GAM	N
4.54805	4.54804	2999.706	.21416	480.627	.002712833	.005478	.012667153	1.39786	2

FLOW PROPERTIES MEASURED NORMAL TO WEDGE LEADING EDGE

M1N= 3.374	DELTAN= 8.927	P1= .6375	R1= .0033	T1= 518.29	PT1= 498.9614	GAM1=1.3996	
M2N= 2.868	EPN= 24.088	P2= 1.3039	R2= .0055	T2= 642.43	PT2= 480.6274	GAM2=1.3979	
REYR= 1.327	A1/A2= 1.561	P2/P1= 2.0454	R2/R1= 1.6508	T2/T1= 1.2395	TPR= .9633	N= R	

FLOW PROPERTIES REFERENCED TO SWEPT WEDGE

M1N	M1T	M2N	M2T	M2	P/PINF	R/RINF	T/TINF	GAM
3.37387	3.92747	2.86794	3.52982	4.54805	4.69860	2.94169	1.59807	1.39786

DELTAN	EPSN	AJOC	ACOI2P	ACOI3P	AEOI1P	THETA	DELTAN MAX	EPSN MAX	N
8.92684	24.08782	15.74766	5.80334	1.23208	39.09345	40.66402	36.27601	65.58788	2

M1= 5.178 SWEEP= 49.535 RIDGE ANGLE= 5.803 DE/AD= 1.000 P1= .6375 T1= 518.29

M2= 4.548 P/PINF= 4.6986 R/RINF= 2.9417 T/TINF= 1.5981 GAM= 1.3979

RECOVERY (PT/PTINF) = .9091 KINETIC ENERGY EFF.= .99616

CONTRACTION (AINF/A) = 2.8167 EPS= 15.748 CROSS FLOW= 1.232

FLOW PROPERTIES REFERENCED TO INITIAL XYZ COORDINATE SYSTEM

M2= 4.548 DELTA XZ= 6.000 EPS XZ= 10.277

TOTAL CROSS FLOW (DELTA XY)= 2.907 GAP RATIO (W1/W2)= 2.654

CASE NO 3 WAVE NO 3 (WEAK SHOCK)

K1	K2	K3	K4	K5
2	2	2	0	0

THERMALLY PERFECT GAS

IN FRONT OF WAVE

TOTAL PROPERTIES

M	MCHECK	TO	T/TO	PO	P/PO	R	R/RO	GAM	N
4.54805	4.54804	2999.706	.21415	480.627	.002712833	.005478	.012667153	1.39786	2

BEHIND WAVE

TOTAL PROPERTIES

M	MCHECK	TO	T/TO	PO	P/PO	R	R/RO	GAM	N
4.05131	4.05130	2999.707	.25738	468.989	.005185326	.008502	.020146935	1.39377	2

FLOW PROPERTIES MEASURED NORMAL TO WEDGE LEADING EDGE

M1N= 2.868	DELTAN= 8.927	P1= 1.3039	R1= .0055	T1= 642.43	PT1= 480.6274	GAM1=1.3979		
M2N= 2.453	EPN= 27.384	P2= 2.4319	R2= .0085	T2= 772.05	PT2= 468.9891	GAM2=1.3938		
REYR= 1.265	A1/A2= 1.453	P2/P1= 1.8651	R2/R1= 1.5520	T2/T1= 1.2018	TPR= .9758	N= 3		

FLOW PROPERTIES REFERENCED TO SWEPT WEDGE

M1N	M1T	M2N	M2T	M2	P/PINF	R/RINF	T/TINF	GAM
2.86794	3.52982	2.45253	3.22462	4.05131	8.76346	4.56542	1.92052	1.39377

DELTAN	EPSN	AJOC	ACOI2P	ACOI3P	AEOI1P	THETA	DELTAN MAX	EPSN MAX	N
8.92684	27.38449	18.08956	5.39400	2.17396	37.25537	39.09345	33.17773	65.13902	2

M1= 4.548	SWEEP= 50.907	RIDGE ANGLE= 5.657	DE/AD= 0.000	P1= 1.3039	T1= 642.43
M2= 4.051	P/PINF= 8.7635	R/RINF= 4.5654	T/TINF= 1.9205	GAM= 1.3938	
RECOVERY (PT/PTINF) = .8871	KINETIC ENERGY EFF.= .99514				
CONTRACTION (AINF/A) = 4.2626	EPS= 18.090	CROSS FLOW= 2.174			

FLOW PROPERTIES REFERENCED TO INITIAL XYZ COORDINATE SYSTEM

M2= 4.051	DELTA XZ= 6.000	EPS XZ= 19.117	
TOTAL CROSS FLOW (DELTA XY)= 5.081	GAP RATIO (W1/W2)= 3.827		

APPENDIX B

INLET PERFORMANCE FOR LOW REYNOLDS NUMBER AND UNSTARTED OPERATION

In order to evaluate the inlets operating characteristics better, one test was made with the Reynolds number reduced by a factor of 1/3 to 3.3×10^6 per meter. The resulting static-pressure distributions within the inlet are found in figure 61 where they are compared with the high-pressure tests. Also given in figure 61 are the results of a test in which the model failed to start because of blockage produced by a survey rake.

The low Reynolds number tests had only a small effect on inlet operation as determined by static-pressure level changes produced by slight alterations in shock-wave positions. In the side passage these effects were seen near the cowl in figures 61(f) and 61(h), whereas the center-passage effects are observed in figure 61(k). The high-pressure level indicated on the foreplate (fig. 61(a)) is in error because of the difficulty in measuring the extremely low pressures.

Alterations in static-pressure levels for the unstarted choked inlet were observed throughout the model. High pressures were found on the foreplate (fig. 61(a)), top surface (figs. 61(b) and 61(c)), sidewalls in front of the struts (fig. 61(d)), and on the cowl (figs. 61(f) and 61(g)). The pressure level in the center passage was low and uniform and indicated the absence of shock waves (figs. 61(i) and 61(k)).

APPENDIX C

CAPTURE MEASUREMENT DATA

The primary conclusions from the capture measurement data (Mach number and capture parameter contour maps) taken downstream from the struts are presented in the report in figures 53 and 54. The purpose of this appendix is to include the data from pitot and static-pressure surveys used to produce those results. Like the data taken at the inlet throat, the program used to analyze these data and generate the contour maps is discussed in appendix B.

The static-pressure distribution around the walls of the inlet at the capture measurement station is given in figure 62 where λ is the peripheral distance around the area as defined in the sketch. The static probe survey data are found in figure 63 which also includes the wall values of figure 62. A nominal value of 80 percent was selected for the total-pressure recovery limit at the capture measurement location downstream of the struts. When the static surveys were combined with the pitot surveys of figure 64, the computed total-pressure recovery was above the imposed limit of 80 percent only in the very small region indicated by the dashed line in figure 63(d). The data are seen in contour map form in figures 65 and 66, and a total-pressure recovery map is given in figure 67.

REFERENCES

1. Henry, J. R.; and McLellan, C. H.: Air-Breathing Launch Vehicle for Earth-Orbit Shuttle – New Technology and Development Approach. AIAA Paper No. 70-269, Feb. 1970. (Also J. Aircraft, vol. 8, no. 5, May 1971, pp. 381-387.)

2. Ferri, A.: Review of SCRAMJET Propulsion Technology. J. Aircraft, vol. 5, no. 1, Jan.-Feb. 1968, pp. 3-10.

3. Becker, John V.: New Approaches to Hypersonic Aircraft. Paper presented at Seventh Congress of the International Council of the Aeronautical Sciences (Rome, Italy), Sept. 1970.

4. Becker, John V.: Prospects for Actively Cooled Hypersonic Transports. Astronaut. & Aeronaut., vol. 9, no. 8, Aug. 1971, pp. 32-39.

5. Development of Liquid-Hydrogen Scramjet Key to Hypersonic Flight. Aviat. & Space Technol., vol. 99, no. 12, Sept. 17, 1973, pp. 75-78.

6. Edwards, C. L. W.: A Forebody Design Technique for Highly Integrated Bottom-Mounted Scramjets With Application to a Hypersonic Research Airplane. NASA TM X-71971, 1974.

7. Small, William J.; Weidner, John P.; and Johnston, P. J.: Scramjet Nozzle Design and Analysis as Applied to a Highly Integrated Hypersonic Research Airplane. NASA TM X-71972, 1974.

8. Henry, John R.; and Anderson, Griffin Y.: Design Considerations for the Airframe-Integrated Scramjet. NASA TM X-2895, 1973.

9. Trexler, Carl Arthur: An Experimental Investigation of the Forebody of a Hypersonic Inlet Model and a Comparison With Theory. M.S. Thesis, Virginia Polytech. Inst. & State Univ., Apr. 1971.

10. Pinckney, S. Z.: Semiempirical Method for Predicting Effects of Incident-Reflecting Shocks on the Turbulent Boundary Layer. NASA TN D-3029, 1965.

11. Pinckney, S. Z.: An Improved Static Probe Design. AIAA J., vol. 12, no. 4, Apr. 1974, pp. 562-564.

12. Goldberg, Theodore J.; and Hefner, Jerry N. (With appendix by James C. Emery) Starting Phenomena for Hypersonic Inlets With Thick Turbulent Boundary Layers at Mach 6. NASA TN D-6280, 1971.

13. Pinckney, S. Z.: Turbulent Heat-Transfer Prediction Method for Application to Scramjet Engines. NASA TN D-7810, 1974.

14. Ames Research Staff: Equations, Tables, and Charts for Compressible Flow. NASA Rep. 1135, 1953. (Supersedes NACA TN 1428.)

TABLE I.- THEORETICAL FLOW FIELD PROPERTIES USED FOR FIGURE 5

Bay	M	p/p_1	$p_t/p_{t,1}$	δ_{xz}	δ_{xy}	A/A_1	p_{pitot}/p_1	
1	6.0	1.0	1.0	0	0	1.0	46.8	← Free stream
2	5.18	2.30	.944	6.0	1.7	1.75	80.4	
3	4.54	4.70	.910	0	2.9	2.81	127.0	
4	4.04	8.77	.888	6.0	5.1	4.26	188.0	
5	3.76	12.74	.883	2.0	6.2	5.25	237.0	
6	3.51	18.02	.879	6.0	7.9	6.85	294.0	← Side-passage throat
7	4.75	3.74	.933	10.0	2.8	2.43	110.0	
8	4.21	7.16	.903	4.0	4.5	3.74	167.0	
9	3.77	12.67	.891	10.0	6.9	5.45	238.0	
10	3.40	20.99	.879	6.0	8.95	7.57	322.0	← Center-passage throat
11	3.17	28.91	.871	2.0	10.5	9.29	388.0	
12	4.54	4.70	.910	0	2.9	2.81	127.0	
13	4.04	8.77	.888	-6.0	5.1	4.26	188.0	
14	3.76	12.77	.886	-2.0	6.2	5.46	238.0	
15	3.51	18.02	.879	-6.0	7.9	6.85	294.0	
16	3.08	33.26	.870	10.0	12.2	10.16	422.0	

TABLE II.- THEORETICAL END EFFECTS USED FOR FIGURE 5

(a) Top surface ($\delta_{xy} = 4^o$)

Bay	M	p/p_1	$p_t/p_{t,1}$	p_{pitot}/p_1
2	4.92	3.07	0.939	97.1
3	4.46	5.22	.910	136.0
4	4.13	7.79	.888	175.0
5	3.92	10.25	.883	208.0
6	3.77	12.53	.879	235.0
7	4.67	4.26	.933	122.0
8	4.25	6.80	.903	161.0
9	3.98	9.53	.891	199.0
10	3.72	13.58	.879	248.0
11	3.56	16.47	.871	277.0
12	4.46	5.22	.910	136.0
13	4.13	7.79	.888	175.0
14	3.92	10.27	.886	208.0
On plow*	5.33	1.98	.968	73.3

*In front of bay number 2.

(b) Cowl ($\delta_{xy} = 0^o$)

Bay	M	p/p_1	$p_t/p_{t,1}$	p_{pitot}/p_1
2	4.99	2.82	0.942	91.7
3	4.28	6.48	.907	156.0
4	3.67	14.40	.877	256.0
5	3.35	22.30	.867	333.0
6	3.04	34.90	.854	432.0
7	4.48	5.17	.930	136.0
8	3.86	11.30	.894	222.0
9	3.31	23.60	.870	344.0
10	2.88	43.40	.846	484.0
11	2.62	63.60	.829	592.0
12	4.28	64.80	.907	156.0
13	3.67	14.40	.877	257.0
14	3.35	22.40	.870	334.0

TABLE III.- CORRECTED THEORETICAL FLOW FIELD PROPERTIES

USED FOR FIGURE 27

Bay	M	p/p_1	p_t/p_1	δ_{xz}	δ_{xy}	A/A_1	p_{pitot}/p_1
1	6.00	1.00	1.000	0	0	1.00	46.8
2	5.07	2.54	.922	6.83	2.00	1.80	85.2
3	4.46	5.12	.891	0	3.18	2.96	133.0
4	3.97	9.44	.870	6.00	5.40	4.44	196.0
5	3.70	13.61	.866	2.00	6.52	5.66	246.0
6	3.45	19.14	.862	6.00	8.27	7.07	302.0
7	4.66	4.09	.912	10.83	3.19	2.56	116.0
8	4.07	8.37	.879	4.00	5.20	4.11	182.0
9	3.59	15.55	.858	10.83	8.14	6.16	265.0
10	3.24	25.52	.842	4.83	10.28	8.45	357.0
11	---	----	----	----	----	---	----
12	4.38	5.59	.879	0	3.44	3.13	141.0
13	3.90	10.19	.859	-6.00	5.71	4.65	204.0
14	3.64	14.62	.857	-2.00	6.87	5.91	256.0
*15	3.40	20.40	.852	-6.00	8.66	7.34	313.0
16	3.24	25.28	.835	4.83	11.30	8.38	354.0

*For large center strut.

TABLE IV.- CORRECTED THEORETICAL END EFFECTS USED FOR FIGURE 27

(a) Top surface ($\delta_{xy} = 4^o$)

Bay	M	p/p_1	$p_t/p_{t,1}$	p_{pitot}/p_1
2	4.86	3.25	0.921	100.0
3	4.39	5.61	.891	142.0
4	4.07	8.26	.870	180.0
5	3.88	10.60	.866	210.0
6	3.73	12.90	.862	522.0
7	4.58	4.46	.912	123.0
8	4.17	7.34	.879	168.0
9	3.87	10.60	.858	209.0
10	3.63	14.60	.842	254.0
11	---	----	----	----
12	4.33	5.95	.878	146.0
13	4.03	8.56	.859	183.0
14	3.84	11.10	.857	216.0
*15	3.70	13.40	.852	242.0
16	3.69	13.80	.835	248.0

*For large center strut.

(b) Cowl ($\delta_{xy} = 0^o$)

Bay	M	p/p_1	$p_t/p_{t,1}$	p_{pitot}/p_1
2	4.86	3.25	0.921	100.0
3	4.18	7.22	.996	166.0
4	3.57	15.80	.858	267.0
5	3.28	24.30	.849	348.0
6	2.97	37.80	.835	447.0
7	4.35	6.52	.902	162.0
8	3.68	13.40	.867	240.0
9	3.10	31.10	.829	399.0
10	2.69	56.30	.801	551.0
11	---	----	----	----
12	4.11	8.08	.873	180.0
13	3.50	17.40	.845	283.0
14	3.22	26.60	.838	368.0
*15	2.90	41.10	.822	465.0
16	2.63	59.90	.783	562.0

*For large center strut.

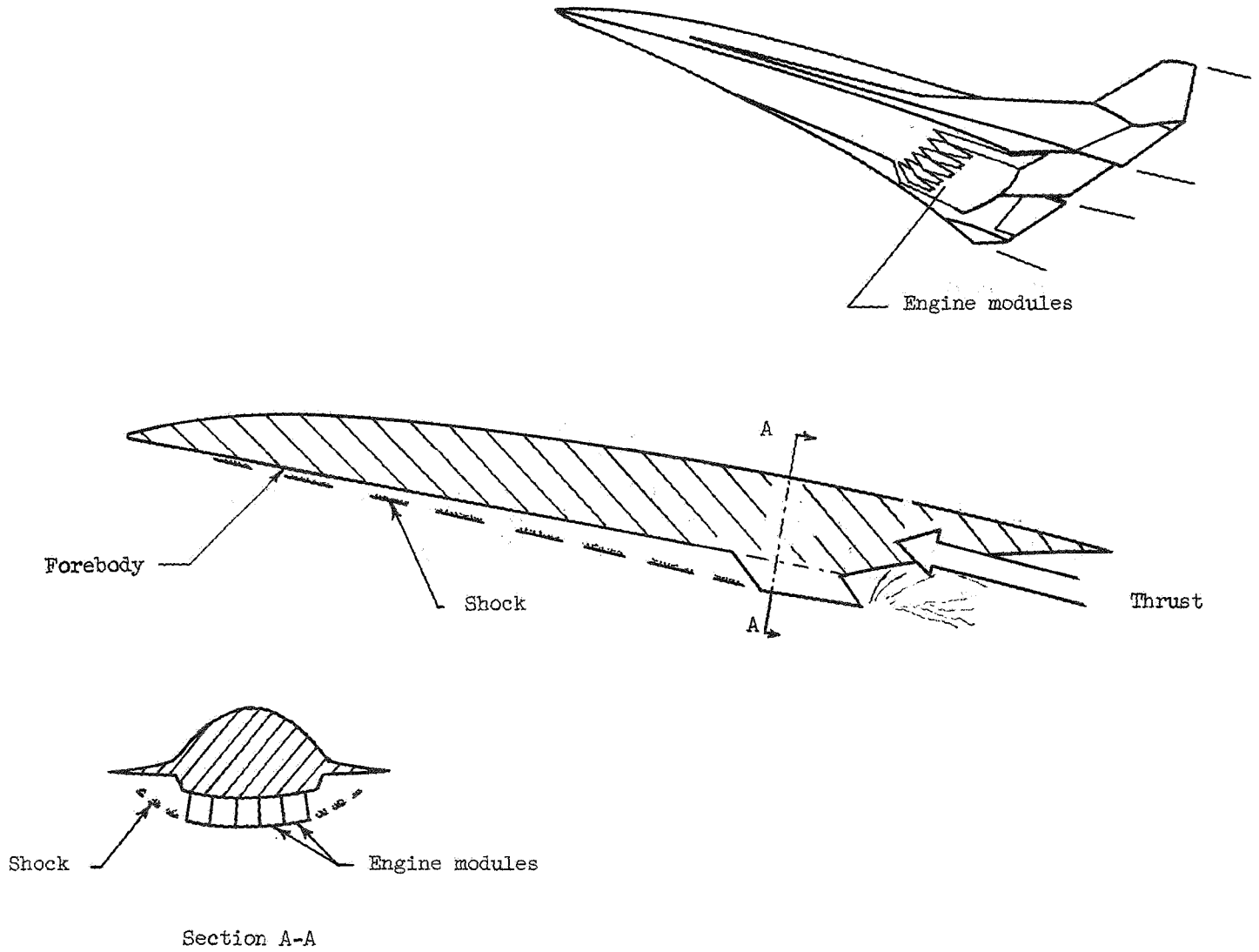

Figure 1.- Airframe-scramjet-engine integration.

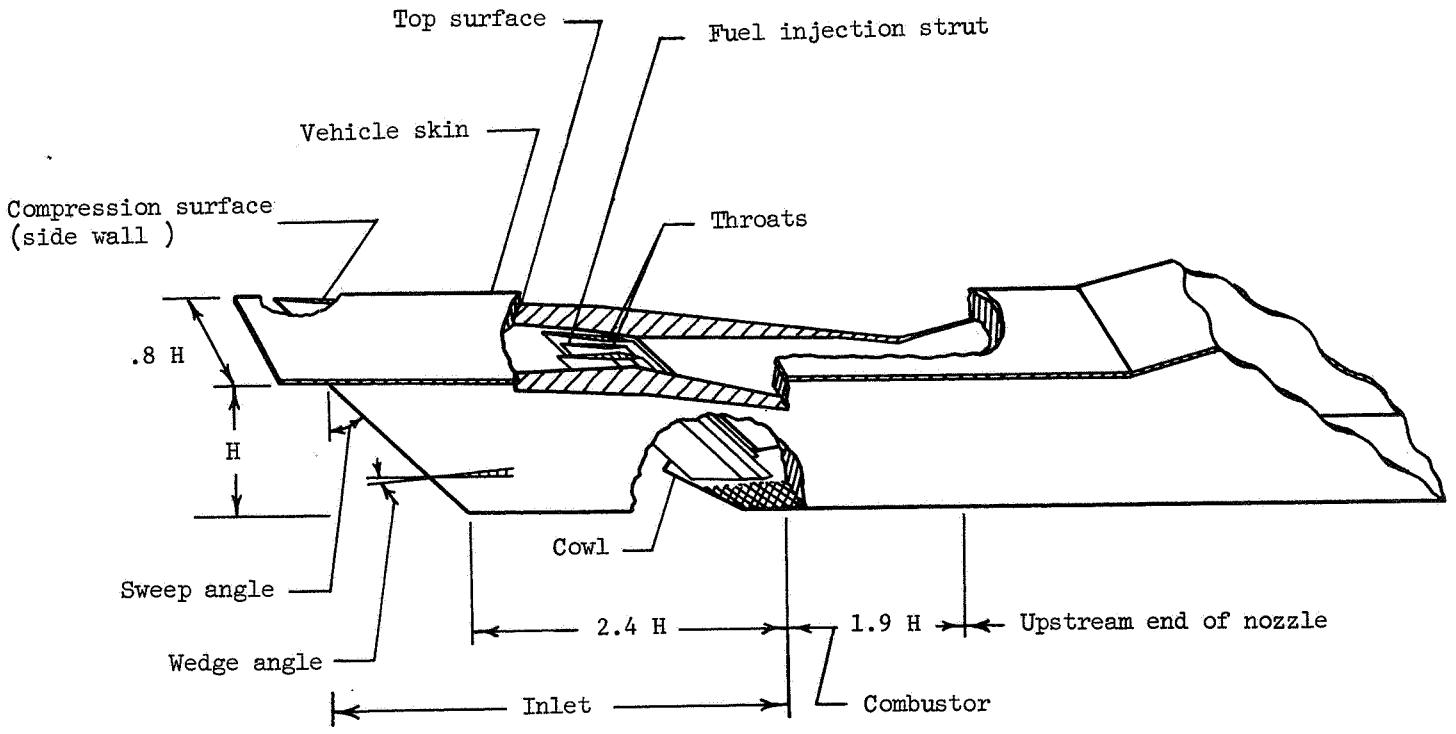

Figure 2.- Inner module of scramjet engine concept (ref. 8).

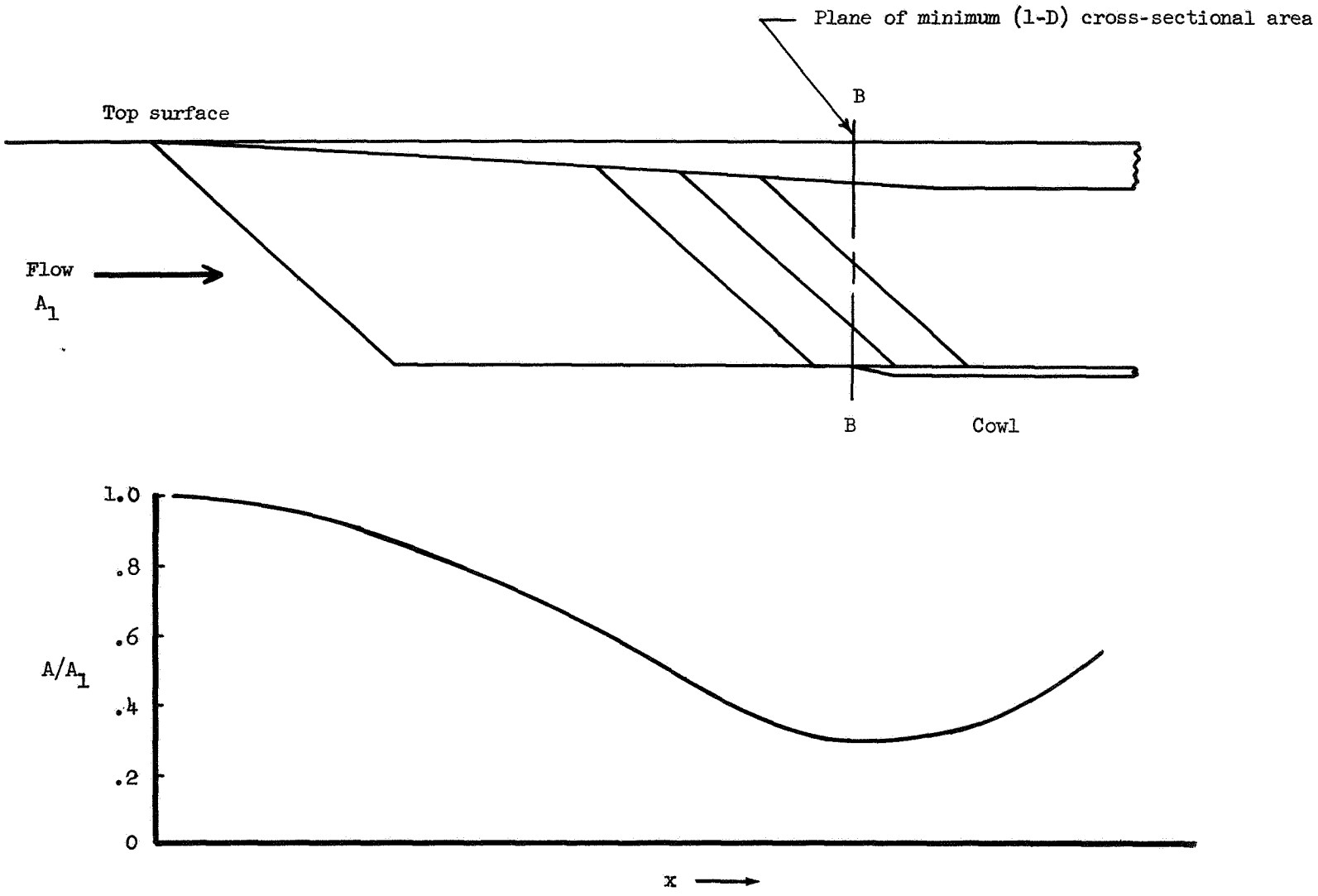

Figure 3.- One-dimensional inlet contraction.

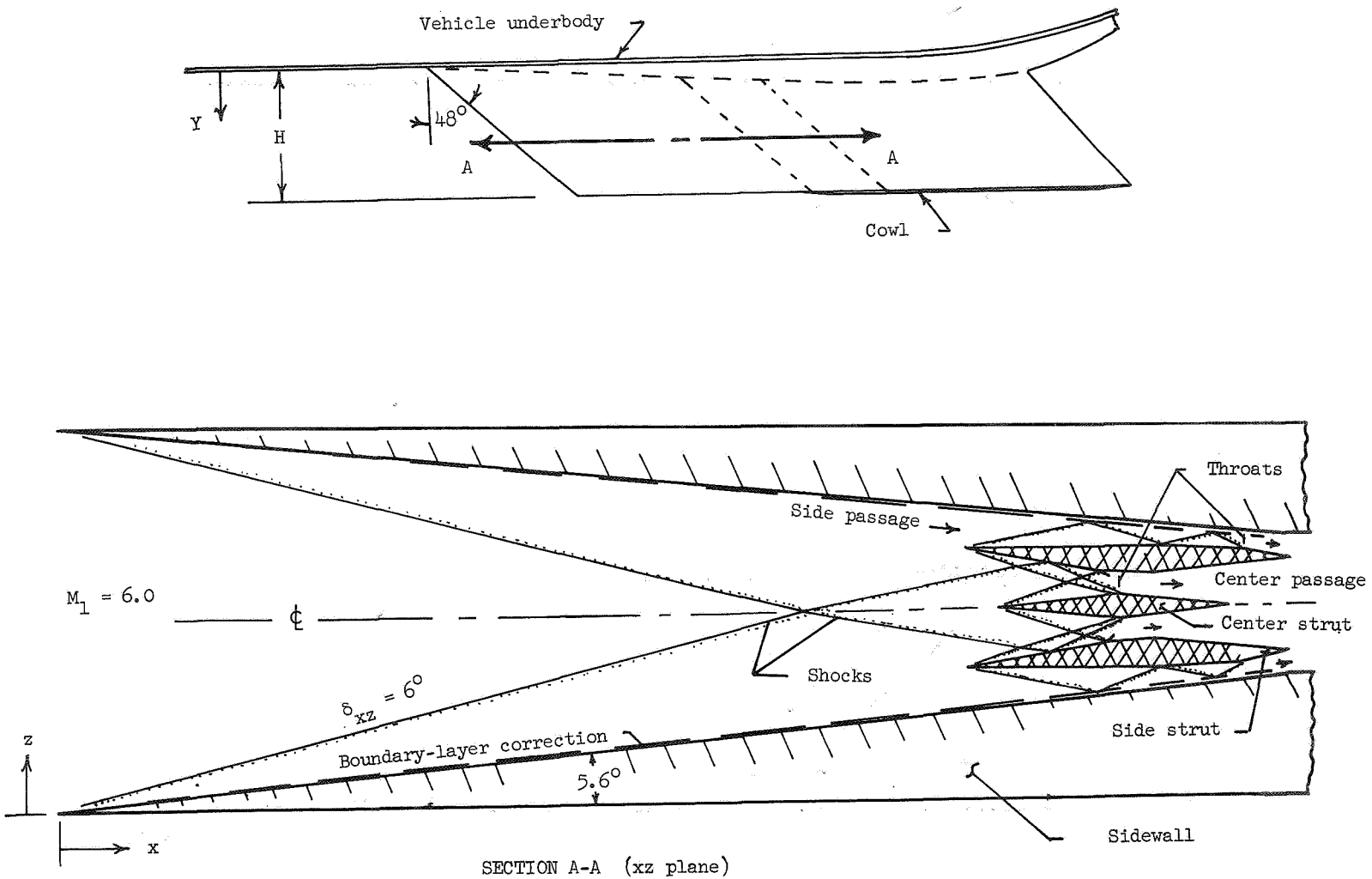

Figure 4.- Inlet model sketch and Mach 6 shock diagram.

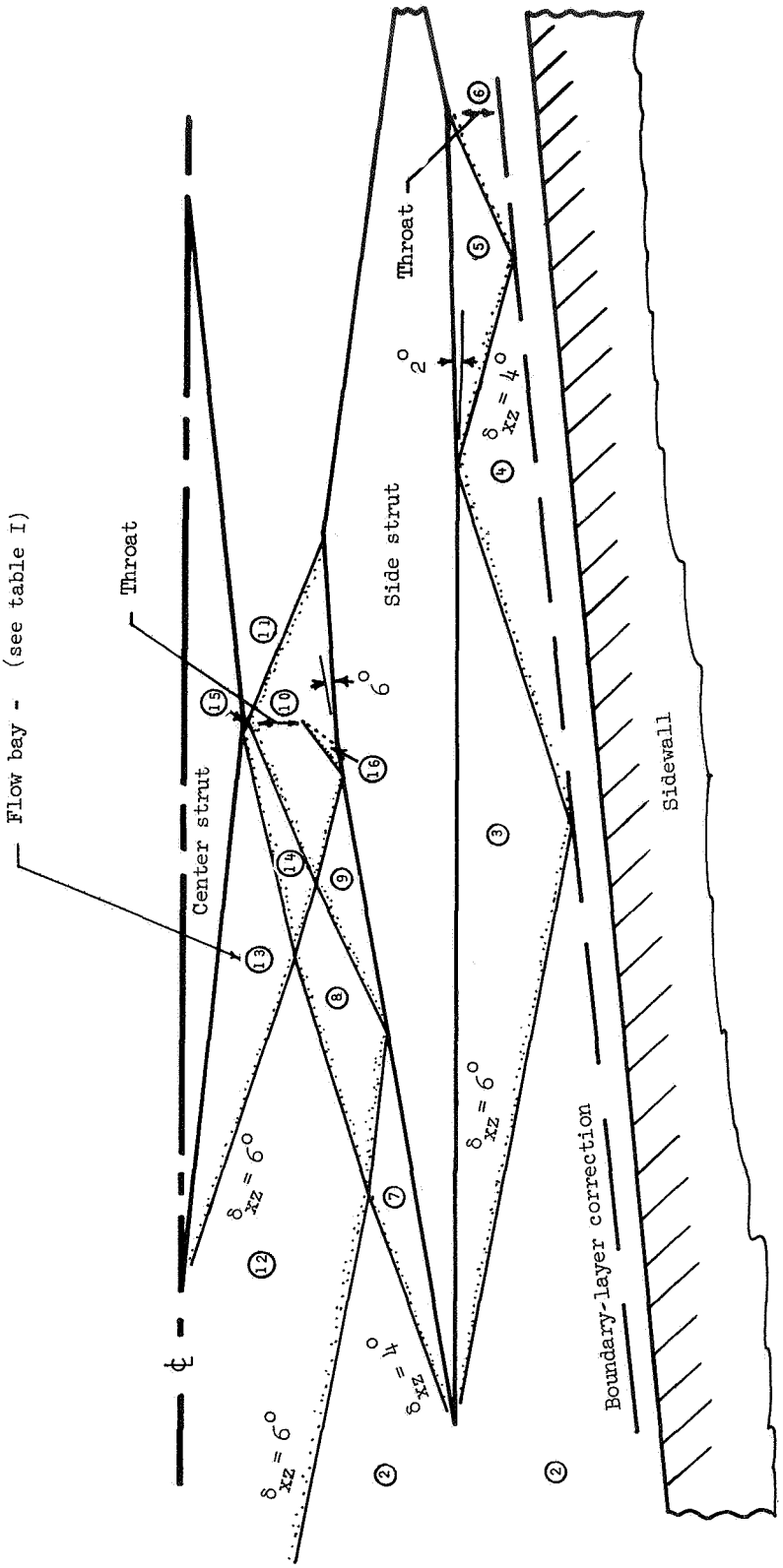

Figure 5.- Shock-wave detail in vicinity of struts. $M_1 = 6.0$.

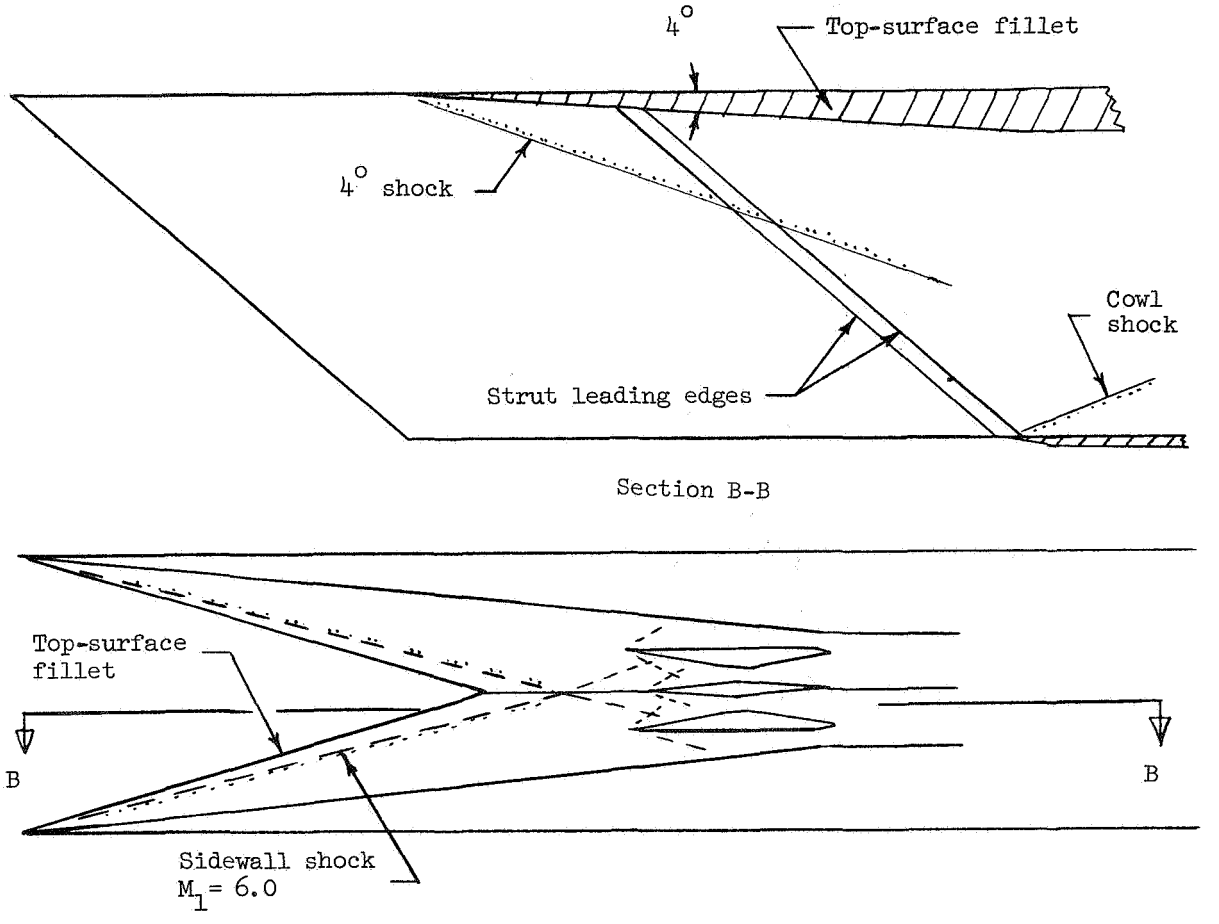

(a) Top surface.

Figure 6.- Theoretical end effects.

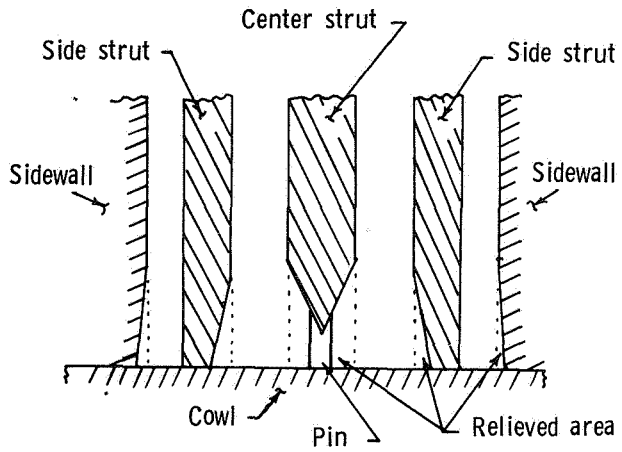

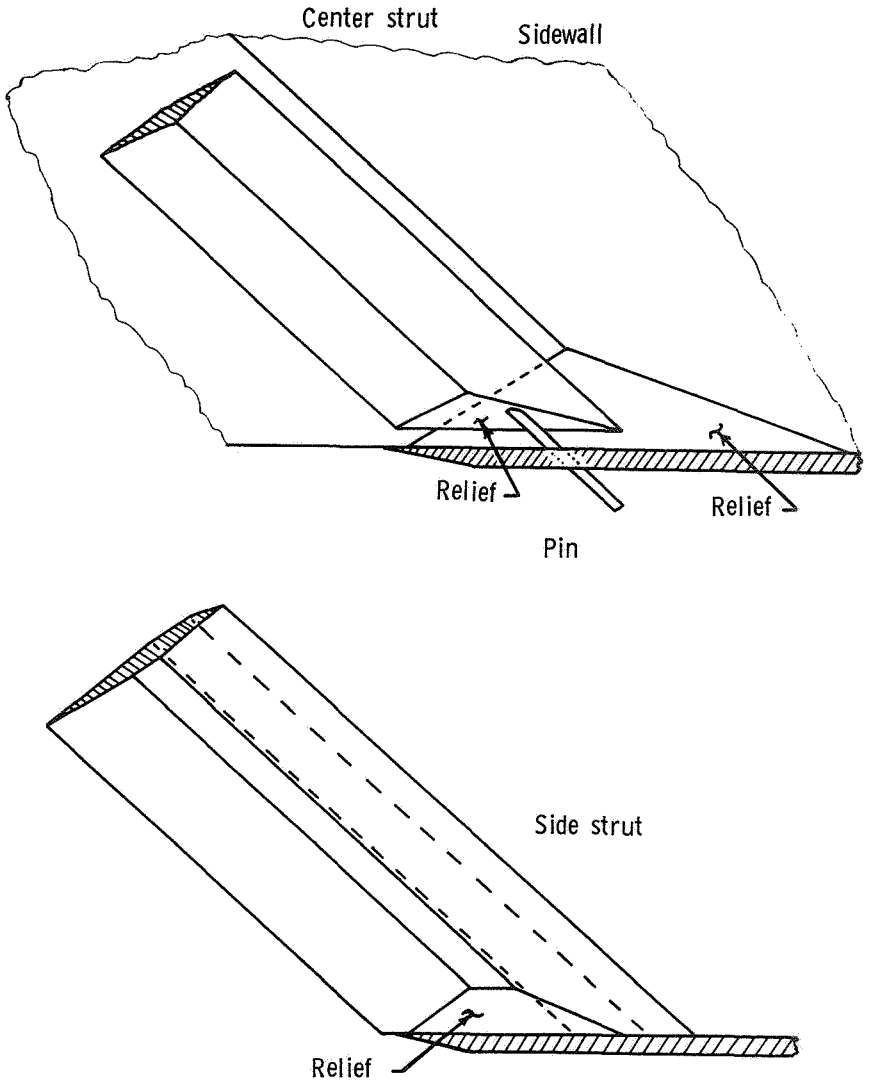

(b) Throat relief next to cowl.

Figure 6.- Continued.

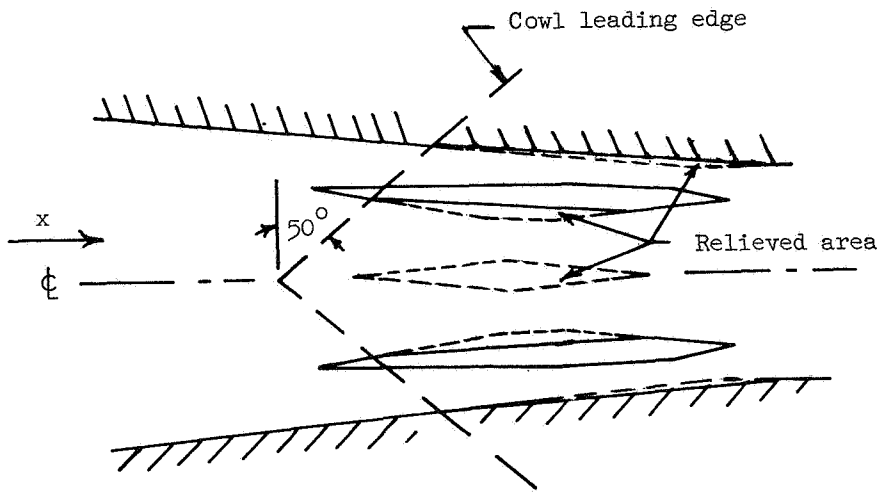

(c) Cowl leading-edge design.

Figure 6.- Concluded.

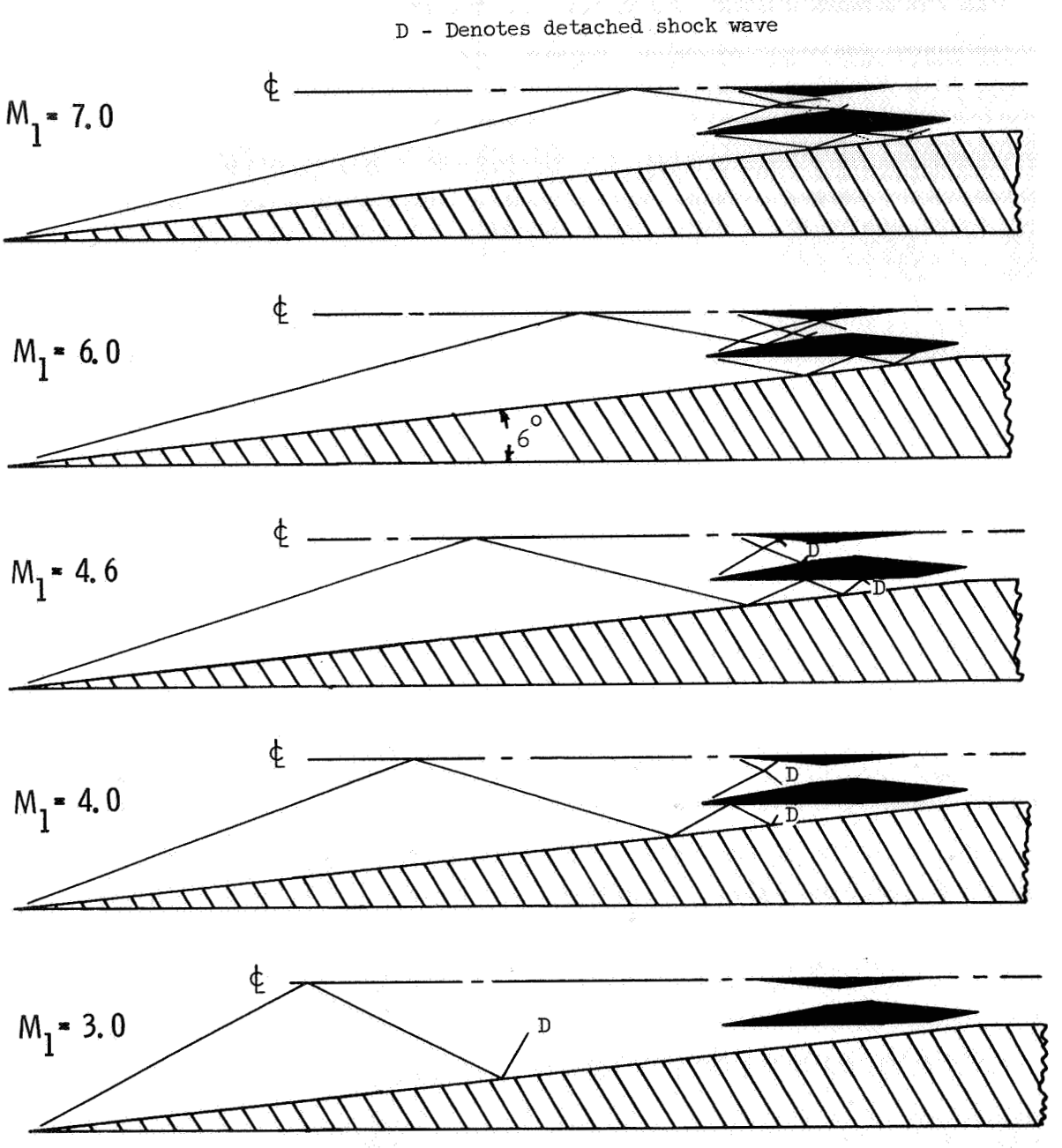

Figure 7.- Off-design shock wave systems (xz-plane). Sweep = 48°.

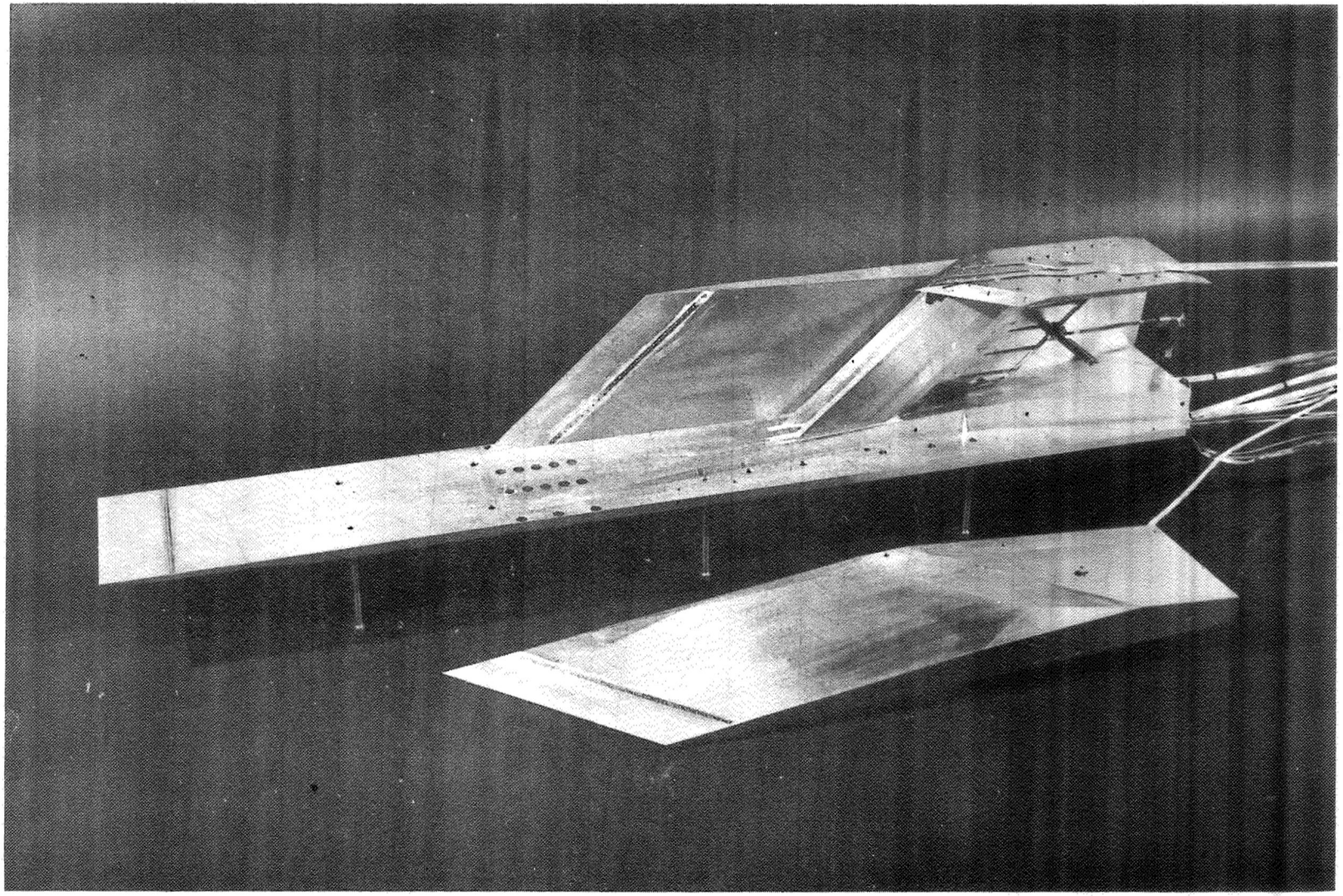

L-72-7495

(a) Side view.

Figure 8.- Model photograph.

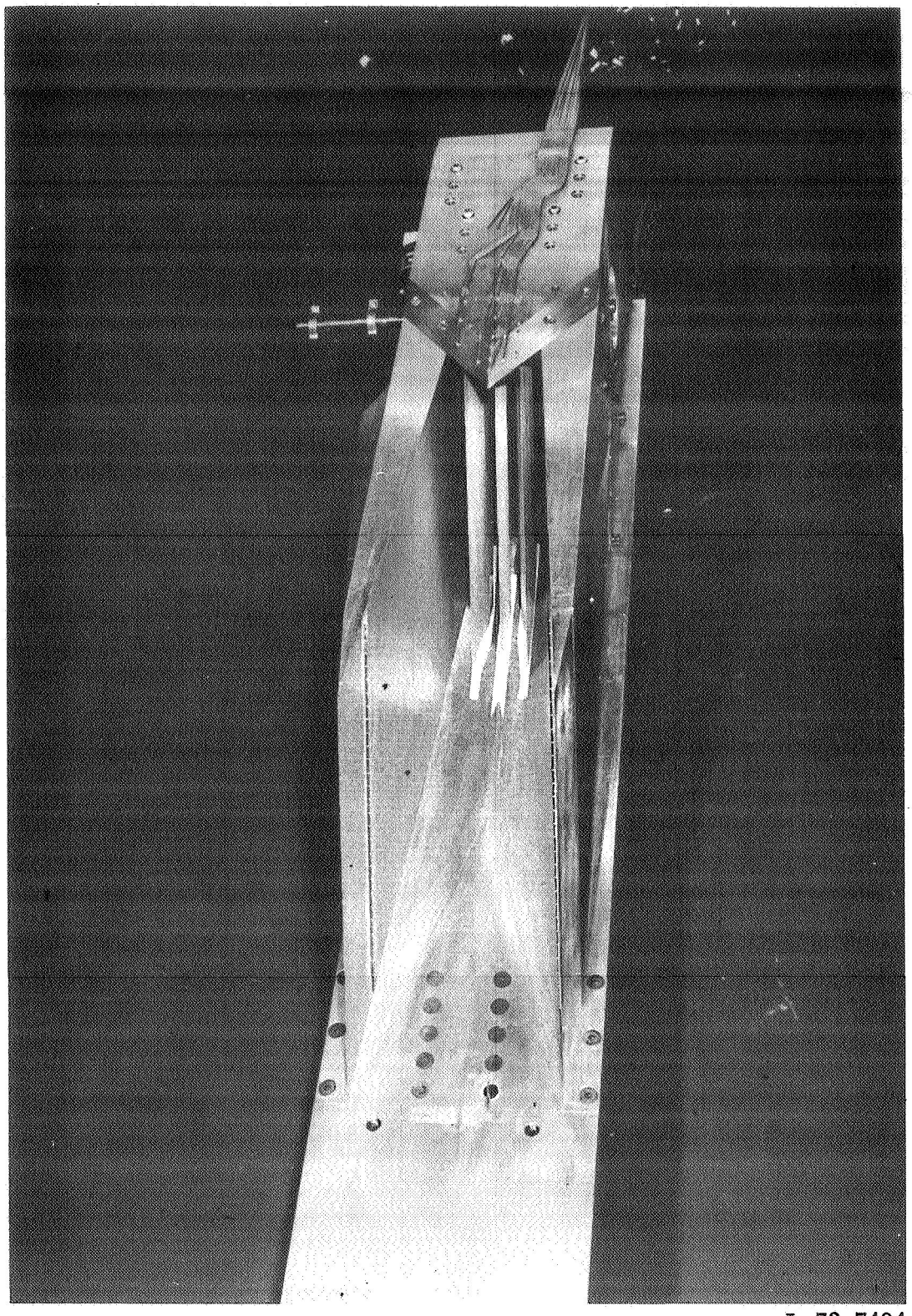

L-72-7494

(b) Front view.

Figure 8.- Concluded.

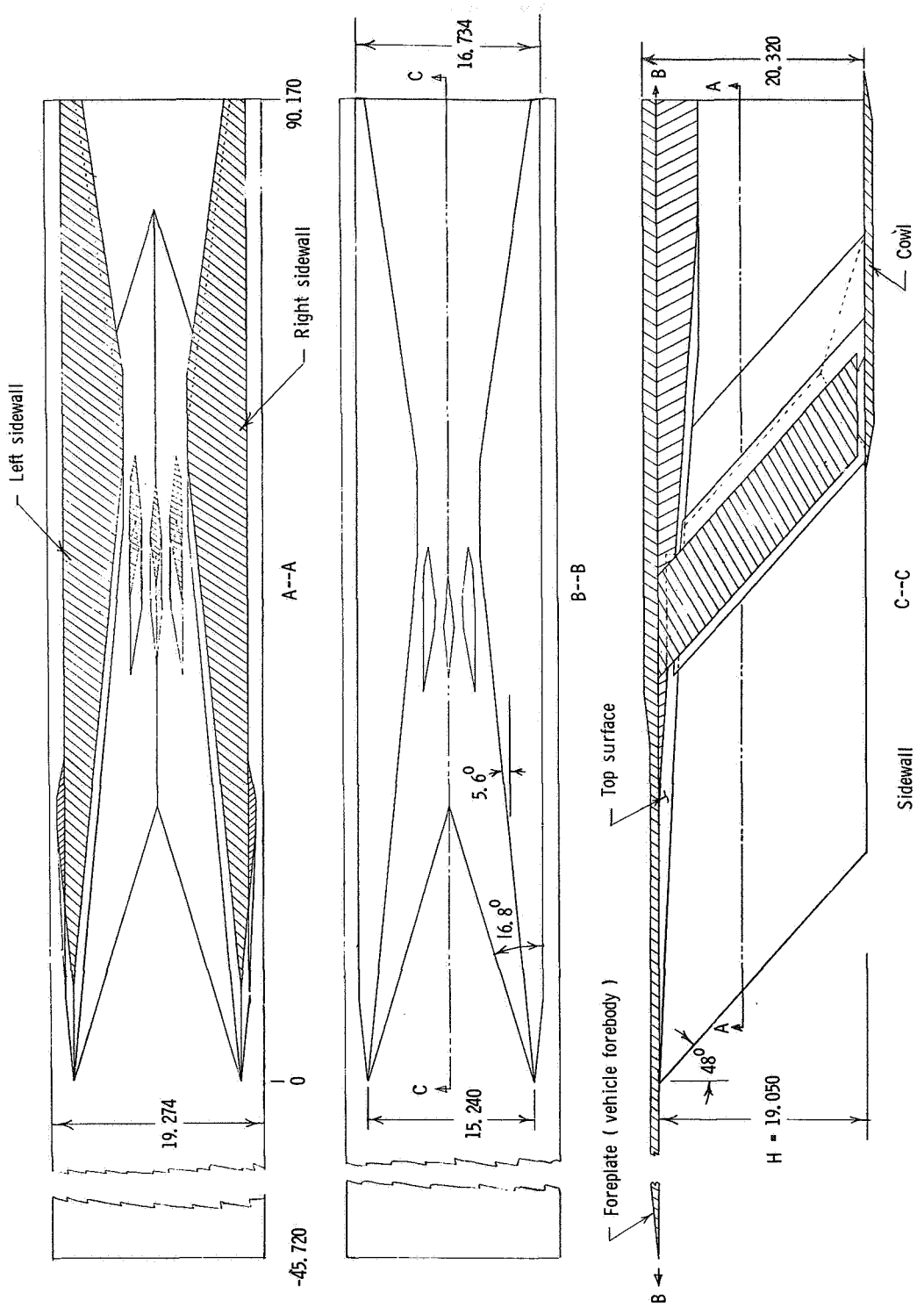

Figure 9.- Model schematics. All dimensions are in centimeters.

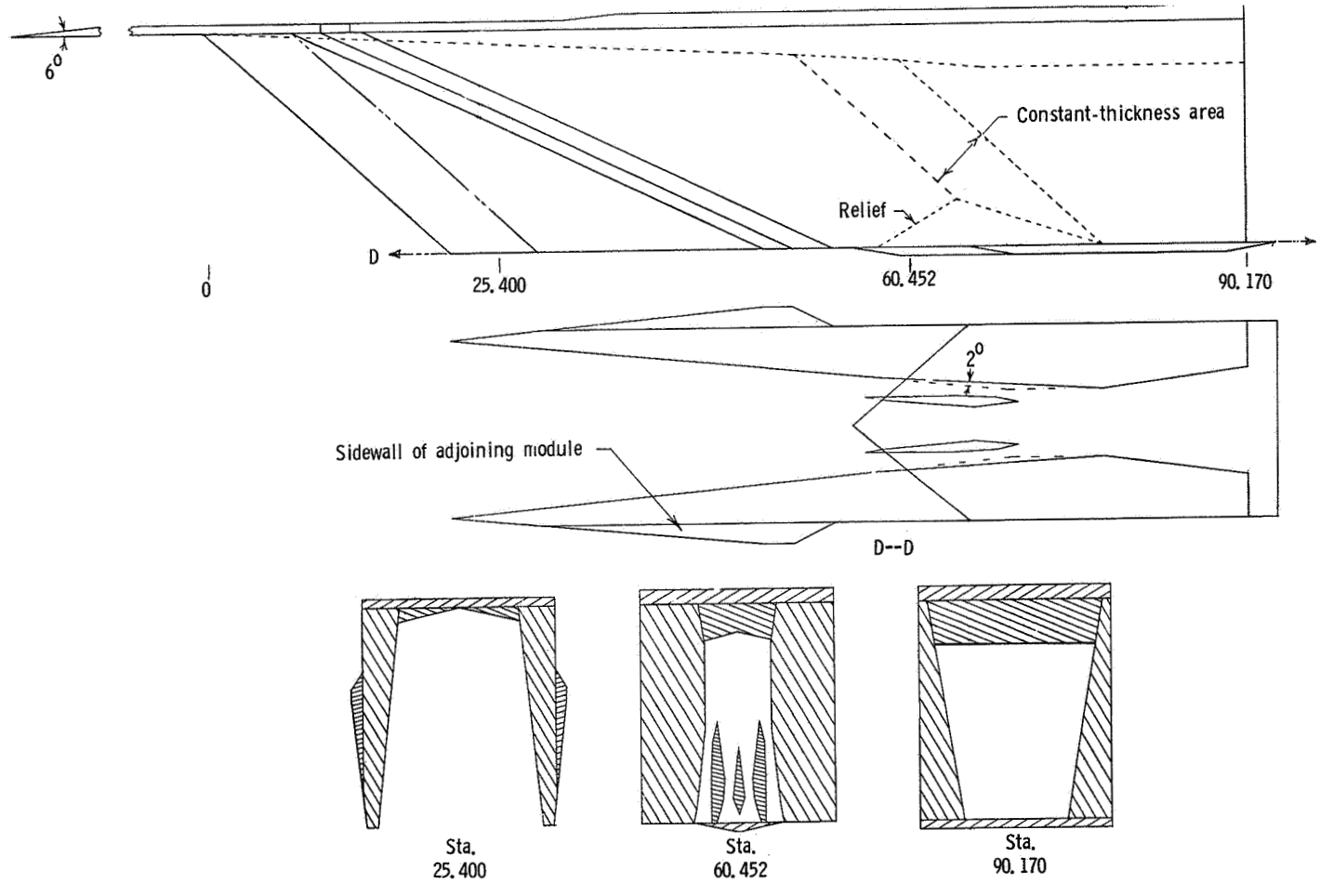

Figure 9.- Concluded.

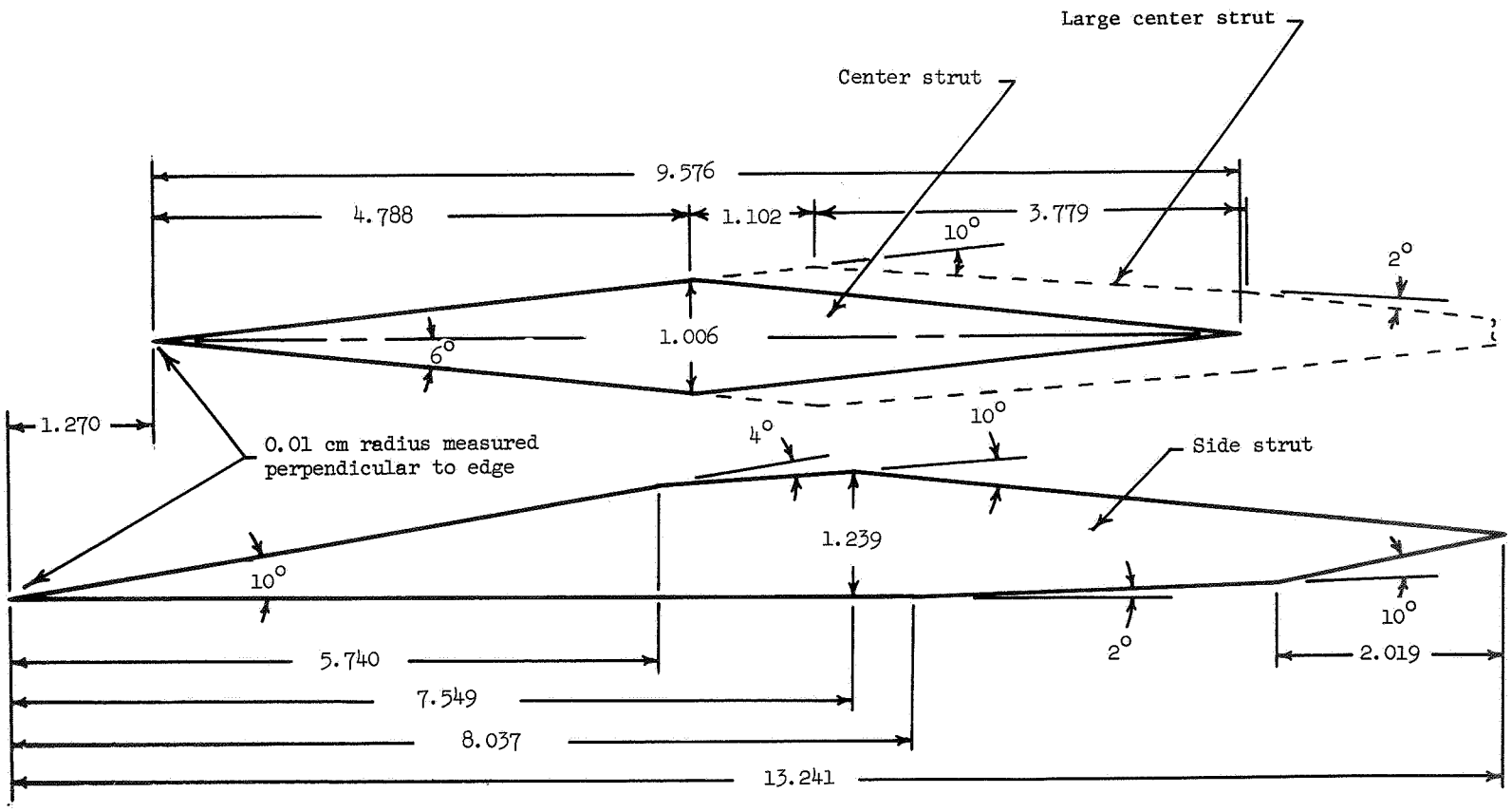

Figure 10.- Side and center strut dimensions as measured in the xz-plane. All dimensions are in centimeters.

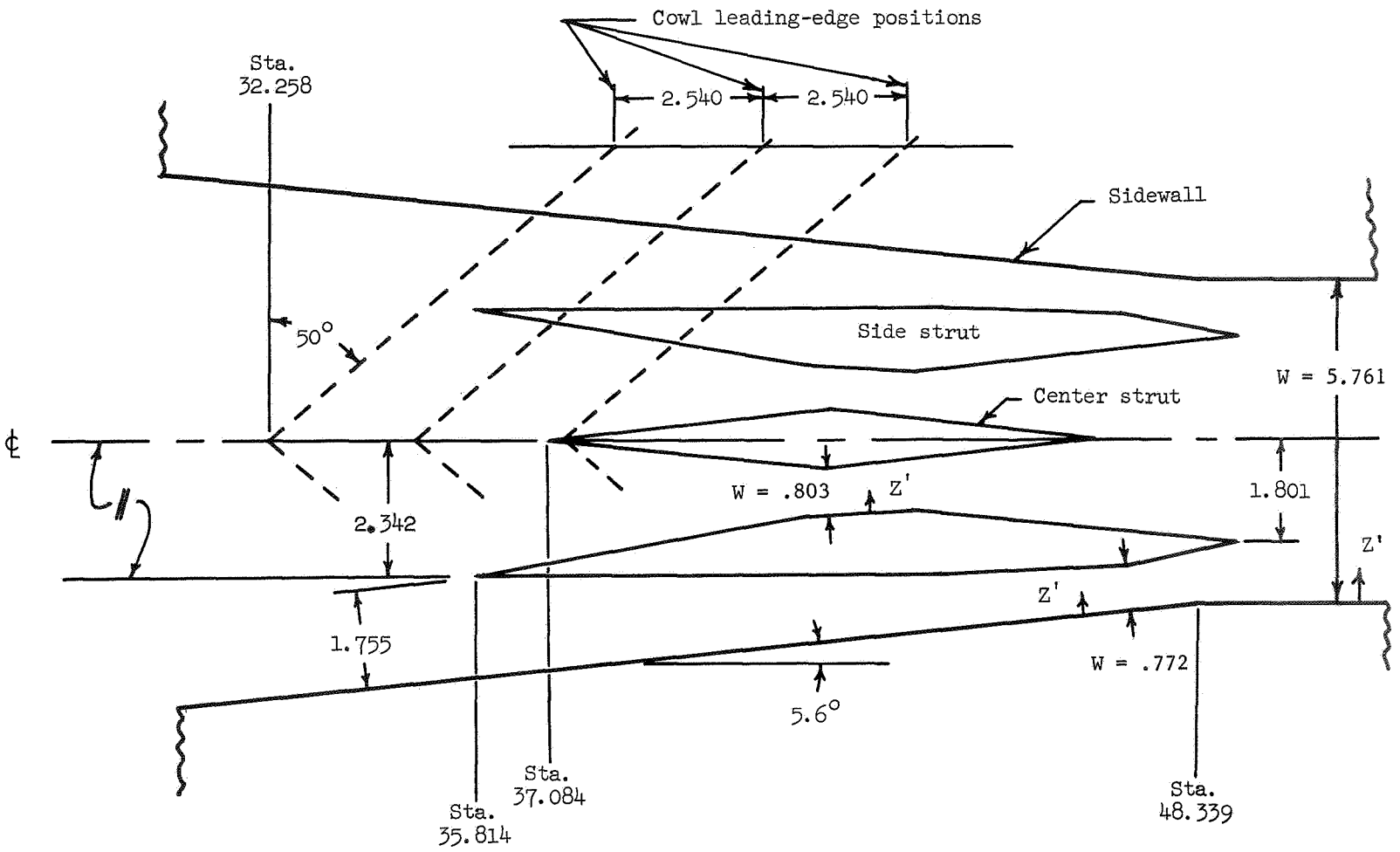

Figure 11.- Relative positions of struts and cowl in xz-planes. All dimensions are in centimeters. Stations are measured relative to sidewall leading edge; cowl leading edge shown at $y = H$.

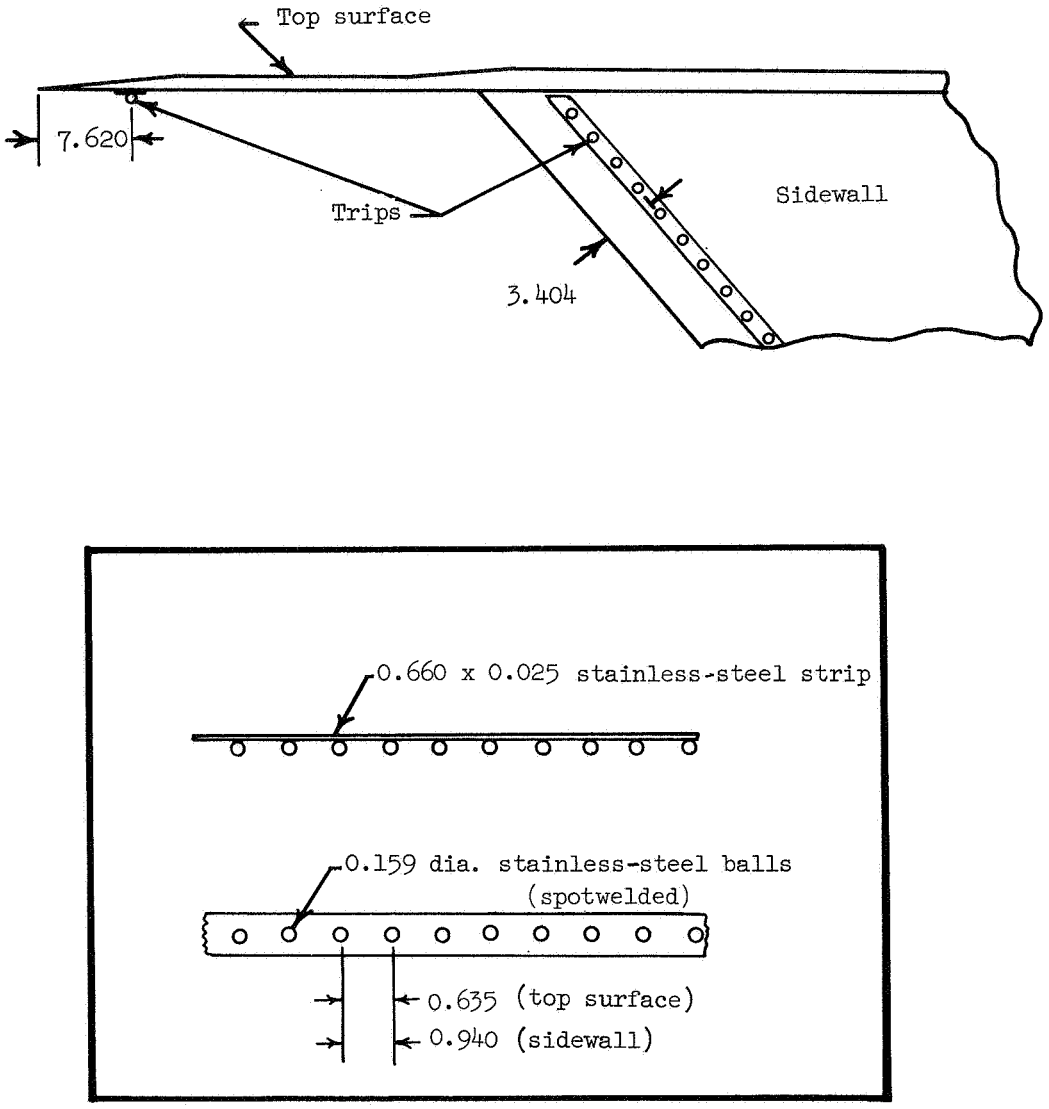

Figure 12.- Boundary-layer trips. All dimensions are in centimeters.

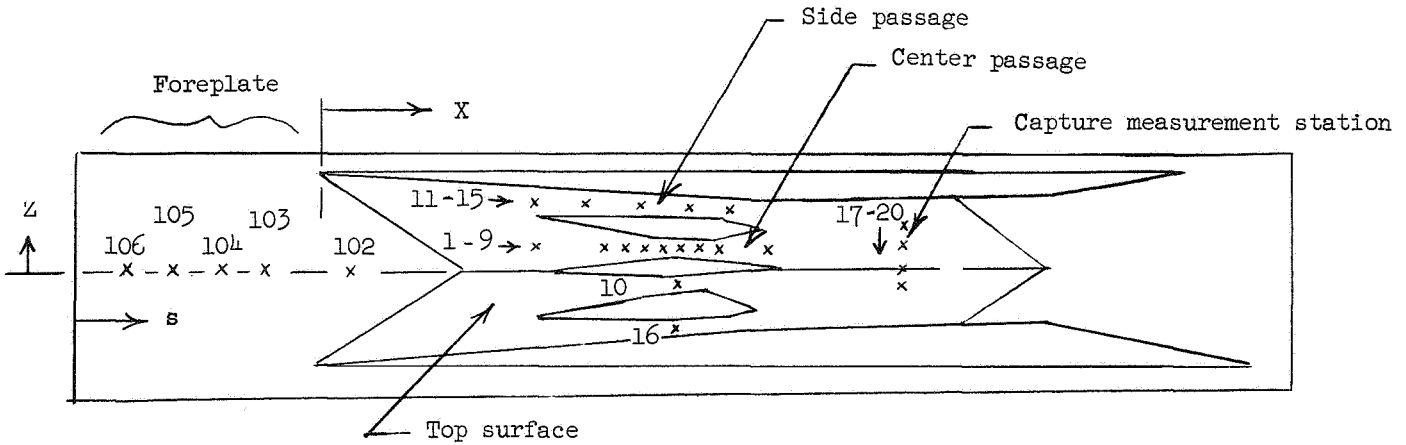

Orifice	s/H	Z/H
106	.733	0
105	1.267	0
104	1.800	0
103	2.333	0
102	3.040	0

(a) Foreplate.

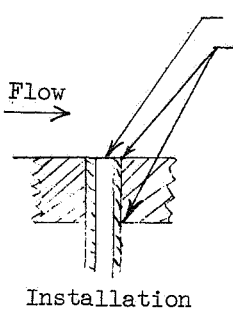

Orifice	X/H	Z/H	Orifice	X/H	Z/H
1	1.747	.058	11	1.693	.175
2	2.013	.053	12	1.960	.163
3	2.080	.052	13	2.227	.151
4	2.147	.051	14	2.427	.142
5	2.213	.050	15	2.560	.136
6	2.280	.049	16	2.227	-.151
7	2.347	.048	17	3.040	.107
8	2.480	.045	18	3.040	.053
9	2.747	.041	19	3.040	0
10	2.213	.050	20	3.040	-.053

(b) Top surface.

Figure 13.- Static orifice locations. H = 19.05 cm.

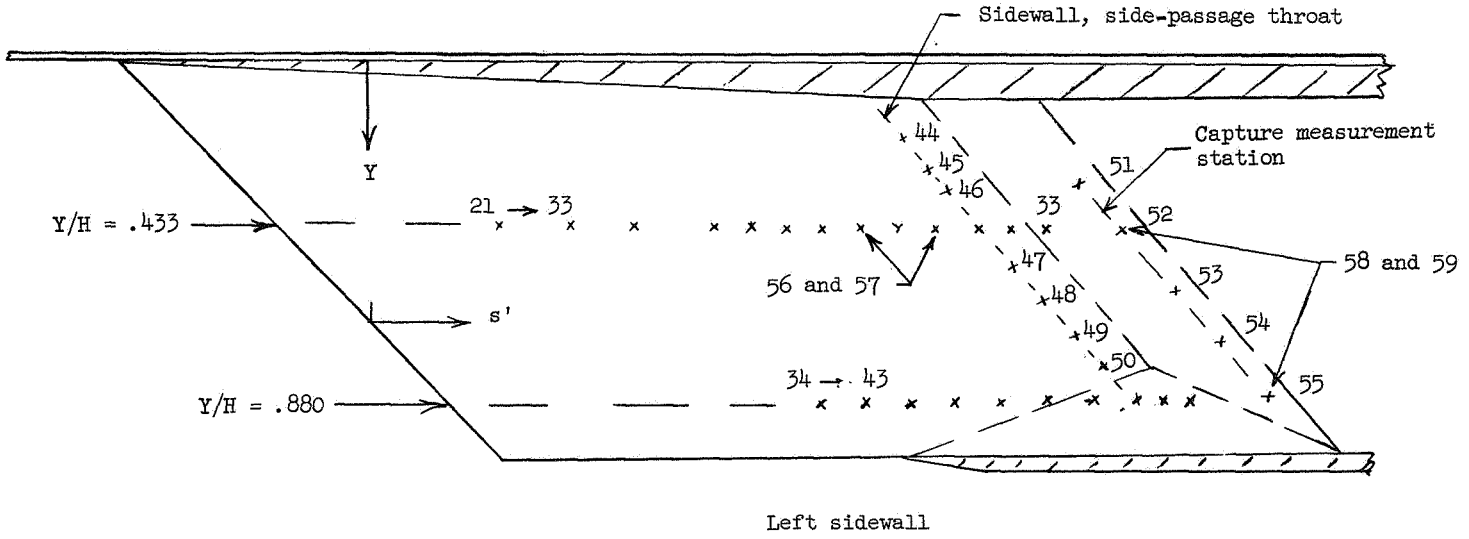

Left sidewall

Orifice	s'/H	Y/H
21	.924	.433
22	1.191	.433
23	1.457	.433
24	1.724	.433
25	1.857	.433
26	1.991	.433
27	2.124	.433
28	2.257	.433
29	2.324	.433
30	2.391	.433

Orifice	s'/H	Y/H
31	2.457	.433
32	2.524	.433
33	2.591	.433
34	1.591	.880
35	1.724	.880
36	1.857	.880
37	1.991	.880
38	2.124	.880
39	2.257	.880
40	2.391	.880

Orifice	s'/H	Y/H
41	2.457	.880
42	2.524	.880
43	2.591	.433
44	2.457	.166
45	2.457	.255
46	2.457	.344
47	2.497	.522
48	2.457	.612
49	2.457	.701
50	2.457	.790

Orifice	s'/H	Y/H
51	2.907	.284
52	2.907	.433
53	2.907	.582
54	2.907	.731
55	2.907	.880
*56	2.257	.433
*57	2.391	.433
*58	2.907	.433
*59	2.907	.880

*Right sidewall

(c) Sidewall.

Figure 13.- Continued.

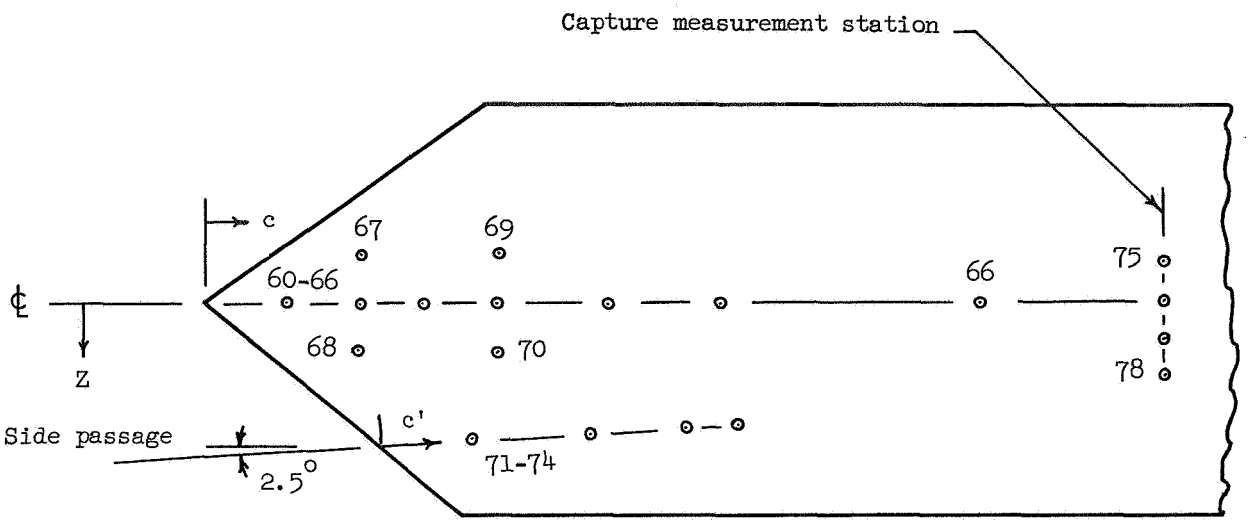

Orifice	c/H	Z/H
60	.093	0
61	.160	0
62	.227	0
63	.293	0
64	.427	0
65	.560	0
66	.827	0
67	.160	-.056
68	.160	.056
69	.293	-.056
70	.293	.056

Orifice	c'/H	Z/H
71	.087	.163
72	.220	.157
73	.353	.151
74	.420	.149
Orifice	**c /H**	**Z/H**
75	1.080	-.053
76	1.080	0
77	1.080	.053
78	1.080	.107

(d) Cowl.

Figure 13.- Continued.

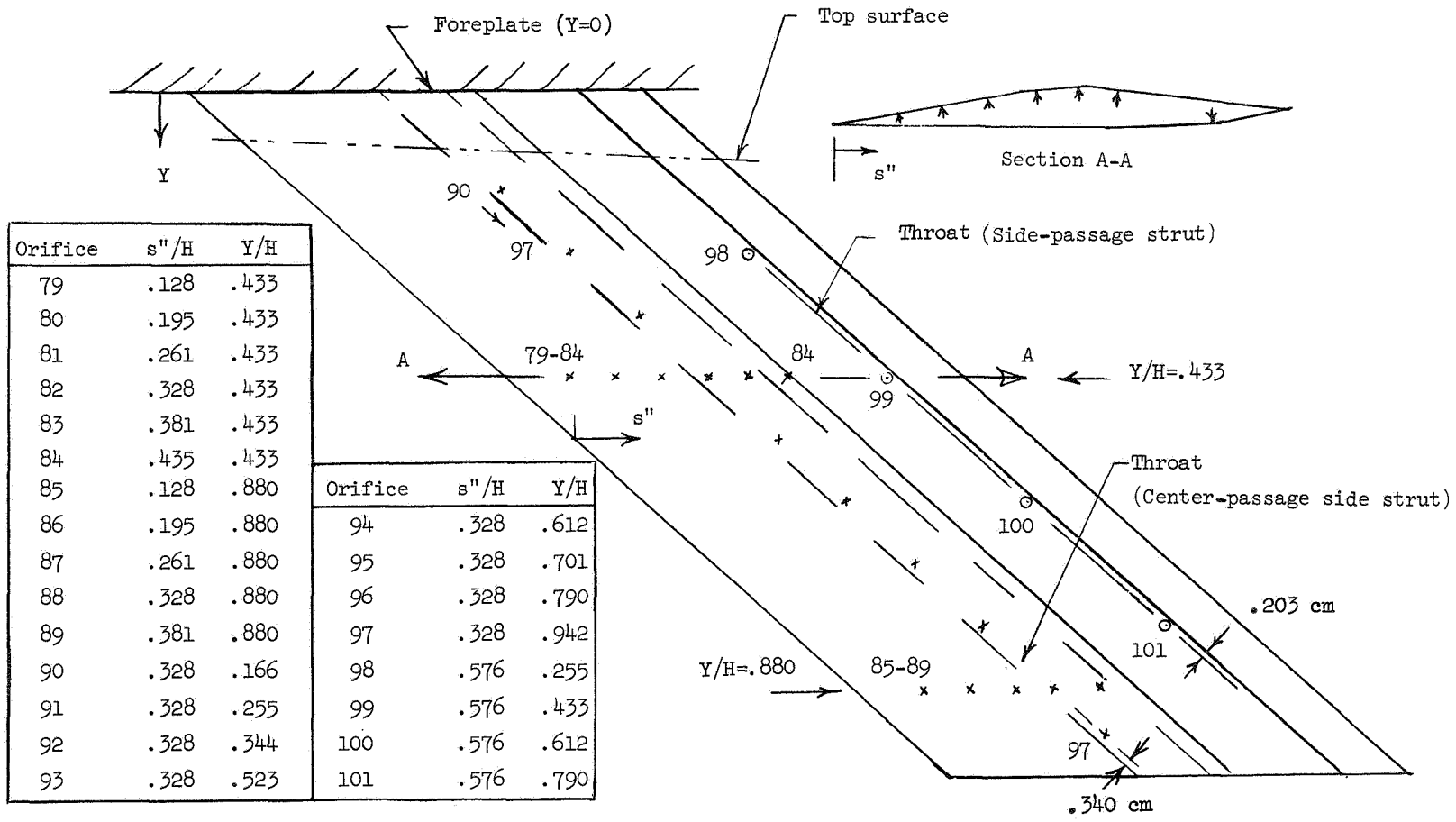

Orifice	s"/H	Y/H
79	.128	.433
80	.195	.433
81	.261	.433
82	.328	.433
83	.381	.433
84	.435	.433
85	.128	.880
86	.195	.880
87	.261	.880
88	.328	.880
89	.381	.880
90	.328	.166
91	.328	.255
92	.328	.344
93	.328	.523

Orifice	s"/H	Y/H
94	.328	.612
95	.328	.701
96	.328	.790
97	.328	.942
98	.576	.255
99	.576	.433
100	.576	.612
101	.576	.790

(e) Left side strut.

Figure 13.- Continued.

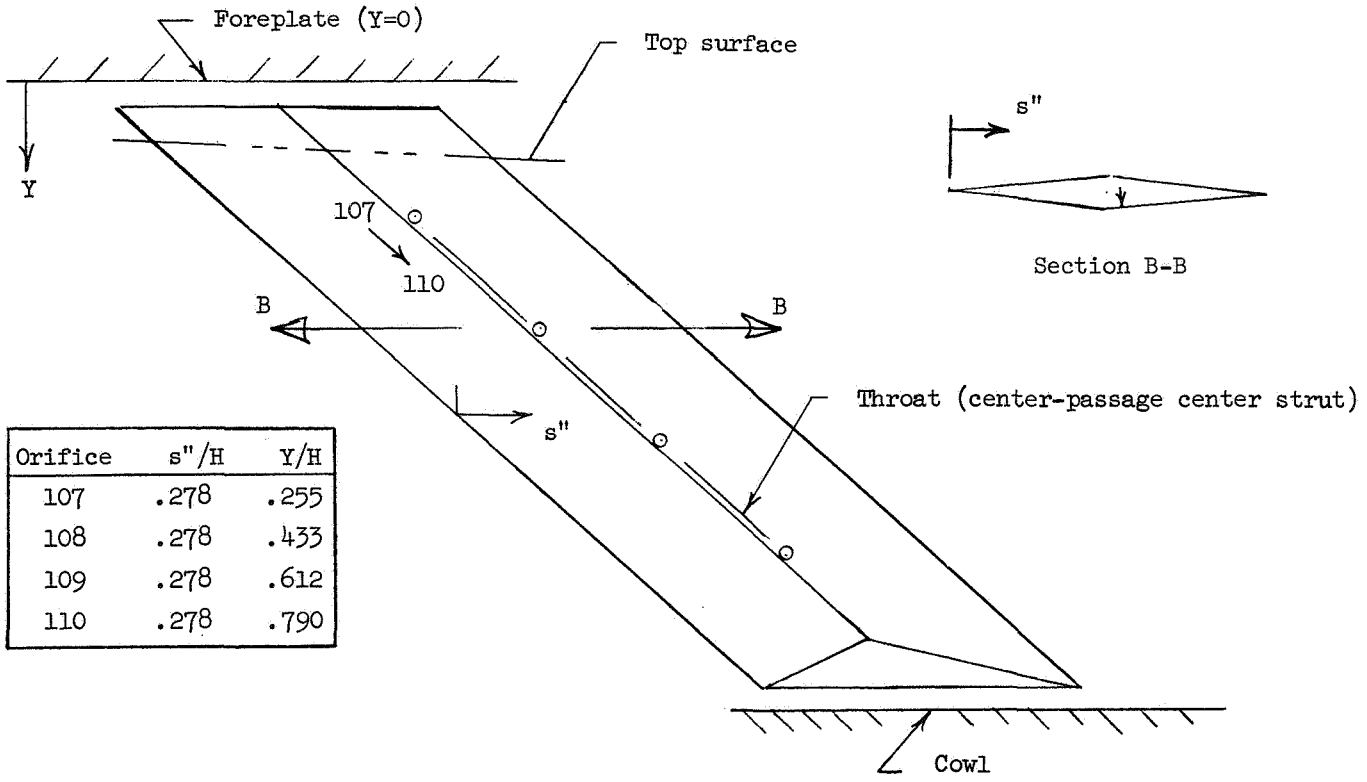

Orifice	s"/H	Y/H
107	.278	.255
108	.278	.433
109	.278	.612
110	.278	.790

(f) Center strut.

Figure 13.- Continued.

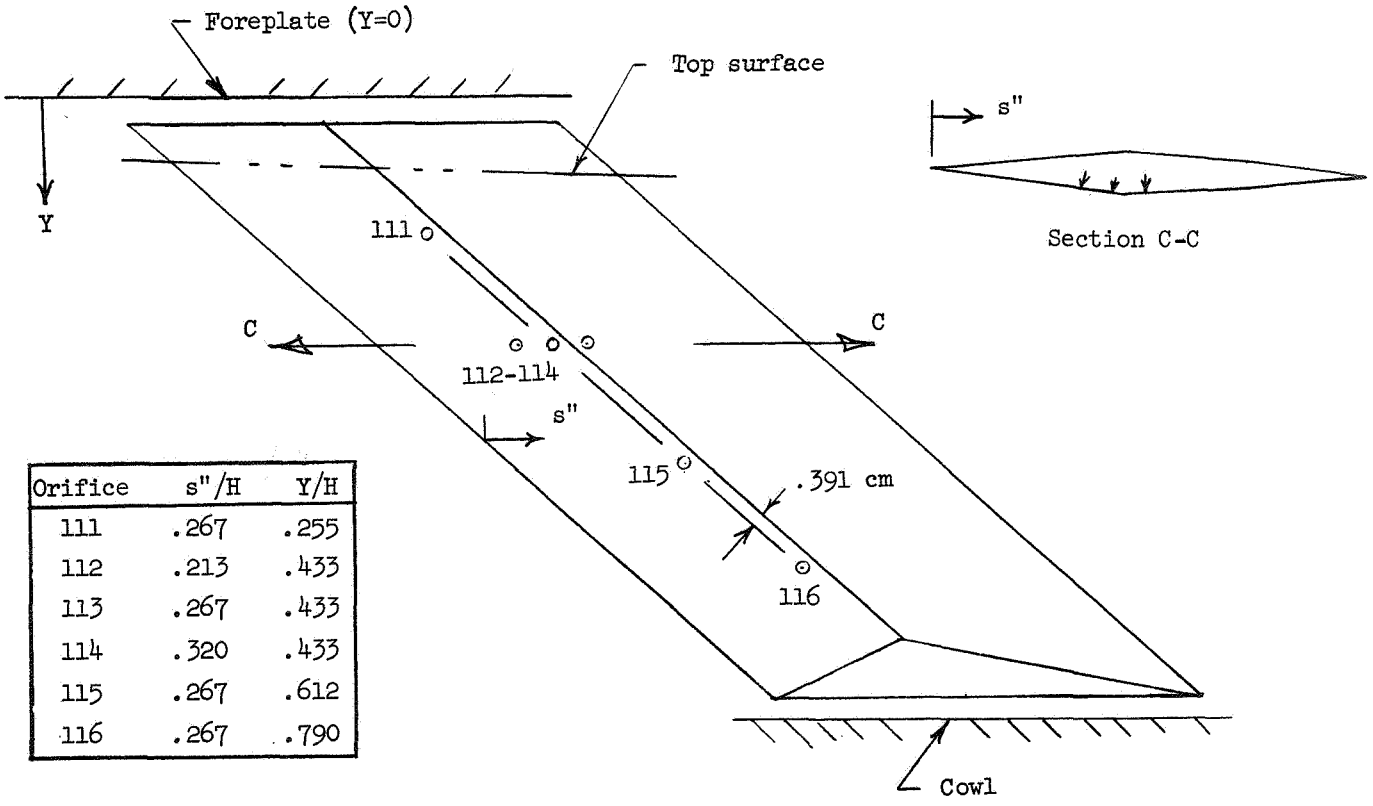

Orifice	s"/H	Y/H
111	.267	.255
112	.213	.433
113	.267	.433
114	.320	.433
115	.267	.612
116	.267	.790

(g) Large center strut.

Figure 13.- Concluded.

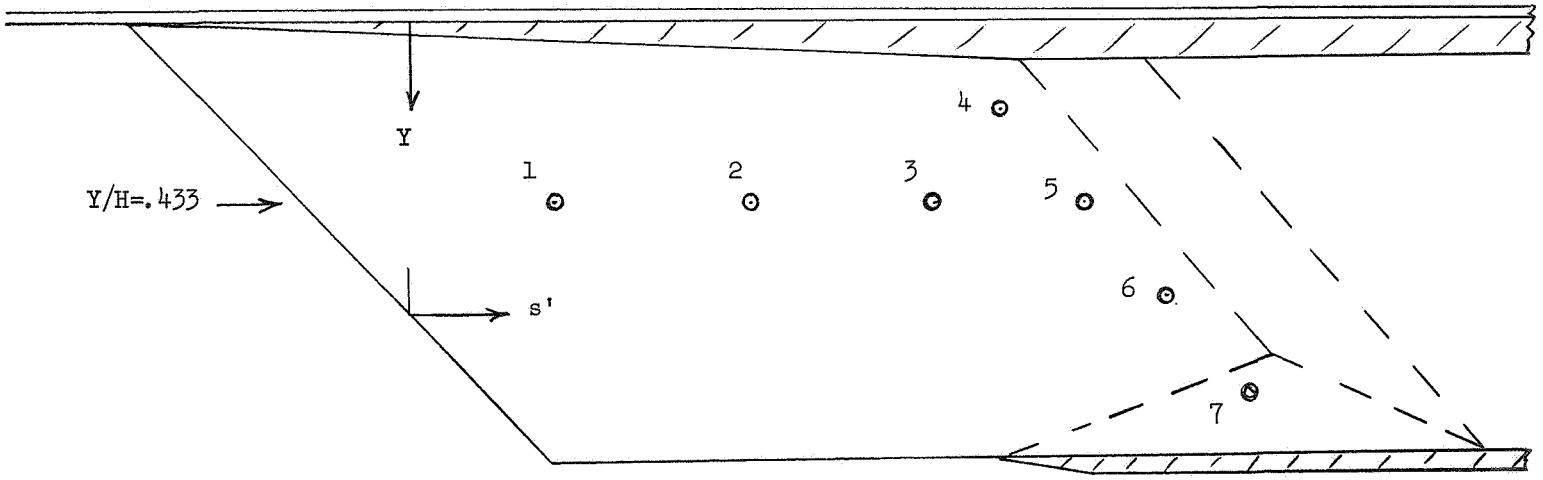

Right sidewall

Thermocouple	s'/H	Y/H
1	.924	.433
2	1.591	.433
3	2.057	.433
4	2.457	.210
5	2.457	.433
6	2.457	.656
7	2.457	.880

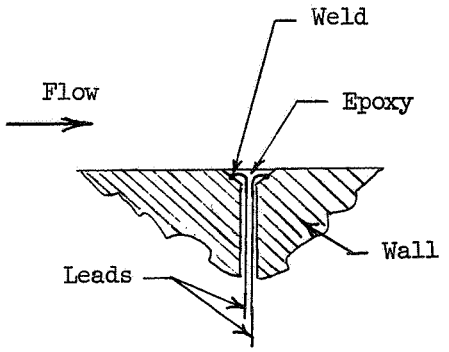

Thermocouple installation

Figure 14.- Thermocouple locations. H = 19.05 cm; 24-gage iron-constantan.

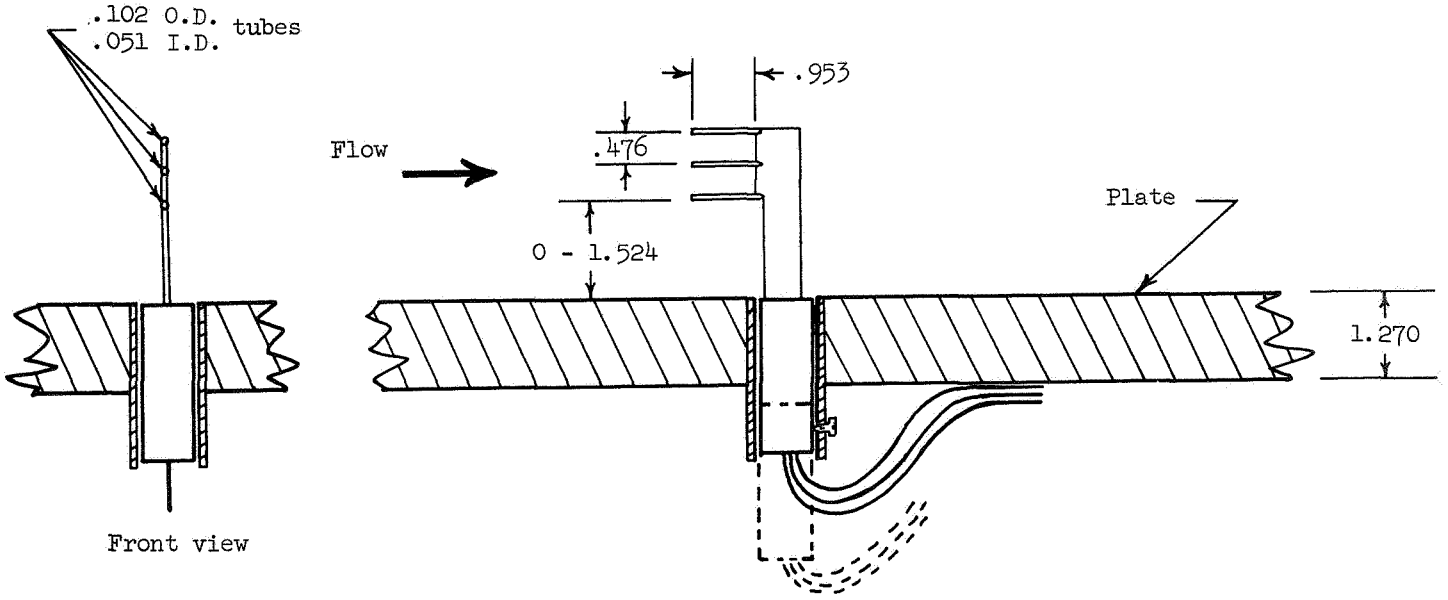

Figure 15.- Foreplate boundary-layer probe. All dimensions are in centimeters.

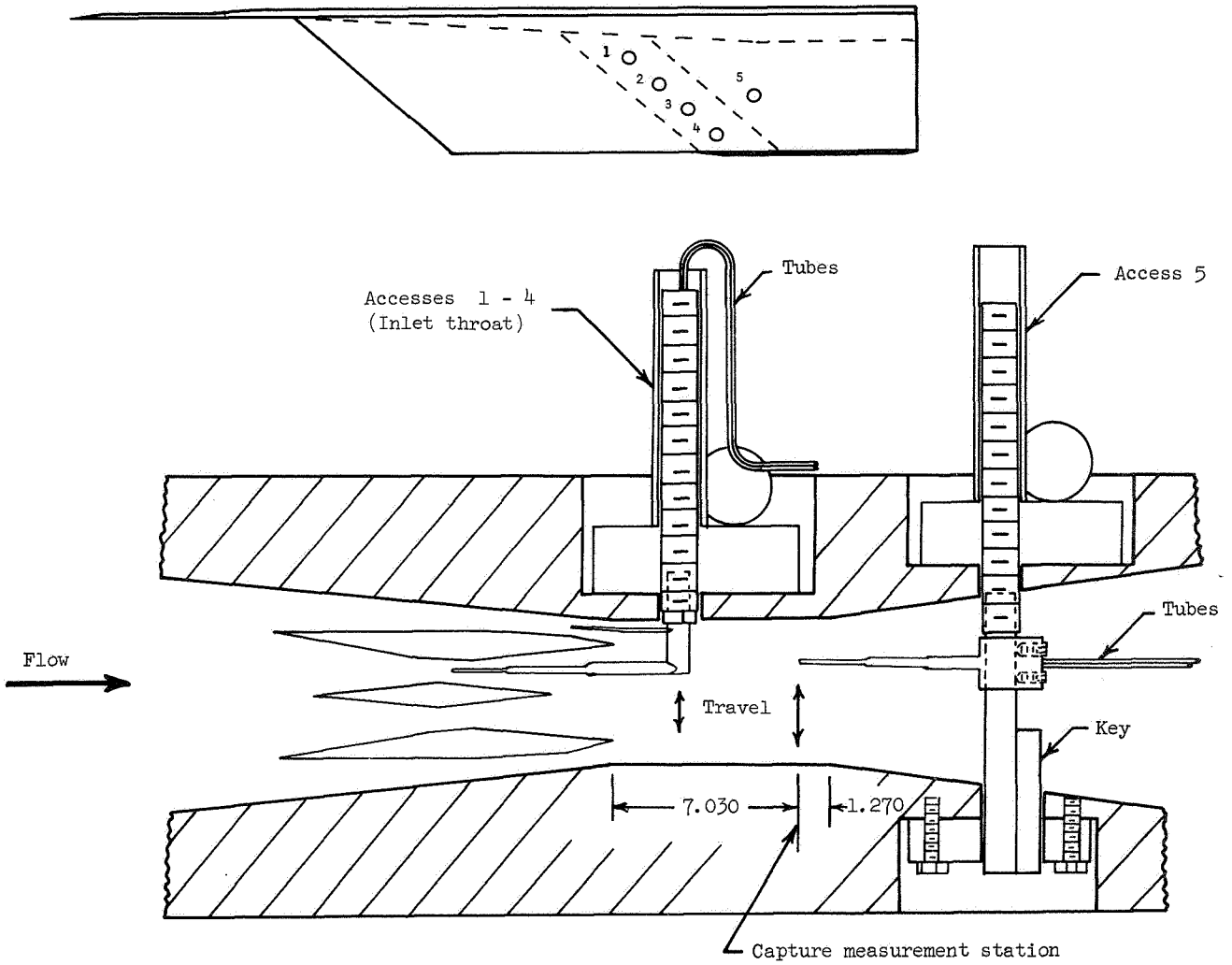

Figure 16.- Survey probe mechanism and access locations. All dimensions are in centimeters.

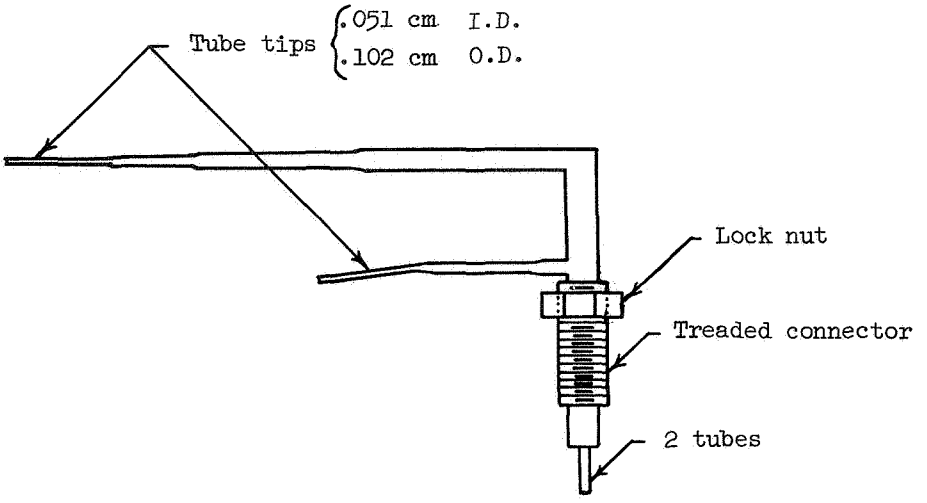

(a) Pitot probe 1. Tube tips bent to aline with inlet throats for each test, and onsight calibration performed.

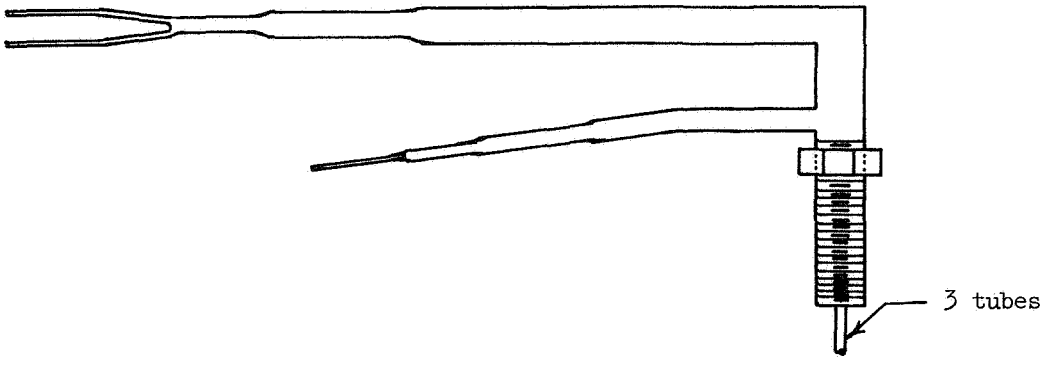

(b) Pitot probe 2. This probe used with modified strut configuration which had wider gap in center passage.

Figure 17.- Throat survey probes. All dimensions are in centimeters.

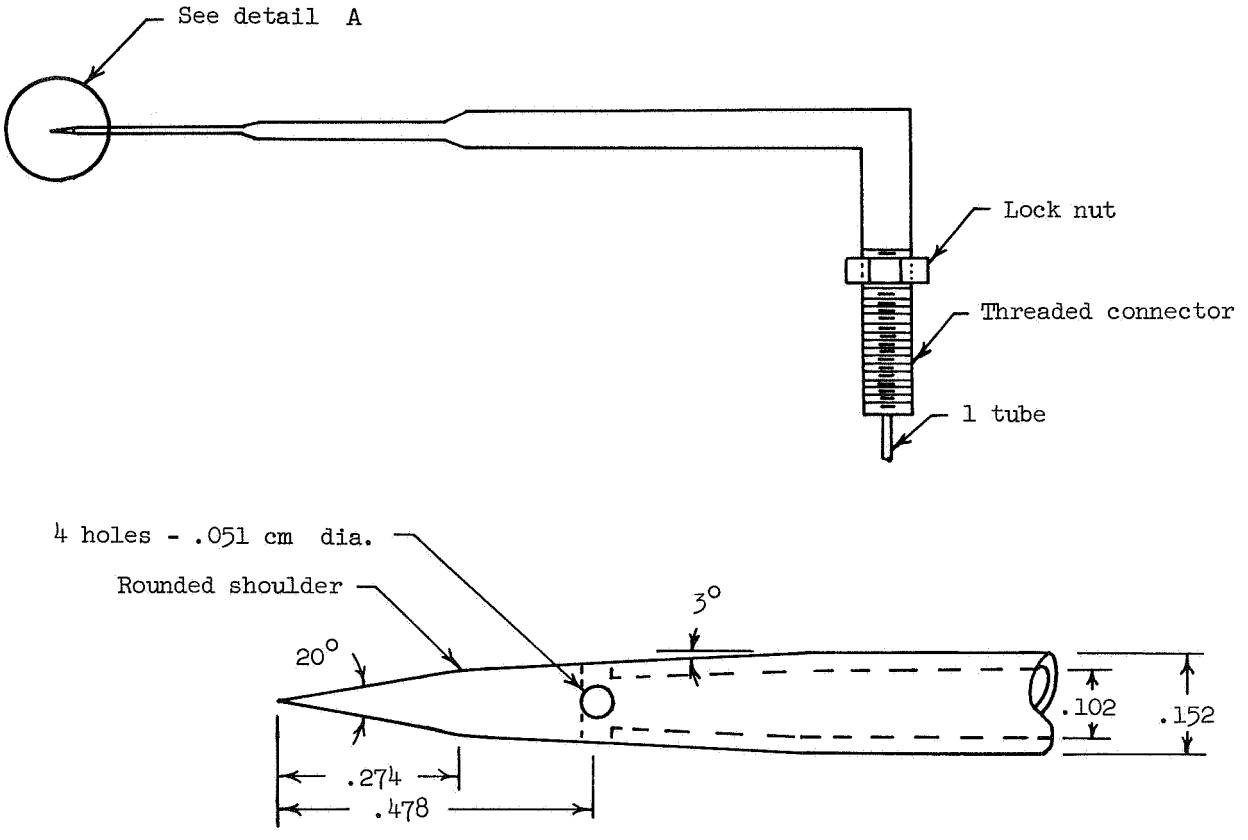

(c) Static probe of reference 9.

Figure 17.- Concluded.

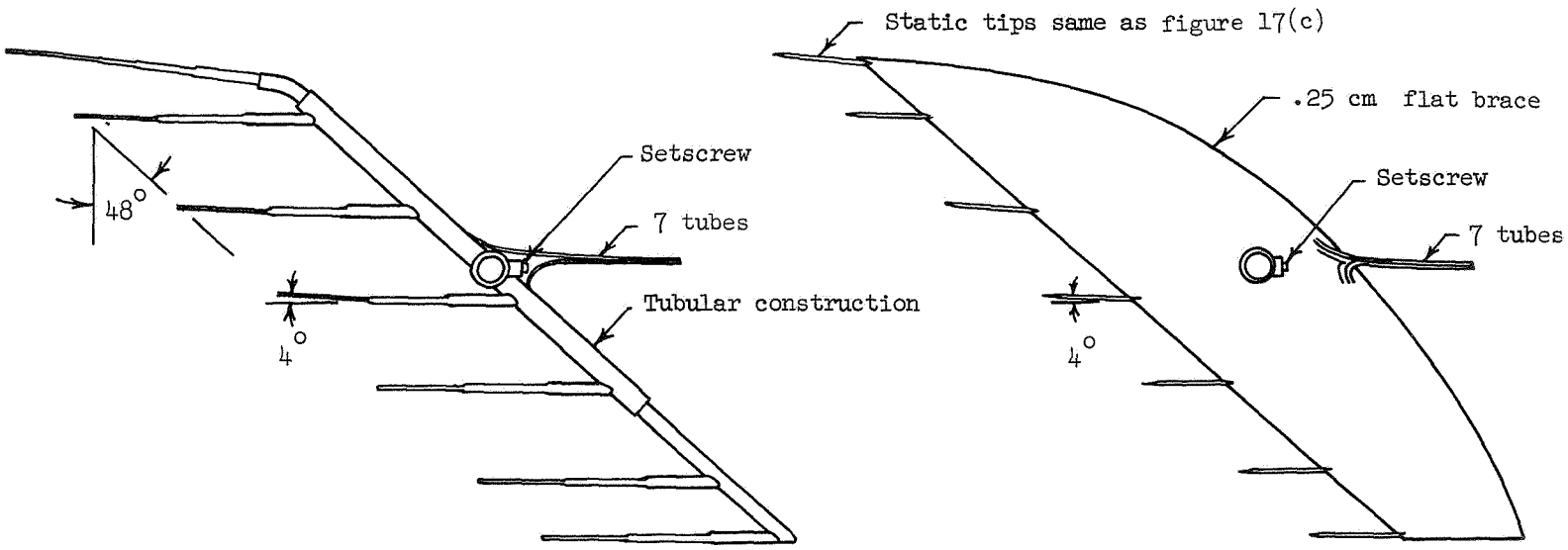

(a) Pitot probe.

(b) Static probes.

Figure 18.- Capture measurement survey probes.

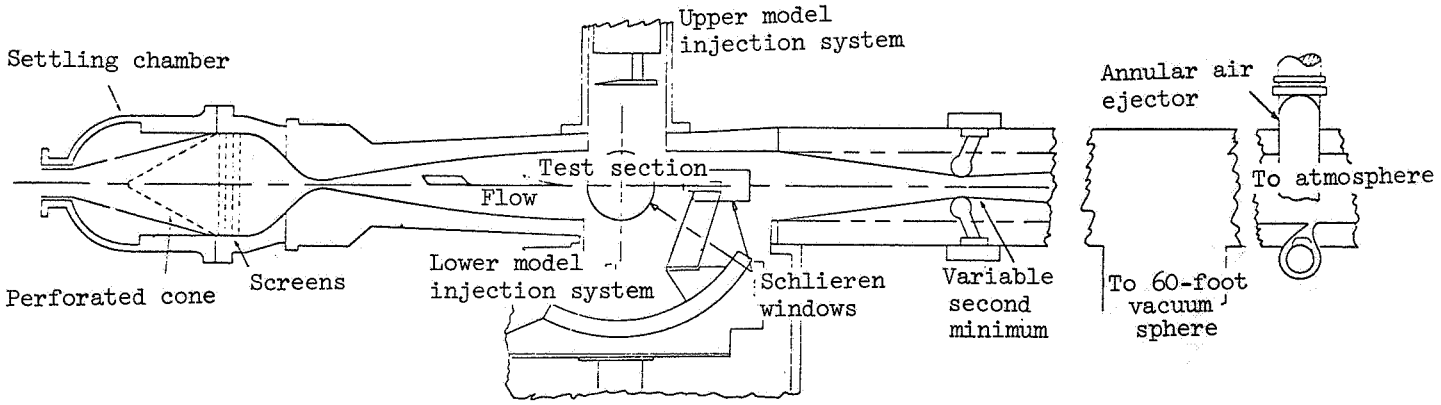

Figure 19.- Langley 20-inch Mach 6 test facility. (See ref. 12.)

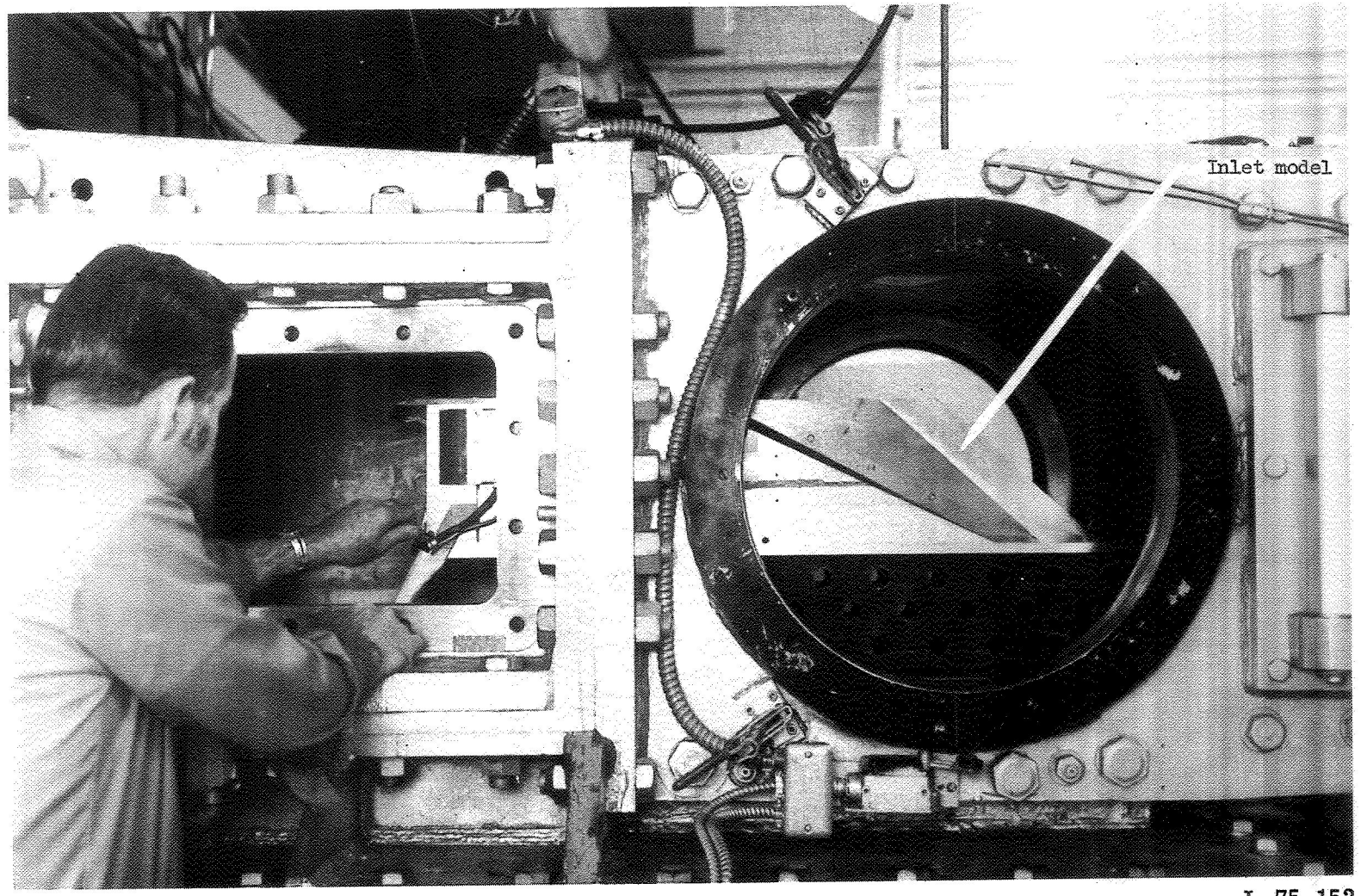

L-75-152

Figure 20.- Inlet model mounted in test facility.

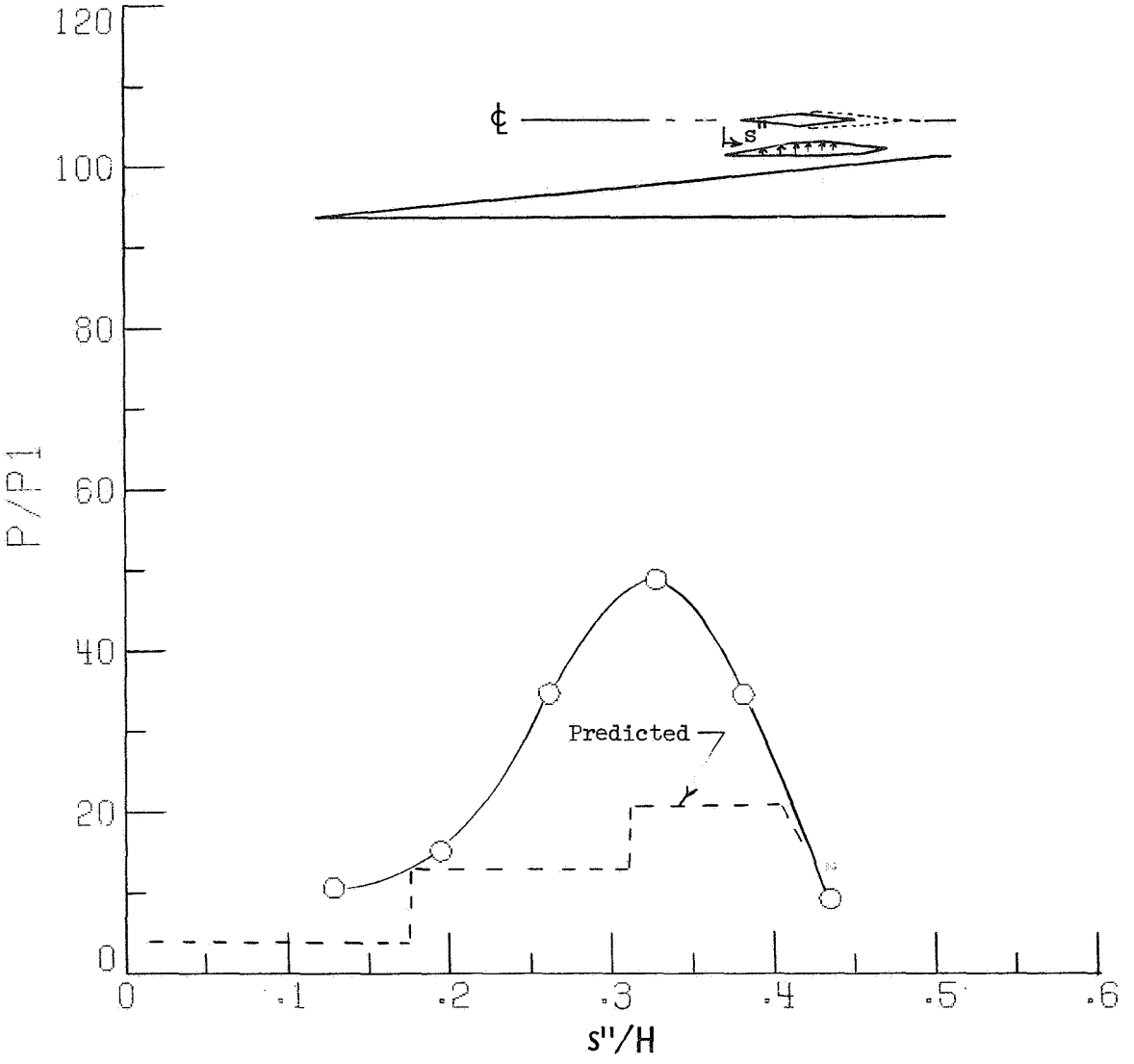

(a) Side strut; Y/H = 0.43.

Figure 21.- Center-passage static-pressure distribution.

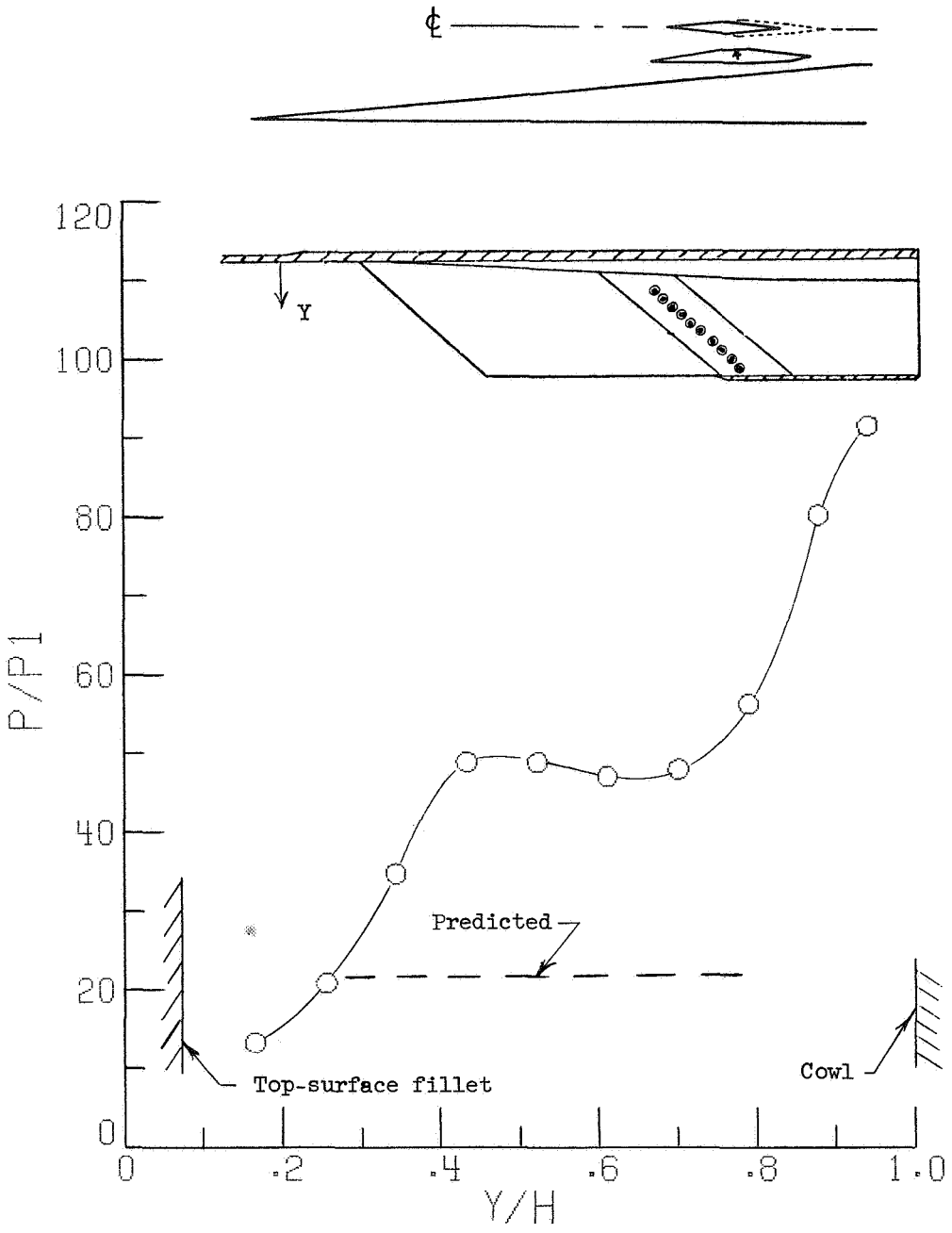

(b) Side strut; throat.

Figure 21.- Concluded.

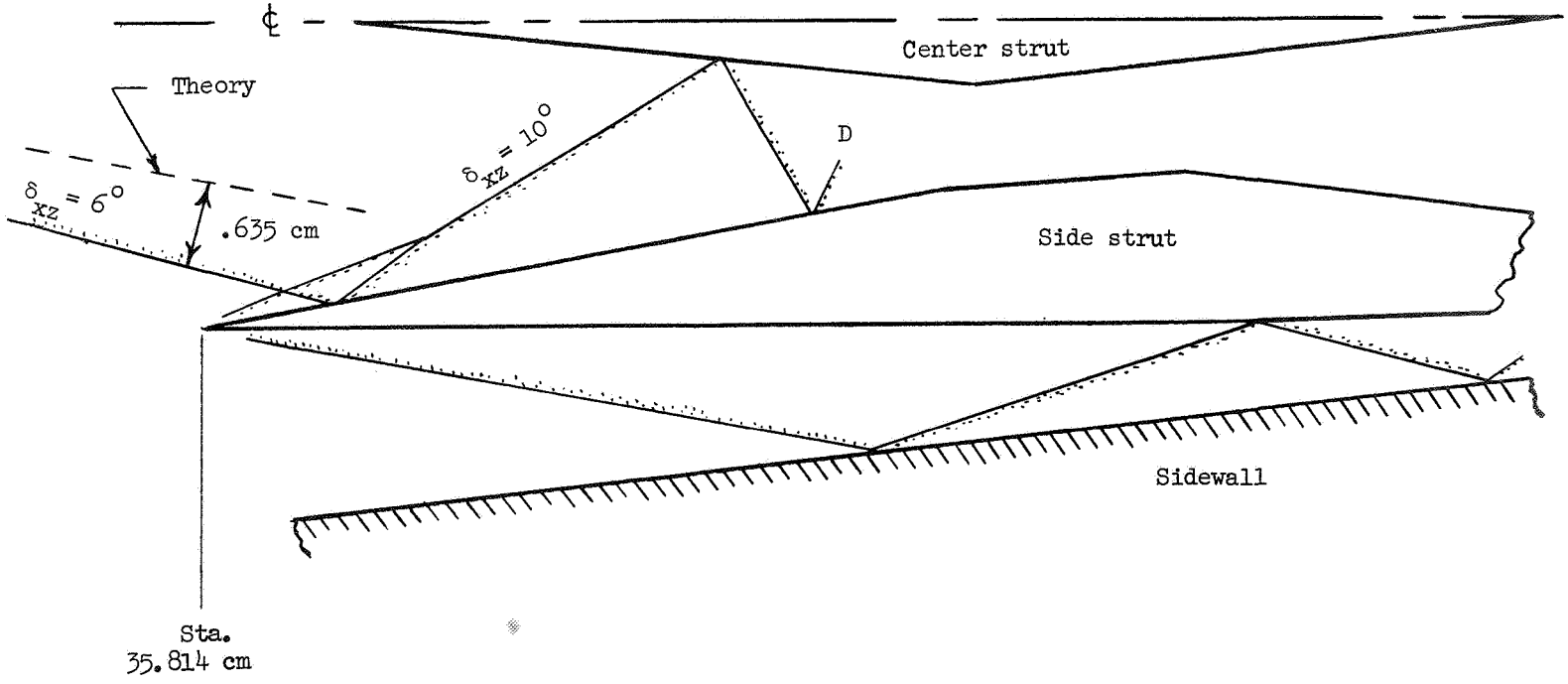

Figure 22.- Effect of shifted shock wave on center passage (xz-plane).

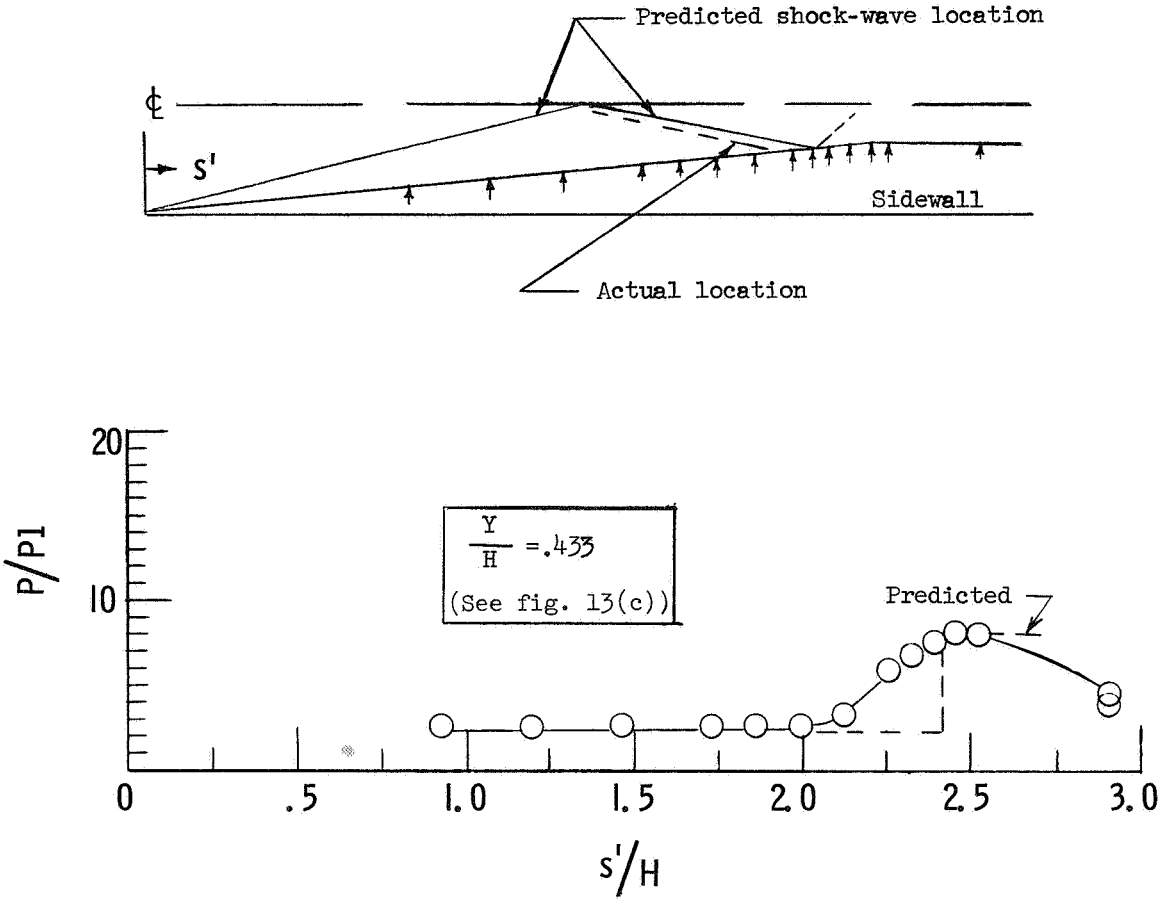

Figure 23.- Sidewall static-pressure distribution. No struts.

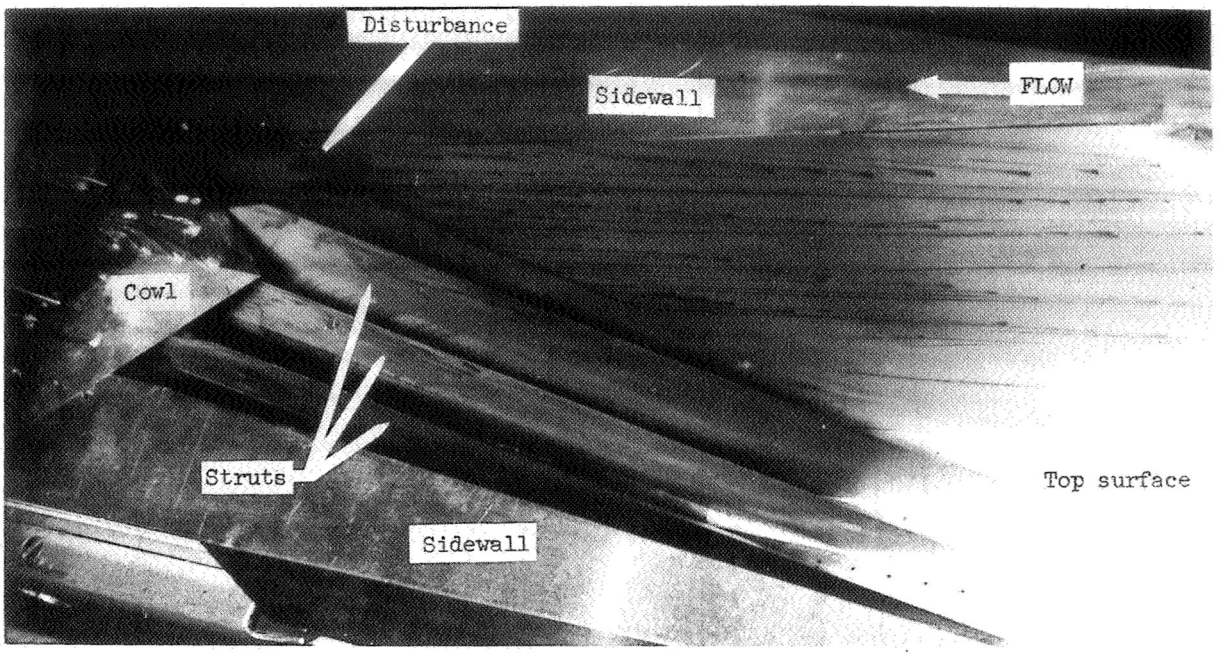

(a) Three-strut configuration (Capture = 81 percent).

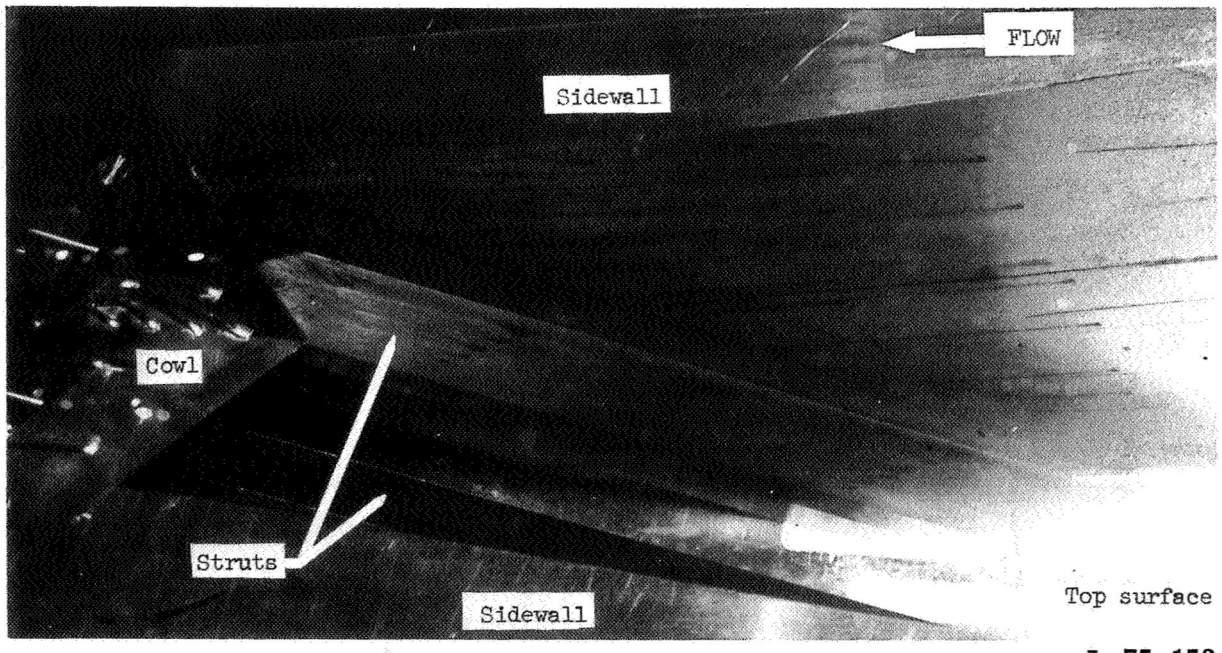

L-75-153

(b) No center strut (Capture = 92 percent).

Figure 24.- Oil-streak photograph.

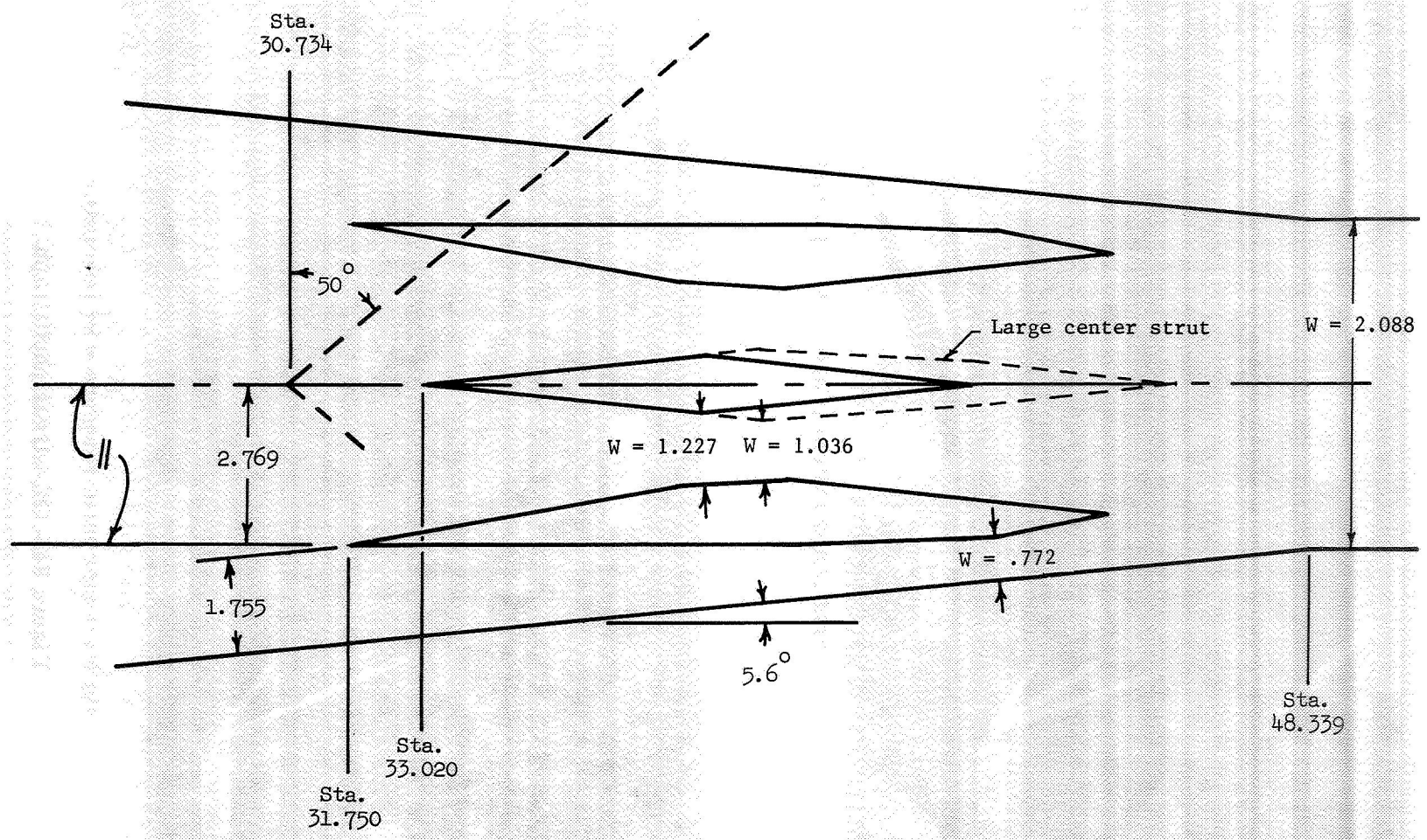

Figure 25.- Modified strut positions (xz-plane). All dimensions are in centimeters.

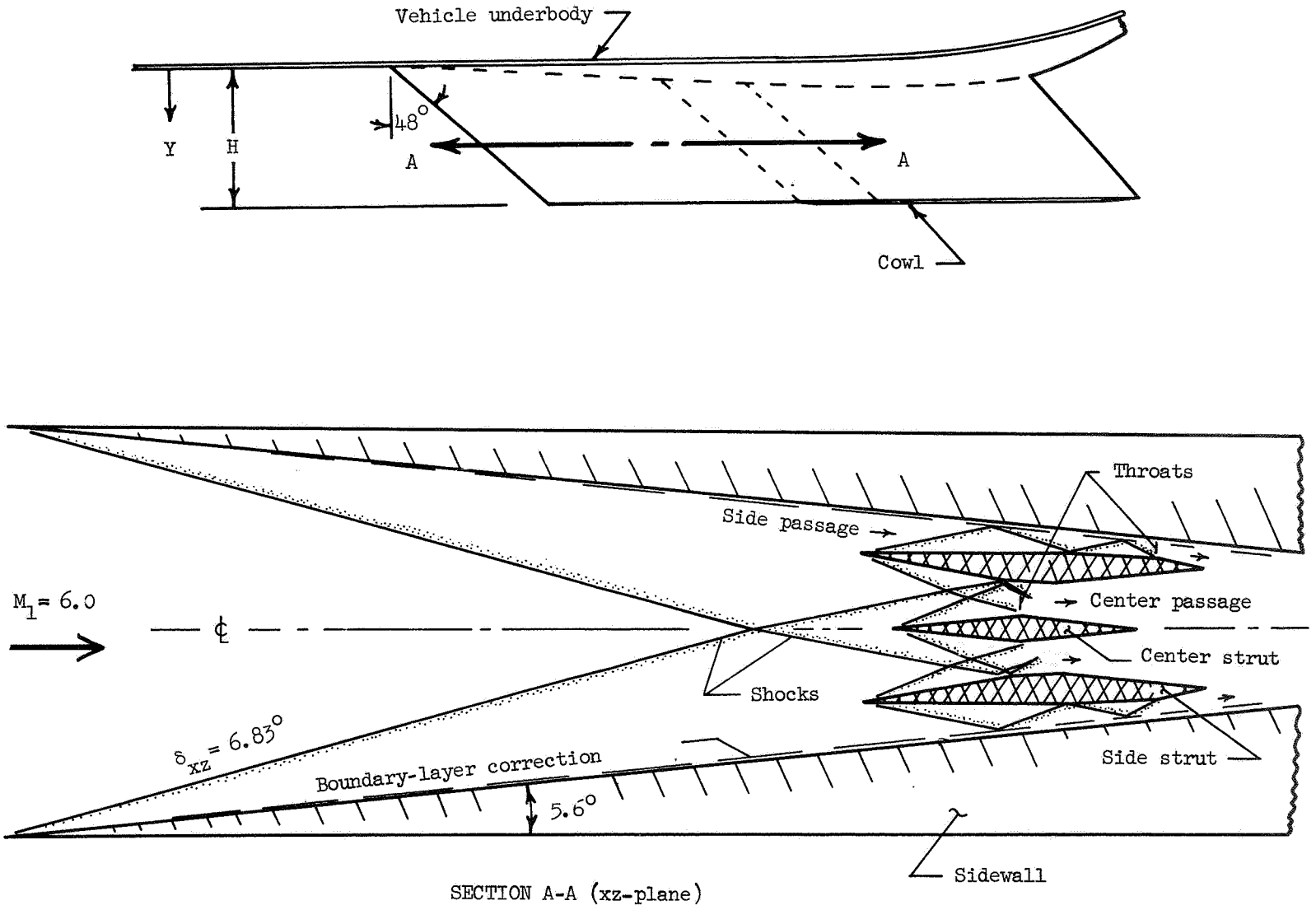

Figure 26.- Corrected Mach 6 shock diagram.

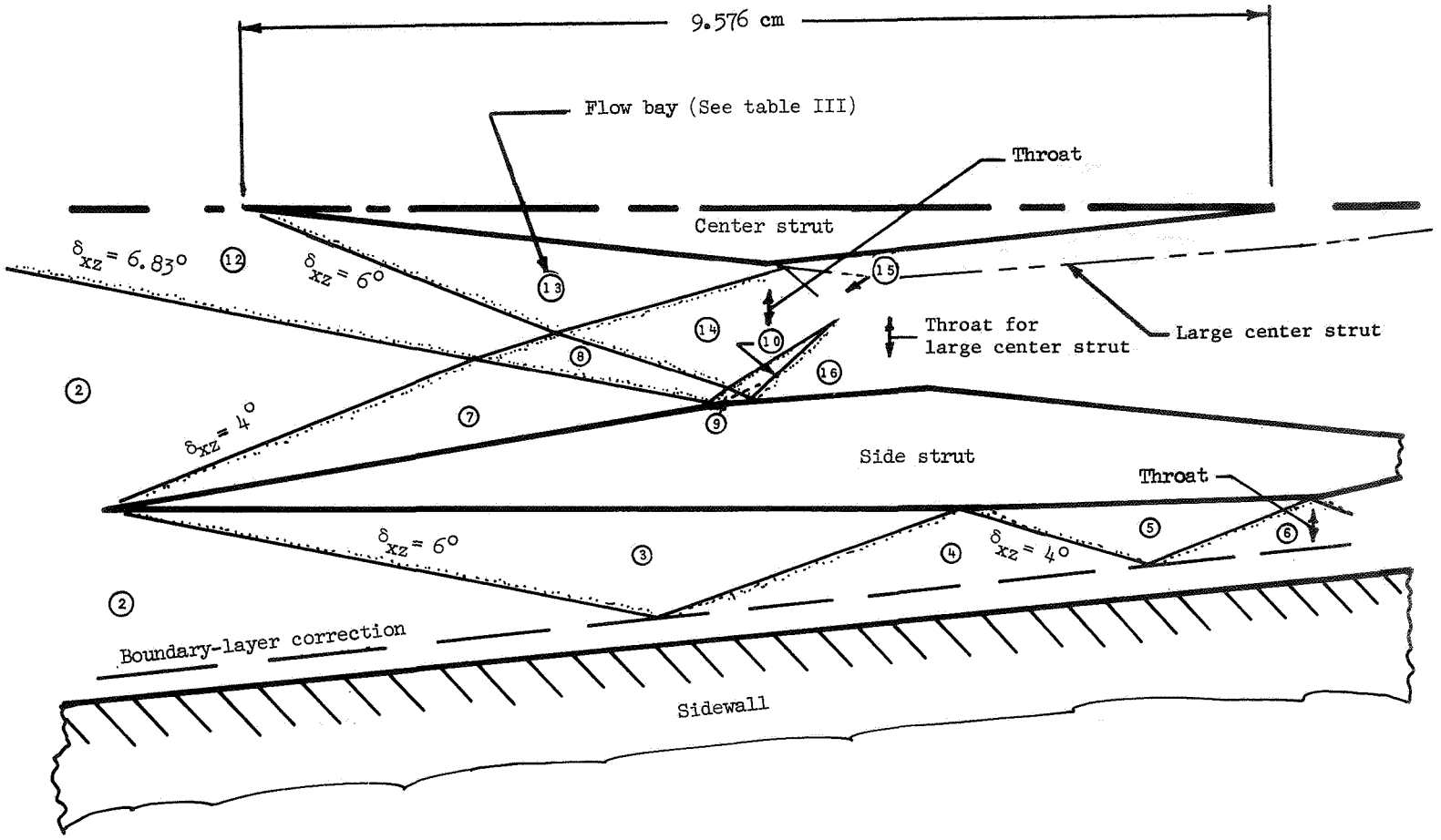

Figure 27.- Corrected shock-wave detail in vicinity of struts. M_1 = 6.0.

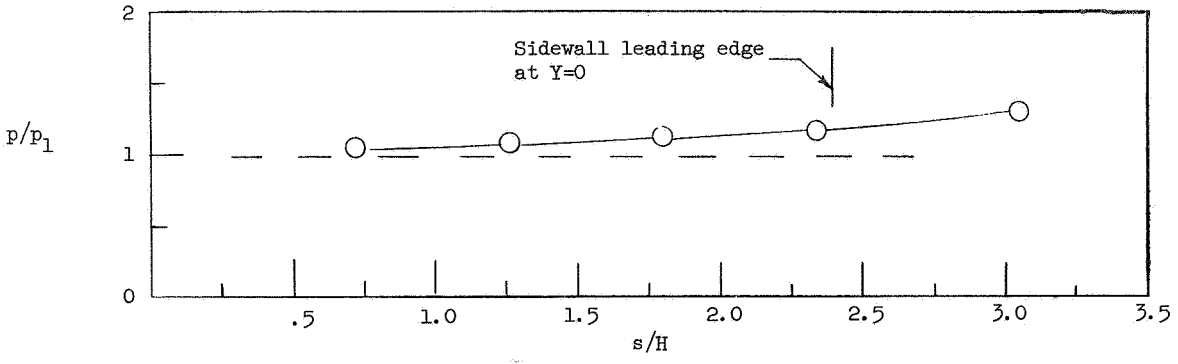

(a) Static pressure on foreplate. Z/H = 0.

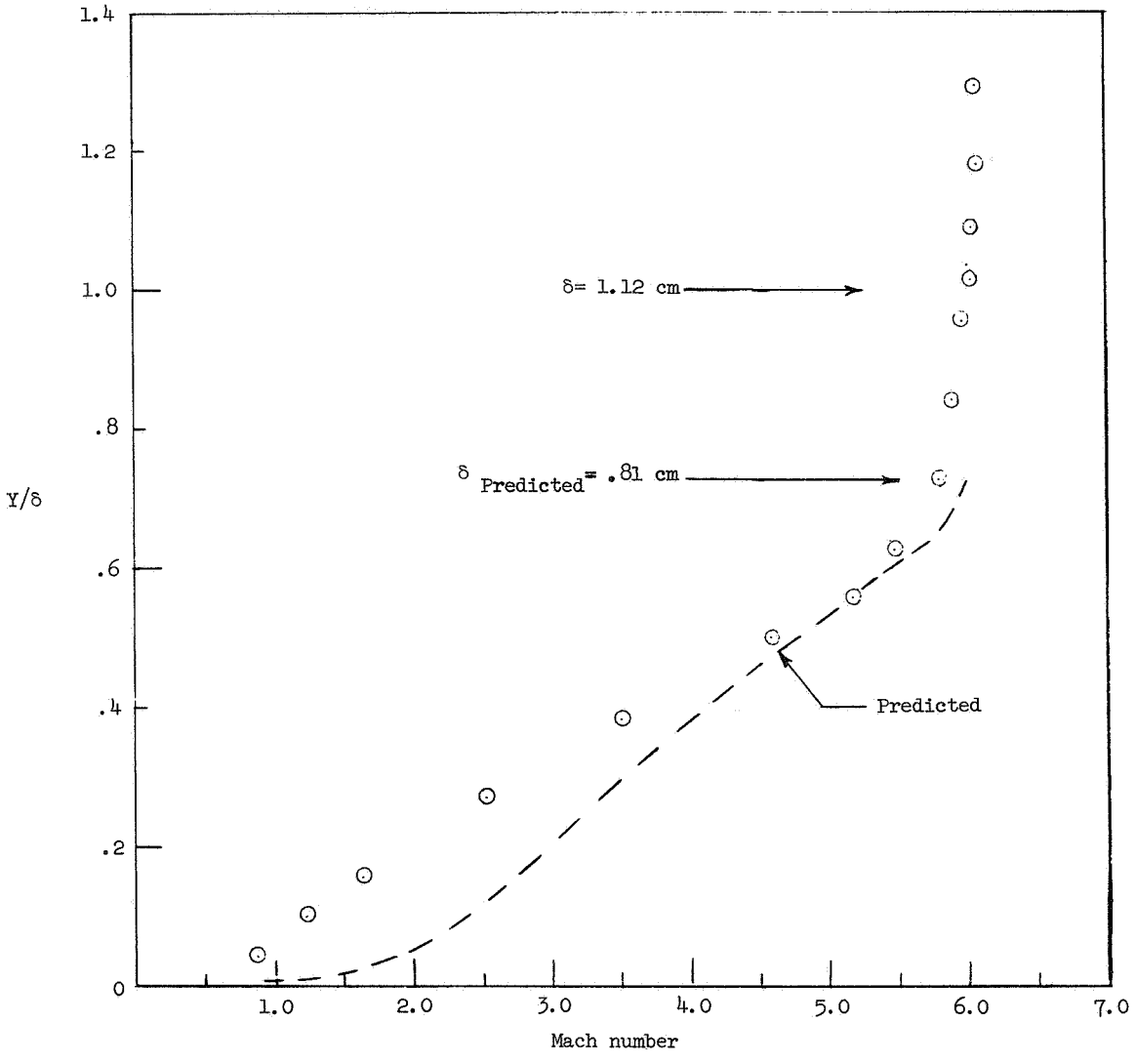

(b) Foreplate boundary layer. s/H = 6.096; Z/H = 0.133.

Figure 28.- Foreplate conditions.

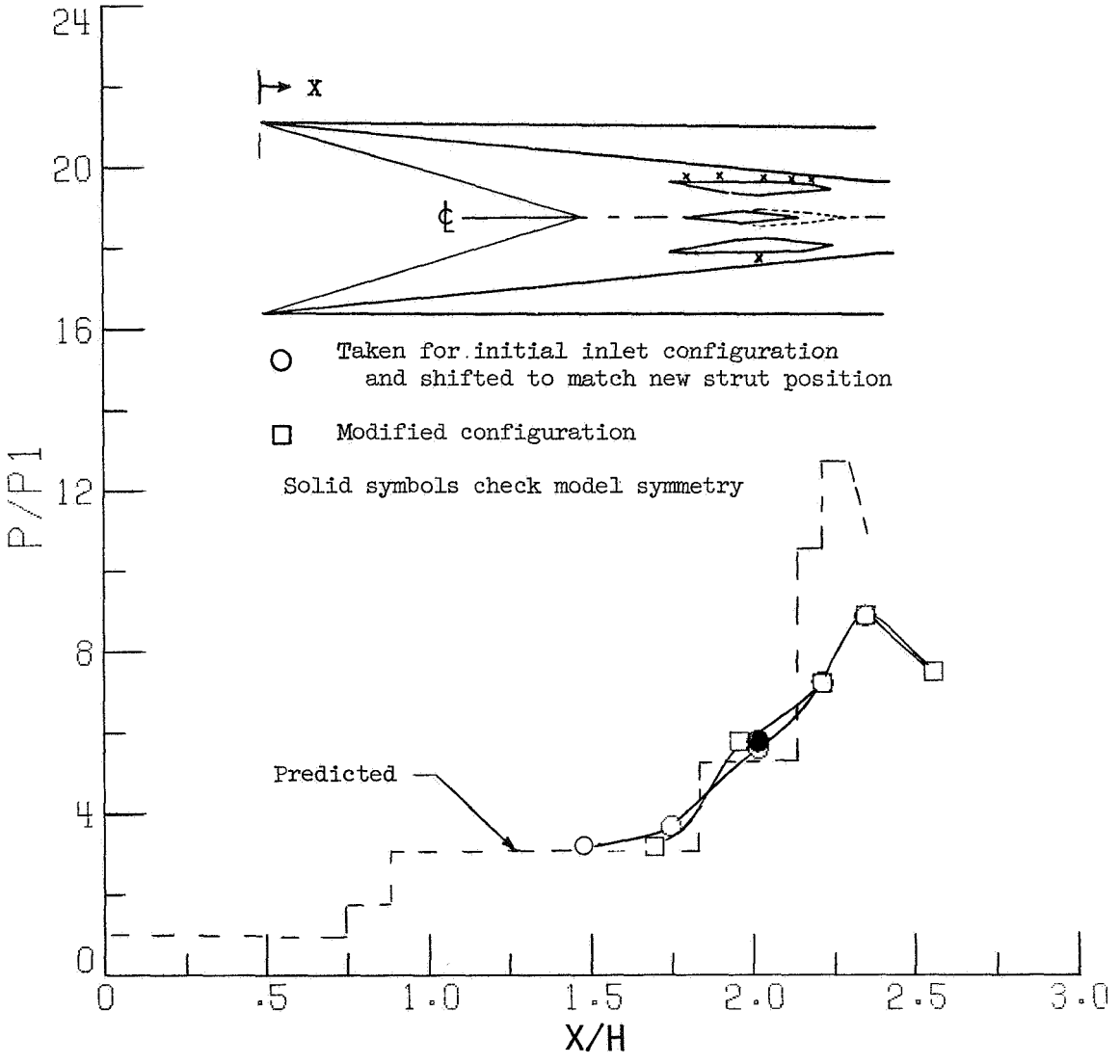

Figure 29.- Static-pressure distribution. Top surface (side passage).

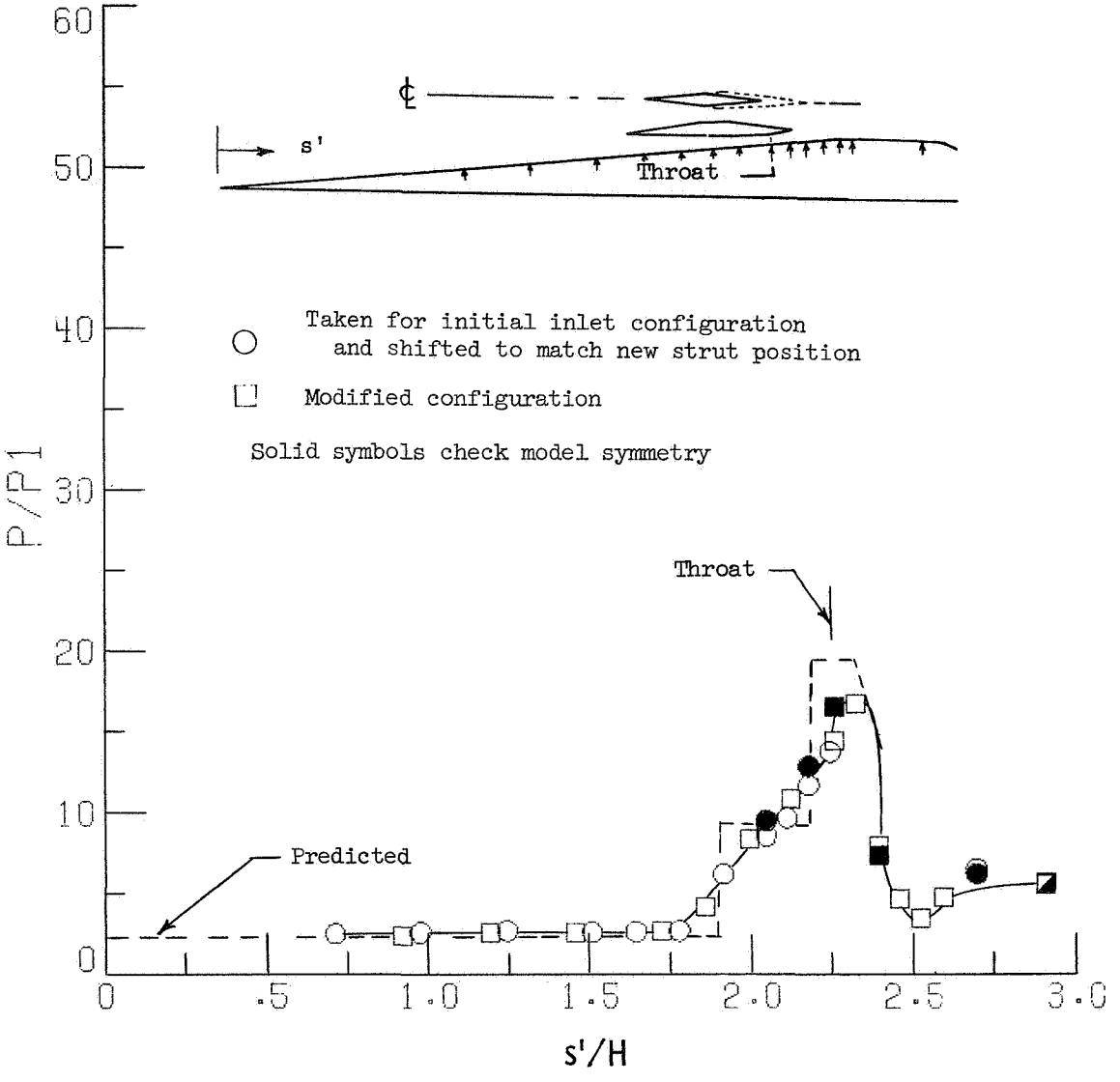

Figure 30.- Static-pressure distribution. Sidewall; Y/H = 0.43.

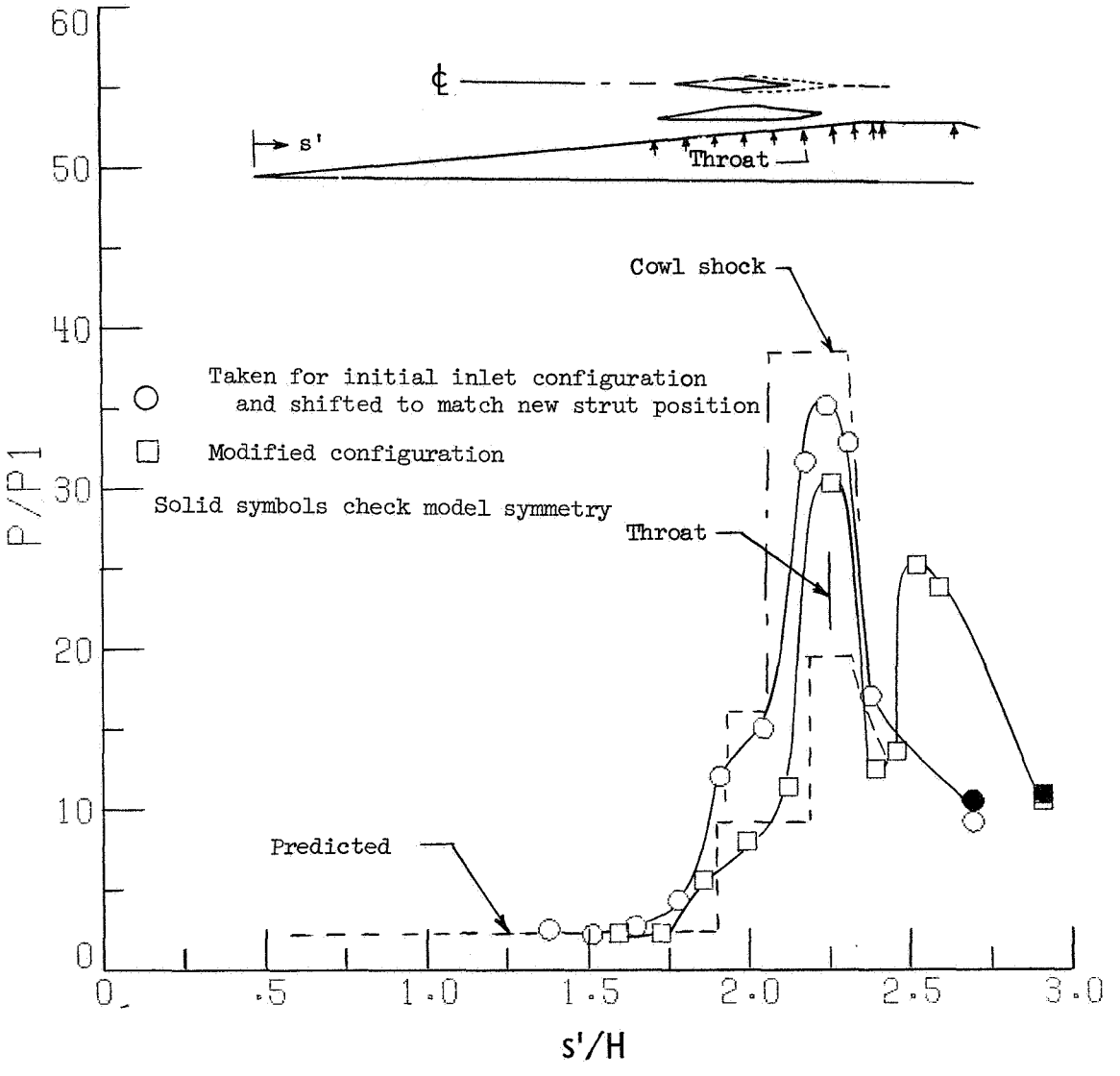

Figure 31.- Static-pressure distribution. Sidewall; Y/H = 0.88.

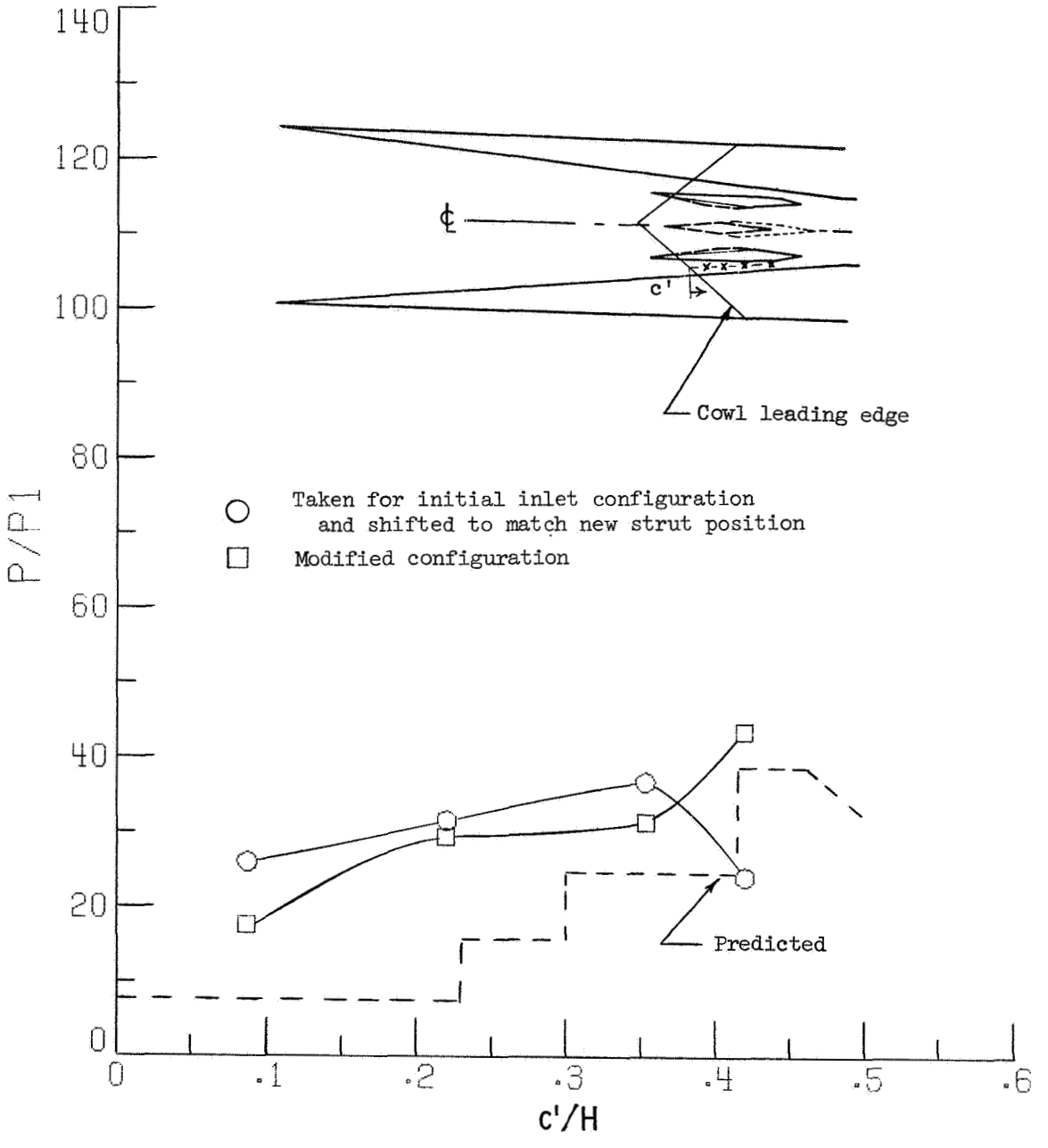

Figure 32.- Static-pressure distribution cowl. Side passage.

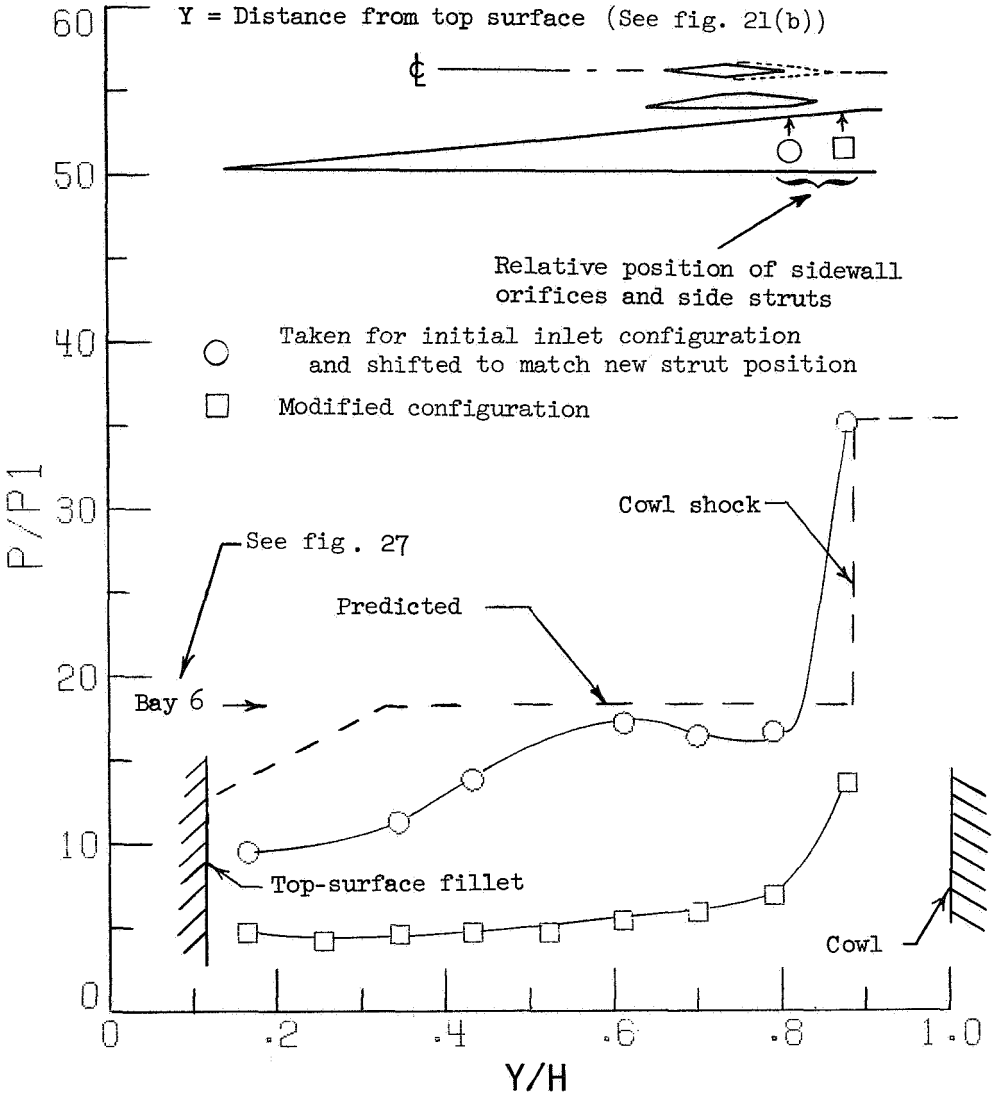

(a) Sidewall.

Figure 33.- Static-pressure distribution. Side passage throat.

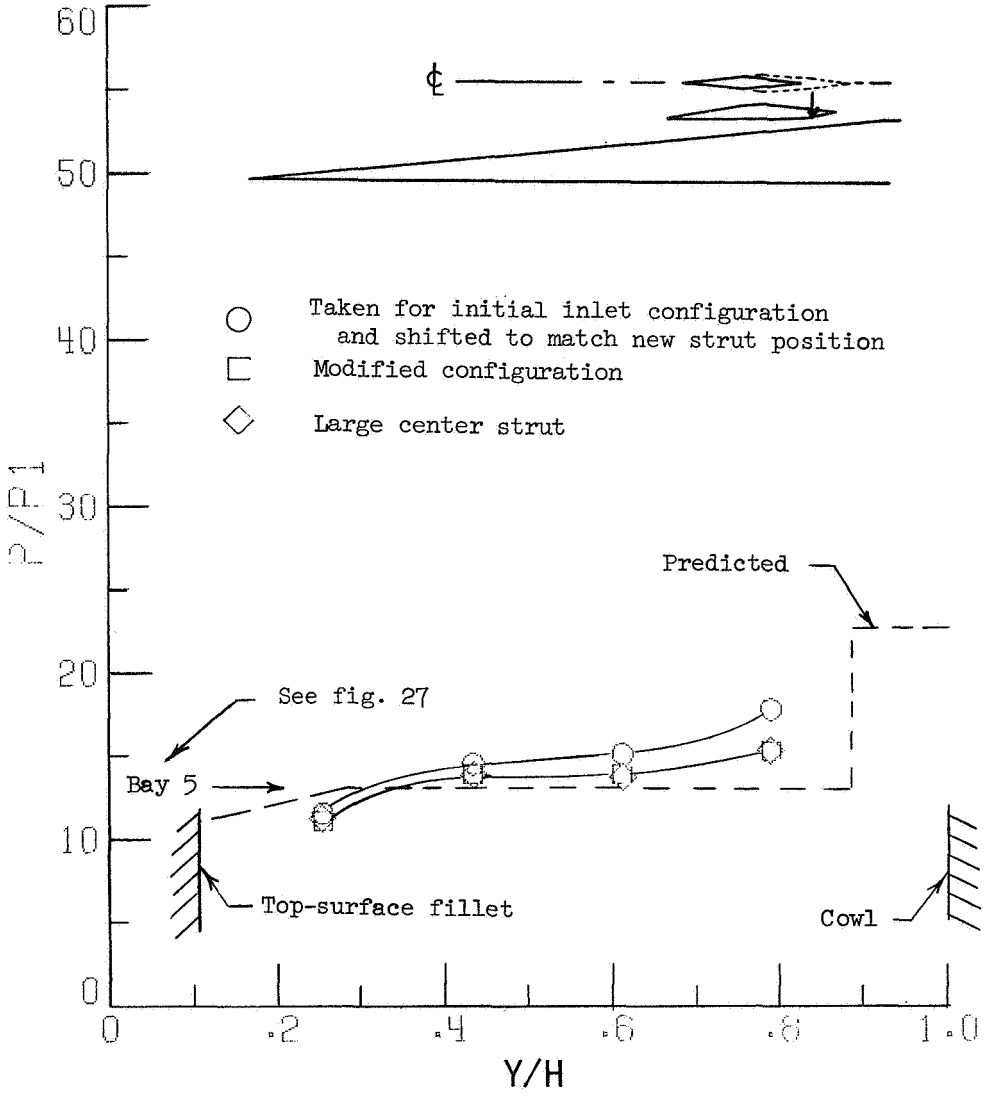

(b) Side strut.

Figure 33.- Concluded.

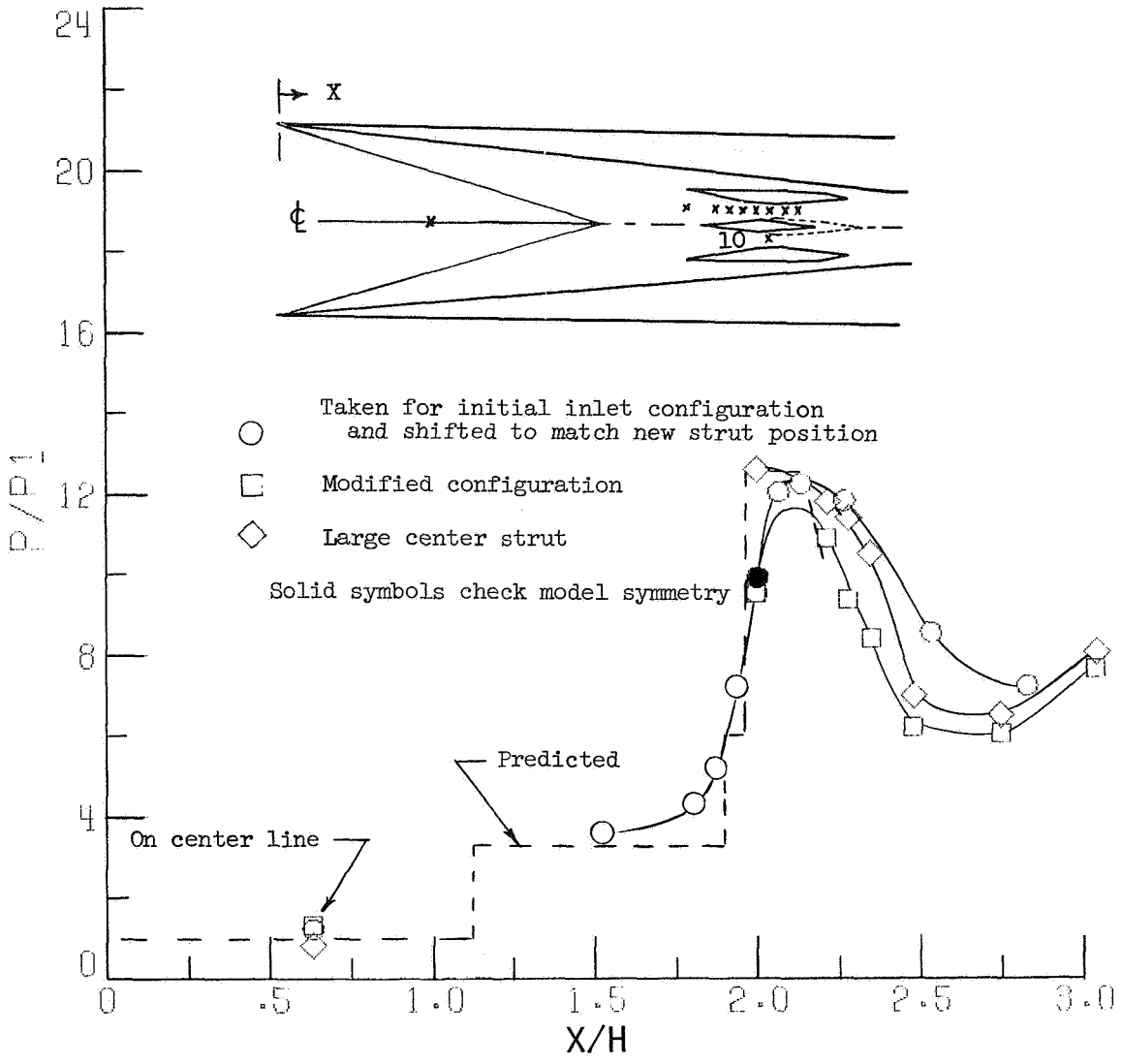

Figure 34.- Static-pressure distribution top surface. Center passage.

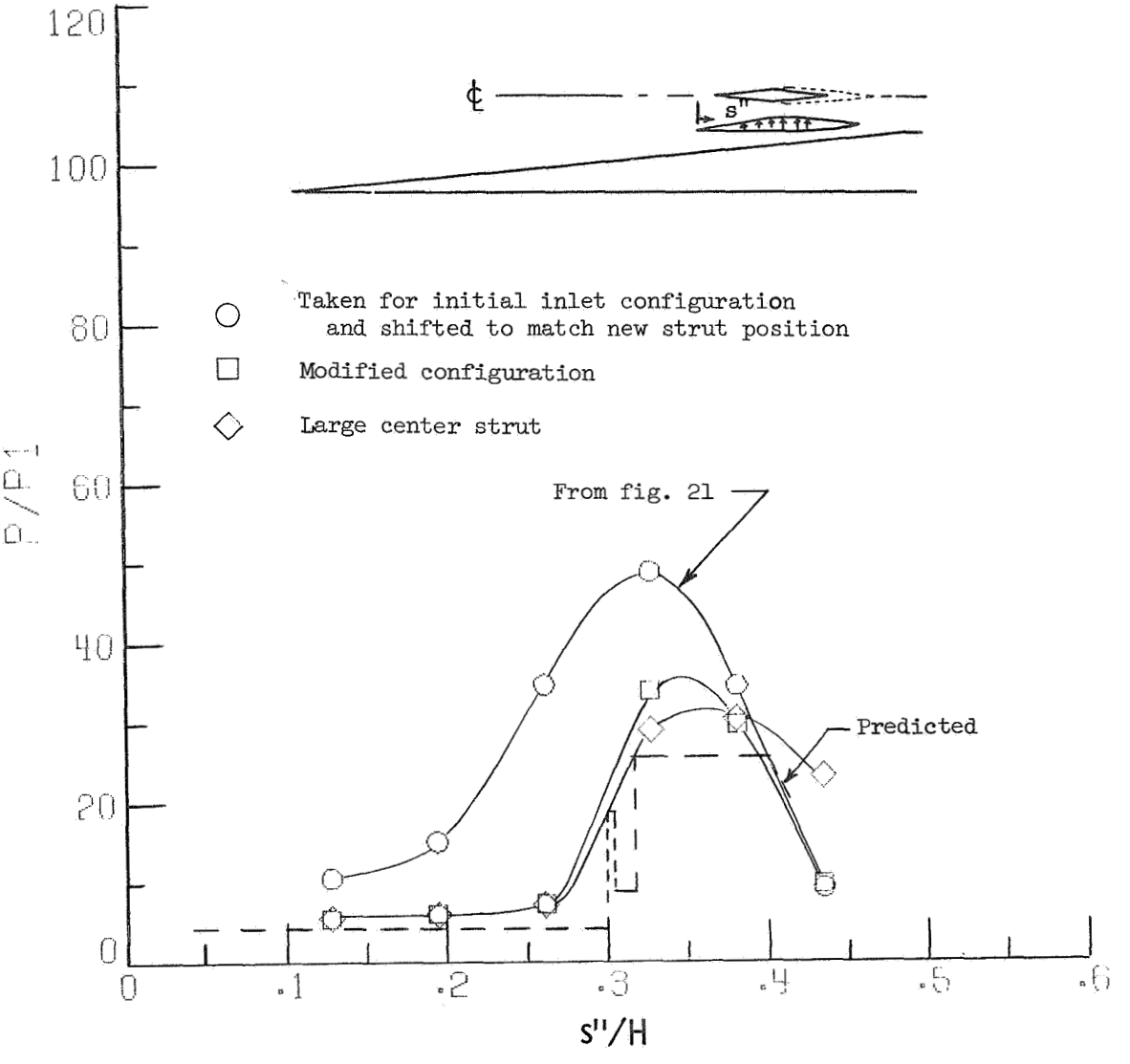

Figure 35.- Static-pressure distribution center passage. Side strut; Y/H = 0.43.

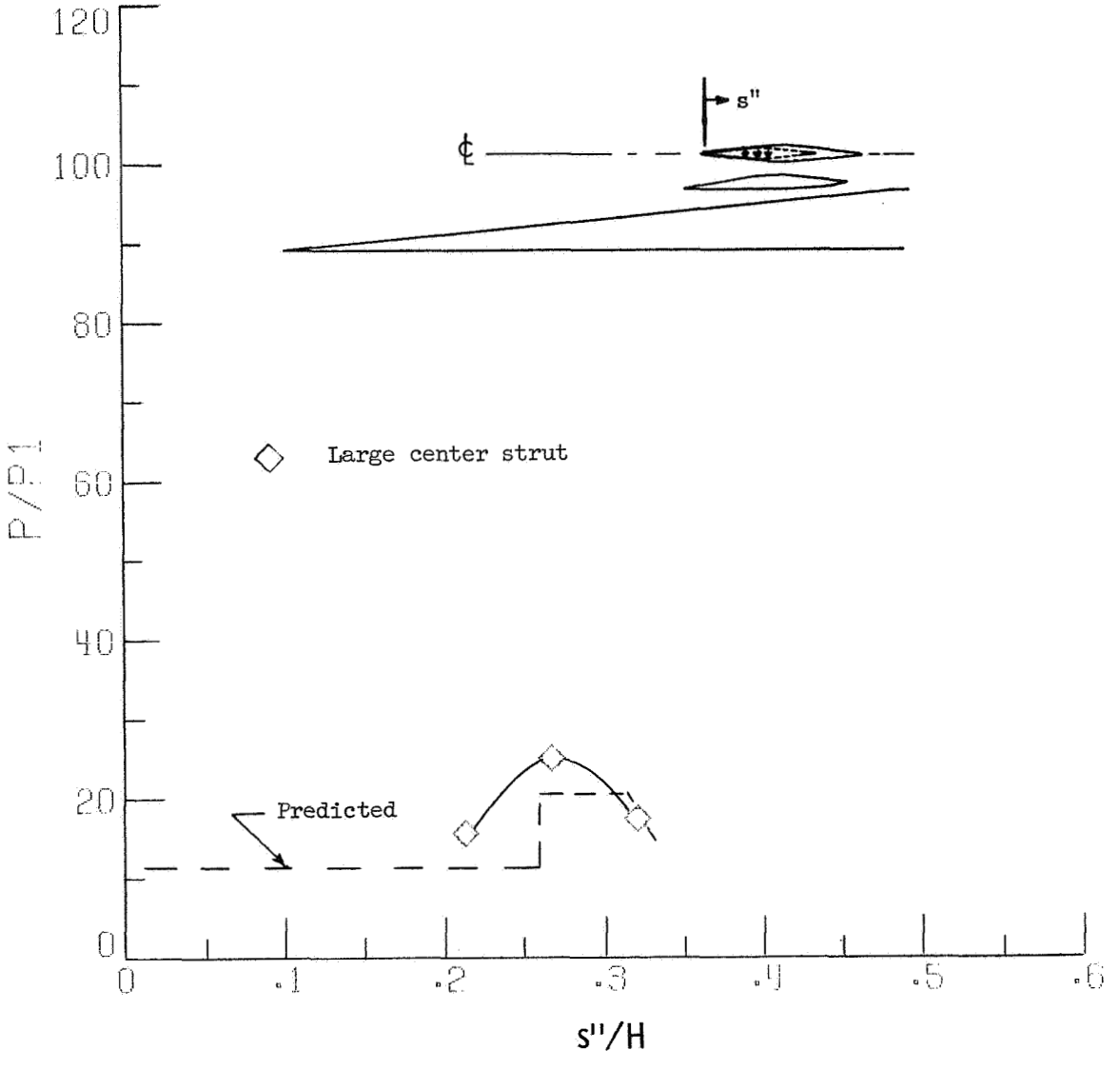

Figure 36.- Static-pressure distribution center passage. Center strut 2; Y/H = 0.43.

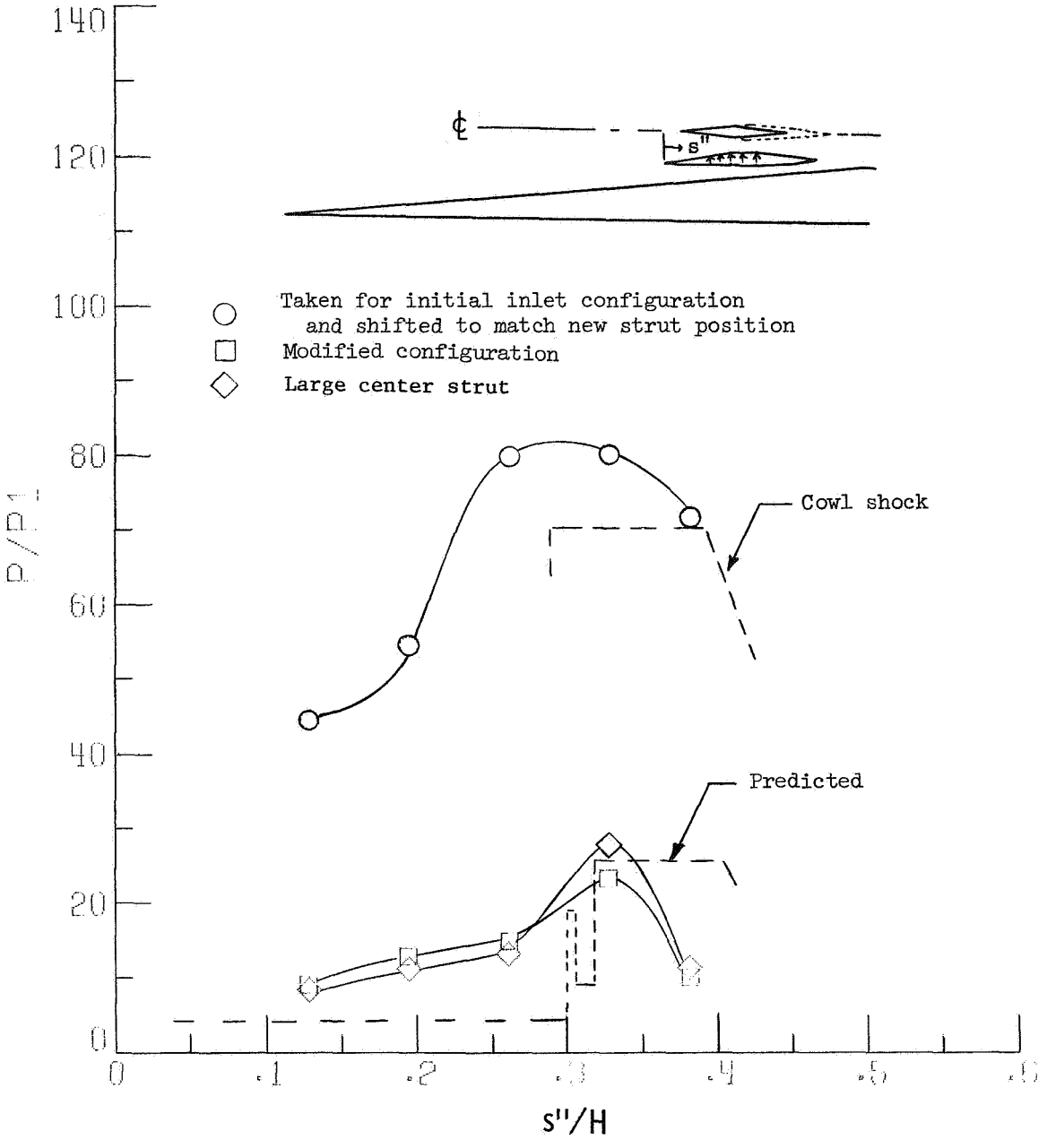

Figure 37.- Static-pressure distribution center passage. Side strut; Y/H = 0.88.

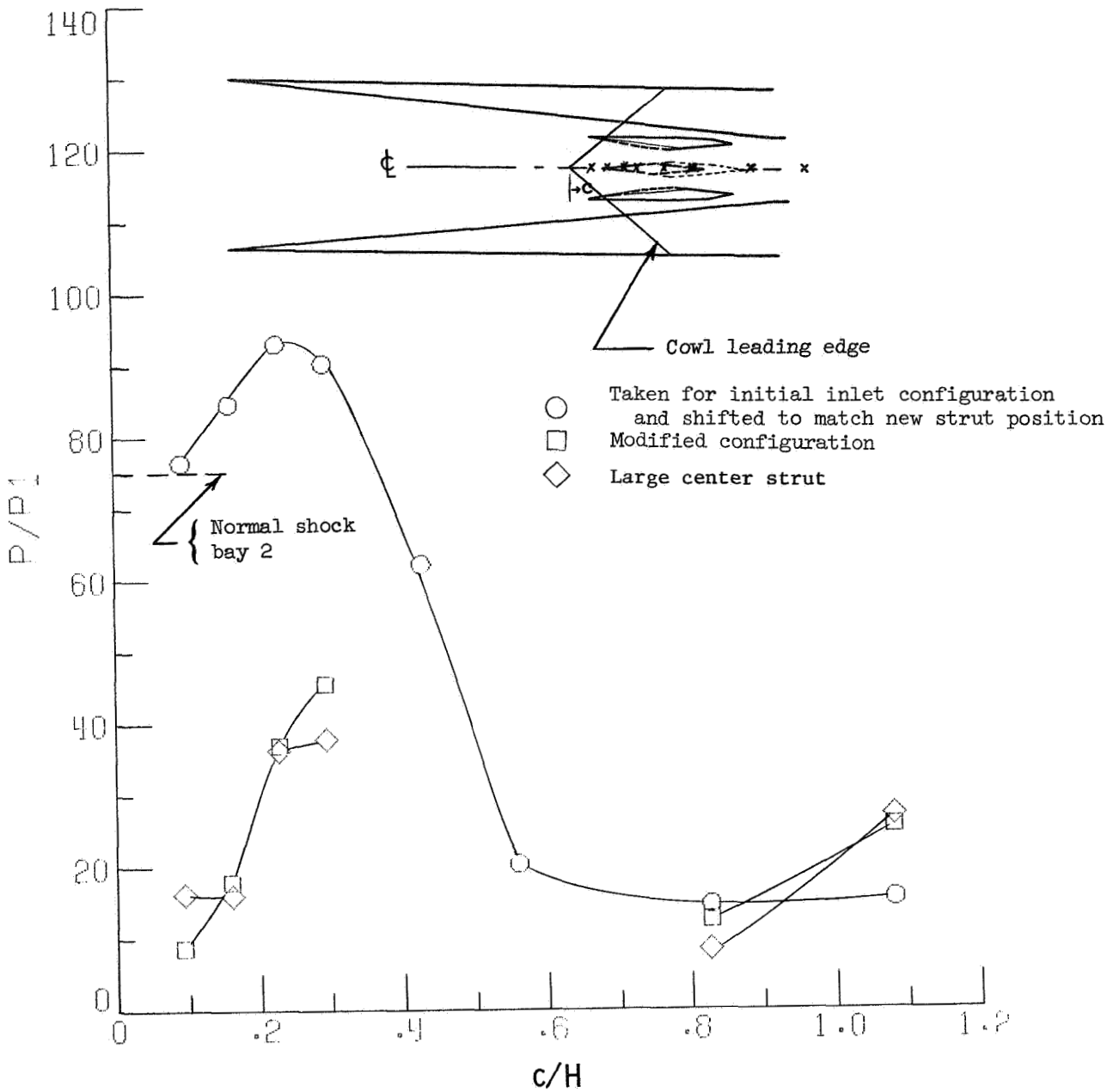

Figure 38.- Static-pressure distribution. Cowl (center line).

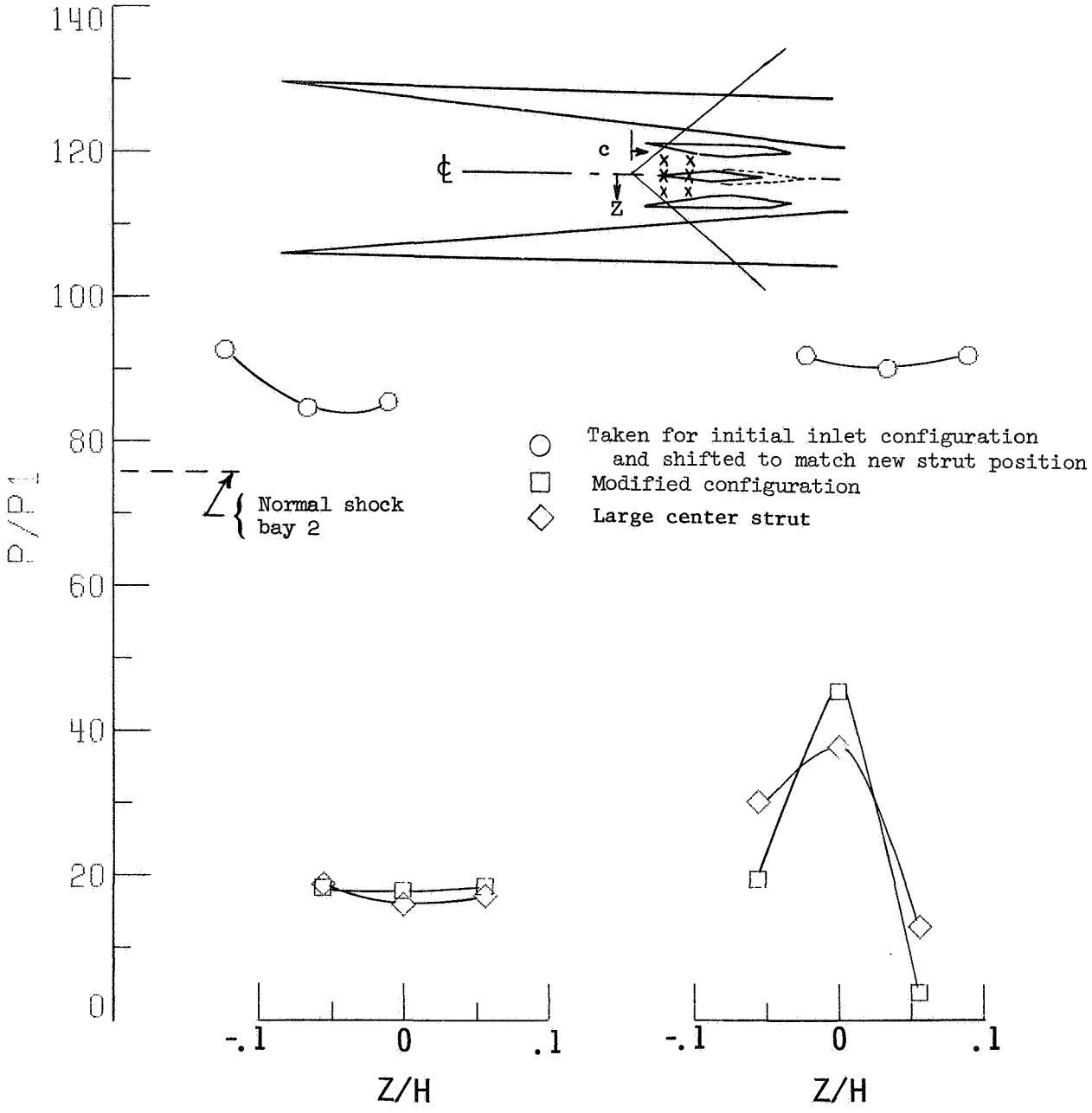

(a) c/H = 0.160.

(b) c/H = 0.293.

Figure 39.- Static-pressure distribution. Cowl (Z-direction).

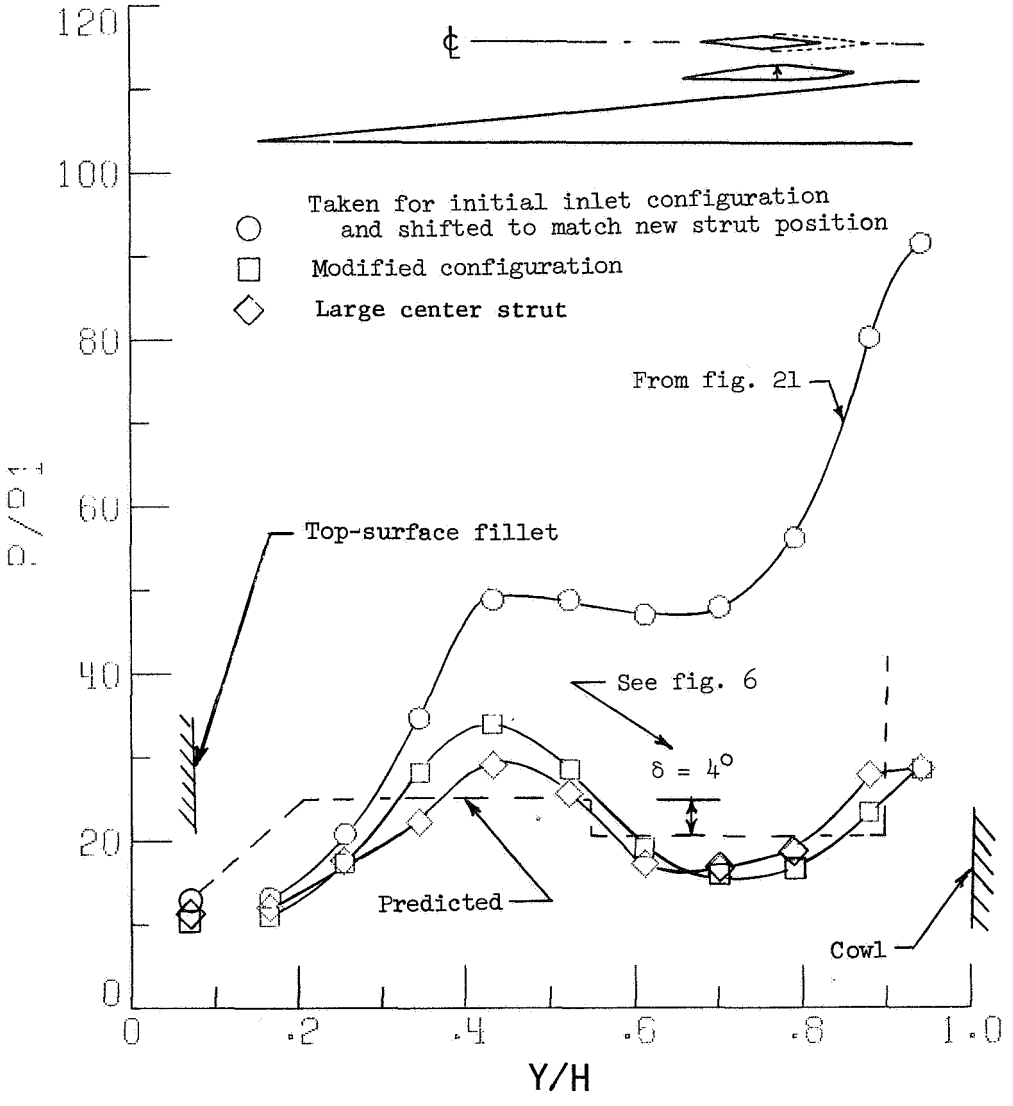

Figure 40.- Static-pressure distribution. Throat (center-passage side strut).

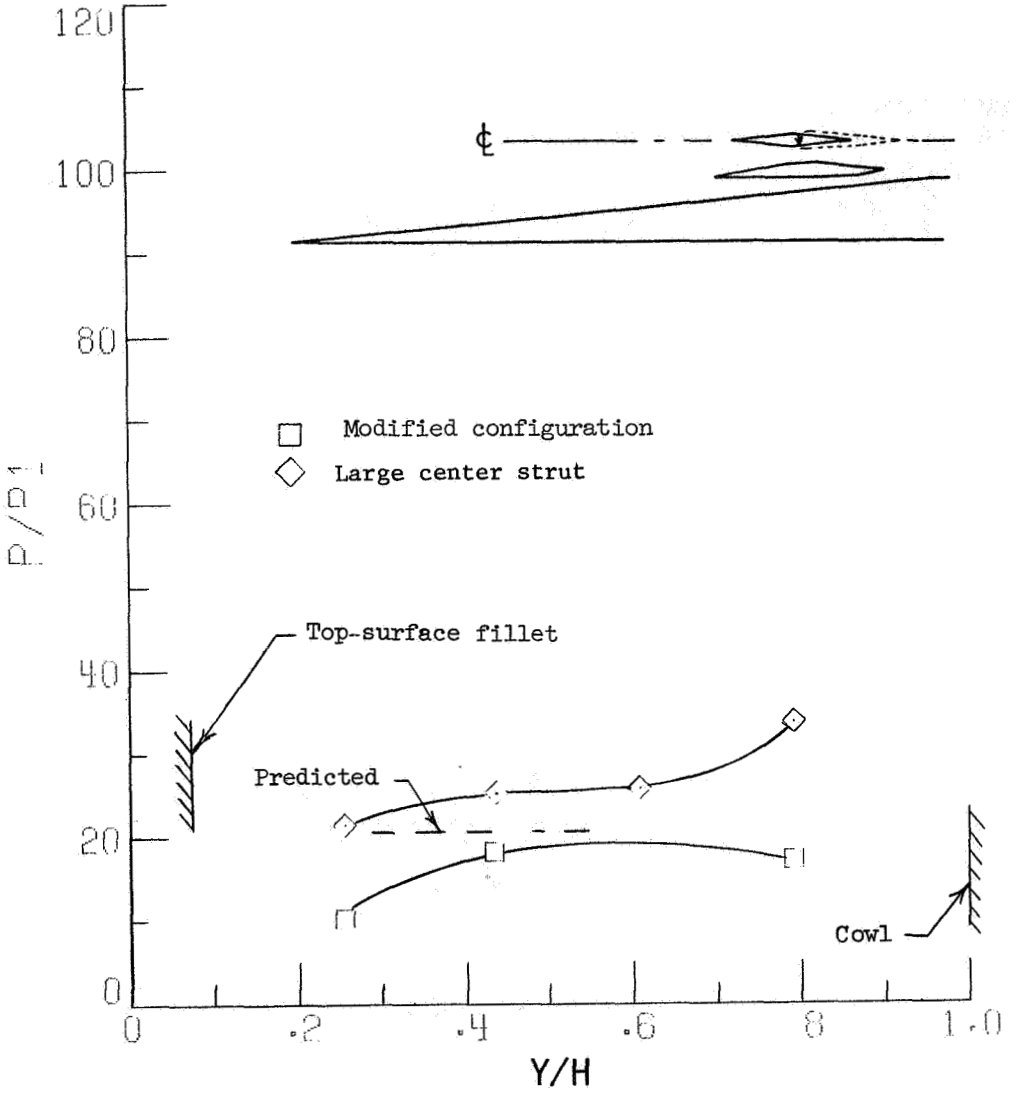

Figure 41.- Static-pressure distribution. Throat (center-passage center strut).

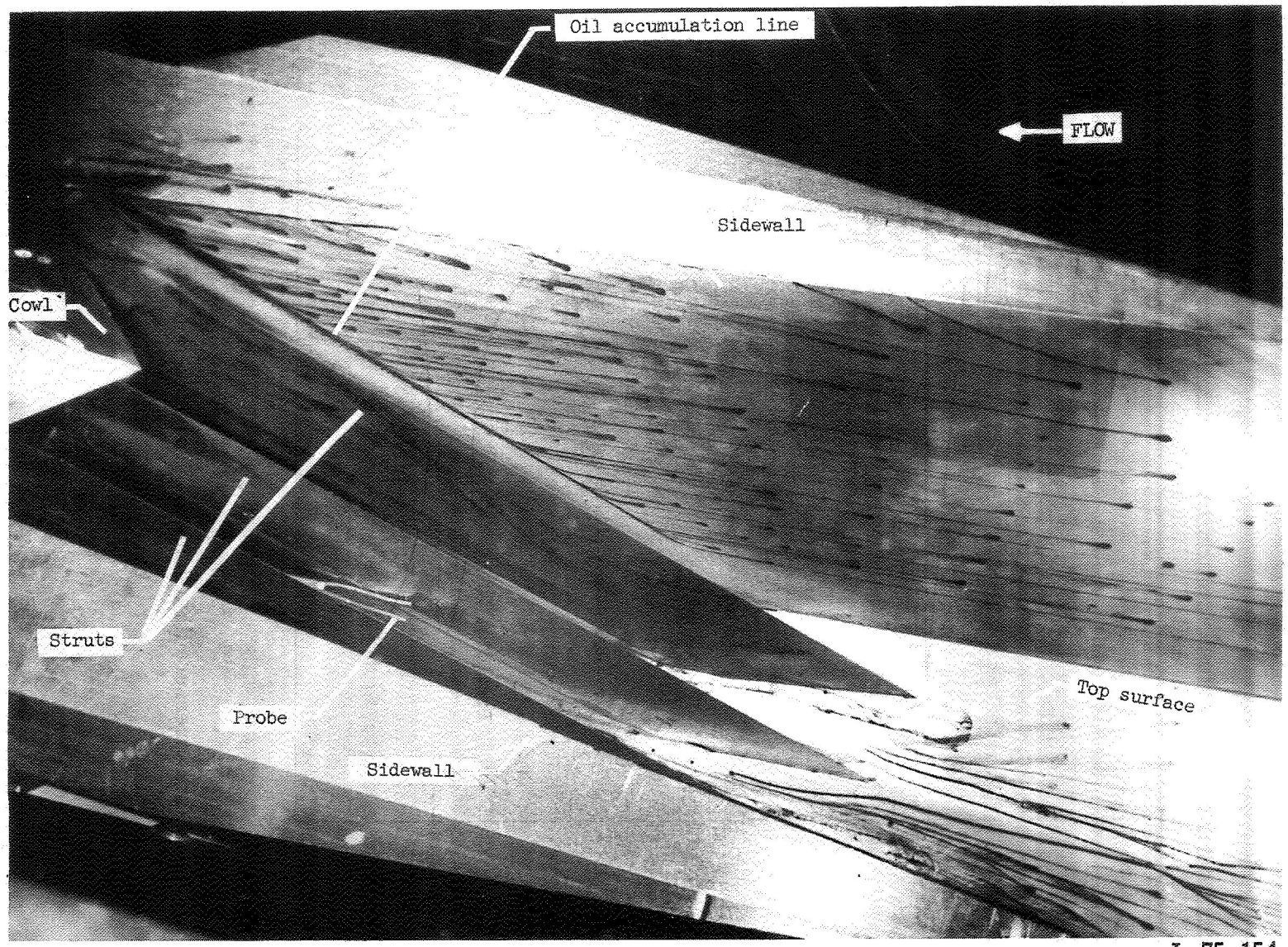

Figure 42.- Oil-flow study.

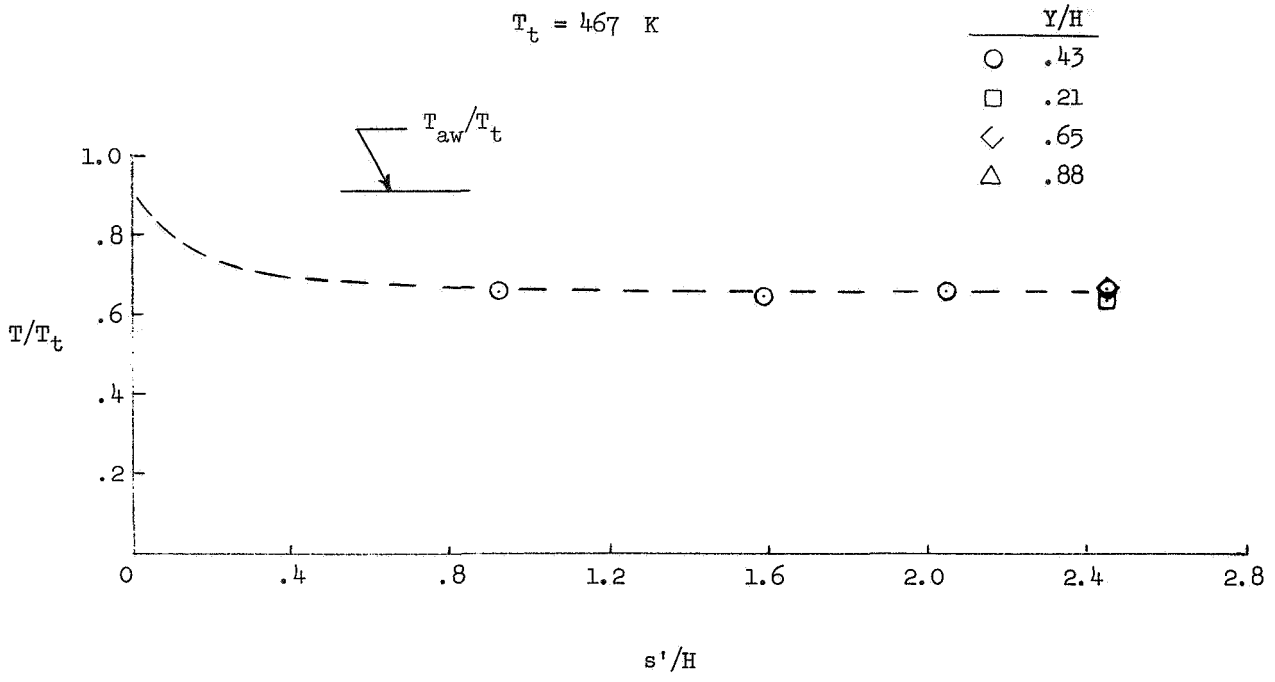

(a) Sidewall.

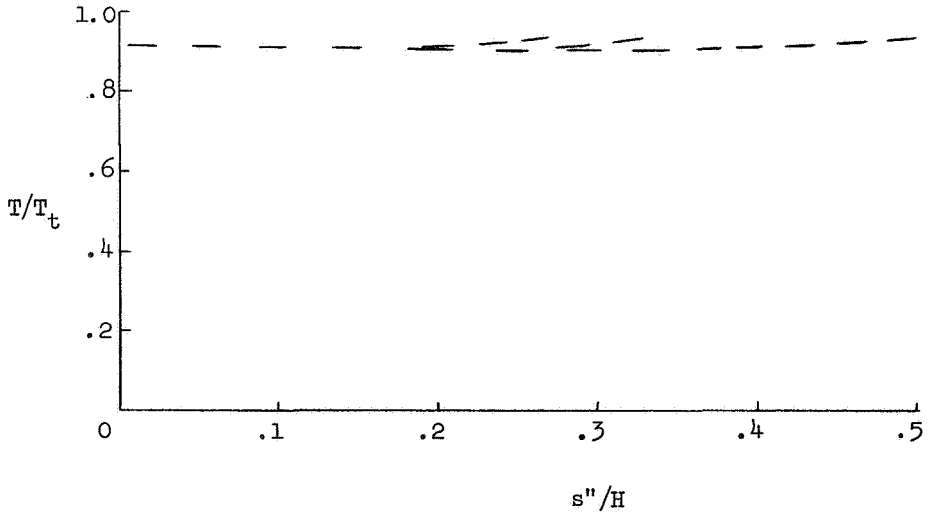

(b) Struts.

Figure 43.- Temperature distributions after 80 sec. M_1 = 6.0.

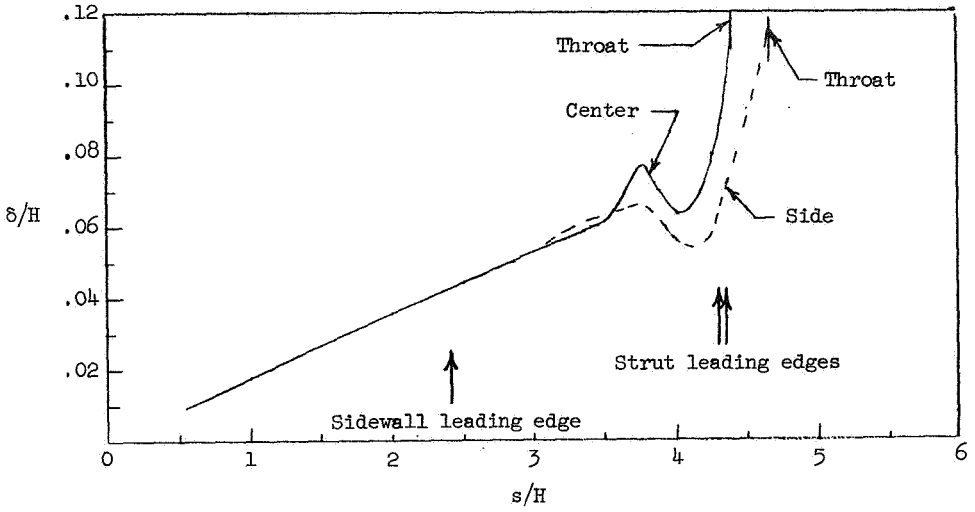

(a) Top surface.

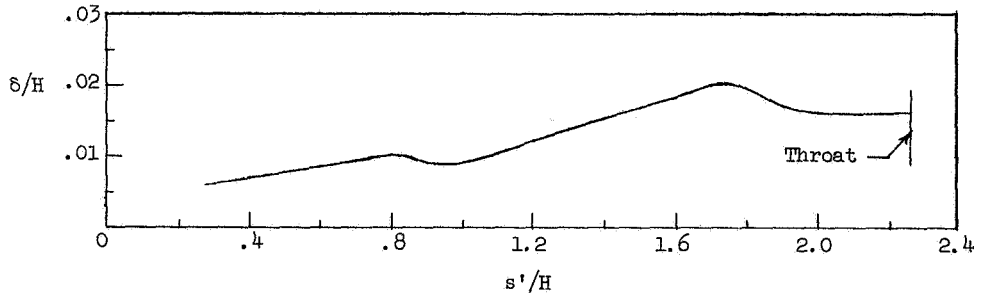

(b) Sidewall (xz-plane).

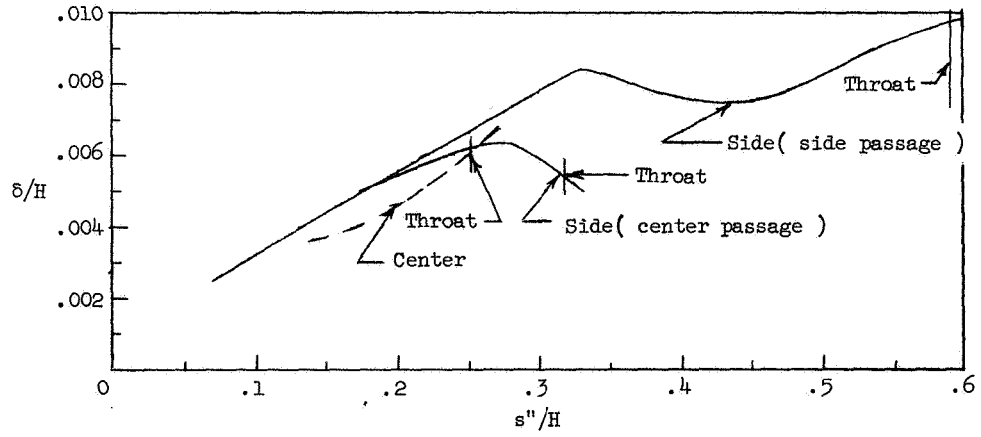

(c) Struts (xz-plane).

Figure 44.- Inlet boundary layers.

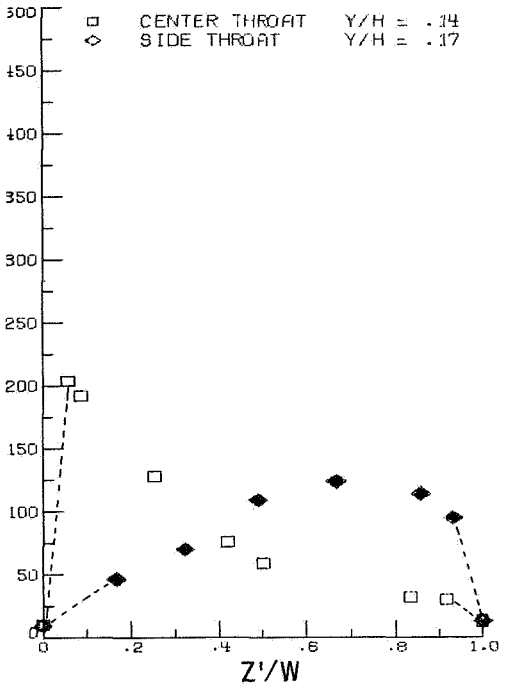

(a) Y/H = 0.15.

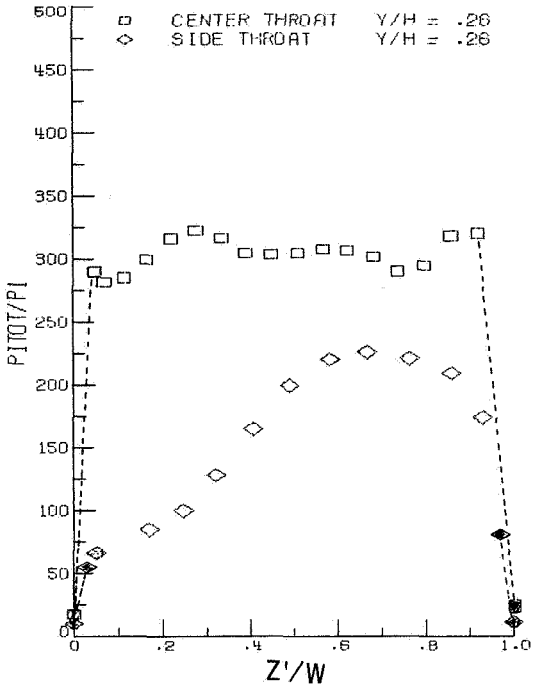

(b) Y/H = 0.26.

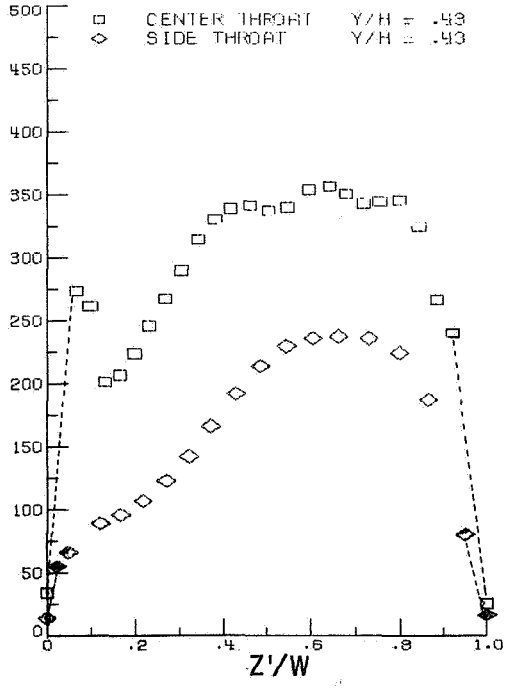

(c) Y/H = 0.43.

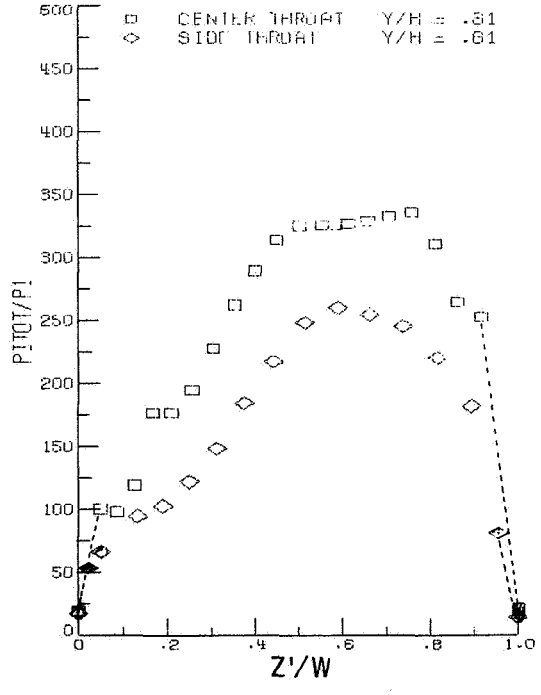

(d) Y/H = 0.61.

Figure 45.- Throat pitot pressure surveys. The solid symbols represent theoretical boundary-layer calculations.

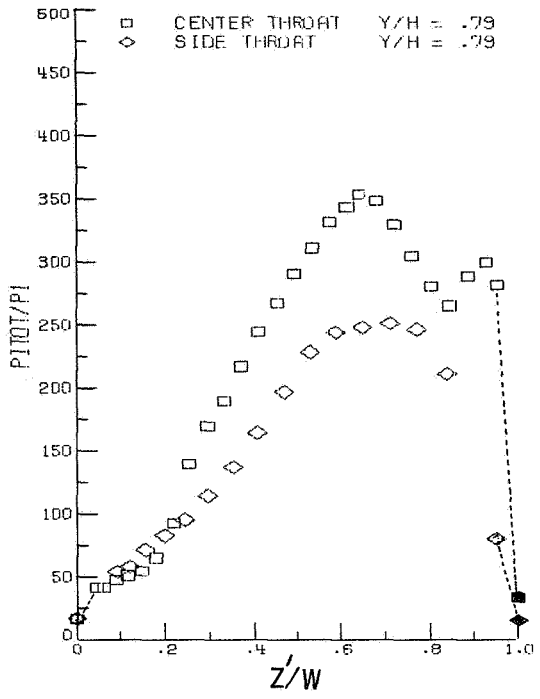

(e) Y/H = 0.79.

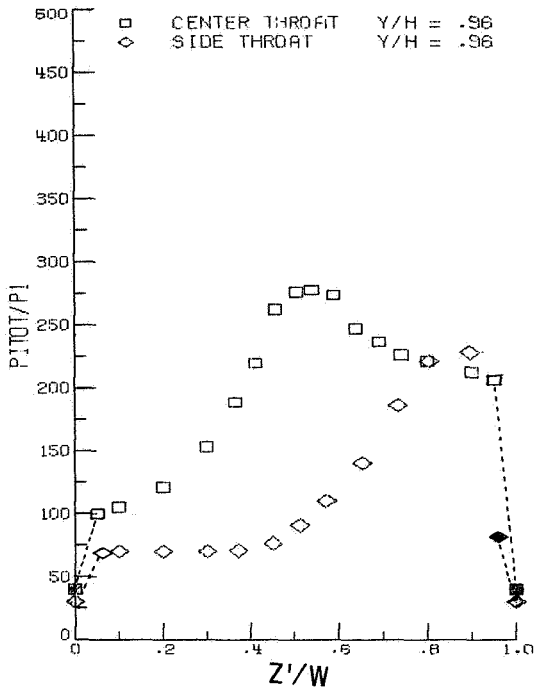

(f) Y/H = 0.96.

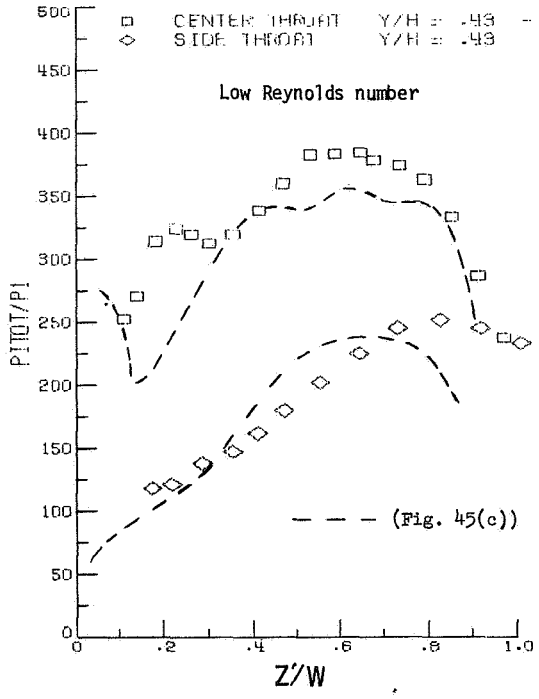

(g) Y/H = 0.43.

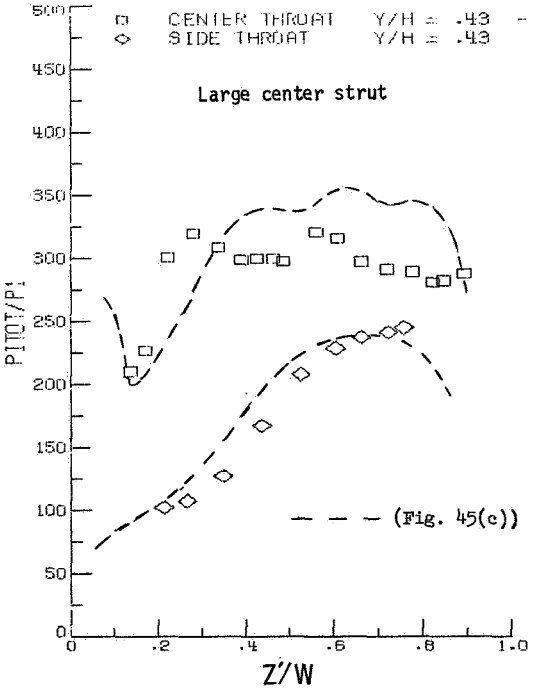

(h) Y/H = 0.43.

Figure 45.- Concluded.

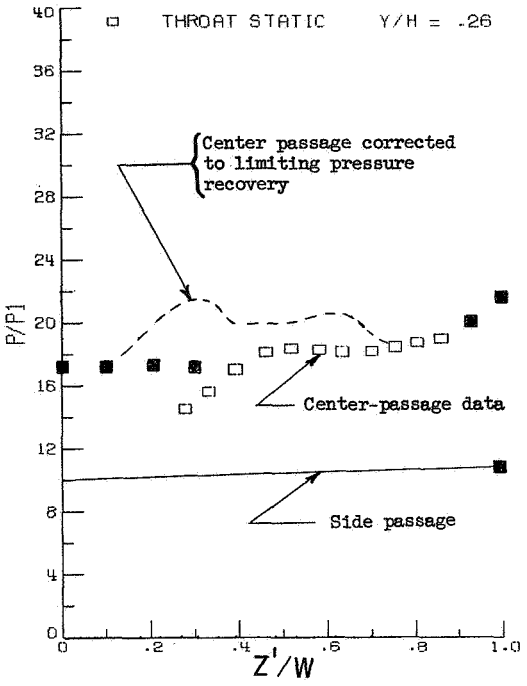

(a) Y/H = 0.26.

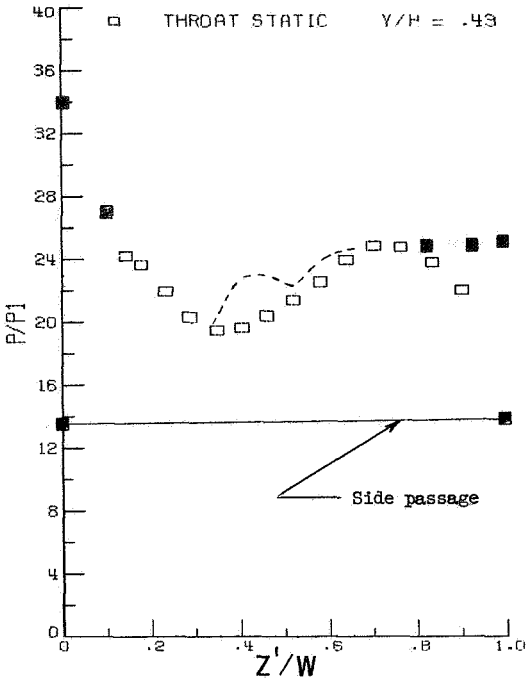

(b) Y/H = 0.43.

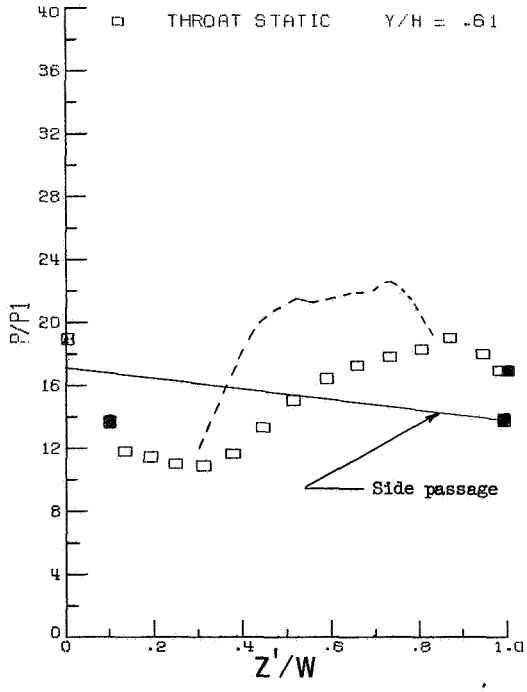

(c) Y/H = 0.61.

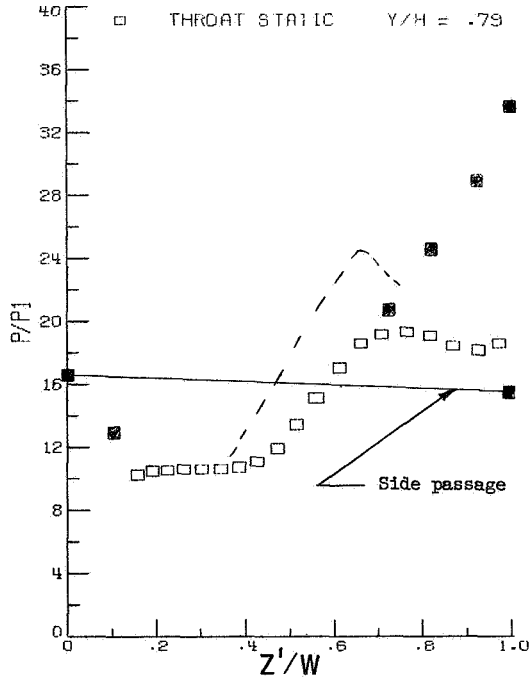

(d) Y/H = 0.79.

Figure 46.- Throat static-pressure surveys. The solid symbols represent data faired to the wall static pressure.

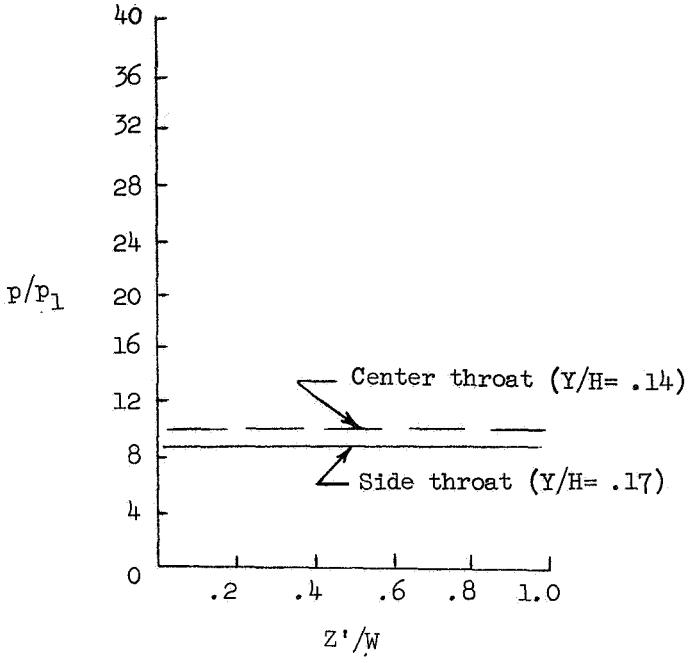

(a) Near top surface.

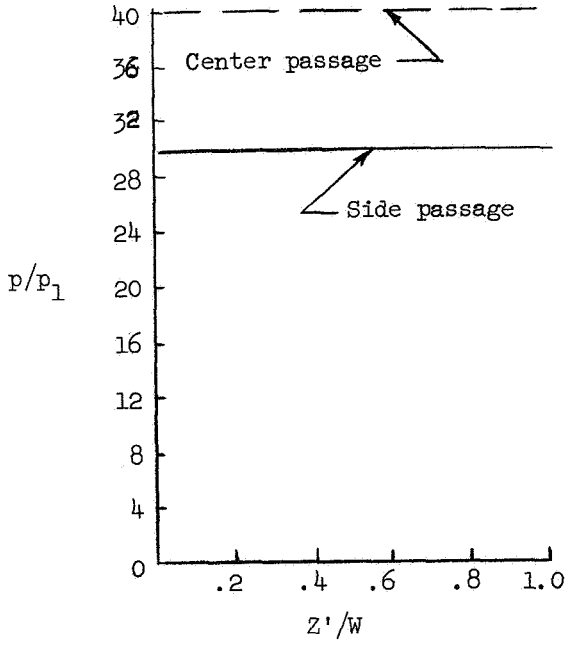

(b) Near cowl; Y/H = 0.96.

Figure 47.- Additional estimated throat static distributions.

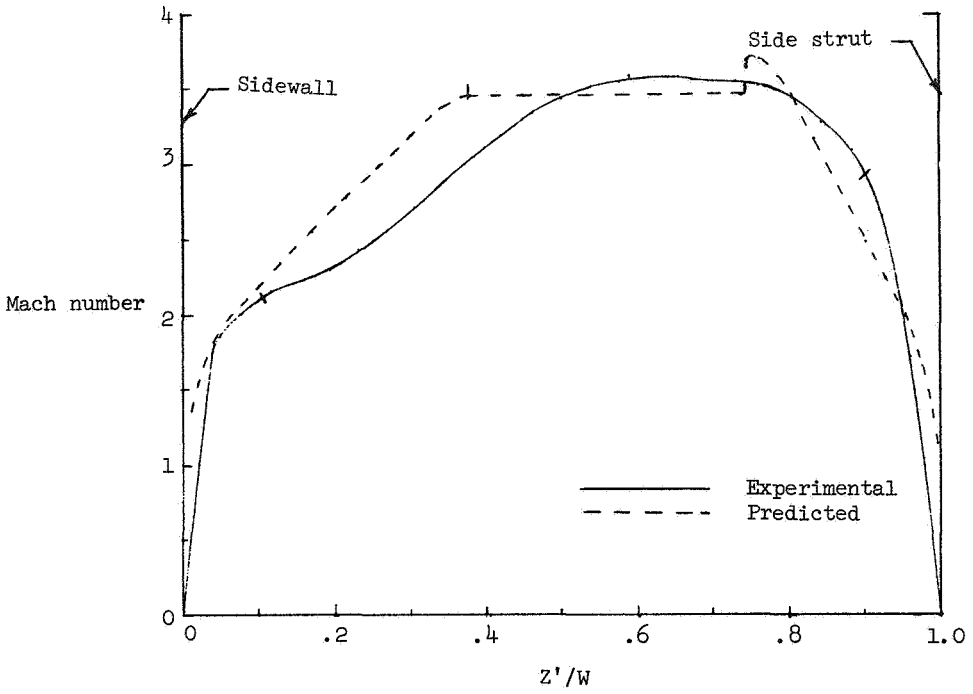

(a) Side passage; Throat gap = 0.772 cm.

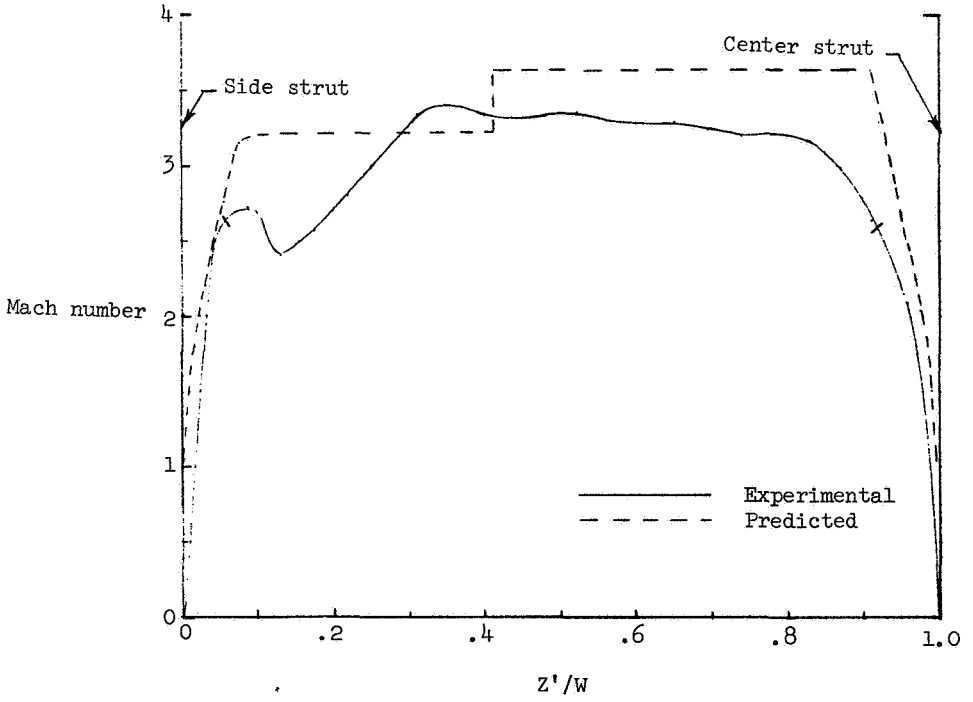

(b) Center passage; Throat gap = 1.227 cm.

Figure 48.- Mach number distribution at throat. Y/H = 0.43.

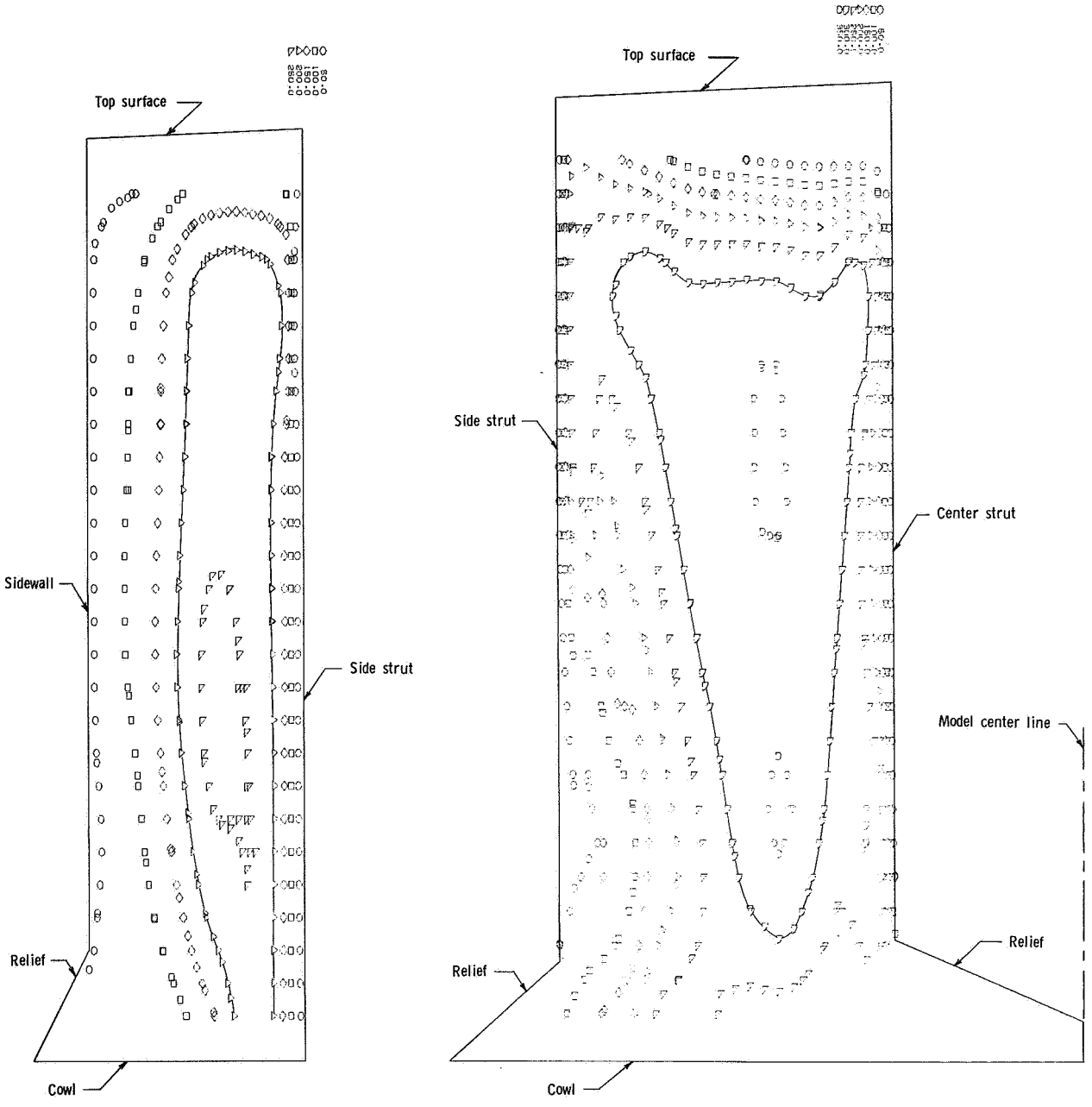

(a) Side passage.

(b) Center passage.

Figure 49.- Throat map of p_{pitot}/p_1.

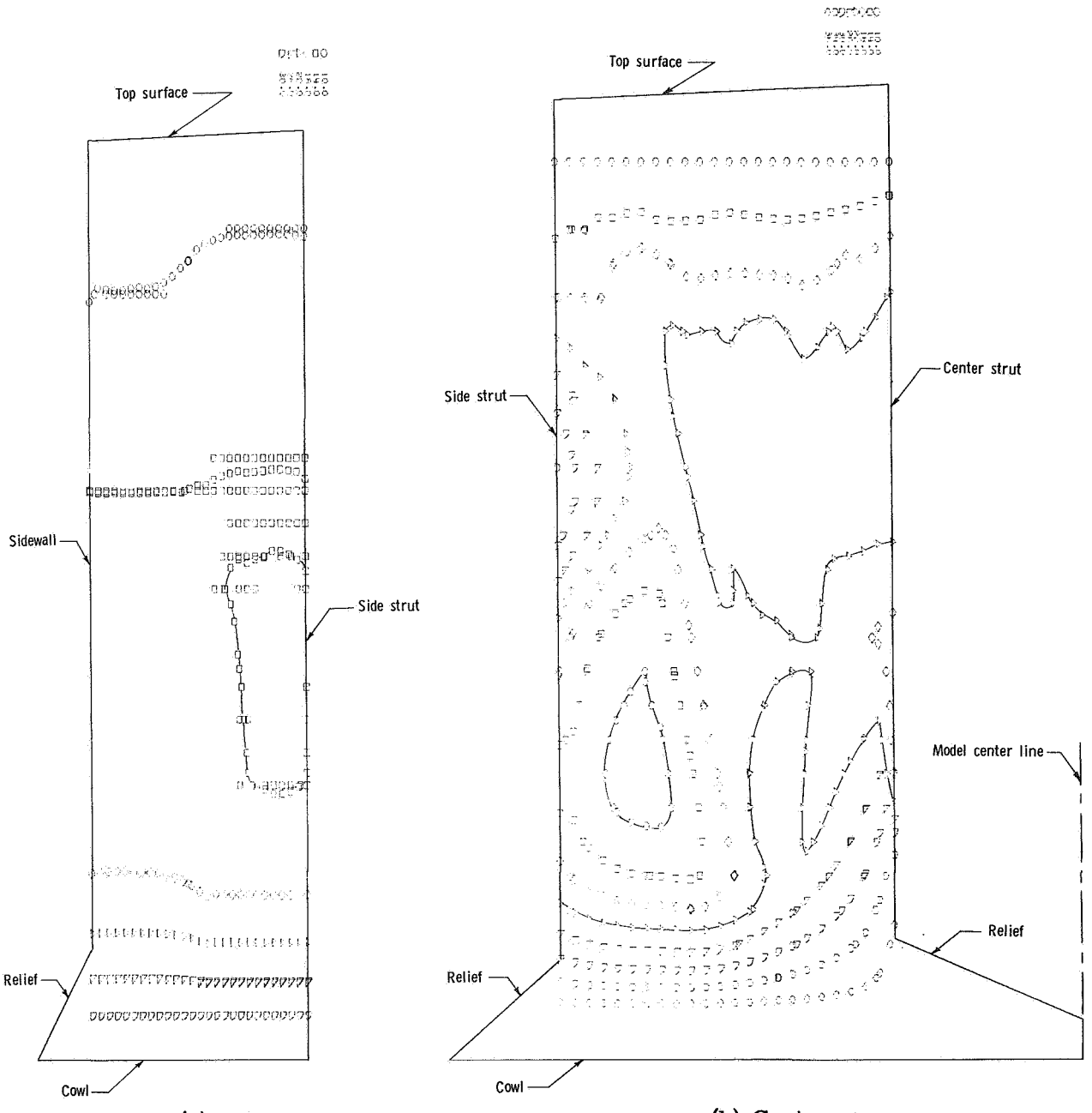

(a) Side passage.

(b) Center passage.

Figure 50.- Throat map of p/p_1.

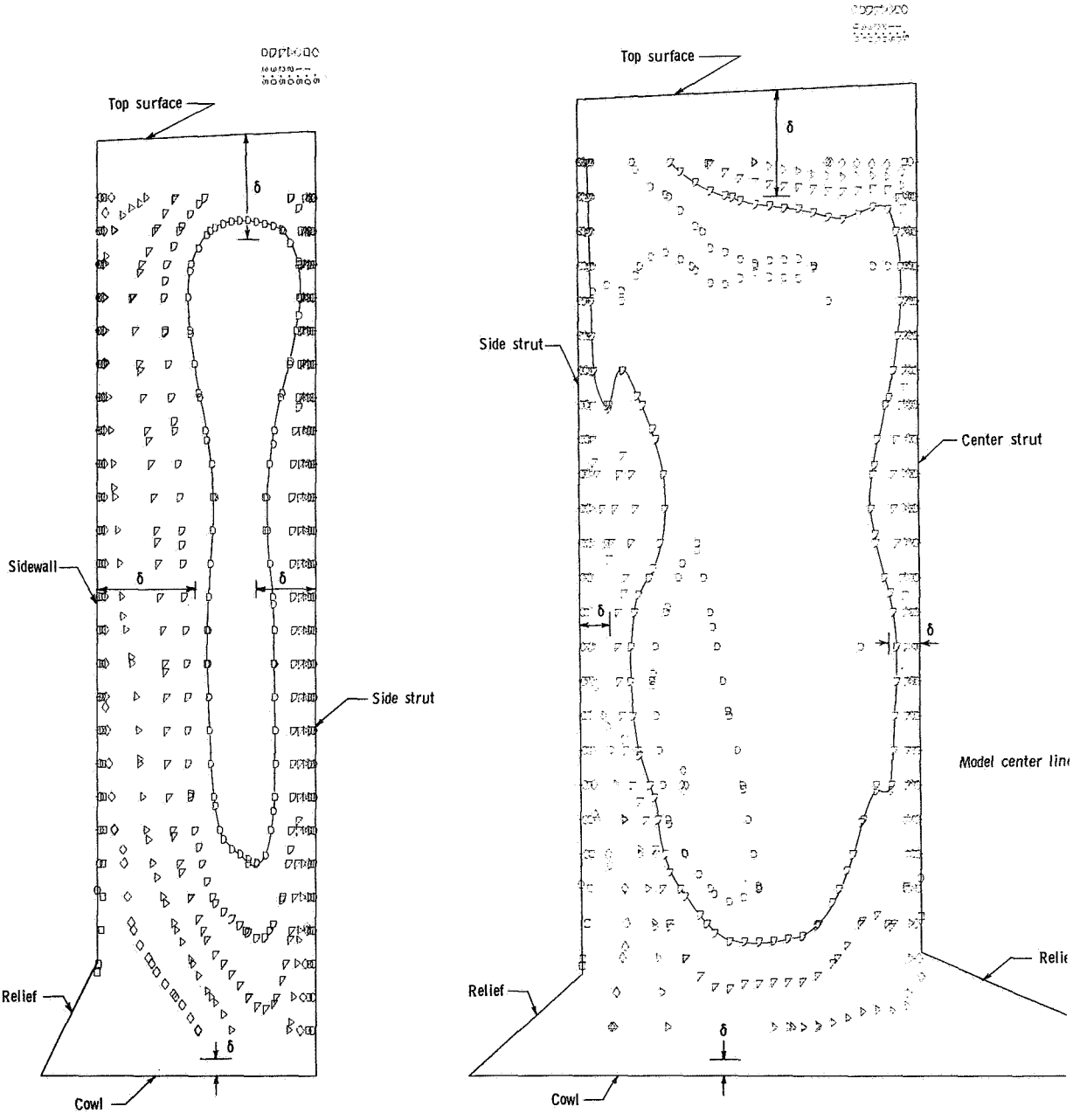

Figure 51.- Throat map of Mach number. $M_1 = 6.0$.

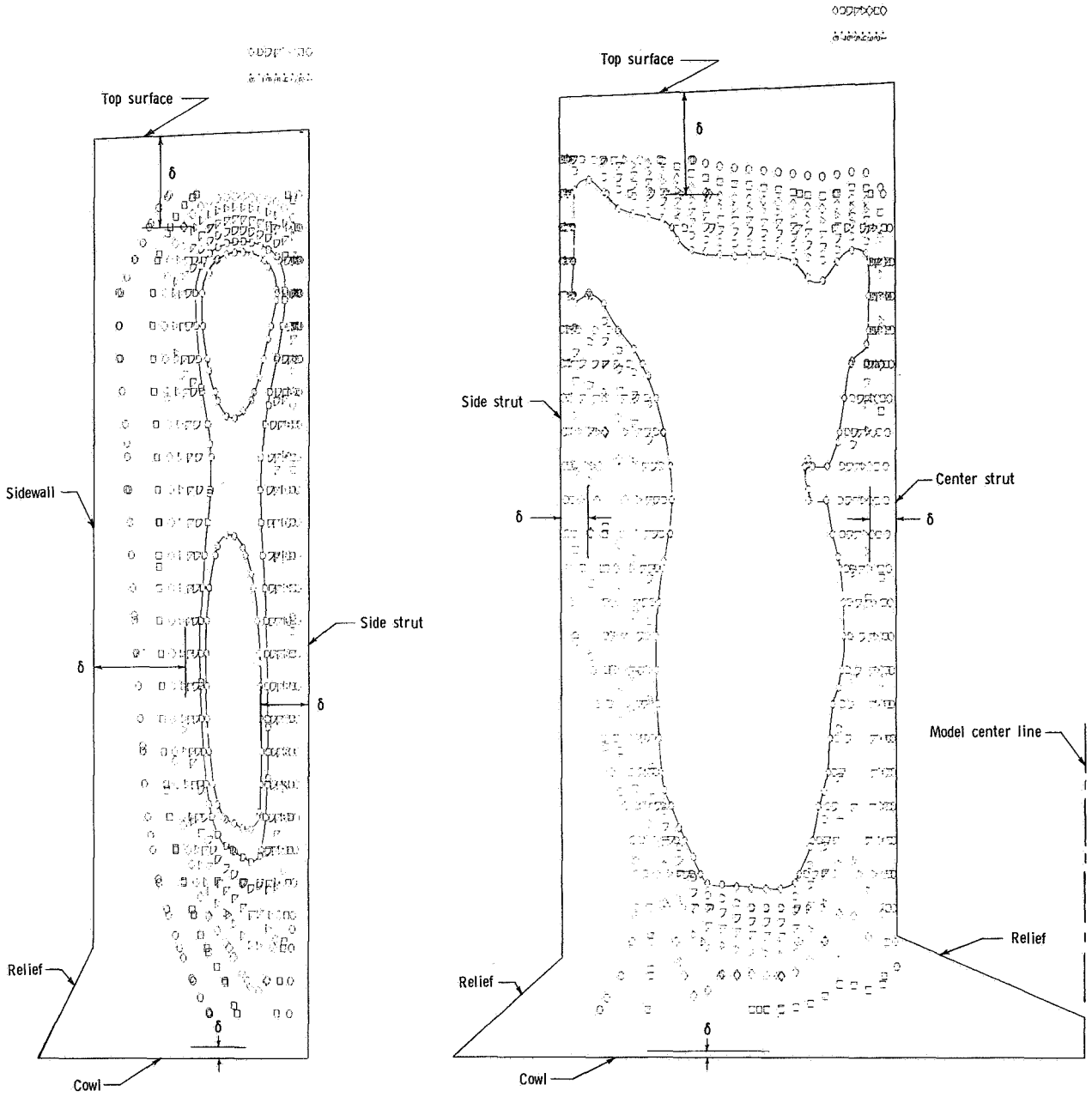

(a) Side passage. (b) Center passage.

Figure 52.- Throat map of total-pressure recovery.

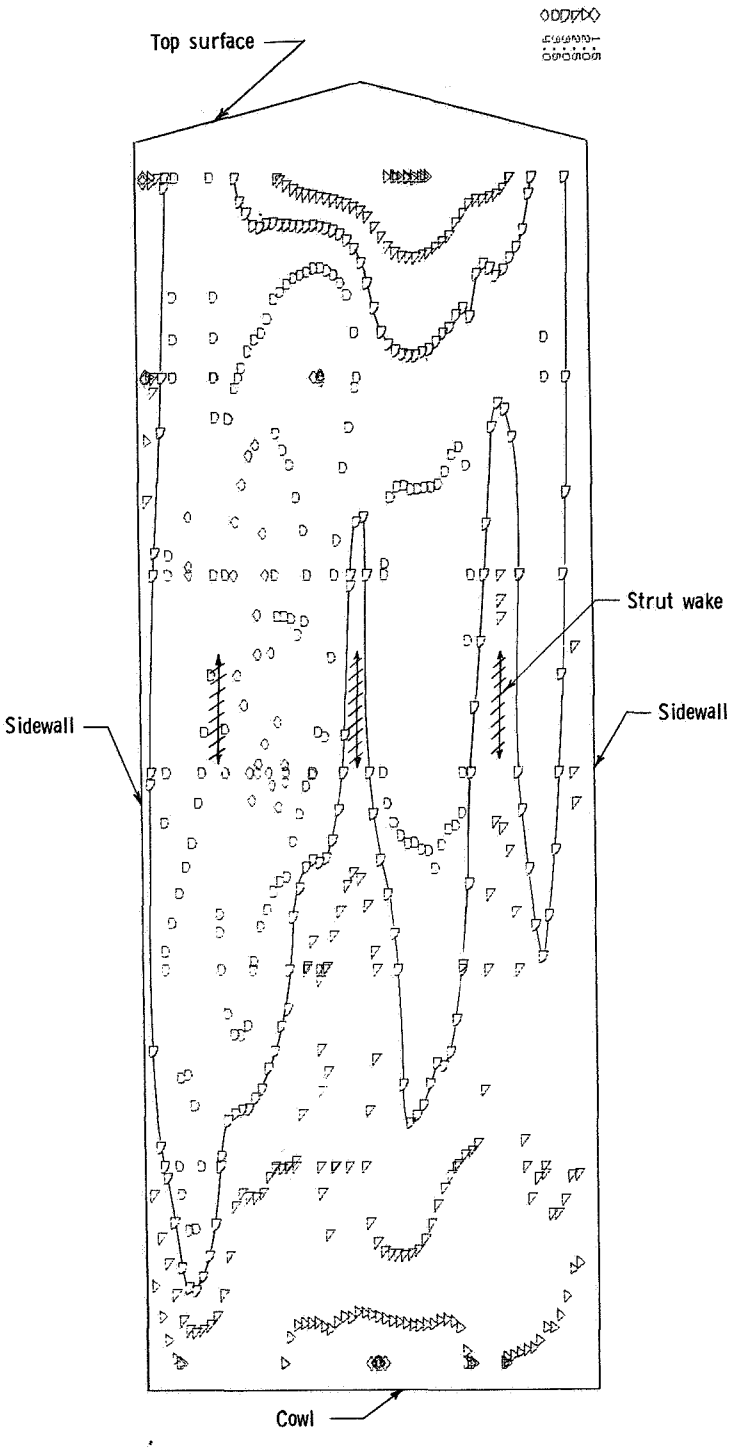

Figure 53.- Mach number distribution at capture station. $M_1 = 6.0$.

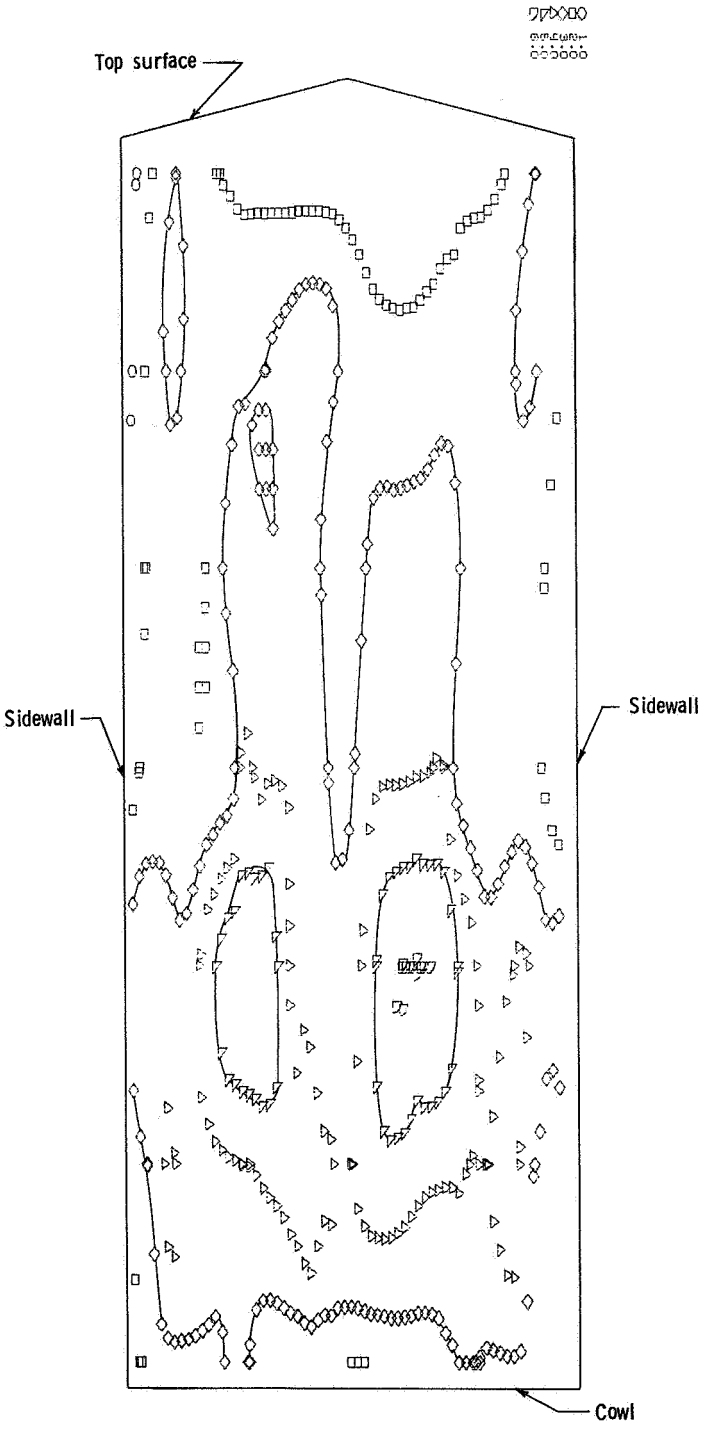

Figure 54.- Capture parameter $\rho v/\rho_1 v_1$.

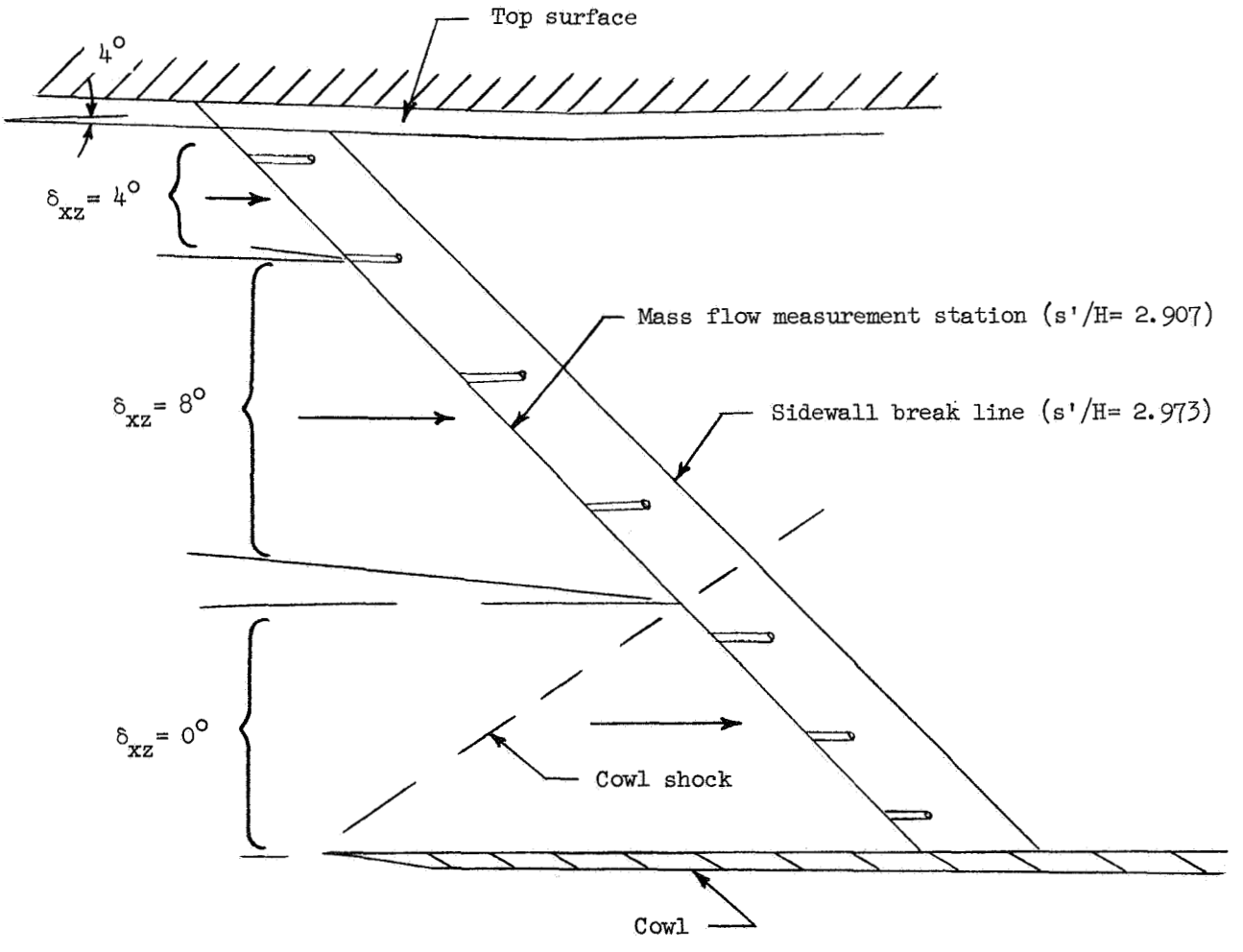

Figure 55.- Assumed flow directions used to compute capture.

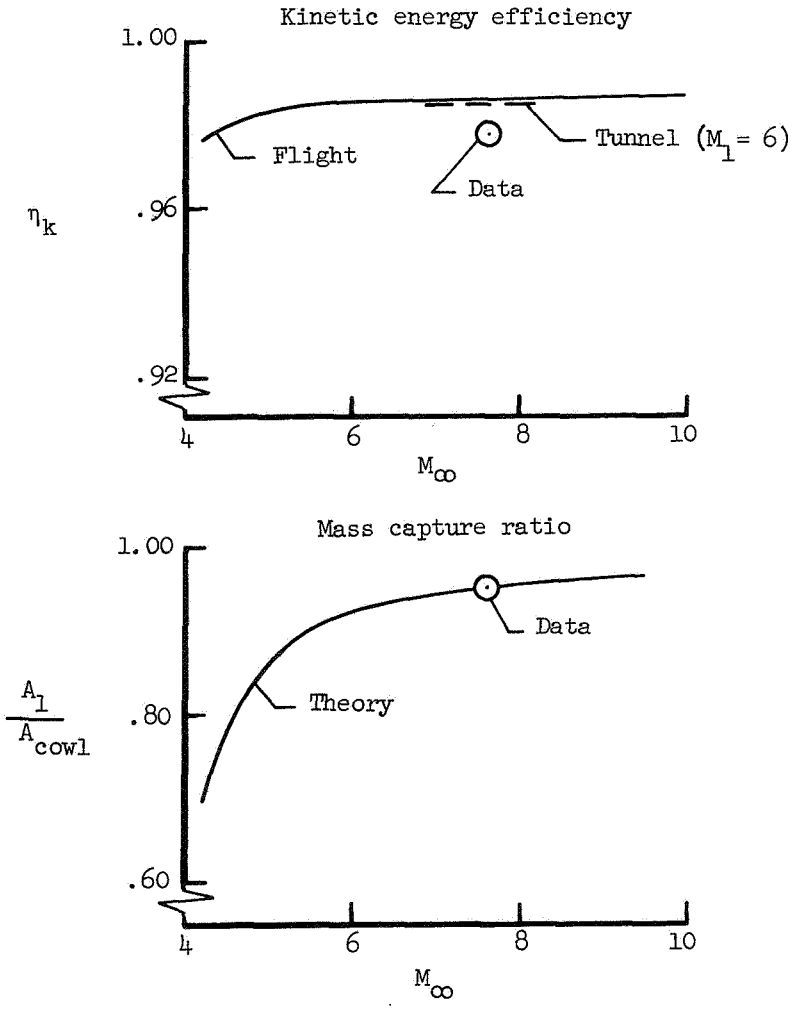

Mass weighted data (M_1 = 6.0)

	Passage		Total* Inlet
	Side	Center	
Contraction ratio	5.8	7.5	7.0
Throat Mach number	3.0	3.1	3.1
Recovery	.46	.66	.59
η_k	.965	.982	.977
Mass capture	.31	.63	.94

* Flow split based on design

Figure 56.- Integrated performance parameters.

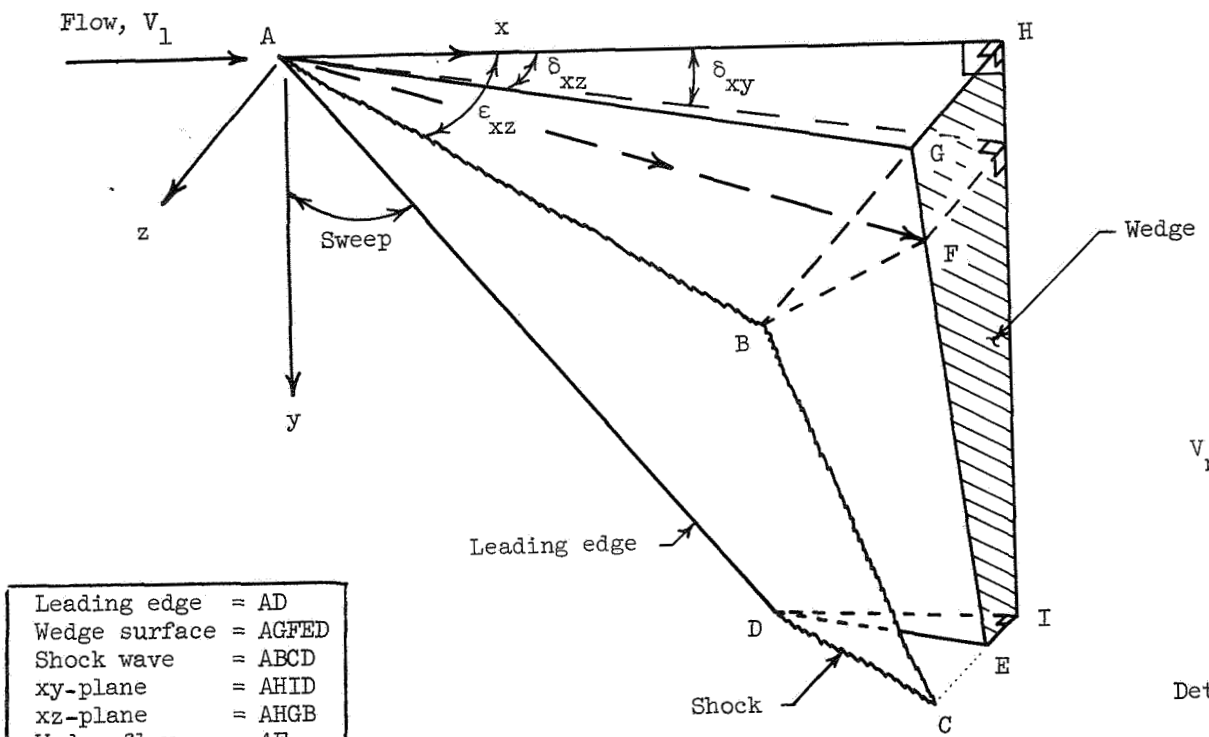

Leading edge	= AD
Wedge surface	= AGFED
Shock wave	= ABCD
xy-plane	= AHID
xz-plane	= AHGB
Wedge flow	= AF
Fillet	= AGFB

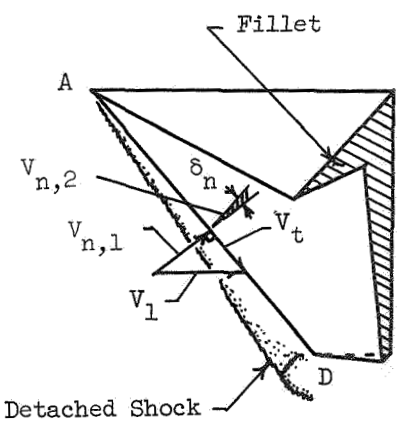

Sketch of flow vectors and a detached shock (Mach number for component $V_{n,2}$ less than 1).

Figure 57.- Swept compression wedge.

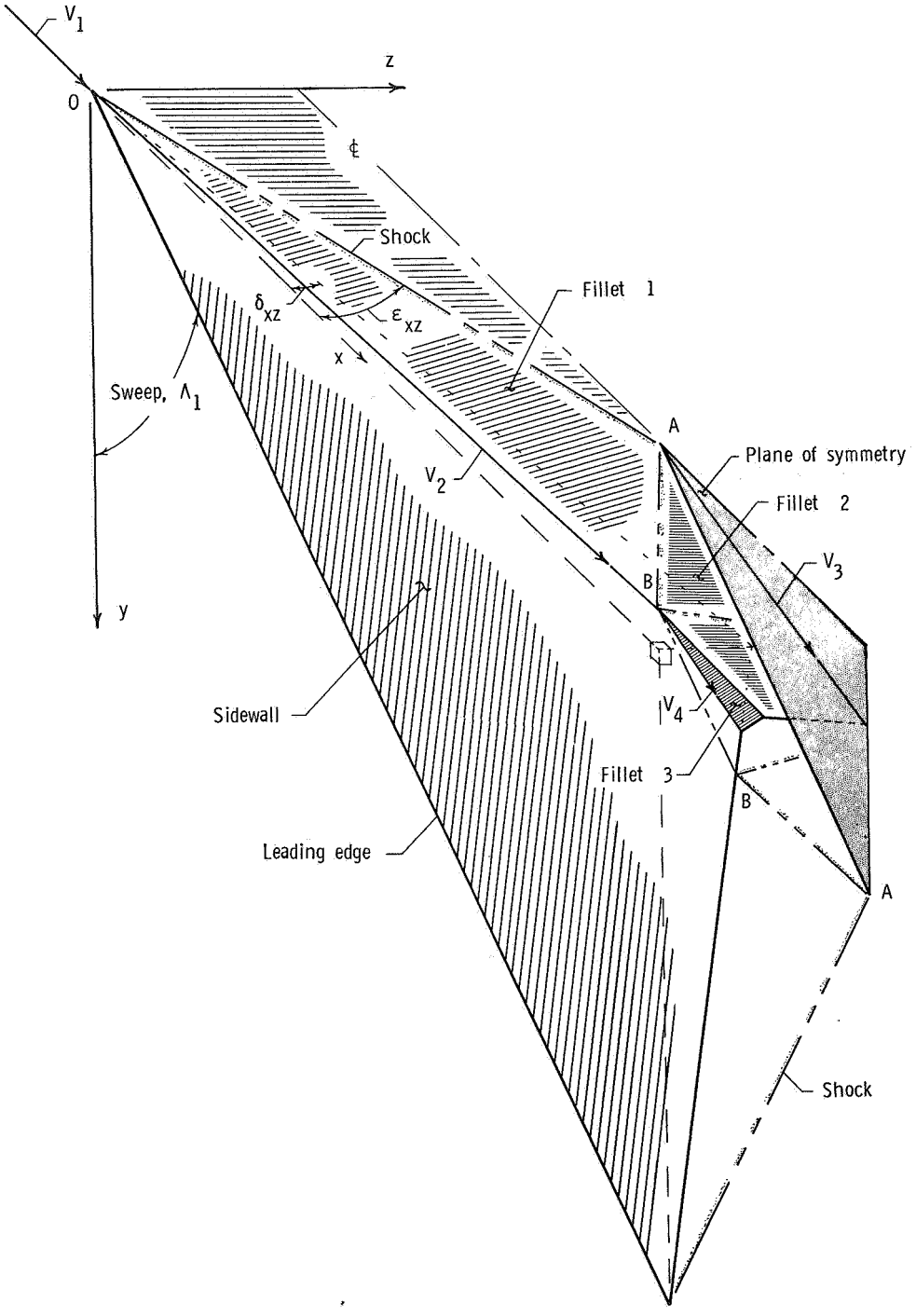

Figure 58.- Train of swept shock waves.

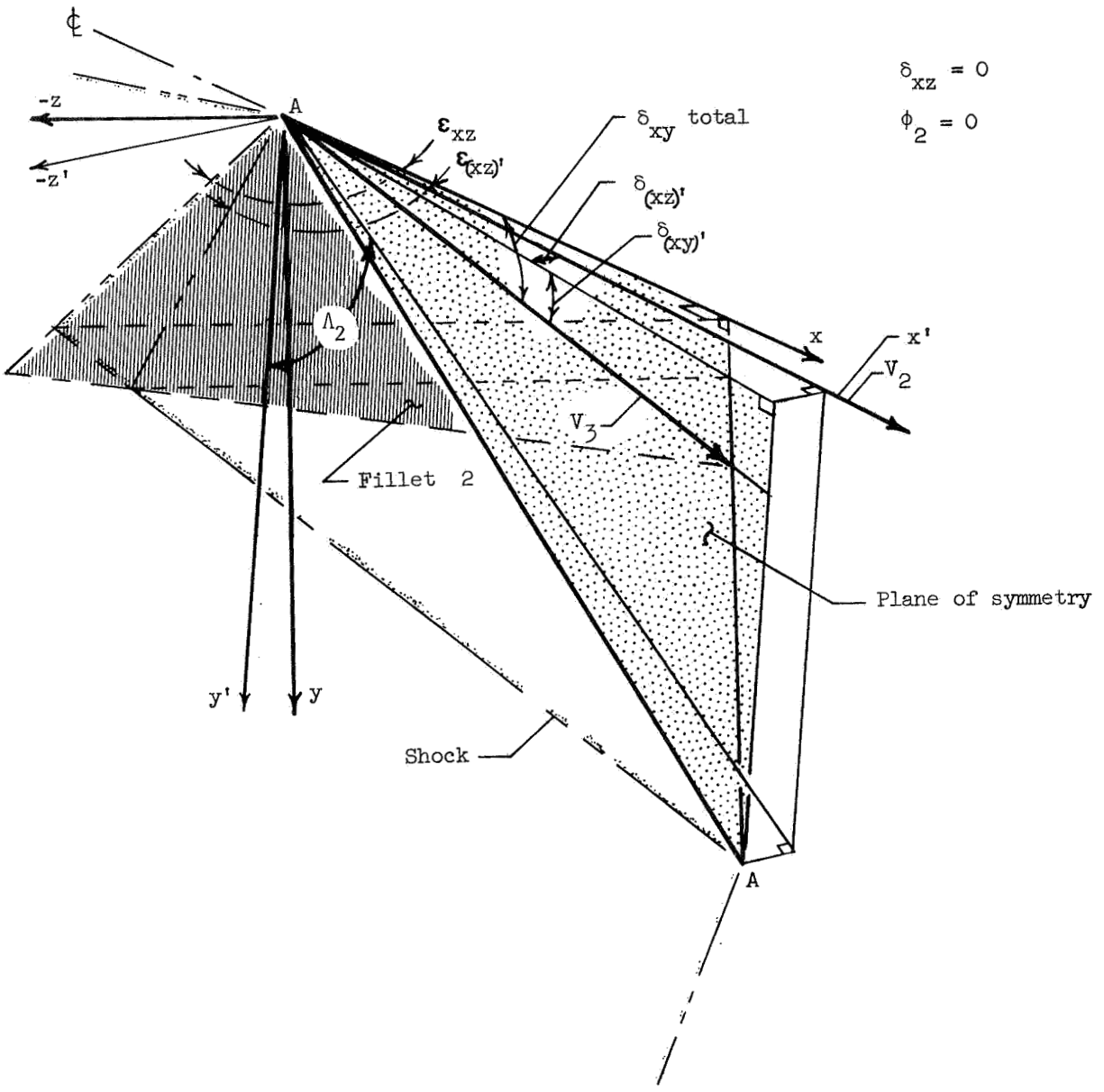

Figure 59.- First reflected shock wave.

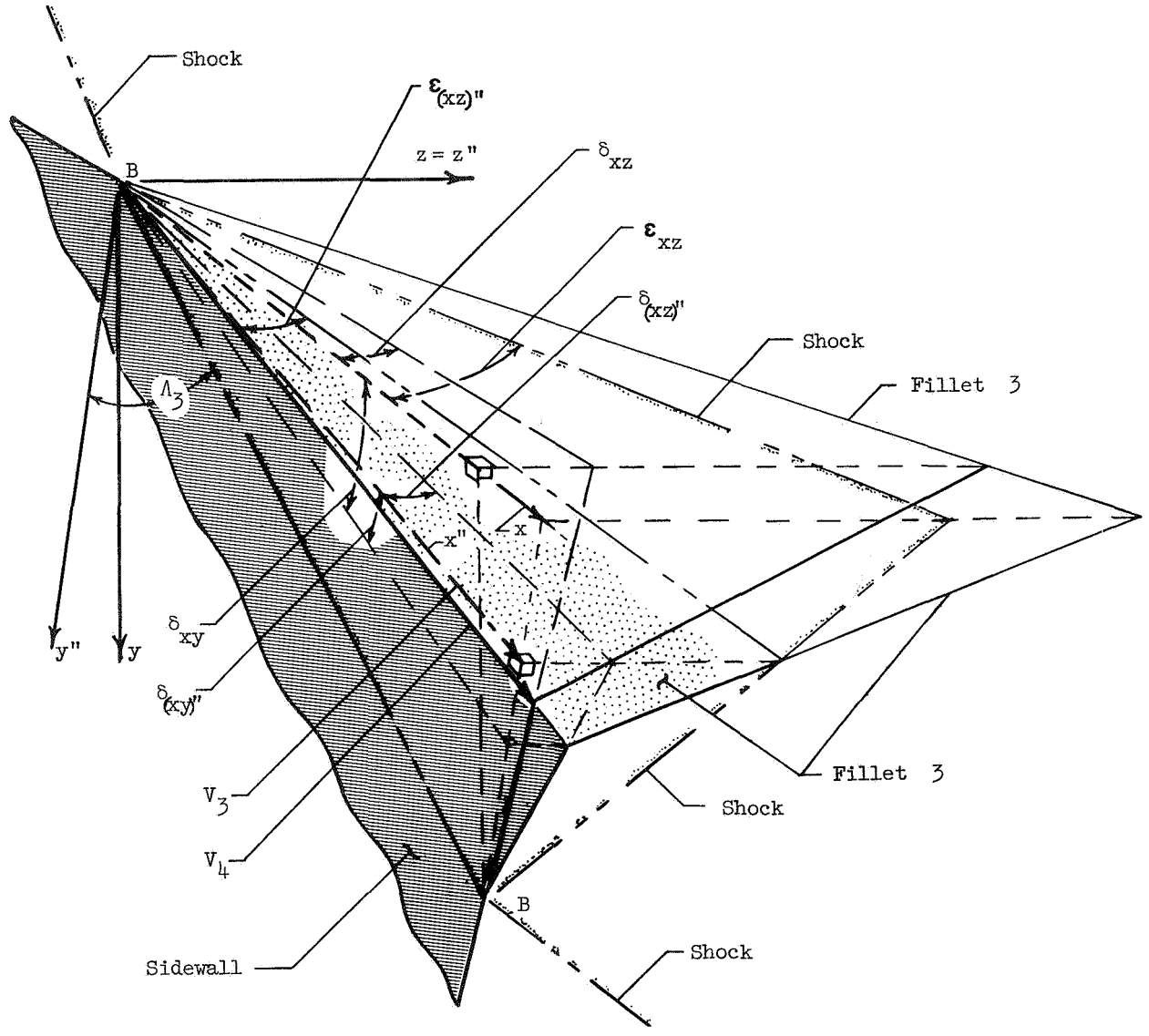

Figure 60.- Second reflected shock wave.

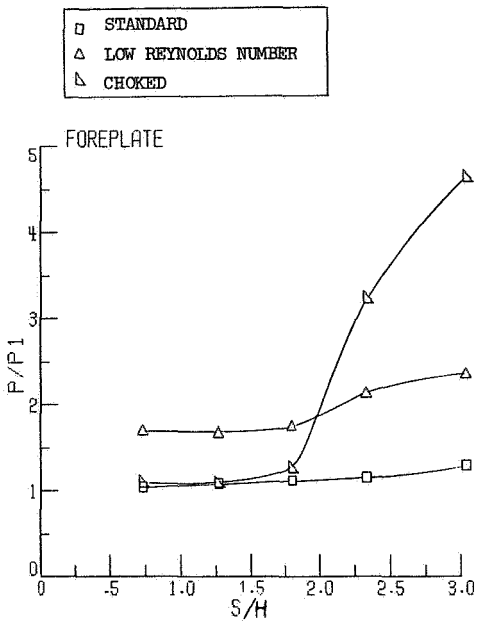

(a) Foreplate.

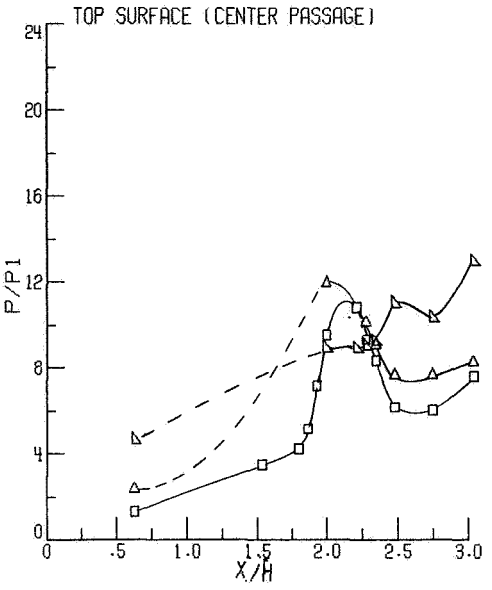

(b) Top surface (center passage).

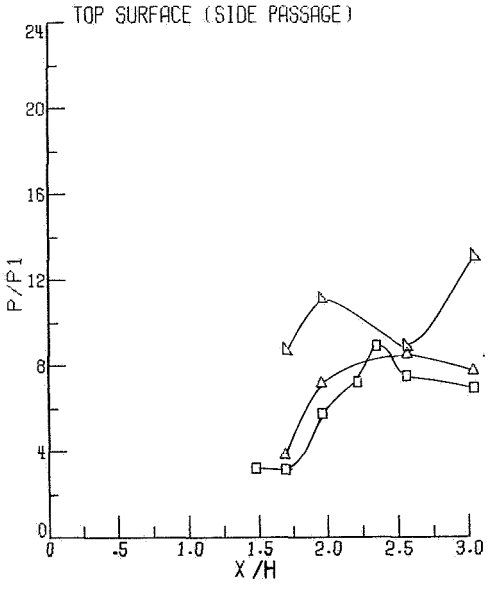

(c) Top surface (side passage).

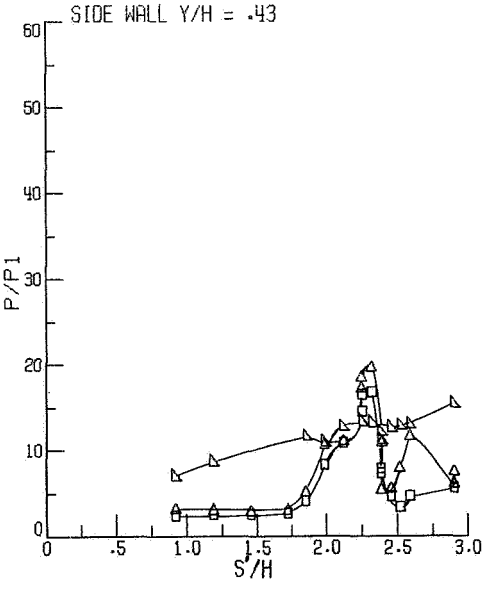

(d) Side wall; Y/H = 0.43.

Figure 61.- Static pressure distributions for low pressure and choked inlet tests. $M_1 = 6.0$.

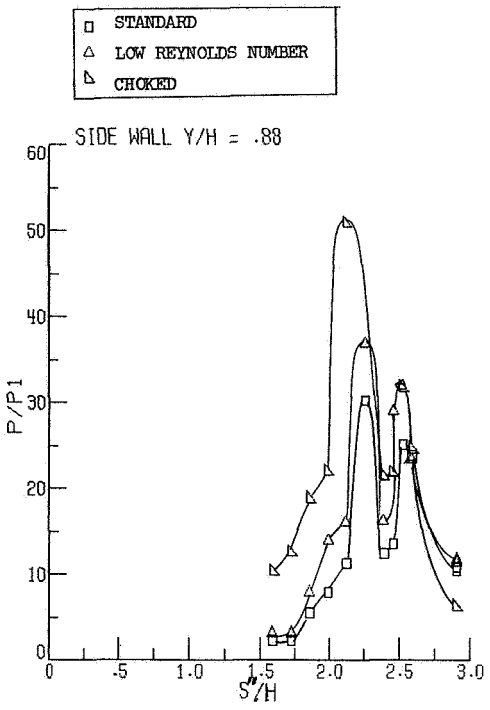

(e) Side wall; Y/H = 0.88.

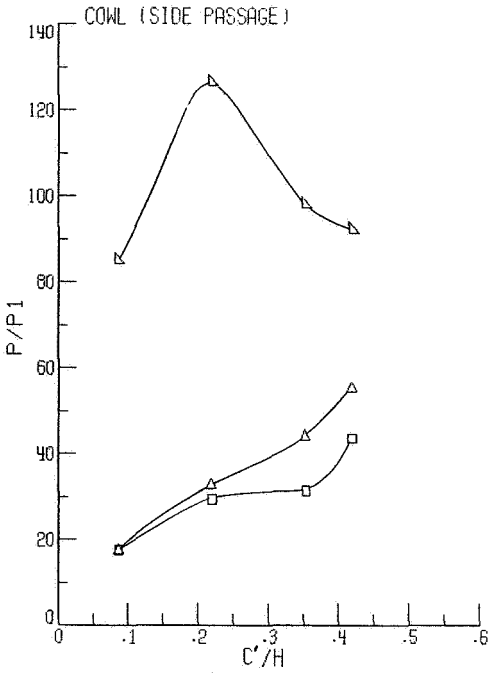

(f) Cowl (side passage).

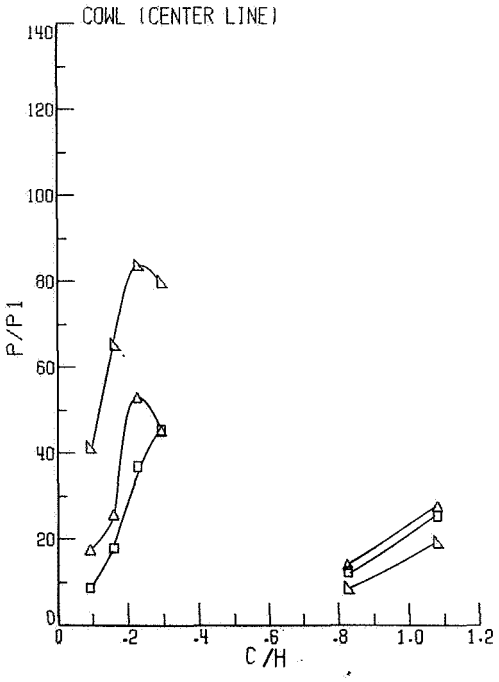

(g) Cowl (center line).

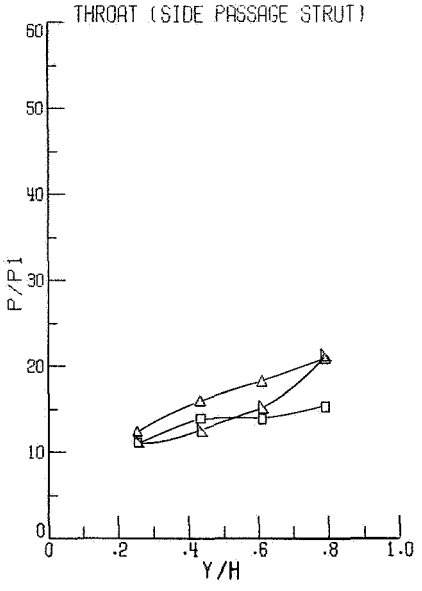

(h) Throat (side-passage strut).

Figure 61.- Continued.

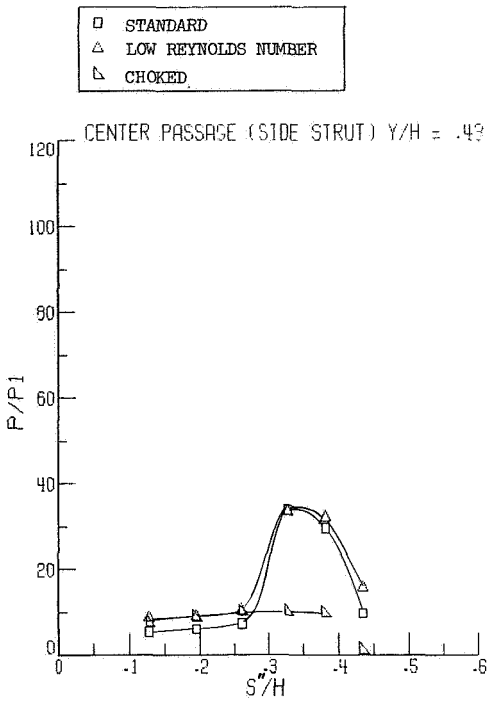

(i) Center passage (side strut); Y/H = 0.43.

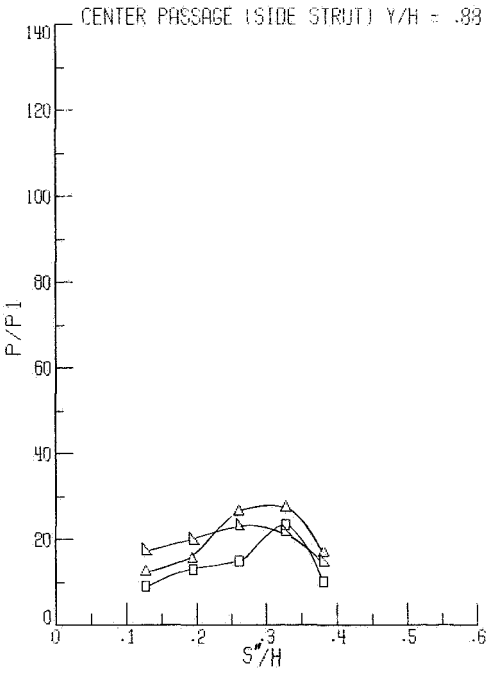

(j) Center passage (side strut); Y/H = 0.88.

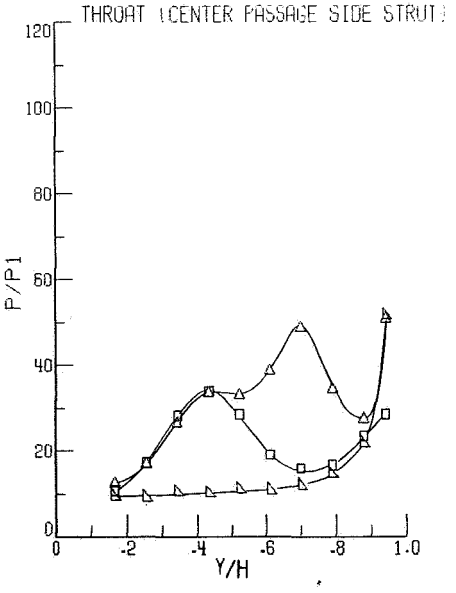

(k) Throat (center-passage side strut).

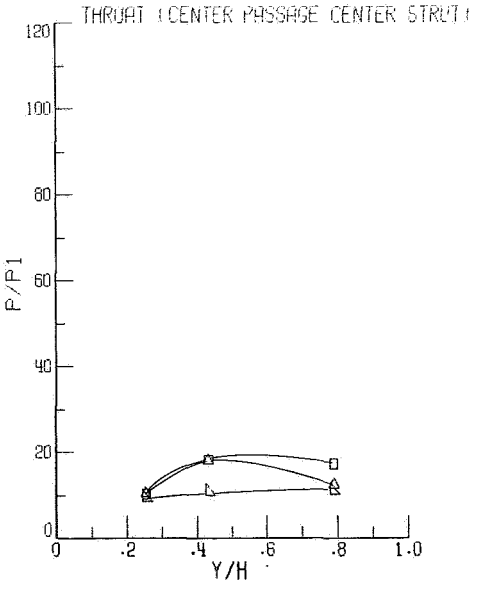

(l) Throat (center-passage center strut).

Figure 61.- Concluded.

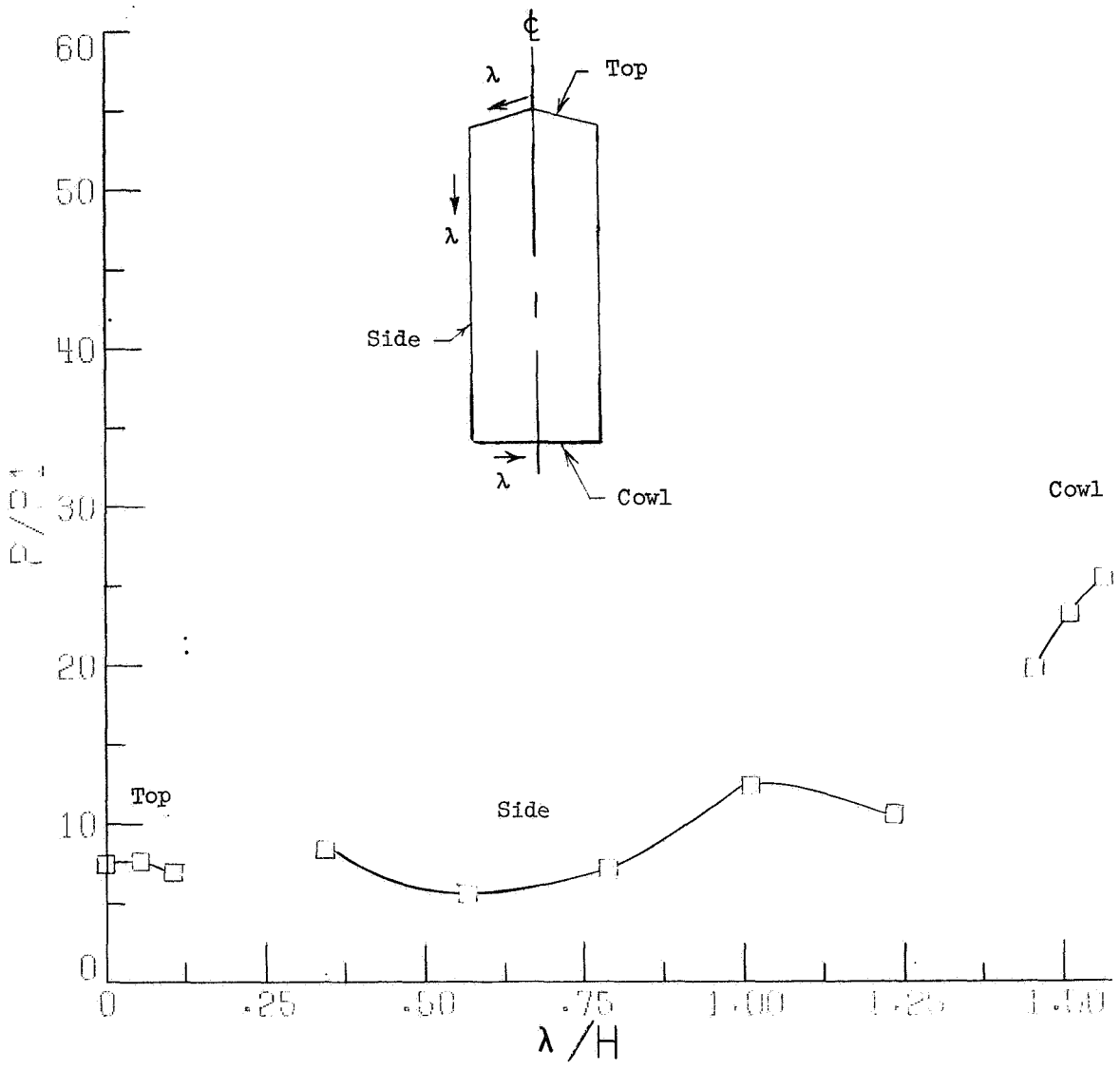

Figure 62.- Wall static-pressure distribution at capture station.

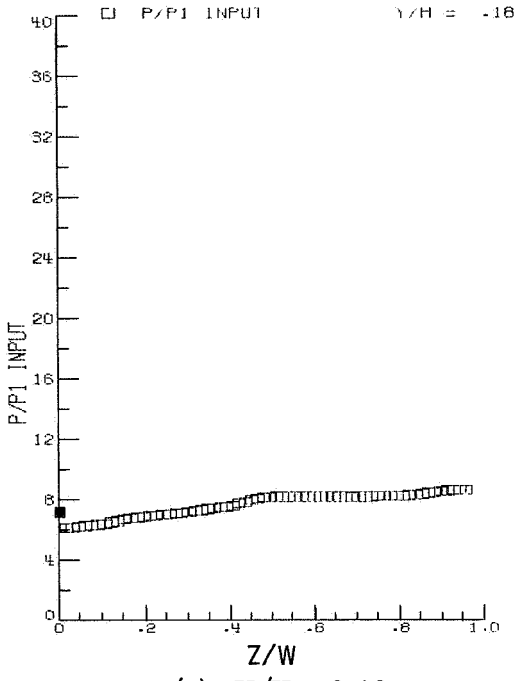

(a) Y/H = 0.18.

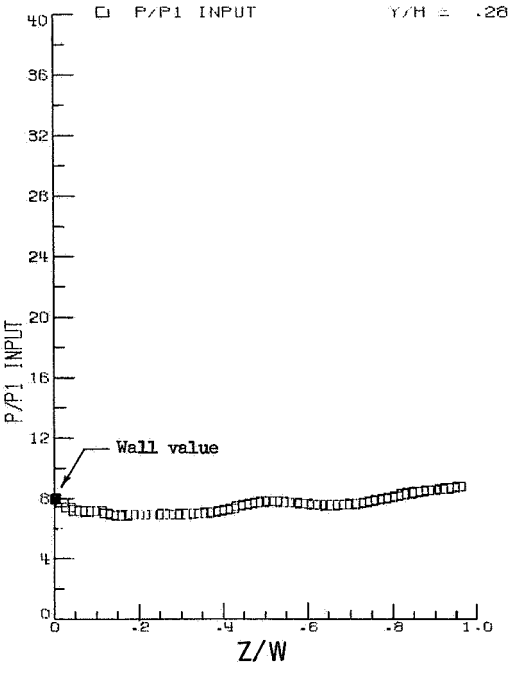

(b) Y/H = 0.28.

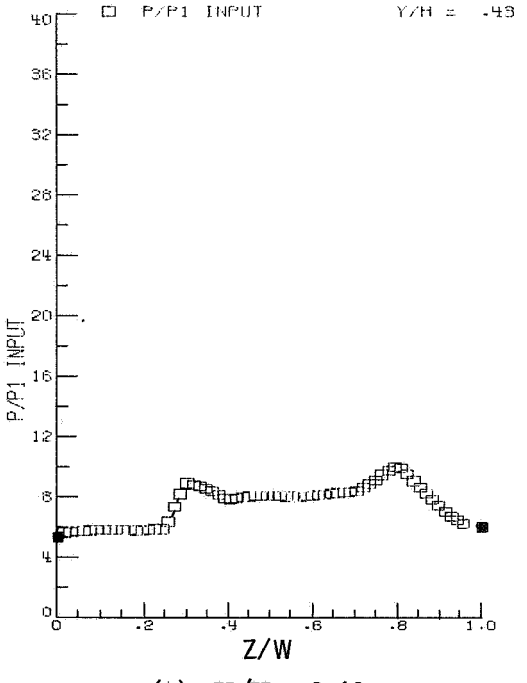

(c) Y/H = 0.43.

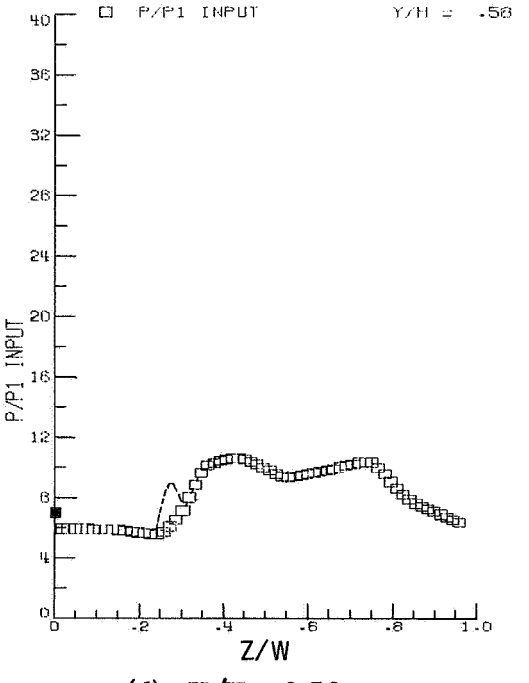

(d) Y/H = 0.58.

Figure 63.- Static-pressure surveys at capture station. $M_1 = 6.0$.

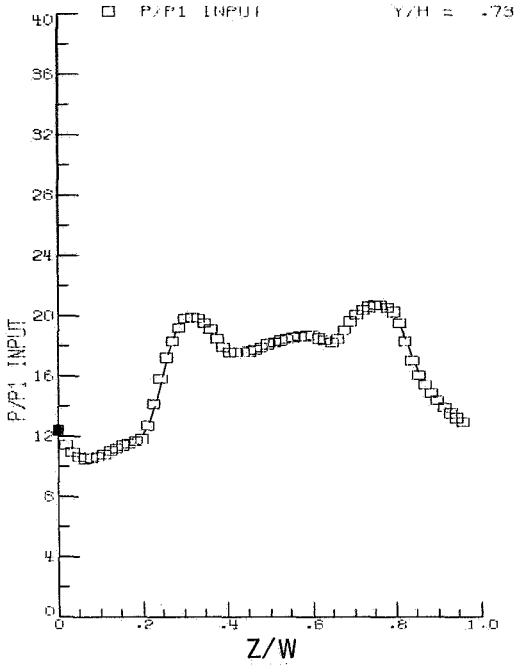

(e) Y/H = 0.73.

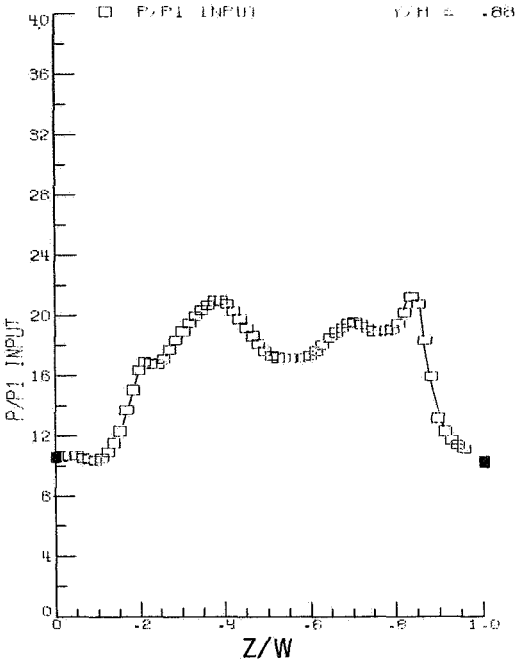

(f) Y/H = 0.88.

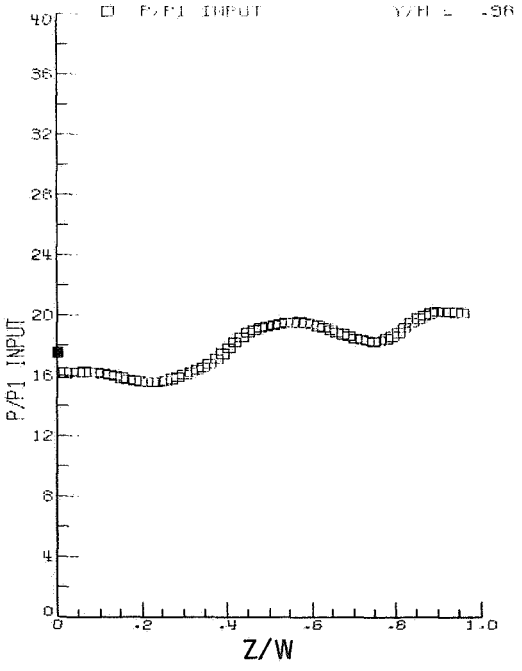

(g) Y/H = 0.98.

Figure 63.- Concluded.

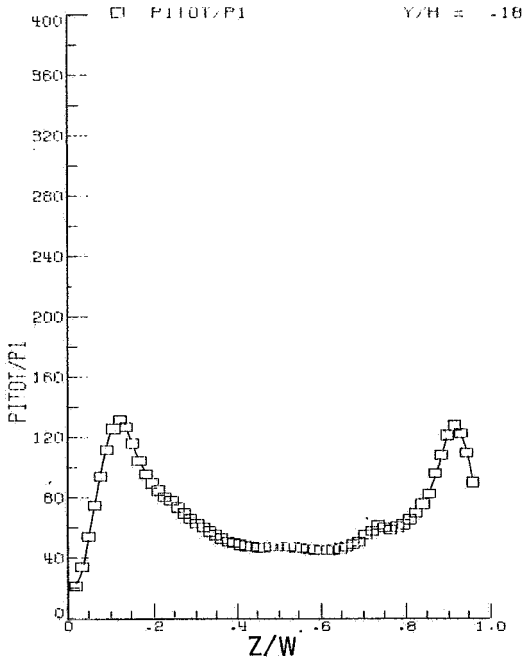

(a) Y/H = 0.18.

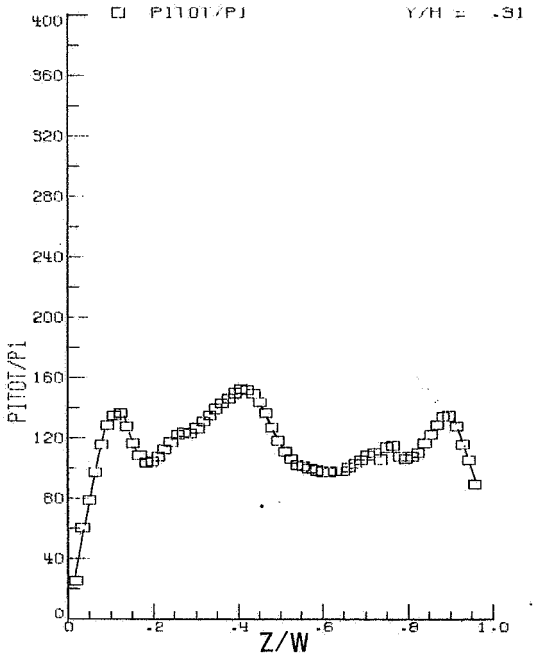

(b) Y/H = 0.31.

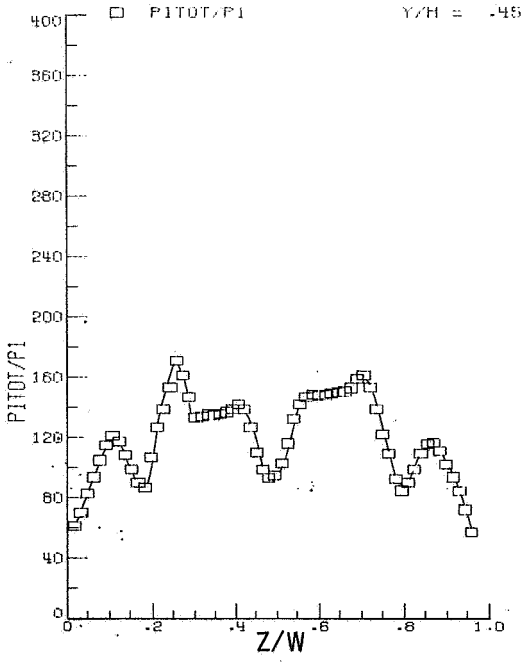

(c) Y/H = 0.45.

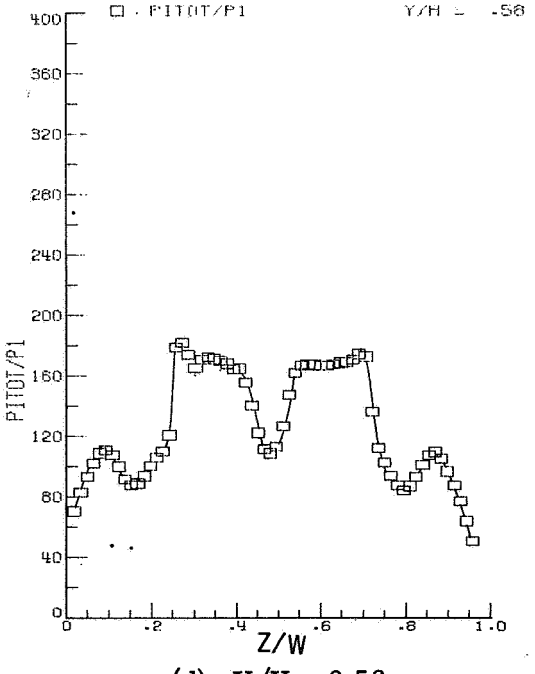

(d) Y/H = 0.58.

Figure 64.- Pitot-pressure surveys at capture station. $M_1 = 6.0$.

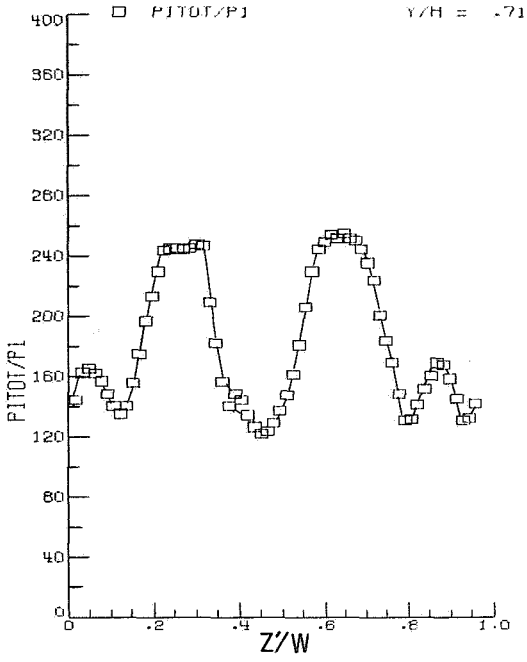

(e) Y/H = 0.71.

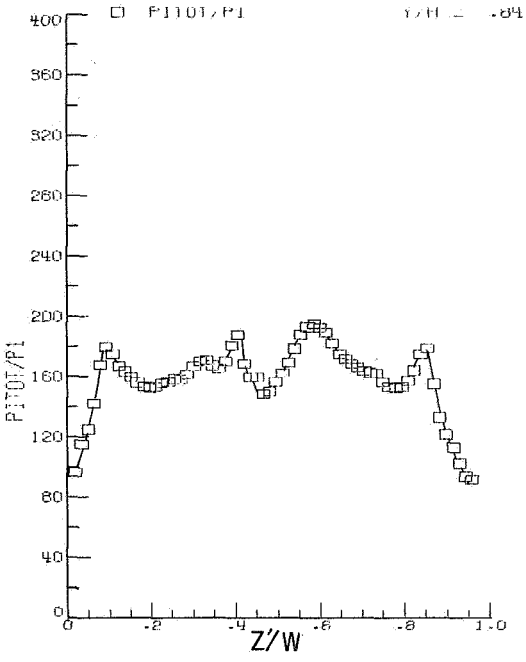

(f) Y/H = 0.84.

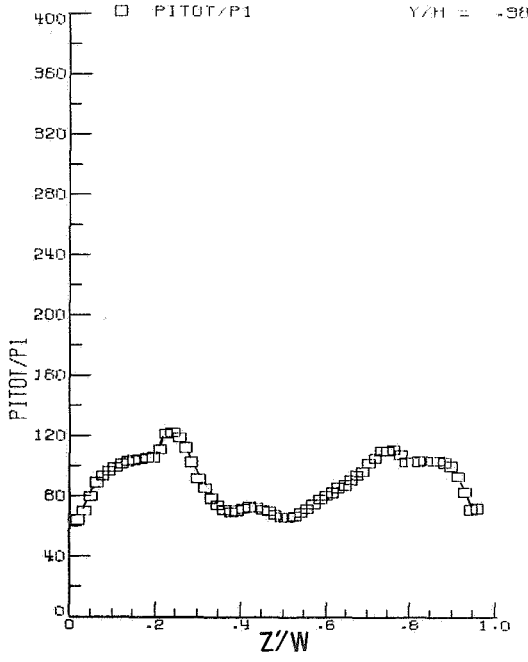

(g) Y/H = 0.98.

Figure 64.- Concluded.

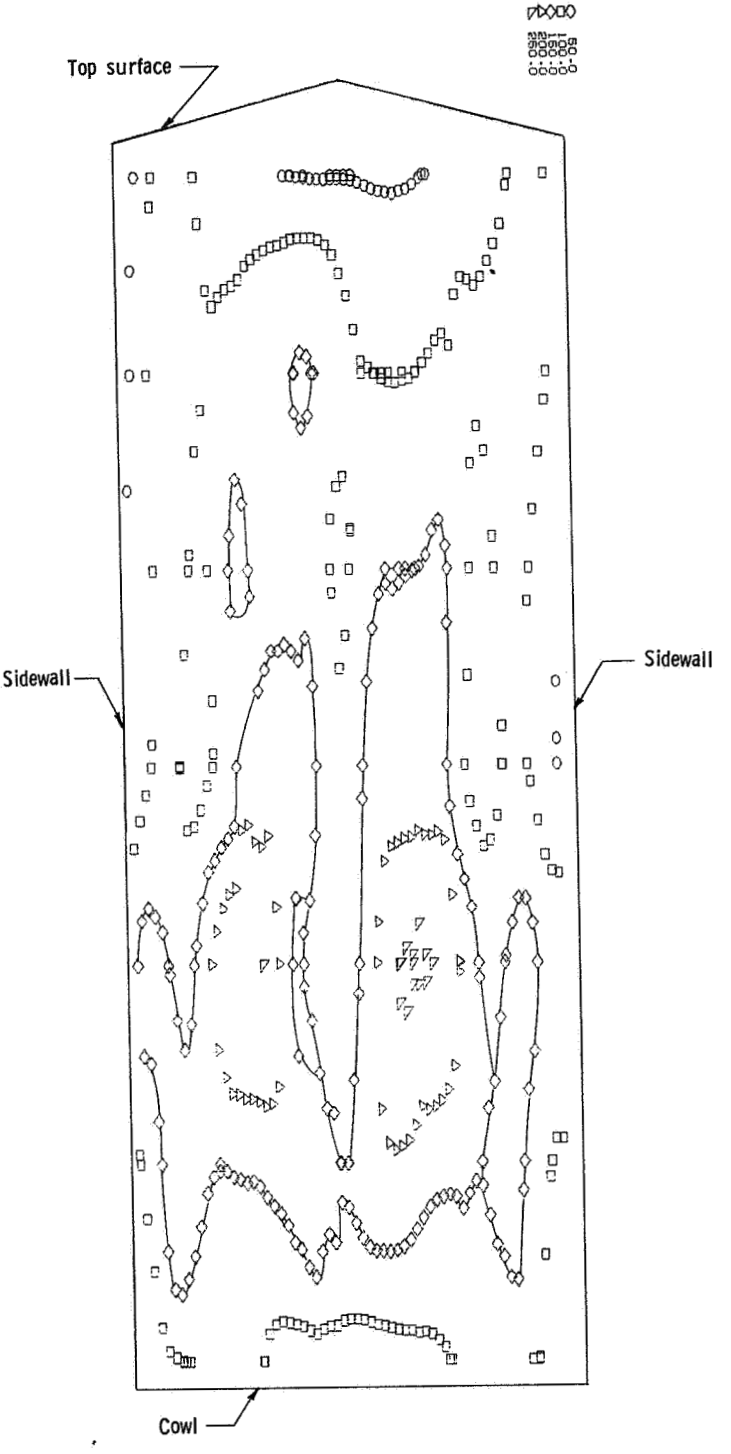

Figure 65.- Capture station. p_{pitot}/p_1.

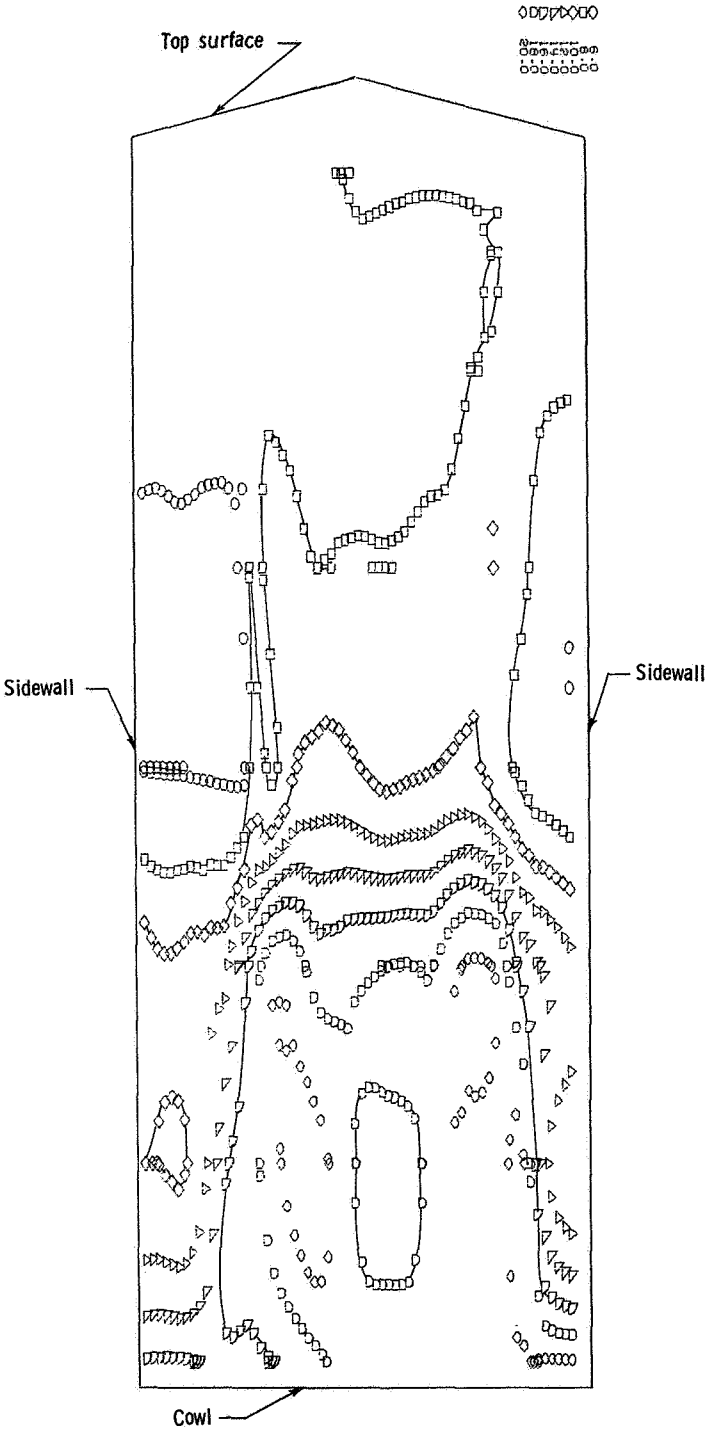

Figure 66.- Capture station. p/p_1.

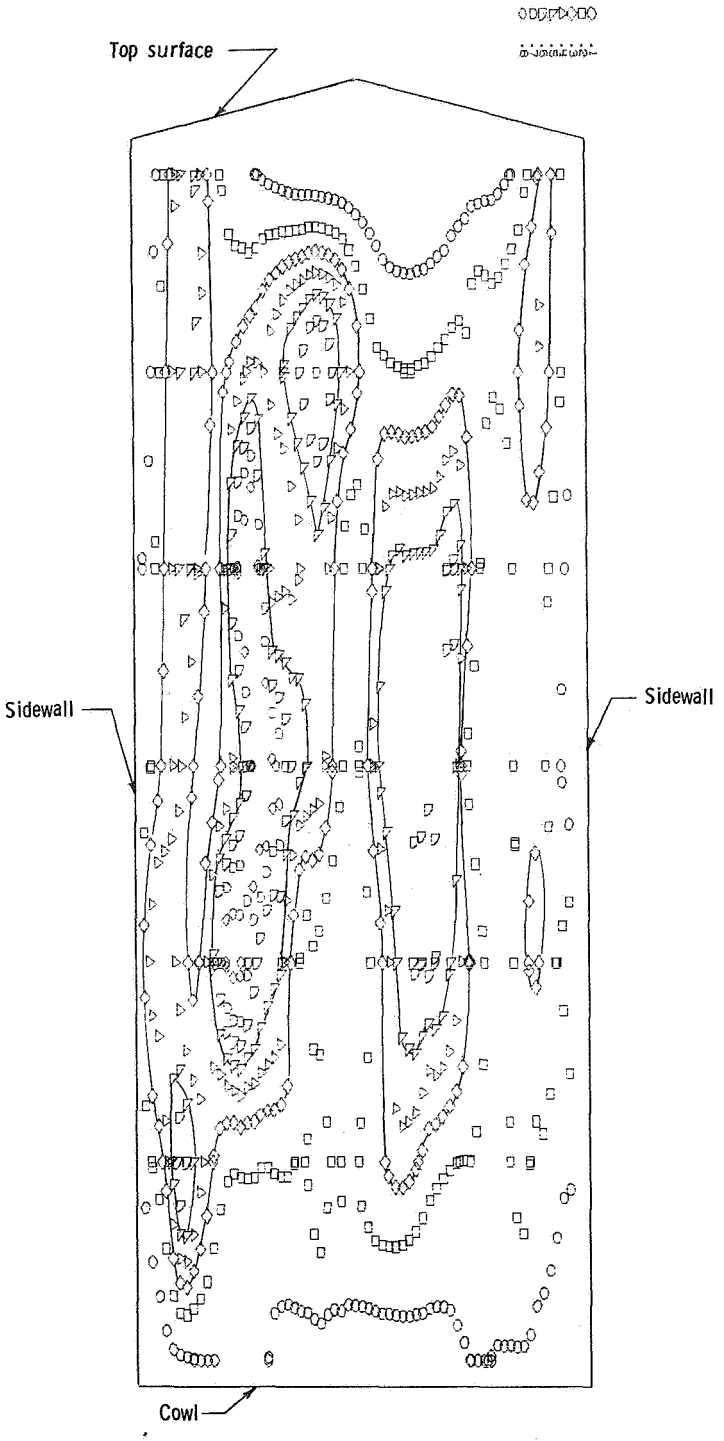

Figure 67.- Capture station total-pressure recovery.

NASA-Langley, 1975 L-10000

NATIONAL AERONAUTICS AND SPACE ADMINISTRATION
WASHINGTON, D.C. 20546

OFFICIAL BUSINESS
PENALTY FOR PRIVATE USE $300

SPECIAL FOURTH-CLASS RATE
BOOK

POSTAGE AND FEES PAID
NATIONAL AERONAUTICS AND
SPACE ADMINISTRATION
451

U.S.MAIL

POSTMASTER: If Undeliverable (Section 158
Postal Manual) Do Not Retur

"The aeronautical and space activities of the United States shall be conducted so as to contribute . . . to the expansion of human knowledge of phenomena in the atmosphere and space. The Administration shall provide for the widest practicable and appropriate dissemination of information concerning its activities and the results thereof."

—NATIONAL AERONAUTICS AND SPACE ACT OF 1958

NASA SCIENTIFIC AND TECHNICAL PUBLICATIONS

TECHNICAL REPORTS: Scientific and technical information considered important, complete, and a lasting contribution to existing knowledge.

TECHNICAL NOTES: Information less broad in scope but nevertheless of importance as a contribution to existing knowledge.

TECHNICAL MEMORANDUMS: Information receiving limited distribution because of preliminary data, security classification, or other reasons. Also includes conference proceedings with either limited or unlimited distribution.

CONTRACTOR REPORTS: Scientific and technical information generated under a NASA contract or grant and considered an important contribution to existing knowledge.

TECHNICAL TRANSLATIONS: Information published in a foreign language considered to merit NASA distribution in English.

SPECIAL PUBLICATIONS: Information derived from or of value to NASA activities. Publications include final reports of major projects, monographs, data compilations, handbooks, sourcebooks, and special bibliographies.

TECHNOLOGY UTILIZATION PUBLICATIONS: Information on technology used by NASA that may be of particular interest in commercial and other non-aerospace applications. Publications include Tech Briefs, Technology Utilization Reports and Technology Surveys.

Details on the availability of these publications may be obtained from:

SCIENTIFIC AND TECHNICAL INFORMATION OFFICE

NATIONAL AERONAUTICS AND SPACE ADMINISTRATION

Washington, D.C. 20546